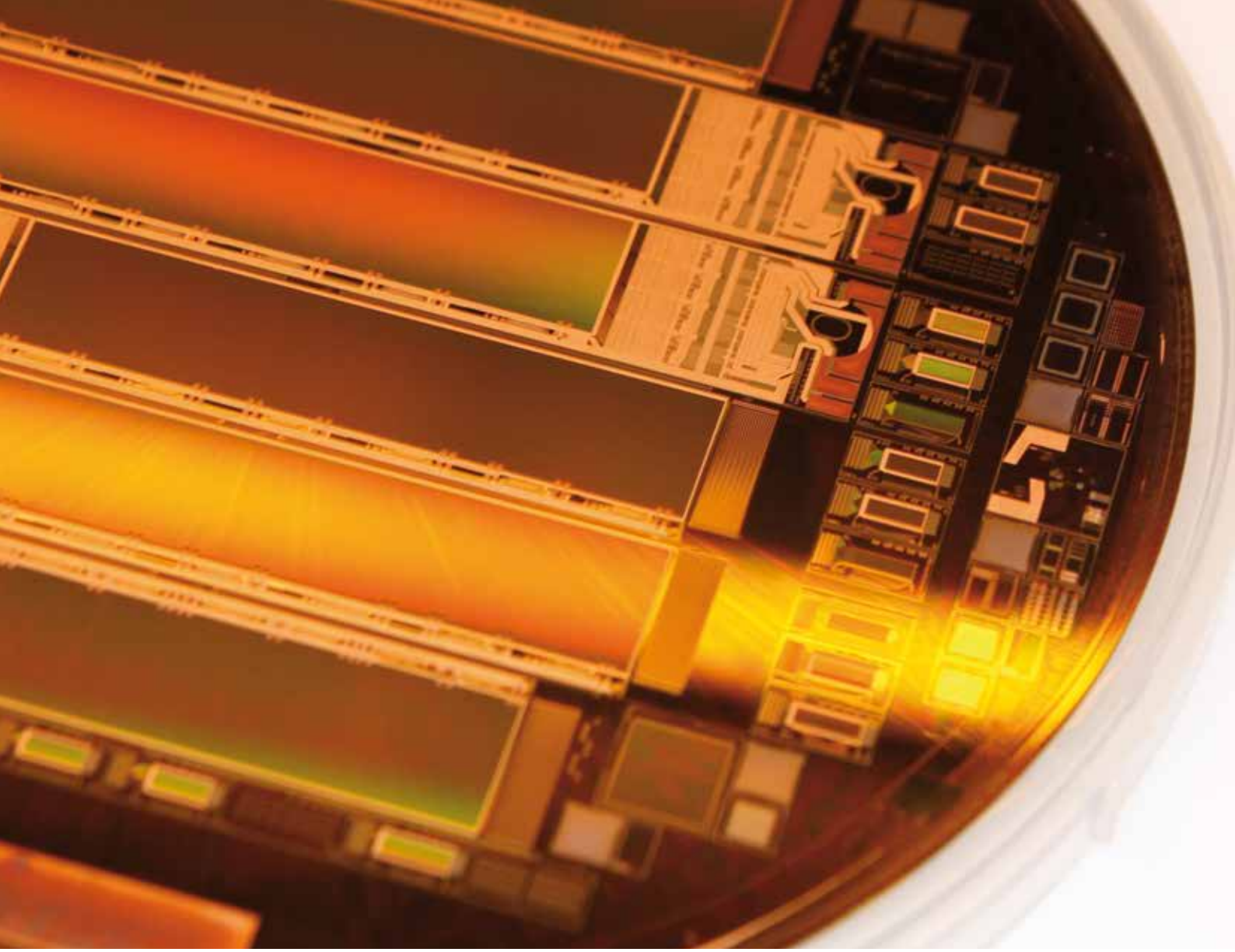

PARTICLE PHYSICS 2014.

Highlights and Annual Report

Accelerators | Photon Science | Particle Physics

Deutsches Elektronen-Synchrotron
A Research Centre of the Helmholtz Association

PARTICLE PHYSICS 2014.

Highlights and Annual Report

Cover
Pilot-run wafer in DEPFET technology for the Belle II pixel vertex detector.

Contents.

The year 2014 at DESY.

Chairman's foreword

In 2014, important decisions were made regarding DESY's financial frame for the coming five years (2015–2019), that is, the so-called third programme-oriented funding period (POF III) of the Helmholtz Association.

DESY is a leading laboratory in the Helmholtz research field "Matter", which has been radically reorganised in order to meet the challenges of the future. The three novel programmes within "Matter" promote the enhanced cooperation between hitherto separate scientific disciplines and between the Helmholtz research centres. One key example is the new programme "Matter and the Universe", which – for the first time – integrates particle physics, astroparticle physics and the physics of hadrons and nuclei. The new programme "Matter and Technologies" promotes the development of enabling technologies for future particle accelerators and advanced particle and photon detectors to a new strategic level.

The Helmholtz evaluation in spring 2014 confirmed the outstanding quality of the research carried out within the research field "Matter" and at DESY. All research activities received highest marks from the international peer review panels. The reviewers also took an in-depth look into DESY's user facilities – the PETRA III synchrotron radiation source and the FLASH soft X-ray free-electron laser – and into the European XFEL X-ray free-electron laser, which is currently under construction (Fig. 1). The resulting new budget lines, with a 3% annual increase for our research programmes and a 4% annual increase for the operation of our user facilities, provide a very solid basis for fulfilling our mission.

DESY's future is intimately linked to its capability to devise and develop forefront accelerator facilities on site, and to visibly participate in European and international large-scale projects for the investigation of matter and the universe. Currently, work at

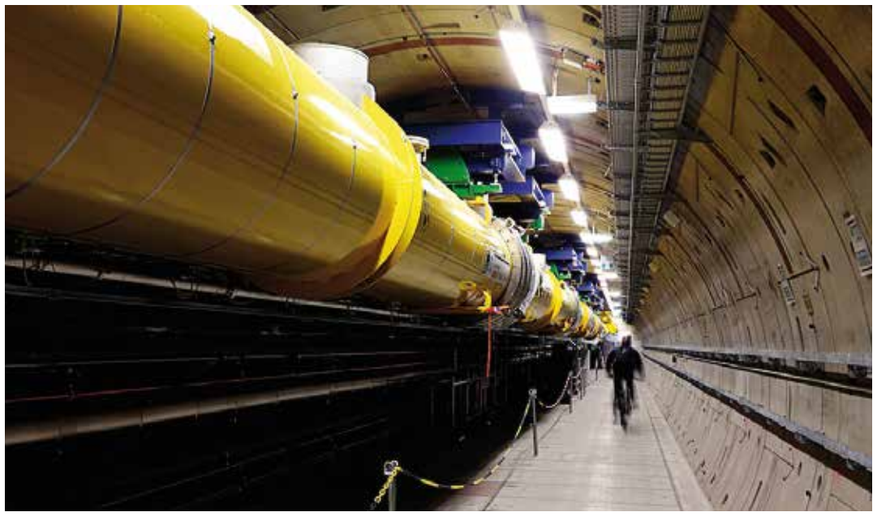

Figure 1
View into the tunnel of the European XFEL X-ray laser with first accelerator modules

Figure 2
Architect's view of the future CSSB building on the DESY campus

DESY focuses on the construction of the accelerator for the European XFEL and on the commissioning of the re-assembled PETRA III storage ring, the two new PETRA III experimental halls and the second FLASH experimental hall.

The construction of the European XFEL X-ray laser is ongoing. Major parts of the infrastructure, such as the electron injector and the radio-frequency system, have been installed in the tunnel. The first modules are already mounted, and the serial production of further modules is running smoothly. DESY is making every effort to meet the overall goal, that is, to close the tunnel by mid-2016. The excellent work of our accelerator team and its friendly and effective collaboration with the members of the Accelerator Consortium are key factors for success.

DESY's soft X-ray laser FLASH is a world-leading user facility with outstanding scientific output, and it continues to be a pathfinder for free-electron laser (FEL) science and technology. With the simultaneous operation of two independent undulator chains, FLASH is leading the worldwide efforts towards multiuser operation of FEL facilities.

Further important activities at DESY are its participation in the upgrade programme of the experiments at the Large Hadron Collider (LHC) at CERN near Geneva as well as in the implementation of the Cherenkov Telescope Array (CTA), a new international gamma-ray observatory. DESY has allocated considerable resources from its base budget for these two mission-critical projects and is currently seeking additional funding.

DESY is embarking into an exciting and brilliant future. The novel research infrastructures at DESY allow radically new ways of exploring matter and materials at relevant length and time scales, opening a new gate to the design of tailored functional materials and better drugs, and to new discoveries in nanospace. In order to exploit these opportunities for scientific breakthroughs, DESY has started to build up its own research capabilities and launched new interdisciplinary research cooperations on the DESY campus. The Center for Free-Electron Laser Science (CFEL) and the new Centre for Structural Systems Biology (CSSB, Fig. 2) are two highlights hereof.

At the same time, DESY has already redirected considerable financial resources for the future operation of the European XFEL. A challenge that DESY is currently facing is to ensure that the long-term German contribution to the European XFEL operation is secured without further reductions imposed on DESY's research programme – which would have a detrimental impact on its future development. I am optimistic that the current negotiations with DESY's funding and advisory bodies will deliver a practical solution.

In future, DESY will take a more strategic approach to technology transfer. To better leverage the potential for innovation, the Senate of Hamburg, DESY and the University of Hamburg decided to build up a new business incubator on the DESY campus. This innovation centre will foster and facilitate enterprise foundations, and start-ups will get support within an inspiring scientific and technological environment. Two start-up companies initiated by DESY scientists are already being co-funded by the Helmholtz Association. The X-Spectrum company will enter the market with a high-technology X-ray detector, and Class 5 Photonics will build very flexible femtosecond lasers generating short, high-power pulses.

I am delighted to thank all our dedicated collaborators for their excellent work and commitment.

Helmut Dosch
Chairman of the DESY Board of Directors

Particle and astroparticle physics at DESY.

Introduction

For particle and astroparticle physics at DESY, the year 2014 was marked by many activities and high expectations for major new projects as well as exciting new scientific results.

At the very start of the year, DESY's strategic proposals for the next programme-oriented funding period (POF III) of the Helmholtz Association were scrutinised by an international team of expert – and found to be of first quality, in both particle and astroparticle physics. These top-rate results lend us the support and stable base funding for our plans for the next five years.

The new POF III period, which started at the beginning of 2015, also saw a reorganisation of the Helmholtz research area "Matter": the former programmes "Elementary Particle Physics" and "Astroparticle Physics" were joined with the activities in hadronic and nuclear physics to form a new programme called "Matter and the Universe", which involves, alongside DESY, the Helmholtz centres GSI, FZ Jülich and KIT. This new organisation bundles the forces of all Helmholtz centres tackling the most fundamental questions in physics – e.g. those about the structure of matter on very different scales and the origin of these structures. With its strong tradition of collaboration in particle and astroparticle physics and the wide-ranging activities of its theory department in these and other fields, the laboratory is optimally placed to benefit from this new structure and bring out its own advantages to the fullest.

A further change for the POF III period is the introduction of another programme, named "Matter and Technologies", to which DESY also contributes significantly. This new programme unites all generic Helmholtz R&D efforts in the fields of detector development and accelerator research, that is, in the development of the very tools required for our research. The programme will open up new opportunities for all contributing centres, and we expect to also benefit from developments in neighbouring disciplines, such as photon science.

DESY's particle physics strategy for the POF III period rests on the three pillars LHC physics, precision physics at electron–positron colliders and theory. As such, it is in perfect accordance with the current roadmaps and strategies in Europe, Japan and the USA. In all three areas, DESY is at the forefront of research.

At the Large Hadron Collider (LHC) at CERN, besides being strongly involved in the data analysis and detector operation, DESY aims to organise and host the construction of major components for the upgrades of the ATLAS and CMS experiments. These activities, which include the construction of one tracker end-cap for each experiment in a new, modern omni-purpose detector assembly facility, are to be carried out together with German university groups and international partners. DESY is currently striving to obtain the necessary funding for the proposal, which will confirm the centre's role as a national laboratory for particle physics. In parallel, the DESY groups are preparing for the restart of the LHC in mid-2015: in the past two years, a lot of consolidation work has been done on the accelerator and the experiments, and preparations for high-energy and high-luminosity running are in full swing.

For several decades, the HERA electron–proton collider was the central building block of DESY's particle physics research portfolio. At the end of 2014, with the start of the POF III funding period, the HERA programme at DESY was concluded, its main analysis goals achieved. The final high-impact measurement of the proton structure was prepared in 2014; the results will be published in early 2015. DESY will preserve the legacy of the world's only electron–proton collider for future purposes; data preservation efforts for the data of the H1 and ZEUS experiments are ongoing. The DESY groups are transferring their experience in proton structure analysis to the LHC, where the uncertainty on the partonic content of the proton is often the limiting uncertainty.

Figure 1
Left: Mock-up for the Belle II vertex detector installation. The alternative installation method (AIM), which was chosen as the default method, is based on a remote vacuum connection system developed at DESY.
Right: Interior of the mock-up. The picture illustrates the narrow space available for readout cables and other services.

In the field of precision electron–positron physics, DESY is a major player in the German-centred vertex detector project for the Belle II experiment of the SuperKEKB collider at the Japanese national particle physics laboratory KEK (Fig. 1). DESY also contributes significantly to preparing the data analysis and computing for Belle II, which is due to start data taking in early 2016. In addition, DESY has farther-reaching plans for projects in Japan: After the site choice for the next-generation electron–positron International Linear Collider (ILC) by the Japanese high-energy physics community, which selected the Kitakami mountain region in northern Japan as their preferred construction site, the site-specific work on the accelerator and detector design has started. DESY is a driving force behind these developments on the detector concept side, but also in the ILC physics programme, in machine development and in questions of accelerator–detector interface.

The DESY theory department is working at the forefront of tool development and data interpretation, and expanding our horizon by devising new models of physics beyond the Standard Model. Particular highlights in recent years were the activities dedicated to the interpretation of the Higgs boson, which was discovered – with major DESY contributions – at the LHC in 2012. Shortly before data taking at the LHC will recommence for Run 2, theorists are now leading the way, working towards results that might overcome the successful but incomplete Standard Model, which has been with us for decades.

In the last years, our strategy at the LHC, the Belle experiment and the ILC as well as in theoretical physics received strong support through the successful recruitment of new leading scientists and professors, who will leave their imprint at DESY and strengthen our role in particle physics. As most of the recruitments were carried out in conjunction with German universities, they also strengthen the coherence of German contributions and the collaboration among the various institutes – a development that will benefit the laboratory as well. In addition, DESY physicists were awarded a number of prestigious grants, among them European Research Council (ERC) Starting and Consolidator Grants, which will also help to shape the future of the research centre.

In astroparticle physics, DESY has developed a rich experimental and theoretical portfolio, with a specific focus on gamma and neutrino astrophysics. DESY is strongly involved in experiments such as the IceCube neutrino observatory and the MAGIC and H.E.S.S. gamma-ray telescopes; it is also a driving force behind the preparations for the CTA next-generation gamma-ray observatory.

In 2014, the international IceCube collaboration successfully pursued its scientific mission, which – in 2013 – had been rewarded by the discovery of highly energetic astrophysical neutrinos (Fig. 2). With its multimessenger approach, IceCube substantially narrows down the possible candidate sources for these spectacular events. At the same time, on the other end of the energy spectrum, the DeepCore subdetector provided more and more stringent constraints on the masses and the mixings of neutrinos. With the PINGU and High-Energy Array projects, the IceCube collaboration is now preparing for a massive extension of its physics reach, and DESY intends to play a major role in these endeavours.

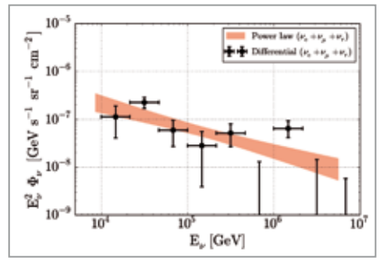

Figure 2
Energy spectrum of astrophysical neutrinos as measured with the IceCube neutrino observatory at the South Pole

In the meantime, the Cherenkov Telescope Array (CTA), a next-generation gamma-ray observatory, is on its way towards realisation. In summer 2014, an interim legal entity, the CTAO GmbH, was established with DESY as one of the founding partners. Construction of CTA will likely begin in 2016, after a site will have been chosen at the end of 2015. DESY will play a decisive role in the construction, operation and management of the experiment. The research centre is responsible for the design and project management of the mid-sized telescopes and has taken over numerous additional tasks in control software, trigger electronics and others. Furthermore, DESY proposes to host the CTA headquarters at its Zeuthen site.

As in particle physics, recruiting of leading scientists and attracting of third-party funding were also successful in astroparticle physics, and one of the ERC Consolidator Grants was awarded to an astroparticle theorist at DESY.

All in all, 2014 was a highly successful year, in terms of scientific output, preparations for important future projects and recruiting. Expectations are therefore high for 2015, but with more data from the LHC coming in and with significant developments in numerous experiments in particle and astroparticle physics, I am confident that at the end of 2015, we will again be able to proudly look back on our achievements!

Joachim Mnich
Director in charge of Particle Physics
and Astroparticle Physics

News and events.

A busy year 2014

January

CMS Achievement Award for Benjamin Lutz

DESY fellow Benjamin Lutz received the CMS Achievement Award 2014 for his engagement in improving the outer layer of the hadronic calorimeter of the CMS experiment at the Large Hadron Collider (LHC) at CERN near Geneva, for which DESY delivered the essential components.

The DESY Team after the upgrade of the central calorimeter ring's last sector. From left to right: Artur Lobanov, Pooja Saxena, Tylor Dorland, Benjamin Lutz

Lutz is acknowledged "for the excellent organisation of the process of carrying out the full replacement of hybrid photodetectors with silicon photomultipliers". The CMS collaboration presents this prize for extraordinary contributions to the experiment.

Benjamin Lutz at the occasion of the CMS Achievement Award 2014 ceremony

DESY presents Bjørn H. Wiik Prizes

Every two to three years, the Bjørn H. Wiik Prize is awarded to younger scientists and engineers for outstanding contributions to DESY's research programme or for technical developments that notably advance projects at DESY. On 23 January, Bjørn H. Wiik Prizes were awarded to particle physicist Kerstin Tackmann, who received the prize for 2012, and photon scientist Ralf Röhlsberger, who received the prize for 2013.

Kerstin Tackmann (35) was honoured for her contributions to the discovery of the Higgs particle by the ATLAS detector at the LHC. With her analysis of the Higgs particle decay to two photons, she played a decisive role in the identification of this particle.

Ralf Röhlsberger (51) was awarded the prize for his fundamental quantum-mechanical experiments with X-rays, which he mainly carried out at DESY's synchrotron radiation source PETRA III.

From left to right: Eckhard Elsen, chairman of the prize committee, Kerstin Tackmann, Ralf Röhlsberger and Margret Becker-Wiik, wife of Bjørn Wiik

February

Milestone for Belle II

A sophisticated test beam campaign, which provided important data for the operation of the vertex detector of the Belle II experiment at the SuperKEKB collider in Japan, was completed at the DESY test beam facility in February. Over a period of four weeks, an international group of more than 30 scientists integrated prototypes of all vertex components for a system test and a thorough check of the functions of the detector together with its entire intricate infrastructure.

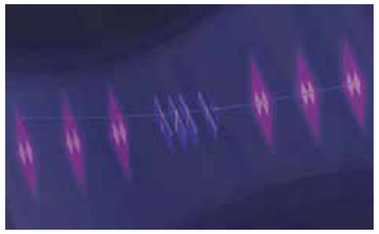

Reconstructed track of a particle flying through the layers of the vertex detector (middle), also traced by the EUDET telescope (left and right) at the DESY test beam facility

The scientists tested, for the first time, the interplay of pixel and strip layers and the corresponding infrastructure in a realistic setup. They mounted the detector components inside a superconducting magnet and subjected them to a massed volley of precisely localised electrons from the DESY synchrotron, thereby carrying out the first tests of the trigger, which is used to select the collisions meriting further scrutiny. With the high collision rate anticipated at Belle II, even its small pixel detector alone will generate about 20 GB per second of data – far too much to be read out unfiltered.

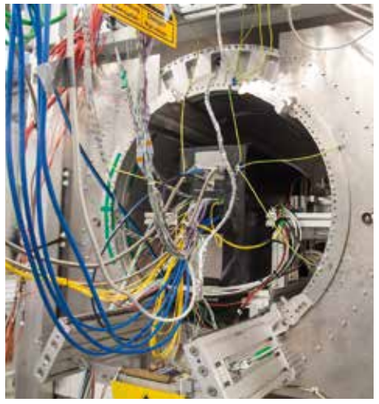

The setup was mounted in a superconducting magnet providing a magnetic field of 1 T.

DESY budget put to the test

Every five years, a committee of international experts evaluate DESY's strategy for the following funding period of the Helmholtz Association. In 2014, the Helmholtz research field "Matter", which includes DESY, was put under scrutiny.

The review process started in February with the programme "Matter and the Universe". Many DESY scientists working in particle and astroparticle physics made decisive contributions to the review, which took place in Karlsruhe. Next on the agenda, at the end of March, was the evaluation of the programme "Matter and Technology", which took place in Dresden with the participation of DESY accelerator physicists and detector developers. Finally, in mid-April, DESY hosted about 200 participants for the evaluation of the programme "From Matter to Materials and Life".

All in all, the programmes with DESY participation received impressive evaluation results. In particle physics, for example, the referees stated that the corresponding research "should be supported fully and with highest priority". DESY thus has the full support of the Helmholtz Association for its research plans in the next five years.

The research landscape of the Helmholtz programme "Matter and the Universe". Objectives marked with an asterisk are common to at least two topics.

February

ICFA and the Linear Collider Board meet at DESY

On 20 and 21 February, the International Committee for Future Accelerators (ICFA) and the Linear Collider Board (LCB) met at DESY. The two strategy groups, whose members come from the world's renowned particle physics institutions, discussed the future of particle physics and its large-scale accelerator facilities.

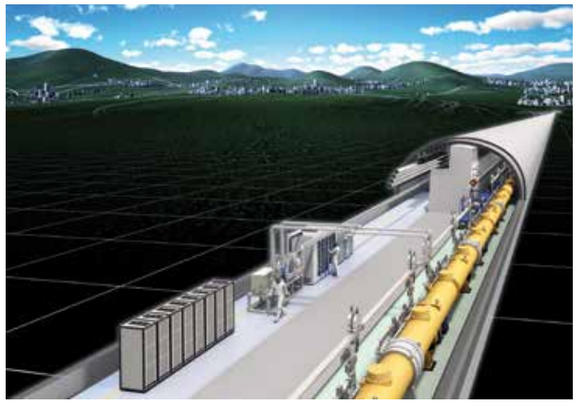

Artist's view of the proposed International Linear Collider (ILC)

ICFA members are experienced specialists working in the field of particle physics all over the world. The LCB was established in 2013 as a subgroup of ICFA, with the mandate of advancing and coordinating the international research work needed to build an electron–positron linear collider for particle physics.

Make your ideas come true

"Make your ideas come true" – some 600 young researchers followed the call and entered about 300 projects into the 2014 "Jugend forscht / Schüler experimentieren" youth science and experiments competition in Hamburg. On 20 and 21 February, the regional competition round took place in the DESY school lab. Dedicated pupils presented a total of 60 projects from the working world, biology, chemistry, geo and space sciences, mathematics, computer sciences, physics and technology. Five projects won a first prize and hence a ticket for the next competition round.

"Jugend forscht" is a talent factory that introduces young people at an early stage to the tools of scientific work. In 2014, "Jugend forscht" applications hit a record with the registration of altogether 12 298 young researchers. This is the highest number of applications in the 49-year history of Germany's best-known young researchers' competition.

Pupils at the regional youth science and experiments competition, which took place at the DESY school lab in Hamburg

Happy birthday, DESY synchrotron!

The particle accelerator "Deutsches Elektronen-Synchrotron" celebrated its 50th birthday. Half a century ago, electrons completed their first lap around the newly built DESY ring accelerator. This marked the start of the particle acceleration era in Hamburg, which eventually saw the DESY research centre (named after the synchrotron) develop into Germany's largest accelerator centre and become a pioneer in technologies for particle detectors and experiments with synchrotron radiation.

On 26 February 1964, DESY director Willibald Jentschke celebrated the successful start of the DESY accelerator together with the accelerator team.

On 25 February 1964, shortly before midnight, the first particles repeatedly rounded the 300 m diameter synchrotron. After two weeks of sometimes frustrating efforts by the accelerator team, everything went very quickly and the first electrons reached an energy of 2.5 GeV in about 8000 rounds. On the following day already, it was possible to obtain 5 GeV.

Eventful years of operation followed, with all kinds of particle physics experiments and with the world's first characterisation studies of synchrotron radiation, whose high value for research was first recognised at DESY. The synchrotron has since then been serving as a pre-accelerator for the large-scale particle accelerators DORIS, PETRA and HERA. Moreover, it is still in demand as a test beam source for the investigation of future detectors.

March

European network GATIS constituted

Under the leadership of the DESY theory group, eleven renowned academic institutions joined forces in the GATIS research and training network, an initiative funded by the European Commission with almost 4 million euro up to 2016.

The scientific goal of the Gauge Theory as an Integrable System (GATIS) network is the development of highly innovative methods for quantum physics calculations. The advancement of technologies from particle physics, mathematics and computer algebra will provide new fundamentals, particularly for the models physicists use to describe, for example, particle collisions at the LHC at CERN.

10th anniversary of International Masterclasses

The International Masterclasses "Hands on Particle Physics" provide a unique opportunity for high-school students to hunt for evidence of particles in authentic data from experiments at the LHC at CERN, the most powerful particle accelerator in the world. The Masterclasses 2014 took place from 12 March to 12 April and attracted about 10 000 participants, as DESY and numerous research institutes around the world opened their doors for the 10th time and invited young people to become particle physicists for one day.
The four LHC experiments ATLAS, CMS, ALICE and LHCb made their data available for the programme. For example, pupils measured the *Z* boson and investigated the structure of the proton. A highlight was the possibility to trace the rare and short-lived Higgs particle in the ATLAS and CMS data, enabling students to experience the discovery of the particle for themselves.

The International Masterclasses took place in collaboration with Netzwerk Teilchenwelt, a German network that aims to expose young people and teachers to particle physics. The Masterclasses are led by Technical University in Dresden and organised by the International Particle Physics Outreach Group (IPPOG), which comprises representatives from CERN, DESY and countries doing research at CERN, with the goal of making particle physics more accessible to the public.

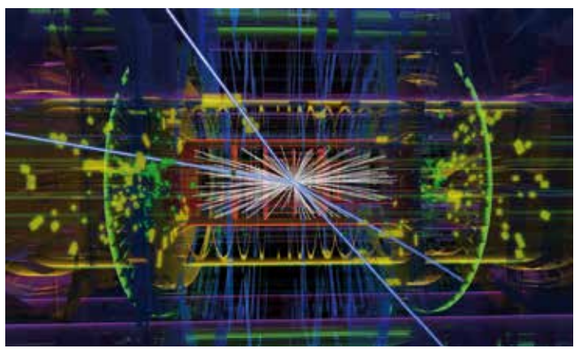

Four muons pass the ATLAS detector after a proton–proton collision (blue tracks)

April

Gay-Lussac Humboldt Prize for Emilian Dudas

Professor Emilian Dudas from École Polytechnique in Palaiseau, France, was awarded the Gay-Lussac Humboldt Prize. During two extended research visits to DESY, Dudas will pursue his work on supersymmetric theories and the interplay of particle physics, string theory and cosmology.

Helmut Schwarz, President of the Humboldt Foundation (left), presents the award to Emilian Dudas.

Dudas is an internationally renowned theoretical physicist specialising in supersymmetric and superstring theories and their implications for high-energy physics and cosmology. He made pioneering contributions to the analysis of unified theories in higher space–time dimensions.

Since 1982, the French research ministry and the Alexander von Humboldt Foundation have been presenting the annual Gay-Lussac Humboldt Prize to internationally renowned German and French scientists who coined and promoted Franco–German scientific collaboration.

April

Matthew Wing wins Humboldt Foundation's Bessel Research Award

Particle physicist Matthew Wing was awarded a Friedrich Wilhelm Bessel Research Award by the German Humboldt Foundation. The 40 year old professor at University College London (UCL), UK, will use the award to stay at DESY for a year, where he will pursue collaborative research in data analysis as well as linear collider and plasma accelerator development together with DESY experts. One of his immediate tasks after winning the award was to lead the major effort of the H1 and ZEUS experiments at DESY's former HERA collider to publish their combined data of the proton structure.

Matthew Wing

May

DESY school lab in Zeuthen celebrates 10th anniversary

On 21 May, the "physik.begreifen" school lab at DESY in Zeuthen celebrated its 10th anniversary. So far, more than 25 000 young people took the opportunity to work like a scientist for one day at the DESY lab and thus gain a lively insight into the world of physics while simultaneously experiencing day-to-day research in all its facets. On the occasion of its anniversary, Martina Münch, Minister of Education of Brandenburg, acknowledged the success story of the DESY school lab: "The school lab is a useful and fascinating complement to natural sciences classes at school."

Pupils at a vacuum chamber experiment in the DESY school lab in Zeuthen

The DESY school labs in Hamburg and Zeuthen invite school classes of different grades to attend experimental days and project weeks in which the pupils can do their own experiments. The experimental programmes are targeted to specific age groups. "physik.begreifen" in Hamburg was the first school lab of this kind launched by a Helmholtz Centre. Today, the DESY school labs are fully integrated into DESY's programmes for promoting the education of young people and are active in numerous networks at the regional and national level.

DESY Golden Pin of Honour for Peter Stähelin

The former DESY research director Peter Stähelin was awarded the DESY Golden Pin of Honour. On the occasion of his 90th birthday, Stähelin was honoured for his great service to the research centre and, in particular, for his pioneering spirit in the exploration and use of synchrotron radiation at DESY.

Peter Stähelin

Nuclear physicist Peter Stähelin was DESY's first research director. From 1960 to 1967, he headed the planning and preparation of high-energy experiments and paved the way for the first very successful experimental particle physics programme. Under his direction, the foundation was laid for the successful collaboration between physicists, engineers and technicians from foreign institutions and DESY in instrumentation, realisation and analysis of experiments that is still key to DESY's success today. From the beginning, Peter Stähelin wanted to use the 6 GeV electron synchrotron DESY also as a source of ultraviolet, vacuum ultraviolet and X-ray radiation. The pioneering work led to the very first measurements with synchrotron radiation at the DESY accelerator in 1964.

July

DESY welcomes record high of summer students

The 2014 summer students in Hamburg

In 2014, DESY welcomed a record 117 summer students to its two locations in Hamburg and Zeuthen near Berlin. During their eight-week stay, the junior researchers from 28 nations gained practical insights into research at Germany's largest accelerator centre. DESY offers one of the largest and most international summer schools in Germany.

The students were incorporated into the DESY research groups in particle and astroparticle physics, accelerator physics and photon science, where they experienced everyday life in science first hand. A series of lectures complemented the practical experience with the necessary theoretical background.

The 2014 summer students in Zeuthen

Helmholtz Fellow Hesheng Chen guest at DESY

Professor Hesheng Chen, who won a Helmholtz International Fellow Award that provided him with funds for two extended research visits to DESY, arrived in Hamburg for his first stay in July 2014. Chen is a renowned particle physicist who was also Director General of the Institute of High Energy Physics in Beijing. He participated in several pioneering experiments, including MARK-J, AMS and Daya Bay.

At DESY, Chen supported the Higgs analyses of the CMS research group and shared his experience of the analysis activities carried out in parallel by Chinese research groups. Discussions with DESY colleagues on the future of global accelerator and particle physics as well as the starting points of future cooperation with Chinese institutes were also on his agenda.

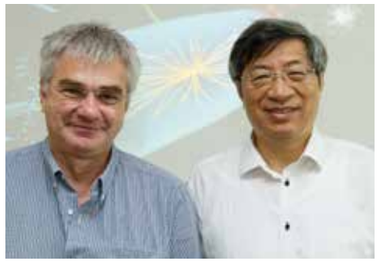

DESY research director Joachim Mnich (left) welcomes Hesheng Chen (right) in the CMS remote centre at DESY.

First H.E.S.S. II data reveal promising pulsar signal

Following the commissioning phase of the largest Cherenkov telescope worldwide, the H.E.S.S. CT5, the High Energy Stereoscopic System (H.E.S.S.) collaboration announced the detection of cosmic gamma rays with an energy of 30 GeV. The H.E.S.S. telescope system, which is located in Namibia, measured pulsed gamma rays in the southern sky for the first time from the ground level, thereby spectacularly demonstrating its performance. The radiation originated from the Vela pulsar, the first pulsar detected by H.E.S.S. and – after the Crab pulsar – the second pulsar ever detected by ground-based gamma-ray telescopes.

H.E.S.S. II is a system of reflecting telescopes of different sizes, which detect cosmic gamma rays in sync. It is run by an international collaboration of 31 institutions in 10 countries. The 28 m CT5 is placed in the centre of four 12 m telescopes, which have been operational for more than 10 years. The CT5 extends the energy range of the array to lower energies and allows for the detection of cosmic particles down to 30 GeV.

The H.E.S.S. telescope system with four 12 m telescopes surrounding the new 28 m CT5 telescope

July

IUPAP Young Scientist Prize in Particle Physics for Kerstin Tackmann

DESY physicist Kerstin Tackmann was awarded the 2014 Young Scientist Prize in Particle Physics of the International Union of Pure and Applied Physics (IUPAP). At the International Conference on High Energy Physics (ICHEP) in Valencia, Spain, she received the prize consisting of an IUPAP medal and a cash award of 1000 euro for her outstanding contributions to elementary particle physics, especially to the discovery of the Higgs boson. Kerstin Tackmann and her Helmholtz Young Investigator Group are members of the ATLAS group at DESY. Together with her group, she made important contributions to the analysis of the two-photon spectrum that were essential prerequisites to the discovery of the Higgs boson.

Kerstin Tackmann

August

DESY and IBM develop big-data architecture for science

IBM and DESY announced their collaboration to speed up the handling and storage of massive volumes of data. The planned big-data and analysis architecture will be able to handle the data output of experiments at DESY's PETRA III synchrotron radiation user facility, which produces more than 20 GB/s of data at peak, and provide researchers with faster access to their measurement data for analysis.

To this end, DESY and IBM Research are developing a solution based on the IBM software-defined storage system code-named "Elastic Storage". The architecture will allow DESY to develop an open ecosystem for research and offer analysis-as-a-service and cloud solutions to its users worldwide.

The solution's scalability will also enable DESY to handle even greater data volumes such as those produced by the new European XFEL X-ray laser, whose annual data output will be comparable to that of the LHC at CERN.

The DESY computing centre

Particle physicists meet in Hamburg

PANIC 2014 conference participants in front of the venue, the main building of the University of Hamburg

In August, elementary particles – including their new superstar, the Nobel-Prize-winning Higgs boson – were in the focus of the Particles and Nuclei International Conference (PANIC) 2014. About 300 scientists met at the University of Hamburg from 25 to 29 August to exchange the newest findings on particle and nuclear physics and discuss future research programmes. The PANIC conference takes place every three years. In 2014, it was jointly organised by DESY and the Institute for Experimental Physics at the University of Hamburg.

"Particle physics is going through a very exciting phase," Joachim Mnich, the DESY director in charge of particle physics, pointed out at the conference. "Following the discovery of the Higgs particle two years ago, the world's largest particle accelerator, the LHC, is currently being upgraded to unprecedented energies. We are eagerly waiting to see what the large LHC collaborations, with substantial DESY participation, will observe in this newly accessible, unexplored energy range."

Minister President of Brandenburg visits DESY

On 6 August, Dietmar Woidke, Minister President of the German federal state of Brandenburg, visited DESY in Zeuthen. On his tour of the campus, he viewed the PITZ photoinjector test facility, the school lab and the workshops. In addition, he was briefed on the current research and development work at the institute.

"DESY is well known worldwide for its top-class research," said Woidke during his visit. "It has been carrying out pioneering work for many years, and it is also regarded as a talent factory." An important aspect for the region is the education and training at DESY in Zeuthen, which is appreciated not only for its academic education and school lab: industrial and technical DESY trainees are regularly among the best in Brandenburg.

Dietmar Woidke, Minister President of Brandenburg (left), and Christian Stegmann, head of the DESY location in Zeuthen, in the DESY school lab

September

DESY Theory Workshop 2014

The 2014 DESY Theory Workshop was held from 23 to 26 September under the motto "Particle Cosmology after Planck". Over 200 participants discussed results from the Planck space observatory and other experiments and their implications for cosmology and neighbouring fields, such as particle and astroparticle physics. One highlight of the workshop was the Heinrich Hertz lecture on "Universe or Multiverse?" given by Andrei Linde of Stanford University, USA.

Andrei Linde during his Heinrich Hertz lecture at the DESY Theory Workshop

Big in Japan

The European Commission funds two projects with DESY participation that promote cooperation with scientists in Japan: the E-JADE and JENNIFER proposals aim to further develop accelerator techniques and enable collaboration on precision measurements of the Standard Model of particle physics, respectively. Both projects were proposed within the Marie Skłodowska-Curie Research and Innovation Staff Exchange (RISE) scheme of the EU Framework Programme Horizon 2020, which supports the posting of EU scientists to non-European countries. The EU now funds the two projects with a total of 3.9 million euro.

The Europe–Japan Accelerator Development Exchange (E-JADE) project deals with the construction of future large accelerator facilities at the highest energies and intends to intensify the cooperation between European and Japanese scientists. Apart from magnet development for the extension of high-energy hadron colliders (LHC), the topics covered by the proposal include the International Linear Collider (ILC), the construction of which is being intensively planned in Japan. The EU will fund the stay of European scientists in Japan for four years with a total of 1.6 million euro.

The objectives of the Japan and Europe Network for Neutrino and Intensity Frontier Experimental Research (JENNIFER) are the preparation and execution of precision measurements and tests of the quark and lepton flavour structure of the Standard Model of particle physics. The Belle II and T2K experiments run by the Japanese KEK laboratory are two world-leading projects in this field. Both experiments can count on a substantial participation from 11 European countries.

Wide-angle view of the accelerator test facility (ATF) at the Japanese KEK laboratory, which recently met the beam focus requirements of the International Linear Collider (ILC)

October

Joint effort for new detector technologies

The Helmholtz Association will fund a joint research project of DESY and Chinese scientists on the next generation of particle detectors. A working group headed by DESY scientist Ingrid-Maria Gregor and Xinchou Lou from the Chinese Institute of High Energy Physics (IHEP) will develop and test new technologies for silicon strip detectors for the LHC experiment ATLAS, which will be operated starting in 2025 at the High-Luminosity LHC (HL-LHC), an upgraded version of the LHC with a substantially higher collision rate. As of January 2015, the cooperation will be funded with 360 000 euro from the Initiative and Networking Fund of the Helmholtz Association. The two research partners will contribute additional funds.

DESY and IHEP scientists will join forces within the Helmholtz-CAS Joint Research Group to develop the new generation of semiconductor detectors. In particular, they will carry out extensive studies of radiation resistance, develop new high- and low-voltage power supplies for the modules, investigate the thermal behaviour of the modules and minimise so-called dead matter in the detector, which slows down particles but does not contribute to the detector performance itself.

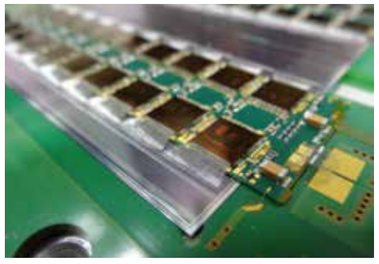

Prototype of a silicon strip module for the ATLAS detector

New business incubator on the DESY campus

The latest advances in physics, chemistry, biology and medicine, in combination with the technical possibilities provided by the radiation sources at DESY, are opening up fresh perspectives for application-oriented research and knowledge transfer. Thanks to an investment grant of 14.2 million euro from the Free and Hanseatic City of Hamburg, a new start-up centre, or "business incubator", situated in close proximity to DESY's scientific expertise and infrastructure, will become an attractive environment for young enterprises and allow DESY and the University of Hamburg to expand their successful science and innovation transfer activities.

To facilitate the founding of new enterprises, part of the centre will be made available rent-free (apart from ancillary costs) to pre-start-ups for a fixed period of time. The remaining area will be allocated to young enterprises and research projects for a modest rent. The target groups are spin-off prospects of DESY and the University of Hamburg as well as small technology enterprises already operating on the market. In addition, existing University and DESY institutions and projects as well as other research institutions on the DESY campus may use the start-up centre. As a longer-term perspective, the new incubator will create the basis for the development of a neighbouring technology park.

Drawing of the planned business incubator building

PhD thesis award 2014

The 2014 PhD thesis award of the Association of the Friends and Sponsors of DESY (VFFD) was shared by Stephan Stern of DESY (CFEL) and the University of Hamburg, and Tigran Kalaydzhyan of DESY (Theory) and the University of Hamburg. The association presents the prize every year for one or two outstanding PhD theses from the two previous university terms.

Stephan Stern and Tigran Kalaydzhyan

Stephan Stern, who was born in 1982 in Magdeburg, Germany, and studied physics at the Otto von Guericke University in Magdeburg, graduated in the Coherent Imaging Division at the Center for Free-Electron Laser Science (CFEL) in Hamburg. His thesis titled "Controlled Molecules for X-ray Diffraction Experiments at Free-Electron Lasers" describes important contributions to single-molecule structure determination and to possible ways of filming chemical reactions with X-ray lasers. Tigran Kalaydzhyan, who was born in 1987 in Yerevan, Armenia, and studied physics at the Lomonosov Moscow State University, graduated in the Theory group at DESY. Kalaydzhyan's thesis, "Quark–gluon plasma in strong magnetic fields", deals with the study of the properties of elementary matter at extremely high temperatures and in the presence of strong magnetic fields.

November

ERC Grant for Kai Schmidt-Hoberg

DESY physicist Kai Schmidt-Hoberg will receive a 1.2 million euro funding grant from the European Research Council (ERC). With the ERC Starting Grant from the European Union research funding programme Horizon 2020, the theoretical physicist will explore new research approaches to understanding dark matter in the coming five years. According to experimental observations, the amount of dark matter in the universe must be five times higher than that of normal matter. But so far, there is no experimental evidence whatsoever of its particle nature.

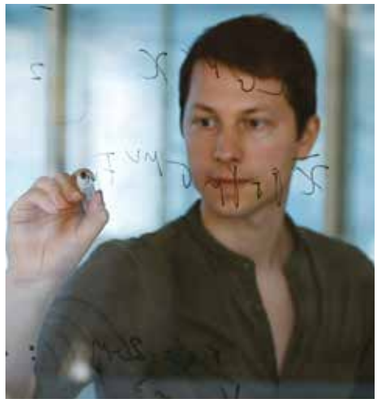

Dark matter hunter Kai Schmidt-Hoberg

Several experiments currently under construction or already in operation, including ATLAS and CMS at the LHC and the Any Light Particle Search (ALPS) experiment at DESY, hope to pin down the nature of dark matter experimentally. These and other experiments promise to supply unprecedented detection sensitivity, leading many scientists to believe that the first experimental evidence for this mysterious form of matter will soon emerge. With his EU-funded project, Schmidt-Hoberg will combine the various paths now being explored to search for dark matter and find new multidisciplinary ways to unravel its puzzle.

December

Annual meeting of the Helmholtz Alliance "Physics at the Terascale"

From 1 to 3 December, the Helmholtz Alliance "Physics at the Terascale" held its traditional annual meeting at DESY. With over 250 participants and numerous high-ranking speakers – among them former ATLAS spokesperson Peter Jenni, theorist Thomas Gehrmann and Argonne National Laboratory interim director Harry Weerts – the workshop was once again an excellent forum for exchange and discussion, displaying the richness of the physics topics being worked on in the Terascale community.

With the Helmholtz funding for the Alliance ending in 2014, the future of the Alliance is currently under debate. A new memorandum of understanding is being prepared among the Alliance partners, and further efforts to establish the Alliance idea in the larger framework of the Helmholtz programme "Matter and the Universe" are being discussed.

Peter Jenni giving his highlight talk at the Terascale Alliance annual meeting at DESY

DESY wins Fast Forward Science video competition

With their amusing and instructive contributions, the winners of the science video competition Fast Forward Science demonstrated that science is anything but abstract or boring. The jury chose the awardees in the categories "Substance" and "Scitainment" from 135 contributions. The winners were honoured on 9 December during the "7. Forum Wissenschafts-kommunikation" in Potsdam.

In the "Scitainment" category, the first prize went to the team around DESY science journalist Ute Wilhelmsen for their video "Particle zoo – on the trail of Higgs, quarks and photons". Strong pictures and lucid explanations help PhD student Mark Wenskat shed light on the wonders of the particle world. Their video clearly shows: research is fun!

The winners of the Fast Forward Science 2014 "Scitainment" prize at the award ceremony in Potsdam

Electron–proton physics.

Seven years after the final shutdown of DESY's electron–proton collider HERA, the analyses of HERA data taken by the H1, HERMES and ZEUS collaborations are still going strong. As the funding for HERA physics from the Helmholtz Association ran out at the end of the last funding period, in December 2014, it is now time to define the final "HERA heritage" – which lies mainly in the field of proton structure analyses, but also in other aspects of quantum chromodynamics (QCD).

The collider experiments H1 and ZEUS are currently publishing their final word on the proton structure ("HERA's crown jewels", p. 20). At the same time, H1 and ZEUS measurements on detailed aspects of QCD, such as the strong coupling constant, reach ultimate precision ("How strong is the strong force?", p. 22). And in the field of heavy-flavour physics, HERA physicists achieved the first-ever measurement of the running mass of the charm quark ("Running masses", p. 24).

The fixed-target experiment HERMES gained new insights into polarised lepton–proton scattering and performed exciting measurements of final-state polarisations using Λ hyperons ("Left, right, up or down?", p. 26).

HERA's crown jewels.

Inclusive cross sections and parton densities

The proton is a subatomic particle with a complex dynamic structure. This structure still remains a puzzle that needs to be solved in order to allow successful searches for new physics phenomena, e.g. at the LHC collider at CERN. Since the proton's discovery at the beginning of the 20th century, numerous experiments were performed to study its substructure, but none have achieved as much as the experiments at DESY's former HERA collider, the only ever existing high-energy electron–proton collider, which was shut down in 2007. HERA has delivered most precise and valuable data, which underpin investigations in fundamental physics such as those using proton–proton collisions at the LHC. The analysis of these HERA riches continues to date.

In the Standard Model of particle physics, the proton is a hadron composed of two up quarks and one down quark that are held together by the strong force, mediated by gluons. These three quarks are responsible for the proton's electric charge and hence are referred to as valence quarks. However, the modern picture of the proton is much more complicated. The gluons inside the proton can produce more gluons and can also split into quark–antiquark pairs – the so-called sea quarks. Therefore, the real proton is full of activity, with valence and sea quarks as well as gluons (together also called partons) continuously interacting with each other. The HERA accelerator was designed to look inside the proton using electrons as probes in order to study proton structure through deep-inelastic scattering (DIS) with its two omni-purpose experiments H1 and ZEUS.

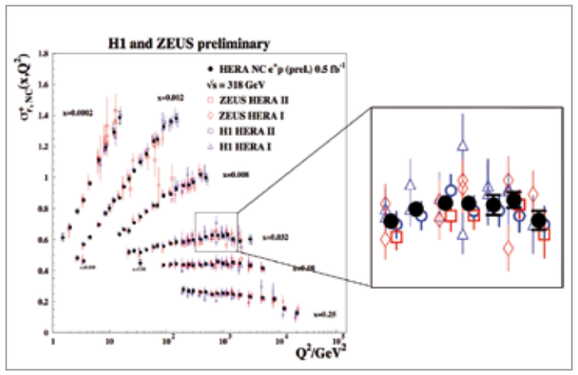

Figure 1

Combination of a subset of the H1 and ZEUS NC measurements.
The insert provides a zoom into one of the measured kinematic bins. The combined measurements are shown as black dots.

In the DIS process, a lepton (in HERA's case an electron or positron) penetrates deeply into the proton and is scattered off one of the proton's constituents via a boson mediator, producing a hadronic shower and a scattered lepton. When the exchanged boson is charged (exchange of W^+ and W^- bosons), the reaction is referred to as charged current (CC) and, similarly, when the mediator is neutral (exchange of Z bosons or photons), the reaction is called neutral current (NC). The cross sections for these NC and CC lepton–proton scattering processes can be directly measured by the experiments, but they can also be calculated theoretically with high precision. Therefore, the measurements can be confronted with our best understanding of the proton substructure, as implemented in the calculations, in order to improve them. The theoretical formalism developed over decades to study the strong interaction is called quantum chromodynamics (QCD). In QCD, the apparent structure of the proton becomes more dynamic with increasing energy at which the proton is probed. In this framework, the proton is viewed as a collection of parton distributions that are mathematically described by probability densities (parton distribution functions, PDFs).

To achieve the highest possible precision, the final H1 and ZEUS DIS cross section measurements were combined [1]. The combined data set benefits not only from increased statistics (a similar amount of data were collected by both experiments), but also from an improved understanding of each separate measurement and from an inter-calibration that occurs because the two collaborations employ different detectors and experimental techniques in their measurements. An example of such improvements can be seen in Fig. 1, where the NC inclusive cross section is shown as a function of the energy available in the interaction (Q^2) for different values of the momentum fraction x carried by the quark struck by the incoming lepton. The separate H1 and ZEUS results are represented as blue and red dots, respectively, and the combination of these measurements is shown in black.

The ultimate precision of the combined HERA data can be used to constrain the partons in the proton. The NC and CC measurements impose strong constraints on PDFs, i.e. NC reactions are mainly sensitive to the gluon and sea quark distributions, while CC data are useful in separating different types, i.e. flavours, of the valence quarks. The open-source QCD software package HERAFitter (see p. 41) was used to analyse HERA data and to extract PDFs by confronting the measurements with state-of-the-art theory. The resulting PDFs, extracted exclusively from the final combined HERA data, are called HERAPDF2.0 [1] and are presented in Fig. 2. The HERAPDF2.0 PDF set has significantly improved uncertainties compared to parton distributions previously extracted at HERA.

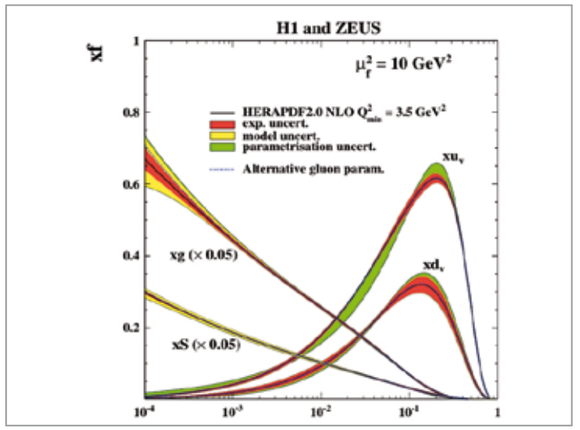

Figure 2

Summary of the HERAPDF2.0 PDF set showing scaled gluon and total sea quark distributions together with the valence quark distributions

Relying on the universality of PDFs, HERAPDF2.0 can be used to calculate accurate predictions for proton–proton processes at the LHC or at any other hadron collider. Moreover, since HERA data are a unique and necessary base of any extraction of the proton's PDFs, the final HERA data combination will soon be used as a crucial input to other theoretical studies needed for LHC data analyses.

The HERA data also beautifully demonstrate the unification of the electromagnetic and weak forces at large energies that is predicted by the Standard Model. The NC cross sections at lower energies are dominated by photon exchange, the mediator of the electromagnetic interaction, and at larger energies by the Z boson, the mediator of the weak force. The CC reactions, in contrast, are purely weak interactions mediated by W bosons. The Standard Model predicts that the electromagnetic force is stronger than the weak force at small energies but equally strong at high energies. Therefore, the fact that the NC and CC cross sections become almost equal at high energy (Fig. 3) is a clear illustration of the electroweak unification. In the figure, HERA data are compared to the theoretical predictions obtained with the HERAPDF2.0 PDF set. Excellent agreement between the two is observed.

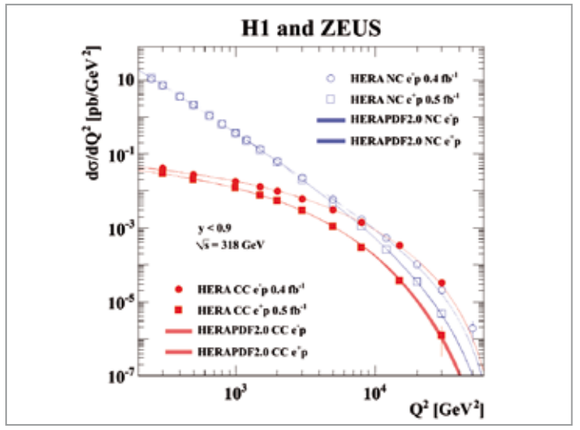

Figure 3

NC and CC cross section measurements as a function of the probed energies.
The plot nicely demonstrates electroweak unification.

With the completion of the data analyses for the inclusive cross section measurements, HERA provides a crucial basis of Standard Model physics, a necessary ingredient to scrutinise our understanding of fundamental physics, such that any potential deviation from the expectations can be used to explore signs of new physics.

Contact:
Achim Geiser, achim.geiser@desy.de
Ringaile Placakyte, ringaile.placakyte@desy.de
Voica Radescu, voica.radescu@desy.de
Katarzyna Wichmann, katarzyna.wichmann@desy.de

References:

H1 and ZEUS Collaborations, DESY-15-039

How strong is the strong force?

QCD, jets and the measurement of the strong coupling constant α_s

The strong force is one of the four fundamental interactions present in the universe. It is characterised by its exceptional change in behaviour with varying distance. Somewhat surprisingly, given that DESY's former HERA collider relied on electroweak interactions for its measurements, HERA was also an ideal place to study this remarkable behaviour of the strong force. By comparing the distributions of so-called jets with theoretical predictions, the HERA experiment H1 recently determined the change of the strong force with distance and also reported the most precise jet-based measurement of its strength yet available.

The HERA collider produced energetic collisions of electrons and protons, which, since protons are composites of quarks and gluons, are effectively electroweak interactions between the incoming electron and one of the proton's quarks. The struck quark and the scattered electron try to escape from the collision; the electron succeeds but, because the quark carries colour charge, it fails to escape unscathed. Instead, in a process known as colour recombination, it produces a narrow spray of colour-neutral composite particles (mainly pions) known as jets. The electron and the particles forming the jets were measured by the H1 detector and used to reconstruct the jets – and thus, to indirectly measure the momentum of the scattered quark.

For the studies of the strong force described here, more than the initial electroweak interaction is needed: a process involving a very high-energy strong interaction must happen. This could be, for example, the production of an energetic gluon during the colour recombination process. If the gluon is sufficiently energetic, it too will produce a measurable jet. Such an event would then be recognisable in the detector as two energetic jets, as depicted in Fig. 1, where two jets as well as the scattered electron are easily visible. Other strong-interaction processes could also lead to two or even more jets.

The theory of the strong interactions, quantum chromodynamics (QCD), has been shown to provide a very comprehensive and successful description of the strong force. However, despite its elegant form and few ingredients, predictions from it are difficult to obtain mathematically. Nonetheless, the distinctive behaviour of the interaction is well predicted: the strong force becomes weaker with smaller distances and stronger with increasing distances. This is in stark contrast with the electroweak and gravitational interactions, whose strength decreases with distance. According to Heisenberg's uncertainty principle, smaller distances are related to higher energies, and vice-versa, thus a measurement of energy dependence is equivalent to a measurement of distance dependence.

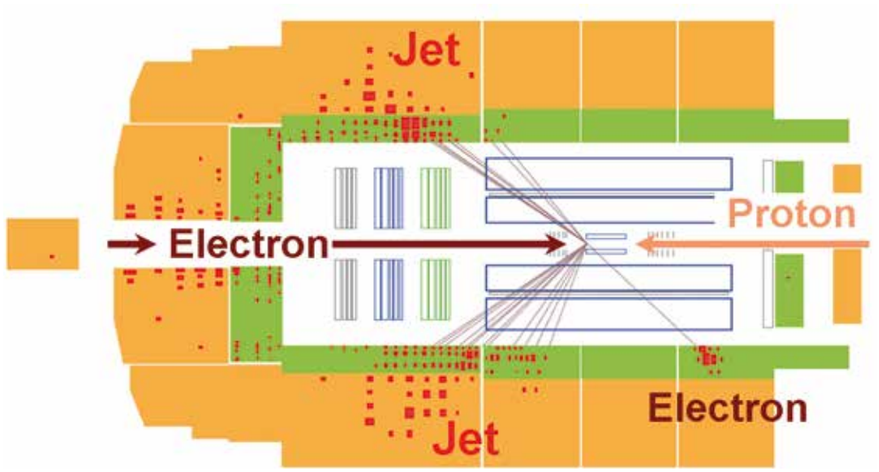

Figure 1
A proton entering the H1 detector from the right collides with an electron entering from the left. The scattered electron (going to the lower right) and two jets (going to the upper and lower left) can be seen. The trajectories of particles (straight lines) are reconstructed from the signals in the detector components.

To a suitably good approximation, the only parameter in QCD that can be determined from experiment is the so-called strong coupling constant, α_s, which gives the strength of the interaction at a given energy (i.e. the energy scale). The exciting questions in the field of strong-interaction physics involve the energy scale at which the processes mentioned above take place and the energy dependence of the strong force. Particularly interesting is the energy range between 5 and 100 GeV, which is ideally measurable at HERA. This region is important since it allows a check of QCD at an energy where the strong force has a large energy dependence while QCD is still able to make precise predictions. At lower energies, the theoretical calculations become intractable, while at higher energies, the energy dependence is reduced to the point that further theoretical challenges would need to be overcome before a meaningful comparison could be made.

The H1 collaboration has now profited from the large amount of data taken in the years 2003 to 2007. The data with exactly one observed jet was employed to obtain a very precise calibration (about 1%) of the H1 detector for the measurement of jet energies. The distributions of the numbers of jets as a function of jet energy were then derived for events with one, two and three jets using improved analysis techniques, and the energy dependence of the coupling strength was determined by comparing the measured points with the theoretical predictions obtained from QCD. The value of the strong coupling constant, $\alpha_s(\mu_r)$, where μ_r is the energy scale of the measurement in GeV, was then inferred for each of five measured points by a statistical technique that compares the QCD prediction to the measurement. Figure 2 shows a comparison of the values obtained to the QCD prediction as well as to other jet-based measurements at similar and higher energies. The energy dependence of α_s predicted by QCD is well reproduced by the data. Given this consistency, the theory can be used to extrapolate all measured points to a common energy scale. The lower part of Fig. 2 shows the value of α_s at the energy scale of the Z boson mass, M_z = 91.2 GeV, as inferred separately for each data point. Finally, the five new data points were combined (as indicated by the blue bands) to give the most precise value of $\alpha_s(M_z)$ yet achieved by a jet-based measurement – four times more precise than the current theoretical prediction.

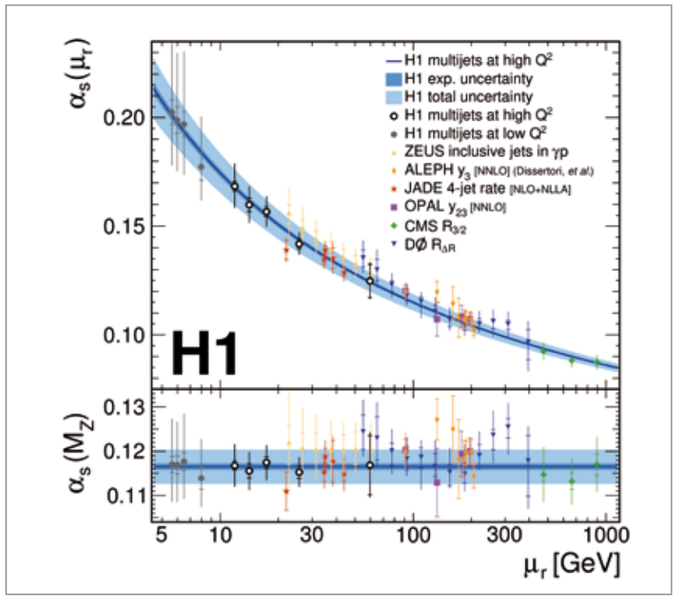

Figure 2
Measurements of the strong coupling constant at different energies from various experiments. The H1 measurements (open circles) are the experimentally most precise values.

Contact:
Daniel Britzger, daniel.britzger@desy.de
Stefan Schmitt, stefan.schmitt@desy.de

References:

H1 Collaboration, Eur. Phys. J. C75 (2015) 2, 65 [arXiv:1406.4709]

Running masses.

The scale dependence of beauty and charm

In particle physics, the strengths of the fundamental interactions depend on the energy scale at which they are evaluated. Thus, quantities like the fine structure "constant" α and the strong coupling "constant" α_s are actually logarithmic functions of the energy scale at which they are evaluated. They are said to be "running" with this scale. Such running behaviour should also apply to other physical parameters such as the quark masses, although details vary among the available theoretical schemes. The running of the mass of the beauty (bottom) quark has now been confirmed experimentally by an analysis of electron–proton collision data from DESY's former HERA collider, and observed for the first time for the charm quark. The observations are in good agreement with theoretical expectations.

The running of the strong coupling constant α_s, discussed in the previous contribution, is well established in the framework of quantum chromodynamics (QCD). It is measured from many different processes, including final-state jet production (jets are bundles of particles emerging from an original final-state quark or gluon) in electron–proton collisions at HERA and in proton–proton collisions at the LHC collider at CERN. Although the HERA experiments stopped taking data in 2007, the corresponding results are still being improved and remain competitive.

In addition to inclusive final states, the HERA experiments can study specific final states, such as those containing heavy quarks. The ZEUS collaboration recently published the most precise measurement of beauty quark production in deep-inelastic electron–proton scattering so far (Fig. 1). This result has been used to extract the value of the running mass of the beauty quark in the so-called $\overline{\text{MS}}$ scheme, in which the running mass is conventionally evaluated at the energy scale of the mass itself, $m_b(m_b)$ = 4.07 ± 0.17 GeV. The measurement is in very good agreement with the world average, $m_b(m_b)$ = 4.18 ± 0.03 GeV.

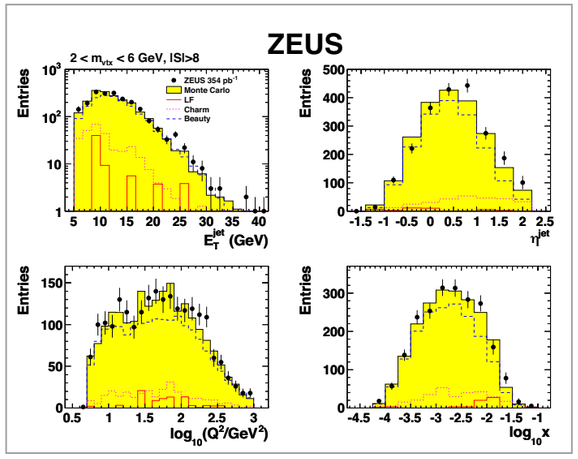

Figure 1

Measurements of the event properties of ZEUS events containing beauty quarks. The data (points) are compared to Monte Carlo predictions (histograms).

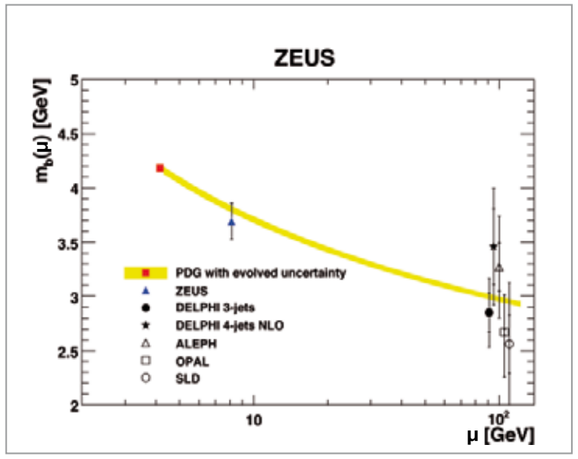

Figure 2

Measurement of the beauty quark mass from ZEUS (blue triangle) in the $\overline{\text{MS}}$ scheme compared to measurements at the *Z* boson scale from the electron–positron collider LEP at CERN (open and closed black symbols) and to theoretical predictions of the running mass (yellow band) normalised to the PDG world average (red point) measured at low scales. The plot clearly demonstrates beauty quark mass running.

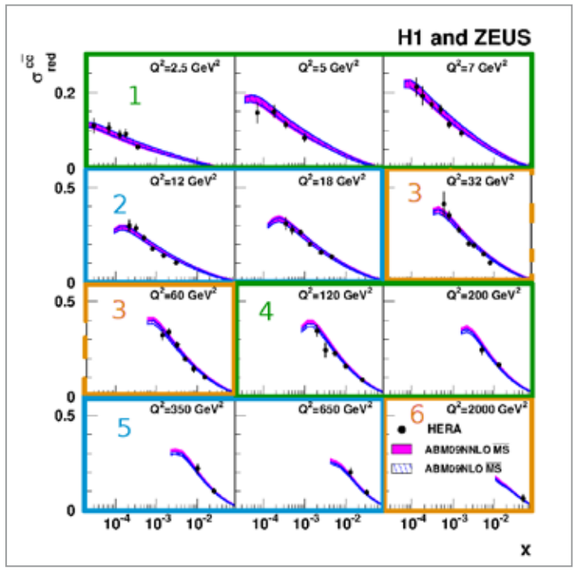

Figure 3

Summary of the combined reduced charm cross section measurements by H1 and ZEUS (points) and comparison to QCD theory (bands). The subdivision into different kinematic regions is indicated by the boxes.

This is the first such measurement from HERA data. Despite the larger uncertainty, it is very relevant, since it was obtained from data at a scale somewhat larger than most of the data entering the world average, and only rescaled to it for comparison.

Figure 2 shows this measurement (blue point), translated back to the scale $2m_b$ ~ 8.2 GeV at which it was actually performed. The scale is two times the beauty quark mass since, at HERA, beauty quarks and antiquarks are produced in pairs by strong interactions. Also shown in Fig. 2 are comparisons to earlier measurements from electron–positron collisions at the former LEP collider at CERN at the higher scale of the mass of the electroweak *Z* boson, and to low-scale evaluations mainly from lattice gauge theory calculations by the Particle Data Group (PDG). The running is clearly visible and agrees well with theoretical expectations (yellow band).

A similar measurement of the charm quark mass had already been performed by the H1 and ZEUS collaborations from a combination of several HERA charm data sets, resulting in $m_c(m_c)$ = 1.26 ± 0.06 GeV, which again is in good agreement with the world average: $m_c(m_c)$ = 1.275 ± 0.025 GeV.

Since charm quarks are produced more copiously than beauty quarks, even subsets of these data still have enough sensitivity to constrain the mass. Accordingly, this measurement was recently refined: the charm quark mass was determined in each of six different regions of the QCD scale shown in Fig. 3.

The result is shown in Fig. 4. The running of the charm mass, explicitly observed in this measurement for the first time ever, is in good agreement with expectations from the theoretical prediction normalised to the extraction of the charm mass at low scales, as in the case of the beauty quark.

In summary, the running of the beauty quark and charm quark masses has been confirmed experimentally at HERA, in agreement with QCD expectations.

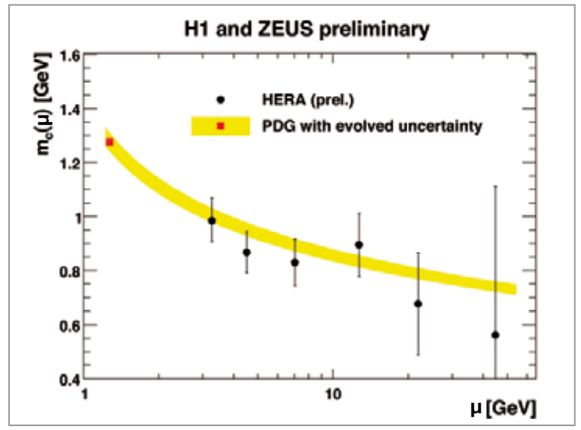

Figure 4

Measurement of the charm quark mass in the $\overline{\text{MS}}$ scheme as function of the probed energy scales. The plot explicitly demonstrates, for the first time, the running of the charm quark mass.

Contact:
Achim Geiser, achim.geiser@desy.de
Katerina Lipka, katerina.lipka@desy.de

References:

ZEUS Collaboration, DESY-14-083
H1 and ZEUS Collaborations and S. Moch, H1-prelim-14-071, ZEUS-prel-14-006

Left, right, up or down?

Inclusive hadron production in lepton scattering from transversely polarised and unpolarised targets

Transverse proton polarisation in lepton–proton scattering breaks the rotational symmetry about the collision axis. Inclusively produced hadrons may then possess a preference in the momentum direction with respect to the polarisation vector of the proton spin. Such preference has been examined for charged pions and kaons at the HERMES experiment at DESY's former HERA collider. Transverse single-spin asymmetry in inclusive hadron leptoproduction can also be studied by final-state polarimetry in unpolarised lepton–nucleon scattering. HERMES has measured the transverse polarisation of Λ hyperons produced on various nuclear targets.

Transverse-spin asymmetries

One of the fundamental properties of particles is spin, their intrinsic angular momentum. A natural question then arising in high-energy physics is whether or not the polarisation of colliding particles has a significant influence on the particles emerging from the collision. For longitudinal polarisation (along the momentum direction of the colliding particles), such spin dependence has indeed been a tool to investigate, also at HERMES, how the spins of the inner constituents contribute to the spin of the proton. In the case of transverse polarisation, the situation is more complex. One of the rather intriguing phenomena in high-energy scattering is the occurrence of transverse single-spin asymmetries. For the last four decades, they have been challenging the understanding of quantum chromodynamics (QCD), the part of the Standard Model of particle physics that describes the strong interaction between quarks and gluons. The prediction from perturbative QCD is that any asymmetry depending on the transverse polarisation of only one hadron involved (either in the initial or final state) should be negligible. However, experimental results did not comply. Already in the 1970s, surprisingly large transverse polarisations of up to 50% were observed in the production of hyperons in the collision of unpolarised hadrons. Moreover, when involving transverse polarisation in the initial state, the produced hadrons had a strong preference for going either to the left or to the right of the proton spin: up to three times more pions were going to one side over the other.

Theorists started to include novel effects that correlate the parton and/or nucleon spin with the transverse momentum of the partons, going beyond the traditional collinear picture in the description of hadron structure in highly energetic collisions. These transverse-momentum-dependent parton distributions were first demonstrated in the observation of the Sivers and Collins effects in semi-inclusive deep-inelastic scattering (DIS) at HERMES. However, despite tremendous progress in this rich field of transverse-spin effects, the large asymmetries observed in hadron collisions (processes much more complex than lepton–nucleon scattering) still give rise to more questions than answers. It is also for that reason that the HERMES collaboration used its unprecedented data set on lepton scattering from transversely polarised protons to look at inclusively produced hadrons and to check whether they prefer to go to the left or right of the spin vector of the proton, if exhibiting any preference at all. In the same spirit, HERMES studied Λ hyperons produced in unpolarised lepton–nucleus scattering to see whether or not they come out of the interaction with a preferred spin alignment.

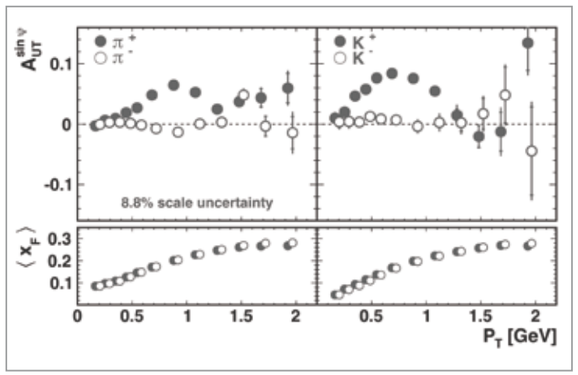

Figure 1

Pion (left) and kaon (right) azimuthal asymmetries in inclusive leptoproduction from transversely polarised protons as a function of the hadron transverse momentum with respect to the lepton beam direction. In the bottom panels, the average value for the Feynman variable, x_F, is given for each bin in P_T.

Inclusive hadron production in lepton–nucleon scattering covers several kinematic regions. Without information on the scattered lepton, two variables are used to characterise the process: the transverse momentum of the hadron with respect to the lepton beam direction, and the Feynman variable, calculated in the lepton–nucleon centre-of-mass system. At low values of transverse momentum, the cross section is dominated by quasi-real photoproduction. At larger values, the virtuality of the photon exchanged between lepton and proton becomes large as well, thus entering the kinematic region of DIS.

Inclusive hadron production at HERMES

The analysis of the data set on transversely polarised protons was carried out by fitting a sine function to the distribution of the hadrons produced around the lepton beam direction with respect to the polarisation vector of the nucleon. Charged pions and kaons were identified using a ring-imaging Cherenkov detector. The resulting sine amplitudes are presented in Fig. 1 as a function of the transverse momentum of the hadron. Significantly positive asymmetries are observed for positive pions and kaons, i.e. they clearly prefer to go to the right of the proton spin vector as viewed by the incoming lepton. The asymmetries exhibit a particular dependence on the transverse momentum: They first rise with increasing transverse momentum and turn over at around 0.8 GeV. At larger transverse momenta, the pion asymmetry rises again. In contrast, the asymmetries for negative pions and kaons are much smaller, mostly consistent with zero. This flavour behaviour is somewhat reminiscent of the Sivers asymmetries in semi-inclusive DIS at HERMES and might give a hint on the underlying mechanism of these asymmetries in inclusive hadron production.

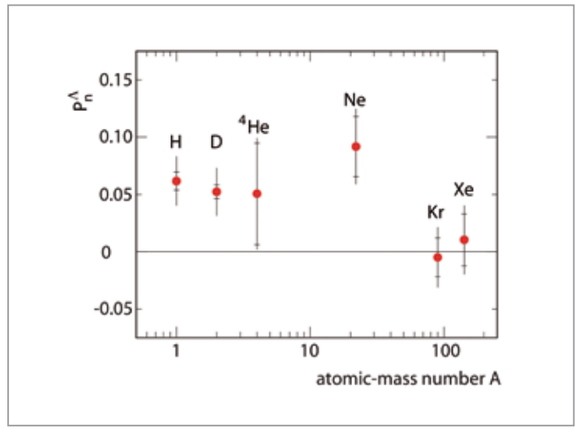

Figure 2

Dependence of the transverse polarisation of Λ hyperons produced in inclusive leptoproduction from nuclei on the atomic-mass number

Turning to unpolarised initial states, transverse single-spin asymmetries require experimentally challenging polarimetry in the final state. Fortunately, nature has provided a tool: the parity-violating weak decay of hyperons. In the decay of Λ hyperons into protons and pions, the proton prefers to go along the direction of the spin vector of the parent Λ (when seen in the rest frame of the Λ hyperon). This has been exploited at HERMES by looking at the decay angular distribution of Λ hyperons produced in lepton–nucleus collisions. Symmetry arguments dictate that any potential polarisation must be orthogonal to both the momentum of the incoming lepton and of the produced Λ hyperon. In other words, if in the laboratory frame the Λ hyperon goes in the horizontal direction, then the polarisation can only be in the vertical one.

Thanks to the versatile target gas storage cell internal to the HERA lepton ring, HERMES was able to measure the transverse polarisation of Λ hyperons for a set of nuclear targets, ranging from the light hydrogen or deuterium to the rather heavy krypton and xenon. The results are shown in Fig. 2, where the average transverse polarisation is presented as a function of the atomic-mass number. For light nuclei, a positive transverse polarisation is observed: When the Λ hyperon is produced to the left (as seen by the lepton beam), its spin vector preferentially points up – and down when the Λ goes to the right. For very heavy targets, the polarisation is consistent with zero.

These results on single-spin asymmetries in inclusive leptoproduction of hadrons serve as important input to understanding the multidimensional partonic structure of the nucleon, and to building models of the underlying processes in hadron–hadron collision. These might eventually explain the decades-old puzzles of large hyperon polarisations in unpolarised hadron collisions and left–right asymmetries in the inclusive production of hadrons from transversely polarised protons.

Contact:
Gunar Schnell, gunar.schnell@desy.de

References:

HERMES Collaboration, Transverse target single-spin asymmetry in inclusive electro-production of charged pions and kaons, Phys. Lett. B728 (2014) 183
HERMES Collaboration, Transverse polarization of Lambda hyperons from quasireal photoproduction on nuclei, Phys. Rev. D90 (2014) 072007

Proton–proton physics.

Since 2006, the DESY ATLAS and CMS groups have been strongly involved in the ATLAS and CMS experiments at the Large Hadron Collider (LHC) at CERN. The DESY groups contribute to the maintenance and operation of existing subsystems, the construction of new detector elements, the analysis of the data samples and the preparation of final results for publication.

The most striking result of the LHC to date is the discovery of the Higgs boson in 2012, to which both DESY groups contributed. They are now exploring its experimental ramifications and refining the measurements of the properties of the newly discovered boson (“Higgs boson under scrutiny”, p. 30). The enormous expertise on the inner structure of the proton and tests of quantum chromodynamics (QCD) that DESY physicists developed during the HERA years is now being brought to bear on the LHC data, which is reflected in several articles in this report: “QCD at the LHC” (p. 36) describes studies of the quark sea in the proton and the analysis of little-studied QCD processes. The HERAFitter project (“HERAFitter – an open-source QCD fit project”, p. 41) has its origins in the HERA community, but the multifunctional software tool, which is used to combine arbitrary data sets (for example from HERA and the LHC) that contain information bearing on the structure of the proton, is now widely employed at the LHC. And the international PROSA collaboration tries to advance the knowledge of the proton structure using data from all available sources by producing the phenomenological tools needed to combine the data sources coherently – for example, recent data from the ATLAS, CMS and LHCb experiments (“Proton anatomy”, p. 40). In addition, the ATLAS and CMS groups at DESY are focusing on rigorous tests of QCD predictions by studying the properties of the jets that are often produced along with a top quark pair (“Confronting QCD with top quark production at the LHC”, p. 38).

Producing such exciting results requires, of course, a detector that is capable of operating in the increasingly extreme conditions produced by the LHC, particularly in the High-Luminosity LHC (HL-LHC) era starting in 2025. Both DESY groups are strongly involved in ongoing upgrades of the detectors and in the design and preparation of entirely new detector subsystems needed for the HL-LHC (“FTK – a fast tracker for the ATLAS trigger”, p. 34, and “Preparing for the HL-LHC”, p. 32).

Higgs boson under scrutiny.

Higgs boson looks much like its Standard Model blueprint

Following their discovery of a Higgs boson in July 2012, the physicists of the ATLAS and CMS collaborations have reworked the complete data sets from their powerful multipurpose detectors at CERN's Large Hadron Collider (LHC) and investigated the observed state in full detail. Comprehensive studies address a wide spectrum of production and decay modes of the new boson with ultimate precision. The legacy analyses based on the full LHC Run 1 data set indicate that the new particle is, at the level of the current data set, compatible with the Standard Model Higgs boson.

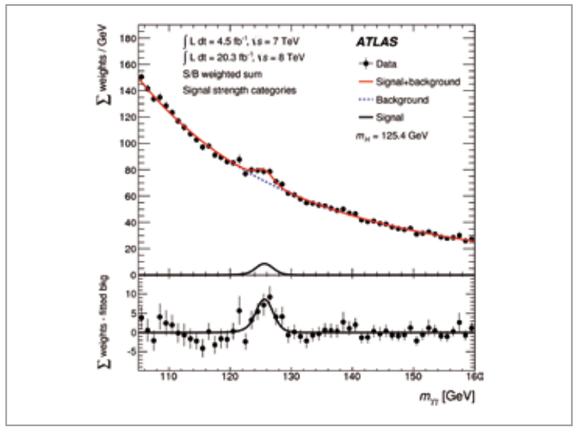

Figure 1

Distribution of the di-photon invariant mass in the ATLAS analysis of the $H \to \gamma\gamma$ channel. The clear peak at a mass close to 125 GeV indicates the Higgs boson signal.

Since the discovery of the new Higgs particle at a mass of 125 GeV, measurements of the properties of the observed state have been essential to establishing its role in the mechanism of electroweak symmetry breaking. Since 2013, the physicists have pushed hard to squeeze every little bit of performance out of the analyses and achieved Run 1 legacy results that are fit for the textbooks. The mass, spin and parity of the new boson as well as its couplings to fermions and gauge bosons and the fiducial and differential cross sections have been measured by the ATLAS and CMS collaborations in a large variety of production and decay channels using the full LHC Run 1 data set.

Improving the performance

Thanks to excellent mass resolution and well-controlled background, the Higgs boson decay into a pair of photons is a showcase channel for the particle's detection and the measurement of its mass and production properties. Recently, the ATLAS scientists have further improved their photon energy resolution by 10% with a refined calibration and reduced the experimental uncertainties on the photon energy scale and resolution as well as on the photon identification.

The selection of the $H \to \gamma\gamma$ events has been meticulously optimised for the characteristics of different production mechanisms, including the fusion of two gluons (ggF), the fusion of two vector bosons (VBF), the production accompanied by vector bosons (ZH and WH), and finally the associated production with a pair of top quarks ($t\bar{t}H$). This results in a considerably improved analysis sensitivity.

The signal strength μ indicates the measured production rate in comparison to the value predicted in the Standard Model (SM). In the new analysis, the signal in the di-photon channel is observed with a local significance of 5.2 standard deviations (σ), in good agreement with the expectation of 4.6 σ. This is illustrated in Fig. 1, which shows the di-photon mass spectrum with a clear signal peak at a mass near 125 GeV over the moderate background. The measurement of the signal strength combining all production modes in the di-photon channel yields $\mu = 1.17 \pm 0.27$, in excellent agreement with the theoretical expectation of $\mu = 1$. Figure 2 shows the results of the first ATLAS measurements of the signal strengths in the various Higgs boson production modes, which are a fingerprint of a true Higgs boson. All of them are consistent with unity within the experimental errors, which indicates perfect agreement with the theoretical predictions.

Combining the channels

A very comprehensive picture of the Higgs boson parameters emerges when measurements performed in various production and decay modes are combined. The CMS collaboration recently completed the final analysis of the Higgs boson properties using all the Run 1 data. These measurements combine three bosonic ($H \to \gamma\gamma$, WW, ZZ) and three fermionic ($H \to bb$, $\tau\tau$, $\mu\mu$) decay modes. The signal has been established in each bosonic decay mode with a statistical significance of ~5 σ or better. The precision of the measurements is further enhanced by performing a statistical combination of the analyses carried out in the individual channels. The Higgs boson mass is determined by combining the di-photon ($H \to \gamma\gamma$) and four-lepton ($H \to ZZ$) channels, resulting in a measured value of 125.0 ± 0.3 GeV. The quantum numbers of the Higgs boson are accessed through the study of the kinematical properties of the leptons emerging in the $H \to ZZ$ and $H \to WW$ decays. The results show preference for the hypothesis of a scalar boson with a positive parity (0^+) as expected in the SM, while alternative spin parity assignments (0^-, $1^\pm$, $2^\pm$) are strongly disfavoured by the data.

Disentangling the couplings

Measurements of the Higgs boson couplings to the SM particles are the crucial test of the Higgs mechanism, which aims to explain the generation of particle masses. In each measurement channel, couplings of the Higgs boson appear both in its production and decay. The combination of the different production and decay channels allows the various couplings to be disentangled. A key property of the Higgs boson is the relation of its "Yukawa couplings" to fermions and its "gauge couplings" to vector bosons. As shown in Fig. 3, these couplings can already be narrowed down quite well and are found to agree with the SM prediction. According to the Higgs mechanism, the Yukawa couplings are proportional to the fermion masses, while gauge couplings are proportional to the square of the weak-boson masses. The verification of this coupling–mass relation, ranging from muons to top quarks, is shown in Fig. 4. The $H \to \tau\tau$ decay mode, which has recently been established with an evidence of more than 3 σ significance, is pivotal in testing this relation. The measurements are found to be in good agreement with the expectation for the SM Higgs boson.

Towards Run 2: precision Higgs physics at the LHC

While the Run 1 legacy Higgs measurements show perfect agreement with the SM predictions, it is by far not excluded that the observed state is only the first visible member of an extended Higgs sector, as predicted by numerous theories of physics beyond the SM. The search for – possibly small – deviations of the properties from the SM predictions is therefore of utmost importance for probing new physics. The higher centre-of-mass energy (13 and 14 TeV) along with the higher luminosity expected in Run 2 will open new opportunities for probing new physics and significantly improve the precision of measurements of Higgs properties.

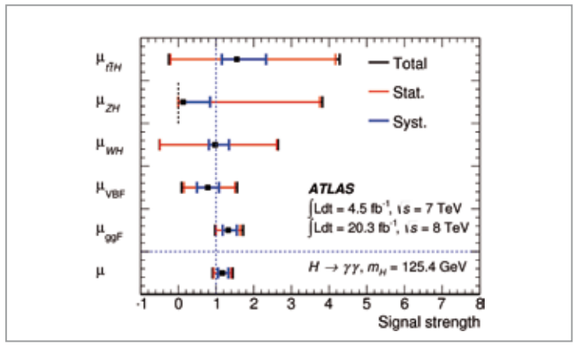

Figure 2

Values of the signal strength μ for various Higgs boson production modes, measured by ATLAS in the $H \to \gamma\gamma$ decay channel

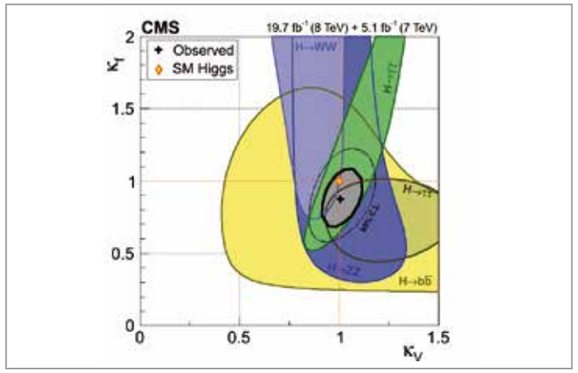

Figure 3

Scan of the fermionic and vector couplings of the Higgs boson relative to the Standard Model values

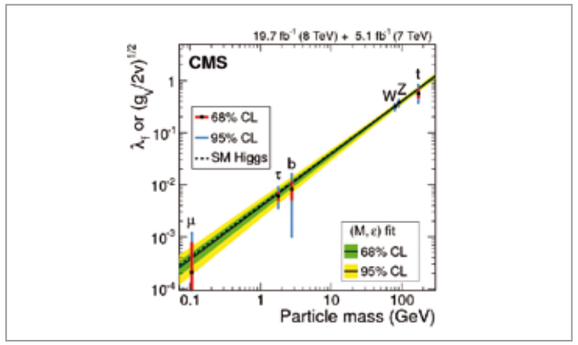

Figure 4

Coupling–mass relation as predicted for the SM Higgs boson, compared to the CMS measurements

Contact:

Yanping Huang, yanping.huang@desy.de
Rainer Mankel, rainer.mankel@desy.de
Alexei Raspereza, alexei.raspereza@desy.de
Kerstin Tackmann, kerstin.tackmann@desy.de

References:

ATLAS Collaboration, Phys. Rev. D 90 112015 (2014)
CMS Collaboration, arXiv:1412.8662

Preparing for the HL-LHC.

ATLAS and CMS upgrades for high-luminosity operation

After a highly successful first data-taking run, the Large Hadron Collider (LHC) paused in 2014 for an ambitious upgrade, which will allow particles to collide at the unprecedented centre-of-mass energy of 13 TeV. Operation will resume in 2015 with the collection of a data sample that will have grown to more than ten times the size of the present sample by 2022, when the LHC stops operation. In parallel, the experiments are laying the groundwork for the detector upgrades needed for the higher-luminosity version of the LHC, the High-Luminosity LHC (HL-LHC), which will start operation in 2025. DESY is engaged in the upgrades of the silicon-sensor-based detectors of both of the major experiments (ATLAS and CMS) and plans to construct large-scale components of them at DESY.

ATLAS tracker end-cap

The DESY ATLAS group has a leading role in the consortium of German and international institutes who are planning the design and construction of the end-cap regions of the future HL-LHC tracker. Each end-cap will consist of seven 2 m diameter disks, each with 32 wedge-shaped carbon fibre support and cooling structures equipped with silicon strip modules, readout, and control and power electronics on both sides (so-called petals). The DESY ATLAS group is involved in all steps of the design and plans to construct one of the two end-caps. Present and future activities include the module assembly and prototyping, the development of petal cores, the mounting of modules onto petals, the design and construction of macro-structures, and the assembly of petals into the end-cap structure.

At present, the group is focusing on the design, construction and operation of petal prototypes, both electrical and mechanical. Initial prototype objects ("petalets") have recently been manufactured and are being tested at DESY (Fig. 1). The petalets are smaller versions of the full-scale petals, with just three silicon sensors per side, mounted on a carbon fibre support structure with integrated cooling. The DESY ATLAS group contributed significantly to the design of the petalets and assembled numerous silicon modules and support structures, which are providing valuable input for the final petal design and construction.

The next step is the development of full-sized petal prototypes (Fig. 2). A carbon-fibre-based petal core is being built at DESY and will soon be distributed to the collaboration. Full-scale thermo-mechanical objects are being designed and will be manufactured in the coming months. They consist of core structures, comprising close-to-final cooling and structural components, which are populated with electrically inert components with representative thermo-mechanical properties to allow the study of mechanical and thermal properties. Once the petal design is finalised and the electrical components are manufactured, fully functional petal prototypes will be assembled and tested.

Figure 1

Fully functional "petalet" – a smaller prototype of an ATLAS end-cap petal

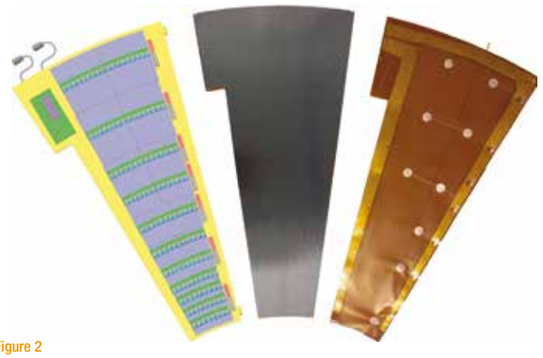

Figure 2

Left: 3D model of the fully equipped ATLAS petal with silicon sensors and electronics components. Centre: Carbon fibre support structure. Right: Electrical bus tape.

CMS end-cap prototype

The future CMS tracking detector will comprise a pixel system and an outer tracker based on silicon strips. The outer tracker will consist of barrel-shaped structures surrounding the inter-action region and disk-shaped structures – the end-caps – on both sides along the beamline. Two types of detector modules based on silicon sensors will be used: a strip-strip (2S) and a pixel-strip (PS) module. Both are capable of delivering trigger information to the level-1 trigger. The DESY group is one of the key partners in the team developing the detector modules and support structures for the future tracker. Together with German university groups, the DESY group plans to build and integrate one of the outer track end-caps, consisting of five double-disks with a diameter of 2.4 m and a length of 1.5 m. For better handling, disks are split into half-disks. Each half-disk is equipped with modules on both sides. The half-disk is a highly integrated support structure with embedded cooling pipes, routed in overlapping sectors, and positioning elements for both module types. Figure 3 shows a CAD model of an end-cap equipped with modules.

The DESY CMS group is now building a small-scale prototype structure that includes all features of a full-sized half-disk. Figure 4 shows a CAD model of the prototype with a light-weight foam core (1), carbon fibre facings (2), two overlapping cooling sectors (3), inserts for cooling and positioning of 2S modules (4), and positioning pins (5) and cooling blocks (6) for PS modules. The region of the prototype labelled (7) shows the overlap with the sibling half-disk.

The two prototype structures will be available for testing by mid-2015. The final design of the end-cap support structures will greatly benefit from the experience gained from their production and tests of their thermal and mechanical properties.

Detector assembly hall

Drawing from the experience of detector construction at DESY and other institutes, an estimated 600 m² of lab space, including 250 m² of cleanroom area, will be required for the production and quality control of the components of the ATLAS and CMS tracker end-caps. An additional space of 200 m² with crane access will be needed for the final assembly, integration and testing. Several options are being considered, including the refurbishment of a hall at DESY's former DORIS accelerator. In parallel, the cleanroom area and required infrastructure are being designed.

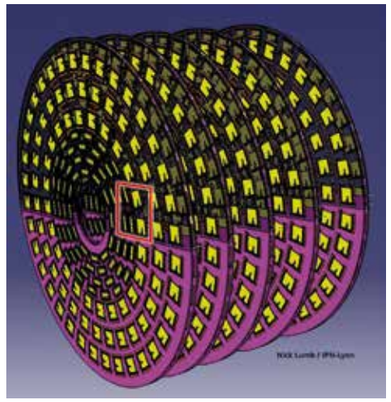

Figure 3

CAD model of one CMS end-cap

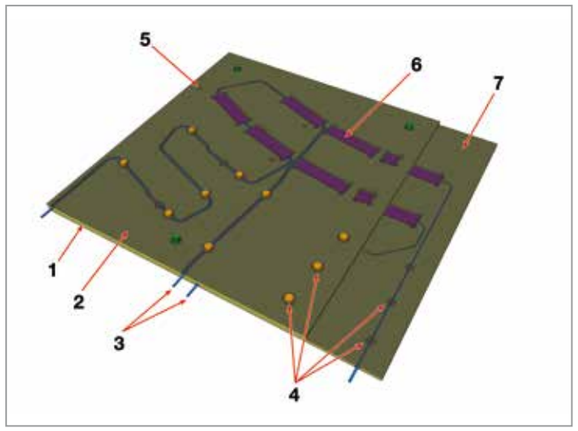

Figure 4

CAD model of the CMS end-cap small-scale prototype

Contact:
Ingo Bloch, ingo.bloch@desy.de
Ingrid Gregor, ingrid.gregor@desy.de
Sergio Diez Cornell, sergio.diez.cornell@desy.de
Andreas Mussgiller, andreas.mussgiller@desy.de
Guenter Eckerlin, guenter.eckerlin@desy.de

FTK – a fast tracker for the ATLAS trigger.

Measuring thirty million particle trajectories per second

When the Large Hadron Collider (LHC) at CERN resumes operation in 2015, it will produce the highest-energy proton–proton collisions ever seen in a particle accelerator. Not only will the collision energy be increased, but the rate of interactions will have grown to the point where it will stretch the capabilities of current technology. The ATLAS detector will need new and innovative techniques for dealing with this phenomenal interaction rate whilst maintaining a high level of scientific precision. The fast tracker (FTK) is a new system designed to boost the capabilities of the ATLAS trigger system for rapidly selecting the most interesting events from a vast quantity of ordinary ones by exploiting the tracks left by charged particles in the ATLAS inner detector.

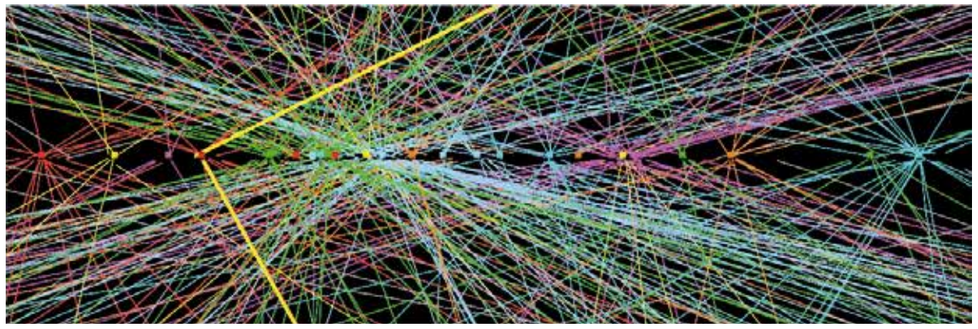

Figure 3
Tracks of one simulated event, extrapolated to the collision region, as viewed from the side, with the beams entering from the left and right

When beam particles collide in the centre of the ATLAS detector, new particles are created. The ATLAS detector, acting like a giant camera, takes pictures of them – in fact, millions of pictures per second. However, present computing and hardware limitations prevent recording all but a tiny fraction of them. Thus a trigger system, which plays a role analogous to a film editor deciding which frames are best, must be used to capture only the very tiny fraction of really interesting collisions, perhaps containing a Higgs boson or some exotic particle never before seen among the particles produced.

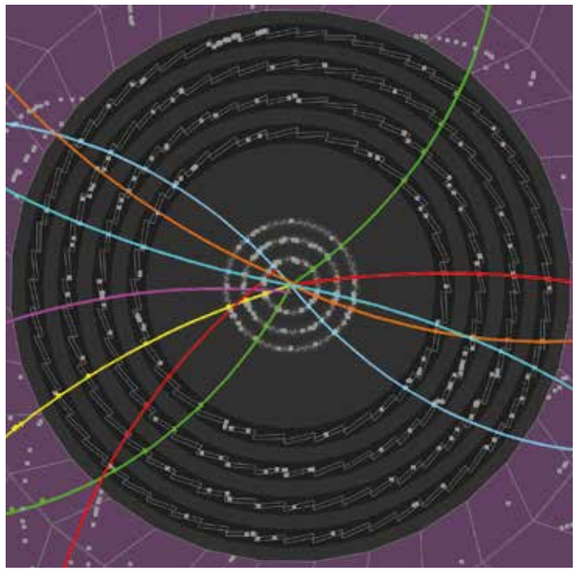

Figure 1
Event display showing the silicon layers of the ATLAS inner detector in its 2013 configuration as viewed from the beam direction. The beams run through the centre. The dark grey region shows the silicon detector, with another tracking detector (not used by the FTK) surrounding it. The individual silicon detectors, shown as grey rectangles, are arranged in seven concentric layers (an eigth layer has since been added). Hits are indicated by dots and reconstructed tracks by smooth curves.

The ATLAS trigger consists of three filtering levels, divided into electronics-based and software-based trigger systems. The first level (L1) uses dedicated electronics to skim off about one hundred thousand of the most interesting events from the 40 million events produced per second. The advantage of the hardware decision is that it is fast (taking less than 3 μs), albeit at the expense of an inherent crudeness compared to a software decision. The second (L2) and third (EF) levels, collectively called the high-level trigger (HLT), are both software-based and capable of making complex trigger decisions but at much lower rate (around 100 kHz). Following the HLT decision, selected events are written to a storage medium, at a rate of no more than 400 Hz.

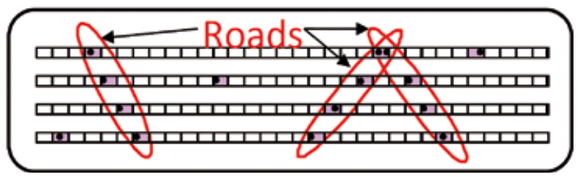

Figure 2
Roads and hits in four layers of the FTK system. The hits are shown in black and the roads in red.

The FTK is a new trigger system, now being commissioned, which will not actually make trigger decisions but will supply valuable information to L2 on all events triggered by L1, before the start of L2 processing. It will process information supplied by the first detector encountered by the particles produced in a collision as they leave their points of creation, namely the inner detector (ID). The ID, consisting of 12 silicon layers arranged in concentric layers like the skins of an onion, is among the most sophisticated and precise components of the ATLAS detector. As a charged particle traverses the ID layers, it leaves behind hits, which can be read out of the detector and further processed. An example is shown in Fig. 1. A typical event has hundreds of tracks, which make thousands of hits. A particle track can be inferred by selecting those hits that are consistent with having come from a single traversing particle. By eye, this appears to be an almost trivial job, thanks to the extraordinary image-processing capabilities of our visual cortices, but a computer or other electronic system has a much harder time of it.

Up to now, the trigger has been limited to using CPU-intensive algorithms running on the HLT trigger computers to reconstruct only a small subset of the tracks produced. In contrast, the FTK is intended to perform the reconstruction of all of the tracks of events triggered by L1 for use at L2 in dedicated custom-designed electronics. This will simultaneously provide the ability to use the complete track set when forming the L2 decision and to allow precious L2 CPU resources to be freed up for use by more refined trigger algorithms.

The FTK will make use of predefined patterns of hits corresponding to tracks stored in an associated memory (AM) system. With the help of the AM system, the FTK will simultaneously compare over one million patterns corresponding to simulated tracks to actual patterns from an event and select the combinations, called “roads”, corresponding to the stored hit patterns, as illustrated in Fig. 2. Once a road is found, the respective hits are used to calculate the track’s parameters. This process is repeated for all selected hit combinations. Figure 3 shows the tracks found in one simulated event extrapolated to the collision region. The tracks can be seen to have emanated from several distinct points corresponding to the individual collisions of two protons. The additional information on the number and positions of collision points is just one of several ways the FTK will contribute to making the L2 trigger decision more selective and precise.

The FTK is presently being commissioned in preparation for parasitic online operation of part of the system in July 2015. The full system will be deployed for operation by the end of 2018. The DESY ATLAS group contributes to the FTK project primarily by calculating the predefined patterns that will be loaded into the AM, by providing software to simulate the complex FTK hardware, by offering FTK-specific software support for the second-level trigger, and through system commissioning.

Contact:
Daniel Britzger, daniel.britzger@desy.de
James Howarth, jhowarth@cern.ch
Stefan Schmitt, stefan.schmitt@desy.de

QCD at the LHC.

Quarks and gluons under the microscope

The knowledge of parton density functions (PDFs) is a prerequisite for data interpretation at CERN's Large Hadron Collider (LHC). LHC data themselves are used to improve the precision of PDFs and to get further insights into details of parton–parton interactions.

LHC data improve constraints on light-quark distributions

The interpretation of most cross section measurements at the LHC relies on the precise knowledge of PDFs that give the probability to find a parton (quark or gluon) with a fraction x of the proton's longitudinal momentum at a given resolution scale. The scale dependence can be calculated in perturbative quantum chromodynamics (QCD), but the x dependence has to be determined from measurements.

Measurements of inclusive W boson or Z boson production are sensitive to the quark distributions inside the proton and are thus used to improve the constraints on parton densities. As an example, the precise measurement of the charge asymmetry in the production of positively or negatively charged W bosons, once included into the QCD analysis of the parton densities, helps to significantly reduce the uncertainty in the distributions of up valence and down valence quarks, as illustrated in Fig. 1 (left). On the other hand, the production of W bosons in association with charm quarks provides the first direct measurement of the strange-quark distribution in the proton obtained at a hadron collider. The results of the ATLAS and CMS experiments on W+charm production at a centre-of-mass energy of 7 TeV are used to determine the proton's strangeness content. While the ATLAS results indicate a somewhat larger strange-quark contribution to the proton light-quark sea than observed in earlier results from neutrino scattering experiments, the CMS result is consistent with the latter, as shown in Fig. 1 (right). In a joined QCD analysis [1] of data from neutrino scattering experiments and the LHC, this indication of a disagreement between the measurements by ATLAS and CMS is resolved.

New observations in Z+jet production

The description of the spectrum of small transverse momenta of Z or W bosons requires the knowledge of the transverse degrees of freedom of the interacting partons, and the transverse momentum of multiparton radiation must also be included. The spectrum of the transverse momentum, p_T, of muon pairs coming from the decay $Z \to \mu^+\mu^-$ in proton–proton collisions [2] is shown in Fig. 2 (left). The cross section is very small for small p_T and reaches a maximum at around 5 GeV. The rise of this spectrum is due to the transverse-momentum distribution of the interacting partons, described by multiparton radiation

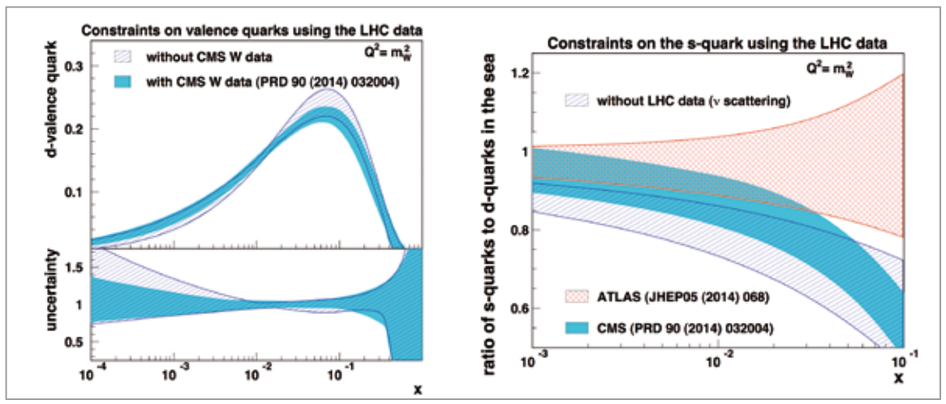

Figure 1
Constraints on down valence quark (left) and strange-quark (right) distributions, improved by using LHC measurements of W boson and associated W boson + charm-quark production

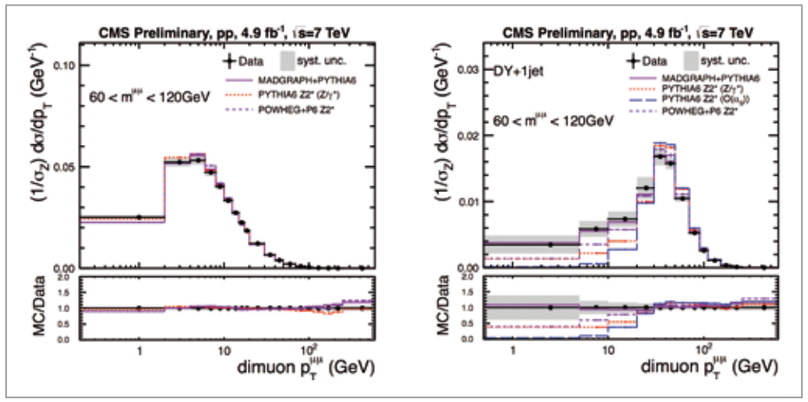

Figure 2
Transverse-momentum spectrum of muon pairs coming from Z decay, $Z \to \mu^+\mu^-$, for inclusive Z boson production (left) and in the presence of a jet (right)

(soft-gluon resummation) in terms of transverse-momentum-dependent PDFs or parton showers. The different theoretical predictions describe the measurement rather well.

A quite different behaviour is observed for muon pairs that are accompanied by a hadronic jet – a collimated flow of hadronic energy – with large transverse momentum, as shown in Fig. 2 (right). While at lowest order in the perturbative calculation of the Z+jet production cross section, a sharp step at the minimum transverse momentum of the jet is expected in the muon pair spectrum, the measurement shows a falling distribution towards small transverse momenta p_T of the muon pair. This behaviour can only occur if more than one jet is appearing in the final state (higher-order calculations). However, even a next-to-leading-order calculation of Z+2jet production – labelled "POWHEG" in Fig. 2 (right) – is not able to describe the measurement. Only a calculation ("MADGRAPH") involving up to four partons in the final state in addition to the muon pair is able to provide a reasonable description of the measurement. This observation is very interesting because it shows that the sensitivity of a quasi-inclusive measurement to higher-order contributions can go beyond what can be achieved by simple perturbative next-to-leading-order expansion.

New observations in multijet production

When the parton densities probed in a proton–proton collision become very large, the probability to observe more than one partonic scattering becomes observable. Such double-parton scattering (DPS) is not described in the standard calculations and needs a special treatment. DPS can be investigated by measuring four jets grouped into two pairs of di-jets with different transverse momenta [3]. If the pairs of di-jets originate from independent partonic interactions, the jet pairs are uncorrelated – this can be seen in the distribution of the azimuthal angle ΔS between the planes of the two di-jet pairs (Fig. 3) at low ΔS values. Simulations including contributions of DPS can describe the measurements, while a simulation without DPS is too low at small ΔS. This measurement shows for the first time the need of DPS in jet production at large transverse momenta in hadronic collisions.

Summary

Precise measurements at the LHC provide important constraints on PDFs, which to a large extent determine the accuracy of the Standard Model predictions for different processes in proton–proton collisions. New effects are observed in events with multiple jets. With the high-energy LHC run, QCD investigations will enter a new and exciting phase.

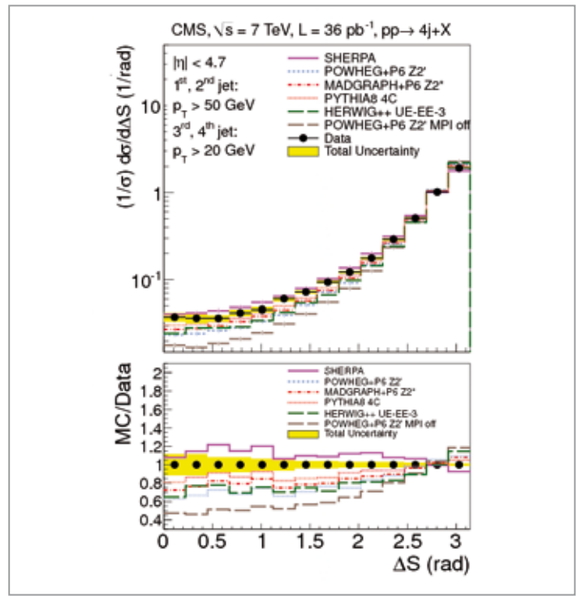

Figure 3
Azimuthal correlation of two pairs of di-jets in proton–proton collisions

Contact:
Hannes Jung, hannes.jung@desy.de
Katerina Lipka, katerina.lipka@desy.de

References:

[1] S. Alekhin et al., arXiv:1404.6469
[2] CMS Collaboration, CMS-FSQ-13-003 (2014)
[3] CMS Collaboration, Phys. Rev. D 89 092010 (2014)

Confronting QCD with top quark production at the LHC.

Measurements of top quark production are starting to constrain theory

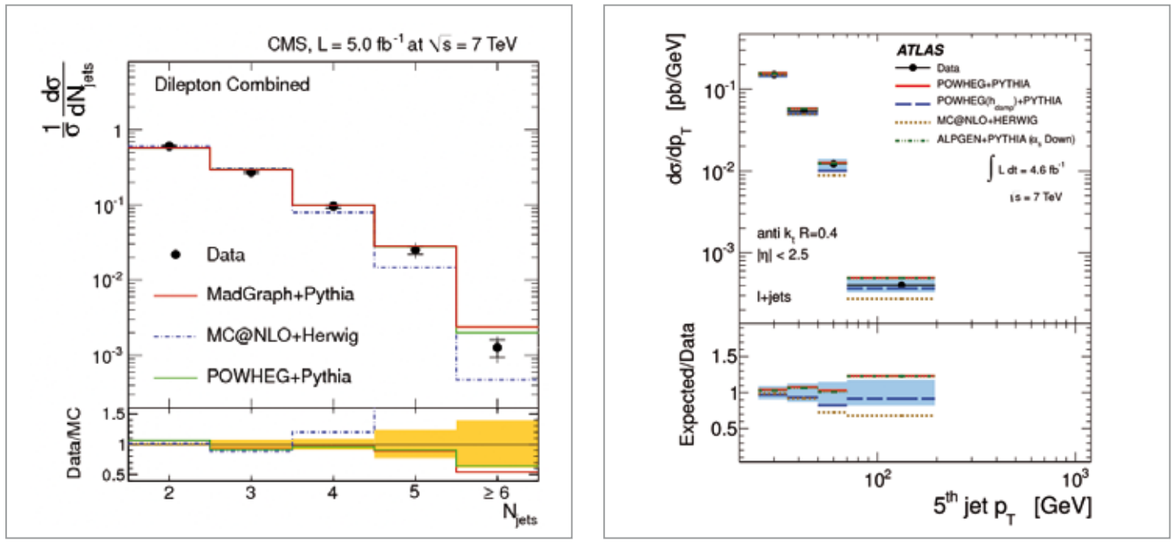

Figure 2

Differential cross section of top quark pair production at 7 TeV as a function of the jet multiplicity in the di-lepton channels (left) and of the first additional jet (right) in the single-lepton channel. The measurements are compared to different SM predictions.

During its first years of operation, the LHC at CERN proved to be a true top quark factory: a total of several million top quark pairs, 100 times more than were produced by the Tevatron collider at Fermilab in Chicago over its 20-year life span, were recorded. The precision of recent LHC measurements of top quark production now equals or even exceeds that of the theoretical calculations and thereby provides essential new information to theorists. Both the ATLAS and CMS groups at DESY have pioneered measurements of the additional high-momentum jets often produced in association with top quark pairs. These measurements are affording rigorous tests of perturbative quantum chromodynamics (QCD), as well as supplying essential information for the measurement of Higgs boson properties and for searches for phenomena not accounted for by the Standard Model, i.e. beyond the Standard Model (BSM) phenomena.

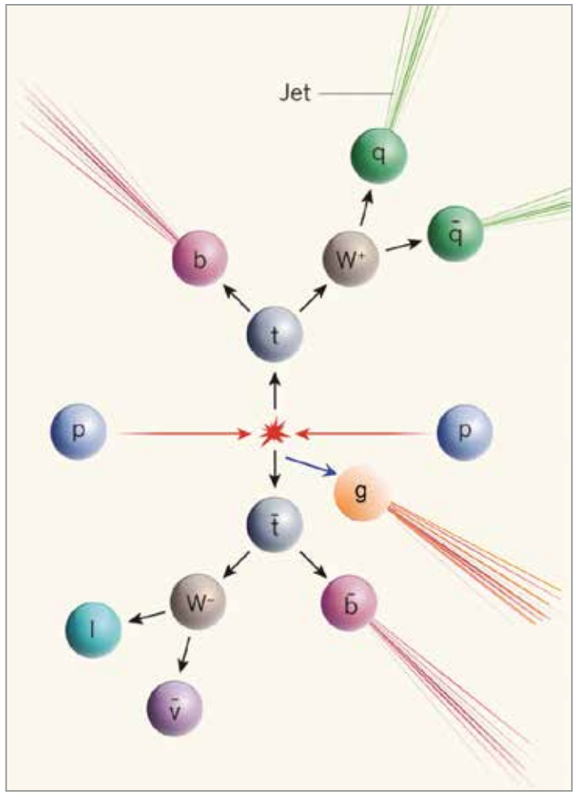

Figure 1

Top quark pair decay with an additional gluon jet (modified from Nature 514, 174–176 (09 October 2014) doi:10.1038/514174a)

Ever since its discovery at the Tevatron collider in 1995, the top quark has been a major research target for particle physicists. Due to its unique properties, in particular its mass (it is by far the heaviest quark known to-date), it serves as an essential testing ground of the Standard Model (SM) of particle physics and plays a key role in the measurement of Higgs boson properties. Moreover, many BSM scenarios expect the top quark to couple to as yet undiscovered particles whose existence might be revealed through measurements of top quark production.

The large data samples collected by the ATLAS and CMS experiments have provided a means to measure the top quark production process with sufficient precision to challenge the accuracy of the state-of-the-art SM theoretical predictions. In addition, stringent limits on the production rates and masses of several hypothetical particles predicted by various BSM models have been derived from them.

At the LHC, a top quark is usually produced along with a top antiquark (a top quark pair, for short). The top quark (antiquark) then decays immediately into a *W* boson and a bottom quark (antiquark), and the *W* boson then decays either into a lepton and a neutrino or into a quark–antiquark pair. For the purposes of analysis, the decay modes are classified according to the decays of the *W* bosons. The ATLAS and CMS groups at DESY focus on measurements in both the di-lepton channel, in which both *W* bosons decay into a lepton and a neutrino, and the single-lepton channel, in which one *W* boson decays into a lepton and a neutrino and the other into a quark–antiquark pair. The outgoing quarks are observed as collimated showers of particles in the detector, called jets. The production of a top quark pair and subsequent decay into the single-lepton channel is illustrated in Fig. 1.

Due in part to the high energy of the LHC, half of the top quark pair events are produced with additional high-momentum jets, which usually arise from radiation processes calculable in high-order perturbative QCD. These additional jets cannot be unambiguously associated with the top or initial-state quark from which they originate. This leads to measurement uncertainties that often limit the measurement precision of many quantities of interest, for example, of the top quark mass. Moreover, events with top quark pairs and additional jets give the largest contribution to the background plaguing the measurement of Higgs bosons produced in association with a top quark pair. This measurement, which will be performed on data collected in the upcoming LHC run, is of particular interest since it allows for the direct determination of the strength of the coupling of the Higgs boson to the top quark. Since the SM confidently predicts that the Higgs boson couples much more strongly to the top quark than to the other, lighter quarks, the measurement is a sensitive indicator of whether or not the boson discovered at the LHC is indeed the Higgs boson predicted by the SM or something even more interesting. Moreover, the signature of top quark pairs produced with additional jets is very similar to that expected by BSM particles since many jets as well as undetectable particles (which would mimic the neutrino from *W* decay) are often among their decay products.

While predictions of the inclusive top pair production cross sections have reached very high precision, the prediction of additional QCD radiation is difficult and significantly less precise. Several theoretical approaches that show significant differences in their predictions of the jet multiplicity distribution and the jet transverse-momentum spectrum are being explored. The ATLAS and CMS groups at DESY have tested these theoretical approaches by performing the first direct measurements of the jet multiplicity distribution and of the jet transverse-momentum spectrum in top quark pair production, as shown in Fig. 2. The measurements have reached sufficiently high precision to exclude some of the models. Furthermore, the results have been used to constrain the theoretical predictions and thereby to yield more precise measurements of the background to Higgs production and BSM particle searches and other interesting quantities and phenomena.

Contact:
Judith Katzy, judith.katzy@desy.de
Maria Aldaya, maria.aldaya@desy.de

References:

[1] CMS Collaboration, EPJ C74 3014 (2014)
[2] ATLAS Collaboration, arXiv:1407.0891 [hep-ex]

Proton anatomy.

Joint experimental and theoretical efforts

With the discovery of a Higgs boson in proton collisions at the LHC, the quest for new phenomena in particle physics enters a new era of precision. Uncertainties in the phenomenological description of proton–proton interactions will limit the LHC discovery potential in the upcoming high-energy run. These uncertainties arise from the very nature of the proton–proton collisions and challenge both theory and experiment. The work of the international collaboration Proton Structure Analyses in hadronic collisions (PROSA) is aimed at improving the understanding of the proton structure and the fundamental parameters of the Standard Model. In PROSA, experimental and theoretical efforts lead to the development of phenomenological tools and their immediate application in data analysis and interpretation.

The proton structure can be parameterised by universal parton distribution functions (PDFs), which depend on the fraction x of the proton momentum carried by a parton and on the energy scale Q of the process. The determination of PDFs requires both accurate theoretical calculations and measurements of various physics processes at different experiments, the core data in PDF determinations still stemming from DESY's former electron–proton collider HERA. The HERA measurements, however, do not cover the whole kinematic range of the LHC with sufficient precision. In particular, the uncertainties on the gluon distribution at very low and very high values of x need to be reduced in order to enhance the predictive power of the Standard Model and in turn the discovery potential of the LHC. Fortunately, numerous LHC measurements provide important constraints precisely in the kinematic regions not covered by HERA and can thus be used for proton structure determination. More specifically, at the LHC, heavy quarks (charm, beauty and top) as well as the Higgs boson are predominantly produced in gluon–gluon fusion – processes that are directly sensitive to the proton's gluon distribution.

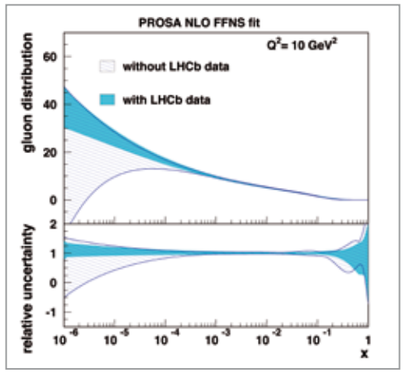

Figure 1

Gluon distribution (upper panel) and its relative uncertainty (lower panel), showing the improvement achieved by the use of LHCb data

Measurements of charm, beauty and top quark pair production at the LHC can therefore be used to probe and constrain the gluon distribution.

The production of charm and beauty hadrons at the LHCb experiment is particularly sensitive to the gluon distribution at very low values of x that are not covered by other experiments. In a recent PROSA QCD analysis at next-to-leading order [1], LHCb measurements of charm and beauty production were used together with HERA data. As a result, the uncertainty of the gluon distribution is significantly reduced at very low x, as demonstrated in Fig. 1. In particular, the uncertainty due to assumptions on the shape of the PDFs in x is strongly decreased.

At the other end of the energy scale, top quark pair production in the ATLAS and CMS experiments probes the gluon distribution in the high-x region, which is particularly important for stringent tests of Higgs production models and for searches for new physics. Different measurements of inclusive and differential cross sections of top quark pair production at the LHC were included in a QCD analysis at next-to-next-to-leading order. This analysis required dedicated phenomenology and tool development and was only possible within the PROSA framework. An improvement of the gluon accuracy at very high x is observed. A more significant reduction of the uncertainty is expected from the even more precise LHC measurements expected from the upcoming LHC run. For the first time, a simultaneous determination of the gluon distribution and the top quark mass becomes possible. The central analysis tool used to obtain these results is the QCD analysis platform HERAFitter.

Contact:

Katerina Lipka, katerina.lipka@desy.de

References:

[1] PROSA Collaboration, arXiv:1503.04581 [hep-ph]

[2] M. Guzzi, K. Lipka, S.-O. Moch, JHEP 1501 082 (2015)

HERAFitter – an open-source QCD fit project.

Unique framework for studying the impact of new data on the proton structure

In 2015, the LHC will resume operation at increased centre-of-mass energy and luminosity, posing new challenges for the understanding of the quark–gluon dynamics of the incoming proton beams. The precise knowledge of the proton's composition plays a dominant role for precision tests of the Standard Model (SM) and is also important for theory predictions for searches for new physics. The HERAFitter project, with its unique expertise in proton structure analysis, aims at providing tools for an improved understanding of SM parameters and scrupulous tests of precision SM measurements.

HERAFitter [1] is a rapidly developing open-source analysis framework for the determination of the parton distribution functions (PDFs) and other free parameters of the SM. Since its launch in September 2011, several versions of the HERAFitter software have been released, and an impressive number of results based on this platform were published. HERAFitter, which unites state-of-the-art theory calculations with an appropriate treatment of precision measurements, covers a large number of different methods used for PDF determination. The project is based at DESY, where the HERA legacy is preserved and two LHC experimental groups (ATLAS and CMS) are hosted, and it enjoys a strong support from the theory and IT expertise on site. The success and growth of the project are driven by the extensive demands from the LHC and HERA collaborations, as well as from the theory community and from individual interests in performing topical studies.

HERAFitter builds on the collaborative open-source paradigm and on active user feedback, and it has a dynamic release cycle. The recent HERAFitter developments had a significant impact on the interpretation of LHC Run 1 measurements, which in turn provide new important precision constraints on the proton structure. Prominent examples of recent HERAFitter publications are a combination of HERA data with the LHC W boson and Z boson measurements that provides a means to disentangle various quark contributions, or a measurement of W bosons produced in association with charm quarks. The latter measurement provides sensitivity to the least constrained quark, the strange quark. In addition, jet production has been studied with the aim of improving the gluon distribution. Moreover, the HERAFitter framework has been used to produce public grids of PDFs that can be used to study predictions for SM or new physics processes.

The HERAFitter developers take an active role in the analyses and interpretation of the LHC data. For example, ratios of di-boson to single-boson production cross sections σ_{WW}/σ_Z are sensitive to effects of physics beyond the SM. The

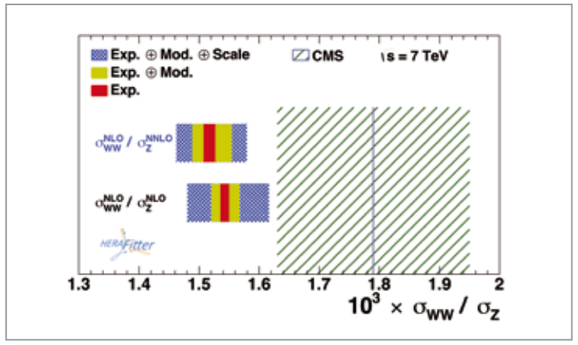

Figure 1

Ratio σ_{WW}/σ_Z calculated at NLO and NLO/NNLO, compared to the result obtained by the CMS collaboration

corresponding experimental data have an increased accuracy that must be matched by consistent theoretical calculations. For the latter, the HERAFitter developers introduced a novel method to determine correlated PDFs, suitable for calculations at different accuracy in perturbation theory [2]. These correlated PDFs are then used for the prediction of σ_{WW}/σ_Z cross section ratios and compared to the recent CMS data, as shown in Fig. 1. The new self-consistent treatment reduces the uncertainty of the theoretical predictions and exhibits a tension with the experimental data. New data from LHC Run 2 are thus eagerly awaited to clarify this seeming discrepancy.

Contact:

Alexandre Glazov (release coordinator), alexandre.glazov@desy.de

Hayk Pirumov (software librarian), hayk.pirumov@desy.de

Ringaile Placakyte (convener), ringaile.placakyte@desy.de

Voica Radescu (convener), voica.radescu@desy.de

References:

[1] "HERAFitter, open source QCD fit project", S. Alekhin et al., arXiv:1410.4412, submitted to Eur. Phys. J. C

[2] "Parton distribution functions at LO, NLO, and NNLO with correlated uncertainties between orders", P. Belov et al., Eur. Phys. J. C 74:3039 (2014)

Electron–positron physics.

Physics at electron–positron colliders – be they circular or linear – is an important cornerstone of DESY's particle physics strategy. At the SuperKEKB collider at KEK, the Japanese national laboratory for particle physics, the Belle II experiment will be commissioned in 2017, and DESY provides important contributions to the experiment ("Preparing for Belle II", p. 44).

At the same time, the efforts towards the next large-scale facility in particle physics, International Linear Collider (ILC), are acquiring more and more momentum. After the publication of the technical design report (TDR) in 2013 and the choice of a potential construction site, site-specific considerations ("Towards a site-specific ILC design", p. 46) and the series production of the cavities ("Cavities en masse", p. 48) are becoming increasingly important. In addition, DESY is participating in the detector designs, the planning of the positron source and the luminosity measurement ("Towards a calorimeter for the ILC", "Positrons non-stop for the ILC" and "Measuring luminosity", pp. 50, 52 and 53).

The article "Catching plasma-accelerated beams" (p. 54) sheds light on another important activity at DESY – the development of novel acceleration concepts for particle physics at the highest energies.

Preparing for Belle II.

Important steps towards the realisation of the project

SuperKEKB is a next-generation *B* factory that is currently under construction at the Japanese national particle physics laboratory KEK. At the same time, the former Belle detector is being upgraded to Belle II. Several German institutes form the core of the international DEPFET collaboration, which is in charge of developing and constructing the novel two-layer pixel detector (PXD) as the inner part of the Belle II vertex detector (VXD). Within the Belle II collaboration, DESY has assumed key responsibilities in the area of VXD integration and installation. The laboratory also contributes significantly to software development and computing as well as to the preparation of the physics analyses.

Project status

At KEK, the work on both the SuperKEKB electron–positron accelerator and the Belle II detector is progressing well. The very ambitious goal of this project is a 40-fold increase of the peak luminosity of SuperKEKB to a new world record of $8x10^{35}$ $cm^{-2}s^{-1}$, which will be achieved by employing the so-called nano-beam scheme. The construction of most machine elements of the main accelerator ring is approaching the final stage, and Phase 1 commissioning is expected to start at the beginning of 2016. This delay of about one year with respect to the original schedule is mainly caused by KEK budget restrictions. The goals of Phase 2 commissioning include first luminosity tuning and detailed studies of machine-induced backgrounds. This requires the completion of essential components of the accelerator complex, such as the damping ring and the superconducting final-focus magnets (QCS). The complex QCS magnets will provide the necessary focusing strength to squeeze both beams to the required beam spot size of about 50 nm in the vertical direction. According to the present schedule, these magnets will be installed in the beamline in the second half of 2016, together with the upgraded Belle II detector but still without the new vertex detector (VXD). Instead, the sophisticated background monitoring system BEAST II, which contains some VXD prototype sensors, will be installed.

The VXD consists of a two-layer pixel detector (PXD), which is currently being built by the international DEPFET collaboration, and a four-layer double-sided silicon strip detector (SVD). In order to avoid damage to these sensitive devices, the VXD will only be installed once the machine background is understood sufficiently well with the help of BEAST II and extrapolations to higher luminosity can reliably be made.

VXD installation

The close proximity of the superconducting magnets to the VXD makes the installation of the vertex detector very challenging. The baseline installation method (BIM) developed by the KEK machine group foresees mounting of the VXD on the tip of one of the QCS magnets before moving the entire package into the Belle II detector. In order to decouple future maintenance work on accelerator components close to the interaction region as much as possible from interventions on the VXD, DESY has developed a remote vacuum connection (RVC) system that will allow the independent installation of the VXD (see *DESY Particle Physics 2012*). To demonstrate the feasibility of all aspects of this alternative installation method (AIM), a detailed mock-up of all essential components of the interaction region was constructed at the MPI for Physics in Munich with the help of DESY and the University of Hamburg and transported to KEK (Fig. 1). In June 2014, a major installation review was held at KEK where the correct functioning of the RVC was demonstrated and both installation methods were compared in the presence of all relevant subdetector experts and representatives from the involved SuperKEKB machine groups. A central point of the discussion was whether the VXD could still be deinstalled in case the RVC was blocked and could not be released anymore, for example after an earthquake. After the successful demonstration of the smooth and reproducible RVC operation and of the emergency deinstallation of the VXD, the decision to adopt the AIM as the new baseline was taken unanimously.

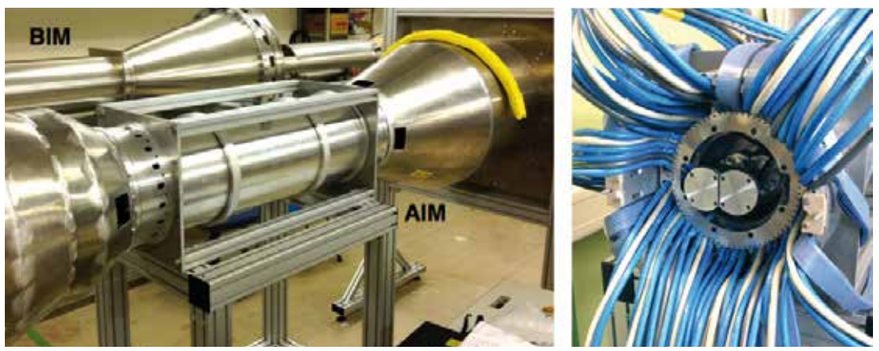

Figure 1

Left: Mock-ups for the two proposed installation scenarios of the Belle II vertex detector. “BIM” stands for “baseline installation method”, while “AIM” is an acronym for the “alternative installation method” that is based on a remote vacuum connection (RVC) system developed at DESY.
Right: Interior of the mock-up. The picture illustrates the narrow space available for readout cables and other VXD services.

Computing challenges

The large increase in luminosity expected at SuperKEKB and the corresponding growth of the Belle II data volumes must be accompanied by a commensurable increase of CPU, network and storage capacities. The Belle II collaboration has developed an ambitious scheme for ramping up the computing resources in a way that matches the luminosity profile expected in the coming years. Regular Monte Carlo production campaigns are being organised to verify that the necessary resources are in place and that the entire system is able to cope with the rapidly increasing demands. In Germany, DESY, KIT and the MPI for Physics in Munich are contributing to this effort with their grid resources. Figure 2 shows a breakdown of the CPU power used in the most recent campaign, which took place in autumn 2014. Thanks to its successful model of opportunistic allocation of free grid resources, DESY was able to contribute a very substantial share of about 30%.

EU funding for commissioning

When the final detector components are produced, the VXD will have to be assembled, tested and commissioned at KEK before it can be installed in Belle II. The detector-commissioning phase will require the presence of a significant number of European experts at KEK over extended periods of time. In order to cover the substantial travel costs related to these activities, several European Belle II groups together with other European institutes that engage in the Japan-based T2K neutrino experiment have submitted a joint proposal, called JENNIFER (Japan and Europe Network for Neutrino and Intensity Frontier Experimental Research), to the EU. JENNIFER was approved in late 2014 and granted a total of 2.3 million euro.

The main goal of the JENNIFER project (Fig. 3) is the support of an intensive scientific and technological exchange with scientists of the host country Japan and among the participating European science and industry partners. For the five German groups that participate in JENNIFER, the funding corresponds to 420 000 euro for the four-year duration of the project.

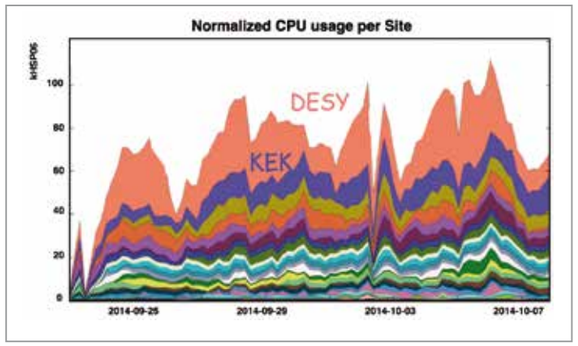

Figure 2

Breakdown of CPU power used for a recent Monte Carlo production campaign. DESY contributed almost 30%.

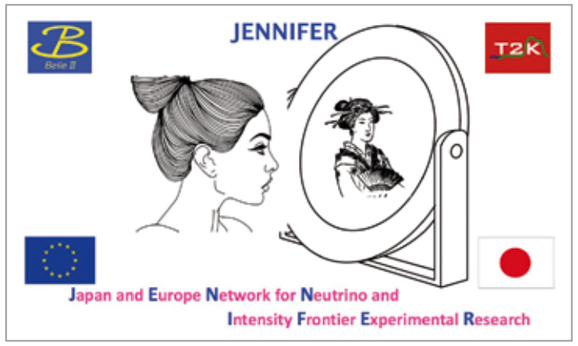

Figure 3

Logo of the recently approved JENNIFER proposal for funding from the EU Framework Programme for Research and Innovation, Horizon 2020

Contact:
Carsten Niebuhr, carsten.niebuhr@desy.de

Towards a site-specific ILC design.

How to fit the ILC into the mountains of northern Japan

Figure 2

Kitakami area with support banner for the ILC

The Japanese government has started a process to evaluate the design and impact of the International Linear Collider (ILC), a next-generation electron–positron collider, as a possible international project to be realised in Japan. In the meantime, a geologically fitting site for the collider has been identified in the Kitakami mountain range in the north of the main island of Honshu. Efforts in the worldwide ILC collaboration are now concentrating on evolving the generic ILC design of the technical design report into a site-specific design for the Kitakami region.

The ILC in Japan?

After the publication of the ILC technical design report (TDR) [1] and the detection of a Higgs particle at CERN's Large Hadron Collider (LHC), the Japanese community of particle physicists has started an effort to propose Japan as a host for the international ILC laboratory. The Japanese government asked the Science Council of Japan (SCJ) to evaluate the project, and the SCJ endorsed the physics case of the collider and raised points for clarification before a decision could be taken. The Japanese science ministry (MEXT) has taken over the charge to evaluate the TDR design, the cost estimates and the potential physics harvest of the ILC with the help of expert committees. A report on the outcome of the evaluation is expected for early 2016. A formal reaction of the Japanese government is then anticipated for no later than spring 2017. A potential proposal to host the ILC as an international project in Japan would be followed by international negotiations, with a possible construction start in 2019 and first beams in 2028.

Figure 1

Possible ILC site (red) in the Kitakami mountain range of northern Honshu

The Kitakami site and the ILC

It is not easy to find a site in Japan where an ILC of approximately 50 km length – fitting not only for the baseline machine with 500 GeV collision energy, but also for an upgrade to 1 TeV – could be built in an underground tunnel. Japanese scientists have been scrutinising every possible location for geological conditions and seismic stability and eventually found the best candidate in the Kitakami mountain range, about 380 km north of Tokyo (Fig. 1). This site offers granite bedrock of very good quality that suits the needs of the ILC. The underground granite slab, which is longer than 50 km, has no active seismic faults and, in case of earthquakes, moves like a big optical bench, i.e. preventing relative motion between the different components of a collider.

The design of the ILC as proposed in the TDR is generic, i.e. not adapted to a specific site, although various sample sites have been studied. Since 2013, efforts have started to understand how the arrangement of the underground and surface facilities needs to be changed to fit into the Kitakami realities.

At the heart of the collider: the interaction region

The most complicated region in the ILC design is the central region, where the particle sources, the damping rings and the interaction region are located. The generic design for an ILC in Japan, as depicted in the TDR, assumed a mountainous region where all access paths into the underground facilities would be routed through horizontal tunnels of up to 1 km length. The Kitakami region is indeed mountainous, but it has broad valleys and mostly moderate slopes (Fig. 2). It is therefore possible to place the ILC in the area in a way that results in a reasonably flat surface above the central region. This would allow vertical access into the detector hall through a big installation shaft. The assembly of the detectors would then predominantly be carried out above ground in an assembly building that is big enough to host both foreseen detectors in that phase. At the same time, the civil construction works on the underground halls and tunnels would proceed, keeping the interference between detector assembly work and construction work at a minimum.

Only late in the construction schedule, about 1.5 years before first beams are expected in the machine, would big preassembled and pretested parts of the detectors be lowered into the detector hall through the vertical shaft. A similar and very successful approach had been adopted for the CMS detector at the LHC. In terms of mass and diameter of the large detector components, e.g. the solenoid coil and the magnet yoke, the ILC detectors are comparable to CMS. Figure 3 shows a 3D CAD model of the ILC central region with a detector hall that has vertical shaft access.

As the detector concept collaborations are widely spread over many laboratories and universities in the world, the design of the interaction region is a good test case for the optimisation of a Japanese-driven design that still has to respect the needs of many users from around the world. Close communication and cooperation across political and cultural boundaries and time zones are a prerequisite. The use of a proper engineering data management system (EDMS) is of utmost importance – only such a system will allow the full documentation of the accelerator and detector design as well as the relevant geographical and geological information to be maintained in a coherent and controlled way. The DESY-EDMS system has been playing this role very successfully for the ILC for many years.

European support for the site-specific work: E-JADE

The European Union has timely issued a call for a Research and Innovation Staff Exchange (RISE) measure within the Marie Skłodowska-Curie actions of the Horizon 2020 Framework Programme for Research and Innovation. DESY, together with the main European players in accelerator research for particle physics (among others CERN, CEA, CNRS, CSIC and Oxford University), has successfully applied for the support of its Europe–Japan Accelerator Development Exchange Programme (E-JADE) proposal. E-JADE aims at sending experienced researchers from Europe to Japan to work on accelerator research towards new hadron accelerators, on LHC upgrades and on linear collider R&D. The latter work package comprises support for the use of internationally accessible EDMSs and site-specific work within the machine–detector interface efforts at the ILC in Japan. These tasks are crucial for a worldwide process where requirements from different ILC developers and potential users are fed into a local engineering design and construction planning effort.

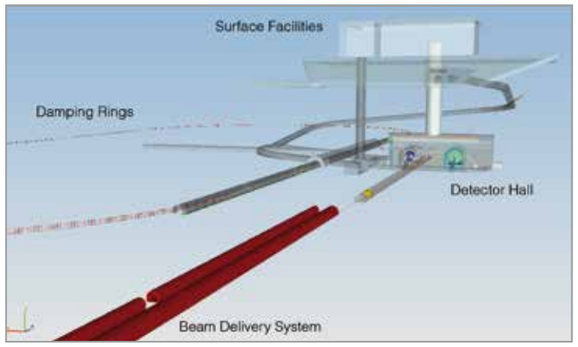

Figure 3

3D CAD model of the central region of the ILC. The detector hall was modified with a vertical shaft fitting into the Kitakami site.

Contact:
Ties Behnke, ties.behnke@desy.de
Karsten Buesser, karsten.buesser@desy.de
Eckhard Elsen, eckhard.elsen@desy.de
Benno List, benno.list@desy.de

References:

[1] T. Behnke et al., "The International Linear Collider Technical Design Report", DESY-13-062

Cavities en masse.

Industrially produced superconducting radio-frequency cavities perform beyond specification

With the mass production of components for the European XFEL X-ray free-electron laser facility in full swing, hundreds of superconducting radio-frequency (RF) cavities have arrived at DESY for acceptance tests at a temperature of 2 K and for installation in cryomodules. For the first time, the performance of industrially produced cavities can be examined with high statistical significance. In addition, about half of the cavities from the ILC-HiGrade programme, produced at the same time, have been specifically prepared for tests of higher performance.

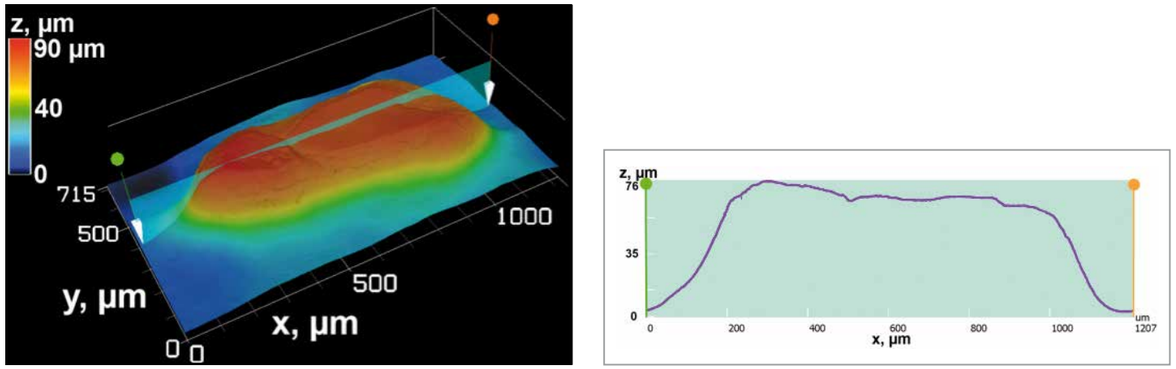

Figure 2

A protrusion of ~100 µm height detected on the surface of a cavity and explored using a silicon replica under a laser microscope. The height profile at the cross section is shown on the right.

International Linear Collider

The International Linear Collider (ILC) is the next large facility for particle physics. It was placed prominently in the European Strategy for Particle Physics and found similar echo in the strategies of Japan and the USA. A world-spanning event in June 2013 concluded the effort of hundreds of physicists to prepare a comprehensive design for this electron–positron collider, the technical design report (TDR) [1]. The multivolume report documents the physics case and the plans for the accelerator and the detectors. The Japanese government is currently examining the scientific and economic impact of ILC construction in Japan. A decision on the project is foreseen no later than 2017. In case of a positive decision, the ILC will be built in a truly global fashion. A site in Kitakami, in northern Japan, is under study as a possible location for the project (see p. 46).

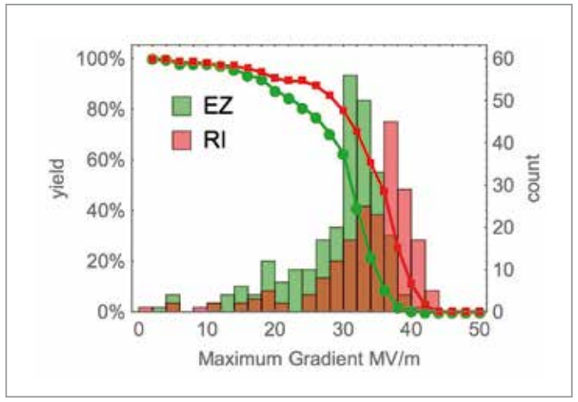

Figure 1

Distribution of the maximum accelerating electrical field (gradient) obtained in the cavities delivered for the European XFEL [2] from two vendors, Research Instruments GmbH (RI) and Ettore Zanon S.p.A. (EZ)

Cavities for the ILC

One of the challenges in compiling the TDR of the ILC was to determine what electrical field could realistically be used to accelerate electrons and positrons towards the collision point. This is an important number since, for a given design centre-of-mass energy, it determines the length of the collider – and because the construction cost of such a facility largely scales with the length. An ambitious goal for the accelerating gradient of 31.5 MV/m had been set at the start of the Global Design Effort for the ILC in 2004. Today, the required energy reach of the next large facility for particle physics is well understood: in order to explore the coupling of the Higgs boson, for example in associated production with the top quark (see p. 30), the collider should provide a centre-of-mass energy of at least 500 GeV. At the time of publication of the TDR, available samples of cavities were small, and the statistical significance of the observed progress in accelerating field remained questionable. Nonetheless, the TDR was able to quote a production yield surpassing 90% for cavities using the foreseen ILC recipe, which includes a second pass of surface treatment.

The linear accelerators of the ILC will be based on the technology of 1.3 GHz superconducting niobium cavities. Such cavities are currently being installed at the European XFEL X-ray laser in Hamburg, which is nearing completion. Some 800 ILC-type cavities will be used for the European XFEL, albeit with a lower gradient requirement of 23.6 MV/m; more than half of these cavities have been delivered. Also, a large fraction of the 24 additional cavities obtained as part of the ILC-HiGrade programme [3] of the Framework Programme 7 of the European Commission have been delivered; they are foreseen for special investigation and performance optimisation.

Figure 1 shows the distribution of the maximum field of the cavities for the European XFEL. Most of these cavities have experienced a single-pass surface treatment only, i.e. buffered-chemical processing or electropolishing (EP) followed by a high-pressure rinse with ultrapure water. The average maximum gradient exceeds 30 MV/m; tails to low fields point to deficiencies in the surface that need to be addressed. The EP-treated cavities (“RI”) yield higher average maximum gradients, confirming an earlier observation based on a small sample of cavities. The ILC recipe will apply the EP treatment.

Detailed surface investigation

The maximum-gradient distribution for the additional ILC-HiGrade cavities looks very similar to the one shown in Fig. 1. The ILC recipe also includes a second treatment after detailed surface investigation. Figure 2 shows an example of a protrusion detected in a cavity and further investigated on a silicon replica placed under a laser microscope. The defect, which results in a limitation of the cavity’s performance, shows an extent of about half a millimetre and protrudes by 100 µm.

Specific removal of such defects followed by a short chemical treatment will improve the performance of the cavities. The ILC-HiGrade cavities should hence exhibit significantly improved performance particularly at low fields. The demonstration of this procedure will help to set the state of the art for industry-produced ILC cavities.

Contact:

Eckhard Elsen, eckhard.elsen@desy.de
Aliaksandr Navitski, aliaksandr.navitski@desy.de

References:

[1] C. Adolphsen et al., The International Linear Collider Technical Design Report - Volume 3.I: Accelerator R&D in the Technical Design Phase, and ibid, Volume 3.II: Accelerator Baseline Design, DESY-13-062

[2] D. Reschke et al., *Analysis of the rf test results from the on-going cavity production for the European XFEL*, 27th Linac Accelerator Conference, Linac2014, Geneva, Switzerland, Aug. 31 – Sep. 5, THPP021

[3] FP7 Preparatory Phase Project ILC-HiGrade, Grant 206711, ilc-higrade.eu

Towards a calorimeter for the ILC.

Constructing and testing a scalable prototype for the hadron calorimeter of an ILC detector

Showing that your idea of a novel detector technology works in principle and performs as well as expected is one thing – building it as a component of a collider detector is quite another story. In previous years, the CALICE collaboration successfully tested a number of novel concepts for the calorimeters at the future International Linear Collider (ILC). Now is the time to show that these concepts can also be realised as parts of a real ILC detector, respecting realistic constraints on size, power consumption and cost. A new prototype of the analogue hadron calorimeter (AHCAL) that demonstrates these capabilities was recently tested in hadron beams at the CERN test beam facility.

CALICE: highly granular calorimeters for linear colliders

In order to reach the physics goals of future linear colliders, an unprecedented energy resolution in the measurement of jets is needed. It has been demonstrated that this is possible with particle flow algorithms, which use the detector component with the best energy resolution to reconstruct each individual particle within a jet: charged particles are measured in the tracking detector, while photons and neutral hadrons are reconstructed in the electromagnetic and hadron calorimeter, respectively. Highly granular calorimeters are necessary to disentangle the energy depositions of each particle. Within the CALICE collaboration, several concepts for such highly granular electromagnetic and hadron calorimeters have been developed and have demonstrated their capabilities in various test beam measurements of so-called *physics prototypes.* Before starting to build a calorimeter as part of a linear collider detector, the next step is an *engineering prototype* that is scalable to the full detector and respects the constraints of such a detector in terms of geometrical dimensions, of space for services like cooling and of power consumption. In addition, cost and effort needed for the production are important aspects.

AHCAL engineering prototype

One of the concepts developed within CALICE is the AHCAL, a sandwich calorimeter with steel absorber layers and active layers consisting of small scintillating tiles (3x3 m²) read out by silicon photomultipliers (SiPMs). In order to cope with the large number of channels (about 8 million for the ILC hadron calorimeter), the readout electronics and an LED calibration system are integrated into the active layers, and the data are zero-suppressed and fully digitised in the detector. For every single channel, the amplitude and time of a potential hit are determined by comparing the signal with a trigger threshold.

Since the calorimeters will be located within the magnet coil, the available space is very limited, and no cooling within the active layers is possible. This puts stringent limits on the maximum power consumption of the electronics. Active cooling of electronics components will only be possible in the gap between the barrel and the end-cap.

A wedge-shaped steel absorber stack of about 1 m³, corresponding to about 1% of the barrel calorimeter of the planned ILC detector, has been assembled at DESY. Up to now, 15 of the 40 slots for the active layers have been equipped (Fig. 1). This configuration already allows for large-scale tests of the system, including cooling and data acquisition. In addition, the active components are arranged in such a way that an identification of the shower start position is possible,

Figure 1
AHCAL engineering prototype in preparation for the beam test at CERN

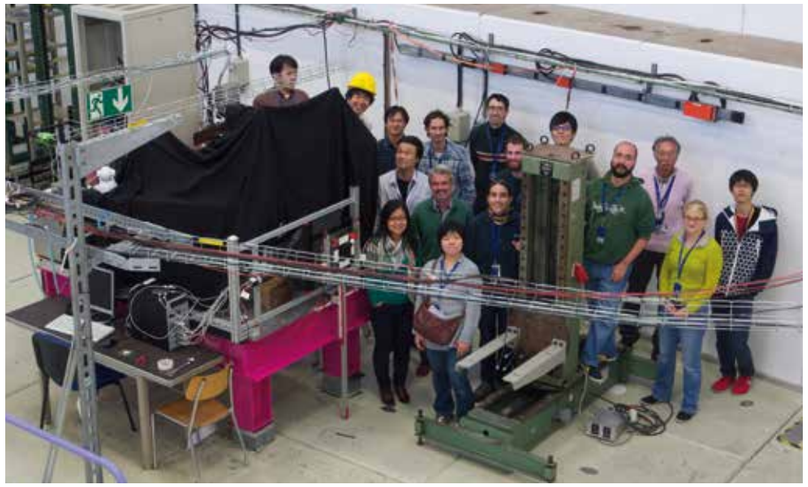

Figure 2
AHCAL engineering prototype (covered with black cloth) together with part of the team at the CERN test beam facility

and hadron shower profiles as well as correlations of hit times within hadronic showers can be measured.

In the active layers, several types of scintillating tiles and SiPMs are used. In the rapidly evolving field of commercially available SiPMs, the flexible AHCAL electronics allows us to profit from the increased dynamic range, improved noise and reduced cost of new-generation devices. In the future, the better device-to-device uniformity of these new SiPMs will probably allow for a reduction of complexity of the electronics. In the engineering prototype, advantages and disadvantages of the various tile and SiPM options can be studied. The first three layers have an even finer granularity, mimicking that of the foreseen electromagnetic calorimeter. They consist of small scintillator strips of size 4.5x0.5 cm² with alternating direction, the information of which can be combined to an effective granularity of 0.5x0.5 cm².

Test beam at CERN

Contributions from the Czech Republic, France, Germany, Russia and the USA as well as from CERN and Japan (the layers for the electromagnetic calorimeter) make the AHCAL a truly international project. After an intensive phase of testing and commissioning at DESY, the AHCAL engineering prototype underwent its first hadron beam time at the test beam facility of the Proton Synchrotron at CERN in autumn 2014. The muon beam also available there provided an important possibility to cross-check the calibration obtained with the internal LED calibration system.

An enthusiastic team of experts and shift crews (Fig. 2) spent several weeks at CERN to operate and monitor the detector during its beam time. Online monitoring software, including a full reconstruction and event display (Fig. 3), was set up and proved to be essential for successful and stable detector operation. A large set of muon data for calibration and hadron data at several energies has been recorded and is now ready for data analysis. In the coming years, more beam tests at higher particle energies are planned at CERN's Super Proton Synchrotron.

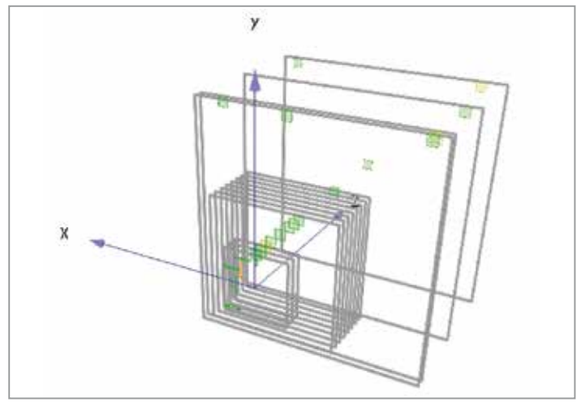

Figure 3
Track of a muon crossing the AHCAL engineering prototype

Contact:
Katja Krüger, katja.krueger@desy.de
Felix Sefkow, felix.sefkow@desy.de

Positrons non-stop for the ILC.

Keeping the target cool

A future high-energy electron–positron collider like the ILC will allow measurements with excellent accuracy if the luminosity is high. A key challenge will be the production of a sufficient rate of positrons – compared to previous accelerators, almost two orders of magnitude more positrons are needed.

In the current ILC design, the positrons are produced by the high-energy electron beam. The electrons are guided through a helical undulator, creating high-energy photons. The photon beam is then steered onto a target to generate electron–positron pairs. The concept of such a source was successfully demonstrated in the E166 experiment at SLAC a couple of years ago.

The design of the positron target represents a significant challenge. In order to limit the thermal load from the impacting photon beam, the target is realised as a wheel of 1 m diameter, spinning at 2000 rpm in vacuum [1]. A first prototype of such a wheel has been built and operated by LLNL [2], and an improved design is shown in Fig. 1. The cooling system will have to remove up to 7 kW from the wheel. Several solutions that use either liquid or radiative cooling are under study.

A detailed simulation of the radiative cooling has been performed (Fig. 2), indicating that even though the average temperature at the rim of the wheel will be higher than for liquid cooling, the cyclic peak load and average heat load are below the recommended limit for the chosen material.

The constant irradiation of the target with high-energy photons will also stress the material, which will thus degrade with time. The properties as a radiative surface will suffer as well. More studies are needed to understand this process and to demonstrate that radiative cooling of the positron target is an option for long-term operation.

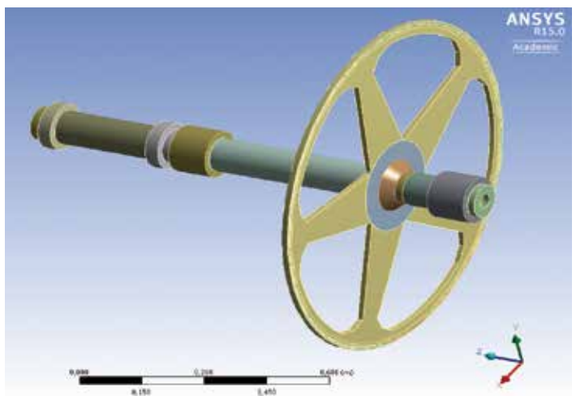

Figure 1

Sketch of the current ILC water-cooled target wheel design. The beam hits the target at the rim; water channels are located inside the spokes and the rim.

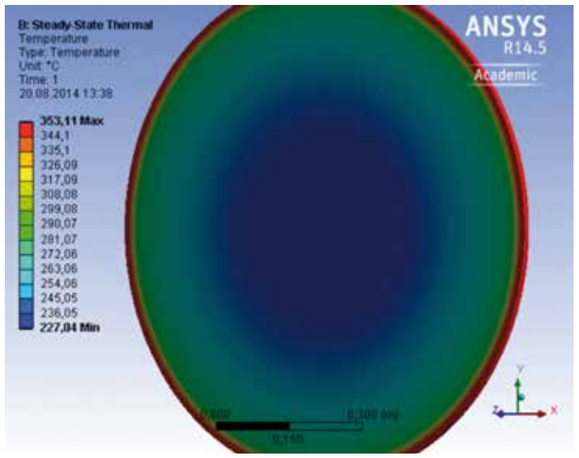

Figure 2

Average temperature distribution in the radiatively cooled titanium alloy target rim (~330°C) and in the inner radiative part (made from copper) of a solid target wheel. (Bearings, shafts and the cooled heat sink are not shown.)

Contact:

Sabine Riemann, sabine.riemann@desy.de
Andriy Ushakov, andriy.ushakov@desy.de

References:

[1] ILC TDR
[2] J. Gronberg et al., arXiv:1203.0070 [physics.acc-ph]

Measuring luminosity.

... from the ILC to the LHC

Luminosity is a key parameter for particle colliders. High luminosity allows precision measurements and access to rare processes. A key challenge is the measurement of the luminosity with sufficiently small errors.

The FCAL collaboration developed the design of a luminosity-measuring detector, or luminometer, for a future electron–positron collider, and successfully tested prototypes of the essential components. Based on these FCAL prototypes, a new luminometer for the CMS experiment at the LHC was built in collaboration with CERN and the AGH-UST University in Krakow, Poland. This new luminometer, the fast beam condition monitor or BCM1F, was recently installed within CMS.

The requirements on this detector were extreme in several respects. The high particle flux at the LHC required radiation-hard materials. The limited space near the beam pipe called for a compact design. Finally, the requirements on the time resolution and count rate were also a challenge, since the LHC will start operating with 25 ns between subsequent bunches in 2015.

Figure 1 shows a fully instrumented BCM1F half-ring. It consists of six single-crystal diamond sensors, each with an area of 5x5 mm^2 and structured into two metallised pads. The pads are read out by dedicated front-end ASICs made with radiation-hard 130 nm CMOS technology. Six such half-rings

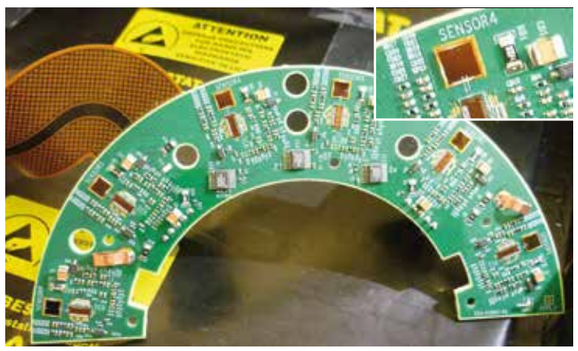

Figure 1

Left: Fully assembled BCM1F half-ring with sensors and front-end ASICs. Right: Zoom showing one two-pad diamond sensor bonded to the front-end ASIC.

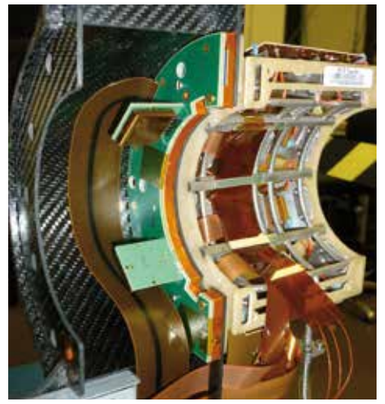

Figure 2

Half-ring of the BCM1F detector integrated with the PLT into a carbon fibre carrier before installation in CMS

were assembled and commissioned at DESY and delivered to CMS. There, they were integrated into a carbon fibre structure with the pixel luminosity telescope (PLT), as shown in Fig. 2.

In addition, a deadtime-free histogramming unit was developed that is able to read out and process high-rate data. The unit maps the arrival time of particles onto a time window corresponding to one turn of the beam in the LHC. The signals from the collision products and the beam halo particles will be counted separately. In particular, this unit allows the luminosity to be measured individually for each proton bunch. Since it is essential for optimising the LHC machine and the data quality at CMS, this bunch-by-bunch luminosity and background information will be transmitted to the CMS and LHC control rooms at 1 s intervals.

Contact:

Jessica Lynn Leonard, jessica.lynn.leonard@desy.de
Wolfgang Lange, wolfgang.lange@desy.de
Wolfgang Lohmann, wolfgang.lohmann@desy.de

Catching plasma-accelerated beams.

On the way to applications of electrons from plasma wakefield accelerators

Plasmas have the potential to offer a quantum leap in particle accelerator technology: they sustain electric fields of the order of 100 GV/m, three orders of magnitude larger than gradients achievable with superconducting radio-frequency cavities (see p. 48). The field of plasma-based particle acceleration has seen impressive progress in the last decade. While plasma-based accelerators are still quite far from supplying the beam quality and average power required for particle colliders at the energy frontier, applications in photon science, such as free-electron lasers (FELs), may become possible in the near future. The FLASHForward facility, which is currently being constructed at DESY, aims at demonstrating, for the first time, a plasma-driven FEL – by putting forward several advances to the current state of the art. Among these developments are a beamline for the extraction, diagnostics and transport of the plasma-accelerated electron beams to the undulators, and techniques to preserve the beam quality along the way.

Plasma wakefield acceleration

A high-current, relativistic bunch of charged particles or an intense laser pulse propagating through a plasma initiates a collective motion of plasma electrons – the plasma wave. The displaced charges generate strong electric fields (wakefields) on the order of 10–100 GV/m. The wakefields co-propagate with the driving beam (particle bunch or laser pulse); another bunch of charged particles, placed behind the driver, may then be rapidly accelerated to relativistic energies by the wakefield.

Laser-driven wakefield acceleration experiments (LWFA) have shown steady progress over the last ten years. Currently, they are producing multi-GeV electron beams over just a few centimetres of plasma, with an energy spread of typically 1% to 10%. So far, much fewer experimental studies have been performed with particle beams as drivers (PWFA), even though this technique may offer several advantages over LWFA, such as improved shot-to-shot stability and significantly higher average beam power. This preference of LWFA is, however, understandable: lasers are much more readily available than accelerators. Fortunately, things are different at DESY, one of the few laboratories in the world to operate accelerators that are perfectly suitable for PWFA experiments.

FLASHForward

FLASHForward will study PWFA by using electron beams from the FLASH free-electron laser. An electron bunch is kicked out of the FLASH bunch train in the extraction section and transported to the beam-matching and -focusing section. Here, it is brought into the shape best suited for the subsequent plasma interaction: parameters such as the transverse beam size have a dramatic impact on wakefield formation and therefore need to be carefully tuned. The heart of the experiment is a vacuum chamber holding the plasma cell – a sapphire capillary with an inner diameter of around 1 mm filled with a hydrogen or helium gas. A high-power laser ionises the gas and creates a plasma, which is struck by the focused electron beam shortly afterwards. The resulting wakefield accelerates the trailing or "witness" bunch, which can be either generated in the plasma itself or injected externally. After the drive and witness bunch exit the plasma, their properties are measured; the drive bunch is then removed by a collimator while the witness bunch is transported to the undulator where it produces the X-ray radiation. Several major improvements set FLASHForward apart from previous PWFA experiments. One example is the high beam quality of the drive bunch: FLASH achieves much smaller emittances and bunch durations than ever used for PWFA, which promises higher quality of the produced bunches. Another example is the usage of newly developed plasma cells that allow e.g. for tunable plasma density profiles, which are needed for some types of experiments as well as to preserve the beam quality (see below).

Beam transport and diagnostics

A further development distinguishing FLASHForward from earlier experiments is a dedicated beamline for the witness bunches. In the past, typically a dipole magnet was placed right after the plasma in order to measure the energy spectrum of the bunches. However, if one wants to use the beam further downstream, e.g. in an undulator, a proper transport system equipped with the necessary diagnostics is required. Such a beamline was developed for FLASHForward (Fig. 1).

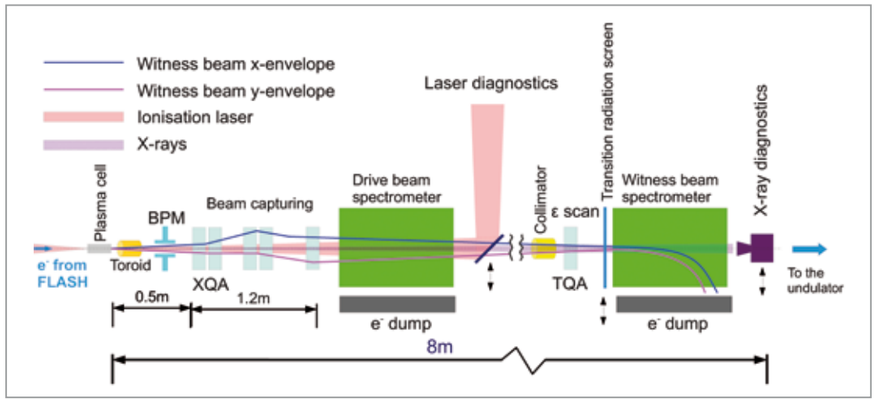

Figure 1
Overview of the beamline for transport and diagnostics of plasma-accelerated electron bunches

The initial section (beam capturing) consists of several quadrupole magnets focusing the divergent witness beam. After the quadrupoles, a dipole magnet acts as a broadband energy spectrometer. Several metres of drift space following the dipole are needed to reduce the size of the witness beam. At the point where the beam is sufficiently small, a collimator is located; it rejects the drive beam while the witness beam passes through unaffected. The emittance measurement section consists of another quadrupole magnet and a profiling screen. Finally, a high-resolution spectrometer precisely determines the energy distribution of the witness beam. Various diagnostics are located along the beamline, such as the longitudinal profile measurement using transition radiation or the diagnostics of the ionisation laser. After passing through the beamline, the beam may be manipulated further to demonstrate lasing in the undulator.

Beam quality preservation

One of the most active areas of research in plasma-based acceleration today is beam quality preservation. Apart from compactness, plasma accelerators have two further great advantages over conventional accelerators: the produced beams have small emittances and bunch durations. This, however, comes at a price. The beams are also highly divergent at the exit of the plasma cell, which leads to their rapid expansion; furthermore, they exhibit a relatively large energy spread of the order of 1%. The overall result is a rapid emittance blow-up.

Special measures have to be undertaken to avoid this quality degradation. One measure at FLASHForward is the optimisation of the capturing section of the aforementioned beamline. The strongest available electromagnetic quadrupoles, placed close to the plasma cell, were chosen in order to focus the beam as soon as possible and hence to minimise the distance over which the emittance growth takes place.

Another important technique is "plasma tailoring". By shaping the plasma density at the transition from plasma to vacuum, it is possible to reduce the divergence of the witness beam, which lessens its expansion on the way to the focusing quadrupoles (Fig. 2). Simulations show that this can practically solve the degradation problem, even with energy spreads as high as 1%. FLASHForward is the first attempt to systematically study and utilise this technique. The generation of high-quality electron beams and the demonstration of FEL-lasing in the undulator will be a major step forward in the field of plasma wakefield acceleration.

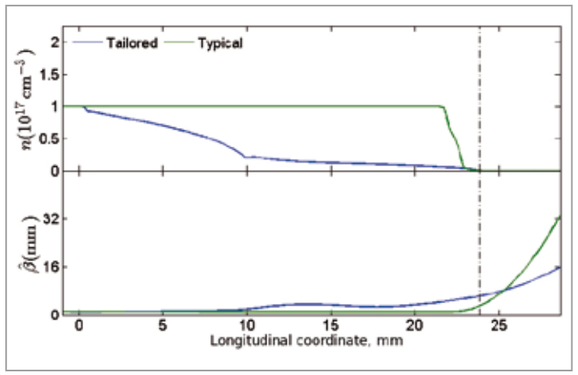

Figure 2
Plasma density (top) and β function, a quantity proportional to the squared beam size (bottom), along the transition from plasma to vacuum. Blue and green curves correspond to the density profiles with and without tailoring, respectively. The vertical dash-dotted line shows the location where the density has already fallen to a negligible value. The reduced beam divergence for the tailored profile (blue) is evident.

Contact:
Vladyslav Libov, vladyslav.libov@desy.de
Jens Osterhoff, jens.osterhoff@desy.de

Astroparticle physics.

Astroparticle physics at DESY explores the universe at high energies using photons and neutrinos. Experimental research at the DESY location in Zeuthen (Brandenburg) focuses on gamma-ray astronomy with the future Cherenkov Telescope Array (CTA) observatory and on neutrino physics and astronomy with the IceCube/IceTop detector at the South Pole (“Neutrino news from the South Pole”, p. 58)

DESY is also engaged in the ground-based telescopes H.E.S.S. in Namibia (“First results from the giant in the desert”, p. 60), VERITAS in Arizona, USA (“Gamma-ray transients observed with VERITAS”, p. 61) and MAGIC on La Palma, Spain, as well as the satellite-borne Fermi-LAT experiment (“Gamma rays from outer space”, p. 62). The data taken and analysed cover the energy ranges of 100 MeV to 50 TeV in gamma-ray astronomy and 10 GeV to several PeV in neutrino astronomy.

The experimental efforts are supported by a strong theory group, which researches a broad range of relevant high-energy phenomena in the universe. Gamma-ray and neutrino astronomy are tightly connected, as energetic gamma rays and neutrinos, being both electrically neutral, point back at their sources, which typically produce both particle types. Thus, combined multiwavelength and multimessenger studies provide insights into the types and mechanisms of cosmic accelerators (such as star explosions, matter-accreting black holes and pulsars) and the structure of the universe, and allow some of the most fundamental principles of physics to be tested.

Beyond the current activities, preparations are being made also at DESY for a next generation of experiments. IceCube-Gen2 is an extension of the currently operating IceCube neutrino telescope towards larger sensitivity for astrophysical neutrinos and lower energies for precision neutrino physics. The IceCube collaboration is currently entering into negotiations with funding agencies and working on a broad range of R&D activities (“IceCube-Gen2”, p. 63). The CTA gamma-ray observatory, built by a large international consortium, will observe the sky with unprecedented energy coverage, resolution and sensitivity. The CTA is rapidly nearing the final technical review and gearing up for the start of construction (“Getting ready for CTA”, p. 64). DESY is a major player in both activities.

Neutrino news from the South Pole.

Neutrino astronomy and neutrino physics with IceCube

In 2014, the IceCube neutrino observatory at the South Pole confirmed its 2013 discovery of astrophysical neutrinos and measured the energy spectrum of the neutrinos with much improved accuracy. Their sources are still mysterious, although IceCube's multimessenger analyses have now ruled out some candidates. In addition, IceCube's DeepCore subdetector delivered strong constraints on the neutrino masses and mixing parameters.

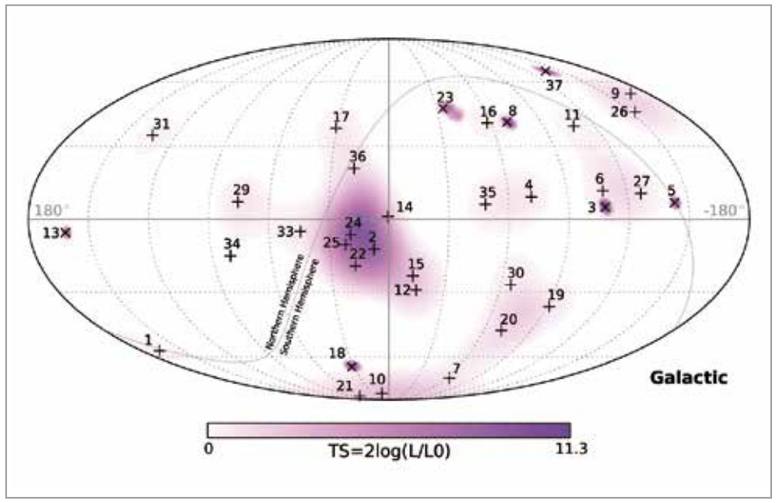

Figure 2

Sky map of predominantly astrophysical neutrinos [1]. (+: shower-like events, x: track-like events.)

The IceCube neutrino observatory

The IceCube neutrino observatory was completed in the winter of 2010/2011 and has since demonstrated, through its observations of neutrino interactions in the thick Antarctic ice of the South Pole, its considerable power to explore the universe. IceCube's array of more than 5000 optical sensors, buried deep in a cubic kilometre of Antarctic ice, records the very rare collisions of neutrinos produced either in the Earth's atmosphere or by distant astrophysical sources (see "Breakthrough of the Year" in *DESY Particle Physics 2013*). After contributing to the construction of the detector, DESY is now strongly involved in its operation and the analysis of its data.

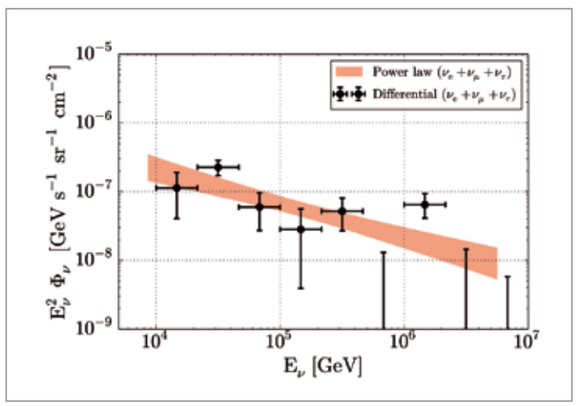

Figure 1

Energy spectrum of astrophysical neutrinos [4]

Neutrino astronomy

Following its discovery of astrophysical neutrinos, IceCube has increased its analysed data set to include a third year of data-taking, and has thereby raised the statistical significance of its observation to more than 5 σ [1] from just one data set. Furthermore, the signal has now been confirmed through the analysis of two other data sets [2, 3]. Finally, an analysis performed by DESY combined all of the available data sets and thereby placed tight constraints on the spectral shape of the astrophysical neutrino flux (Fig. 1); the energy spectrum was shown to be consistent with a power law with a spectral index $\gamma = 2.50 \pm 0.08$, in the energy range between 10 TeV and several PeV [4].

The observation that the sky map of (mostly) astrophysical neutrinos (Fig. 2) is nearly isotropic, implies that the sources of the neutrinos are not inside our galaxy [1]. However, attempts to identify them in the IceCube data have so far failed. Using a multimessenger approach, which correlates sources known through optical observations with the astrophysical neutrinos, the DESY group has shown that one suspect, active galactic nuclei (AGNs) whose jets point towards the Earth (so-called blazars), cannot be the source [5]. A second candidate, gamma-ray bursts, has also been ruled out by the non-observation of very bright and short neutrino bursts [6]. Thus, the hunt for the sources of astrophysical neutrinos continues.

Determining neutrino properties

In addition, scientists are using IceCube to study the fundamental properties of the elusive neutrino itself. Motivated by a 2012 publication showing that the IceCube subdetector, DeepCore, is sensitive to neutrino oscillations, DESY researchers performed a much-improved analysis [7] in the low-energy range. The key observation is that fewer Earth-traversing muon neutrinos in the 25 GeV energy range are seen than would be naively expected from the known rate of atmospheric collisions.

The reason for this is that the flavour of a neutrino can change (e.g. from a muon neutrino to an electron neutrino) due to flavour oscillations. In the data taken between May 2011 and April 2014, about 5200 events were found, while 7000 would be expected if the neutrinos had not oscillated. From an analysis of angular and energy spectra (Fig. 3), competitive constraints on the mass difference for neutrinos differing in flavour and on the neutrino mixing angle were derived; after only three years, IceCube achieved a measurement precision that the Super-Kamiokande experiment in Japan took 15 years to reach. The uncertainties on the IceCube results are larger than, but already comparable to, the most precise neutrino beam experiments, MINOS and T2K. As IceCube takes more data and its analysis methods are further improved, the gap may soon close.

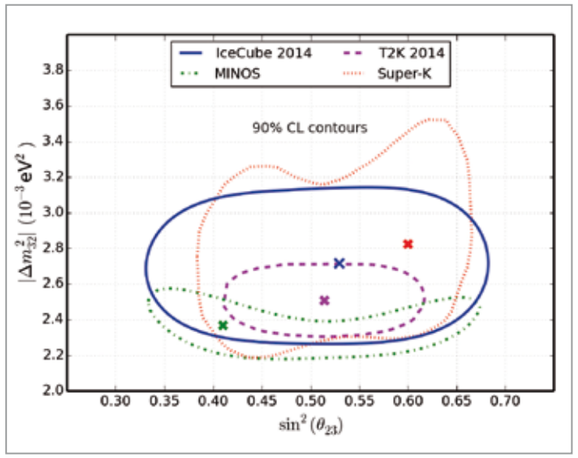

Figure 3

Constraints on neutrino mixing parameters [7]

Contact:
Marek Kowalski, marek.kowalski@desy.de

References:

[1] M.G. Aartsen et al., Phys. Rev. Lett. 113, 101101 (2014)
[2] M.G. Aartsen et al., Phys. Rev. D89 10, 102001 (2014)
[3] M.G. Aartsen et al., Phys. Rev. D91 2, 022001 (2015)
[4] M.G. Aartsen et al., in preparation; L. Mohrmann et al., Proceedings of 13th TAUP (2013)
[5] M.G. Aartsen et al., in preparation; T. Glusenkamp et al., arXiv:1502.03104
[6] M.G. Aartsen et al., in preparation; M. Kowalski, arXiv:1411.4385
[7] M.G. Aartsen et al., arXiv:1410.7227

First results from the giant in the desert.

… and preparations for a major hardware upgrade in 2015

In 2014, the Cherenkov telescope system H.E.S.S. in Namibia performed the first ground-level measurement of pulsed gamma rays in the southern sky. This detection of cosmic gamma rays of 30 GeV, which spectacularly demonstrates the experiment's performance, was announced by the H.E.S.S. collaboration in July. The radiation originates from the Vela pulsar, the first pulsar detected by H.E.S.S. and – after the Crab pulsar – the second pulsar ever detected by ground-based gamma-ray telescopes. DESY engineers in Zeuthen also work on an electronics refurbishment of the four H.E.S.S. I cameras, which will allow the maximum science return of the mixed-size H.E.S.S. II system in its final years before the dawn of the Cherenkov Telescope Array (CTA).

H.E.S.S. II is a system of telescopes of different sizes that detect cosmic gamma rays in sync. The 28 m CT5 telescope, inaugurated in 2012, is placed in the centre of four 12 m telescopes that have been operational for more than 10 years. It extends the energy range of the array to lower energies and allows for the detection of cosmic particle accelerators down to 30 GeV. Astroparticle physicists have now demonstrated this detection capability, with significant analysis contributions from the H.E.S.S. group at DESY: In cooperation with scientists from all over Europe, a tailor-made reconstruction analysis was developed for these low-energy gamma rays. In this way, the scientists were able to detect a pulsed, repeating gamma-ray signal in the energy range of 30 GeV (Fig. 1) and to attribute it to the Vela pulsar.

This result opens the door to new observation possibilities of the inner galaxy.

In order to exploit the powerful mixed-size H.E.S.S. II array more efficiently, an upgrade of the 10 year old electronics of the photomultiplier cameras in the four smaller telescopes (CT1–4) is necessary. At DESY, an entirely renewed electronics concept was designed, which will be deployed on the first telescope in 2015. The system, which already uses technology in consideration for the CTA telescopes, will get a faster readout and network technology, a more versatile architecture of the data flow and several additional features to increase the operating reliability and reduce maintenance costs. Completion of the project is foreseen for summer 2016.

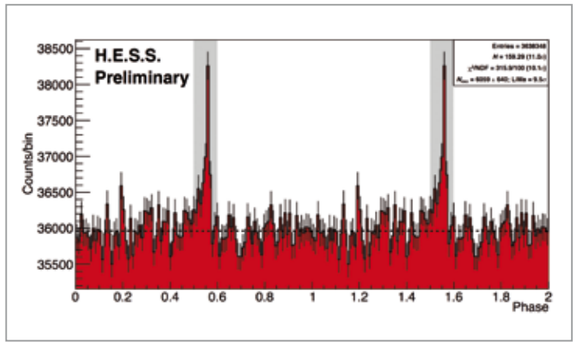

Figure 1

Periodic gamma-ray pulses of the Vela pulsar in the data of the H.E.S.S. experiment. One phase is equivalent to 89 ms.

Figure 2

H.E.S.S. camera test bench in the construction hall at DESY in Zeuthen

Contact:
Stefan Klepser, stefan.klepser@desy.de

Gamma-ray transients observed with VERITAS.

How to catch short gamma-ray flares

The VERITAS observatory, consisting of four 12 m imaging atmospheric Cherenkov telescopes, is sensitive to gamma rays from cosmic accelerators at energies from 85 GeV to 30 TeV. DESY scientists measure and analyse transients and variable emission from gamma-ray sources, such as binary systems, active galactic nuclei and gamma-ray bursts. The DESY group contributed to the discovery of historically bright and fast flares from the binary LS I +61 303 and to the discovery of gamma-ray emission from the blazar RGB J2243+203.

Variable gamma-ray emission on time scales from minutes to months is observed from a number of astrophysical objects. Their sizes and masses extend from active galactic nuclei harbouring supermassive black holes of millions of solar masses to binary systems that consist of a star and a compact companion with masses of a few times the solar mass. Studies of variability shed light on the physical processes responsible for the acceleration; the determination of the characteristic timescales for particle acceleration and gamma-ray emission gives us an understanding of the size and location of the emission region.

The observation of variable emission patterns is challenging, as the rapid and aperiodic flaring is generally not predictable. Additionally, measurements with ground-based gamma-ray observatories are limited to dark nights. The transient nature requires a rapid turnaround of the data, so that flares can be captured during their evolution. This allows the observing schedule to be adapted and alerts to be sent out to other observatories. The DESY group shares responsibility for the VERITAS on-site next-day analysis, which returns high-quality scientific results a few hours after the data have been recorded.

Two scientific discoveries stand out among the VERITAS results in 2014. The binary LS I +61 303 exhibited bright and rapid variability, which had not been seen before in such objects. The system consists of a massive star and a compact object. VERITAS observations showed variability on timescales of less than a day. Gamma rays with energies of up to 10 TeV were measured during the flares, which revealed that the accelerating processes observed might be among the most efficient in astrophysical sources.

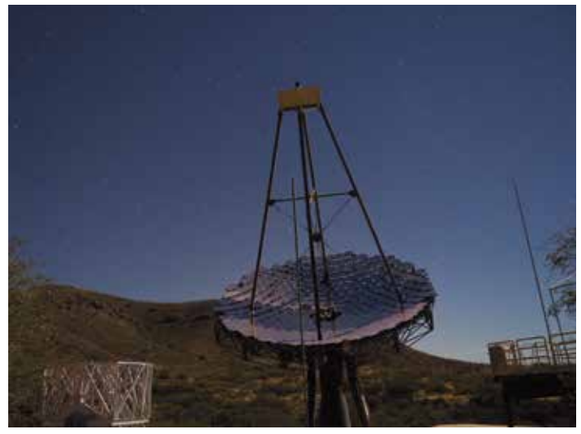

Figure 1

VERITAS telescope in Arizona, observing during moonlight (Credit: M. Hütten, DESY)

The VERITAS discovery of a gamma-ray blazar (RGB J2243+203) over Christmas 2014 increases the number of known gamma-ray blazars to 56. This is yet another step towards a more complete measurement of the blazar population. As the large energetic outflows from active galactic nuclei have a significant impact on their environment, a precise measurement of their luminosity distribution will eventually result in a better understanding of their contribution to the high-energy universe.

Contact:
Gernot Maier, gernot.maier@desy.de

Gamma rays from outer space.

Extragalactic gamma-ray background observed with the Fermi Large Area Telescope

The Large Area Telescope (LAT) onboard the Fermi Gamma-Ray Space Telescope continuously surveys the gamma-ray sky at MeV and GeV energies. A new study, led by a DESY researcher, has measured the intensity of the diffuse glow of gamma rays that reach the Earth from all directions with better precision and at higher energies than ever before.

The gamma-ray sky can be decomposed into individual sources, diffuse emission attributed to the interactions of galactic cosmic rays with gas and radiation fields, and a residual all-sky emission component presumed to be of extragalactic origin. This extragalactic gamma-ray background (EGB) originates from all the gamma-ray sources that are too faint to be detected as individual sources (e.g. sources in distant galaxies) and from gamma rays of processes that occur throughout the universe. Such processes may be astrophysical, or they might involve exotic physics like the annihilation of dark-matter particles into photons. Since the universe is transparent to gamma rays of MeV and GeV energies, the EGB is a measure of the total amount of gamma rays emitted by all the sources and gamma-ray-producing processes in the cosmos. Measurements of the EGB intensity and spectrum are therefore of fundamental importance. They can be used to constrain properties of astrophysical sources [1] as well as new physics models – from primordial black holes [2] to WIMP dark matter [3].

Led by a DESY researcher, the Fermi-LAT team has now measured this gamma-ray background from 100 MeV to 820 GeV with improved precision and at higher energies than ever before [4]. The EGB spectrum shows a significant high-energy cut-off feature and can be well described over nearly four decades in energy by a power law with a spectral index of 2.32 ± 0.02 and an exponential cut-off with a break energy of (279 ± 52) GeV. The total intensity above 100 MeV attributed to the EGB is (7.2 ± 0.6) × 10^{-6} photons cm^{-2} s^{-1} sr^{-1}.

A simple explanation of the measured total EGB spectrum from 100 MeV to nearly 1 TeV would be a single class of extragalactic sources producing gamma-ray spectra with spectral indices of about ~ 2.3, and a roughly constant source density over the history of the universe. Interestingly, the distribution of spectral indices for individual sources

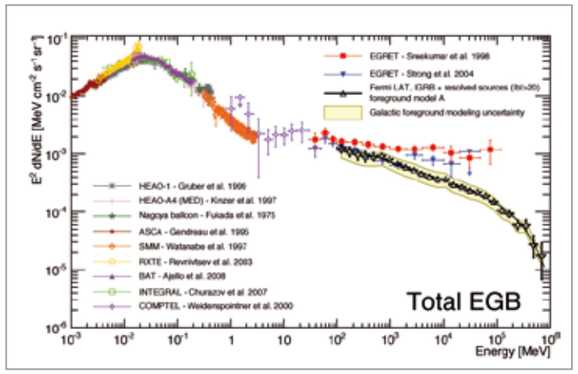

Figure 1

Extragalactic X-ray and gamma-ray backgrounds measured by various instruments. The black dots and yellow band represent the new measurement by the Fermi-LAT [4].

detected by the Fermi-LAT above 10 GeV also peaks near 2.3. However, the actual origin of the EGB might be more complex with various extragalactic source classes contributing to the total emission. More sophisticated analyses are needed to fully understand how sources governed by so diverse physics as we see in the gamma-ray sky can produce a nearly featureless EGB spectrum over almost four decades in energy.

Contact:
Markus Ackermann, markus.ackermann@desy.de

References:

[1] M. Ajello et al., arXiv:1501.05301
[2] B.J. Carr et al., PRD 81, 104019 (2010) [arXiv:0912.5297]
[3] M. Ackermann et al., arXiv:1501.05464
[4] M. Ackermann et al., ApJ 799, 86 (2015) [arXiv:1410.3696]

IceCube-Gen2.

Making IceCube fit for the future

The IceCube-Gen2 project is planning to improve the sensitivity of the South-Pole-sited IceCube neutrino observatory for astrophysical neutrinos and to extend its reach to lower energies to enable precision neutrino measurements. Extensive simulation studies and detector R&D are under way to define the next generation of neutrino telescopes.

Two findings have recently spurred interest in IceCube extensions. First, the discovery of astrophysical neutrinos marks the beginning of a new era of astronomical observation. Second, the DeepCore subdetector, a more densely instrumented array at the centre of IceCube, has demonstrated that precision measurements of neutrino oscillation parameters are possible in a natural medium. Extensions of the IceCube infrastructure (summarised under the name IceCube–Gen2) are now envisioned, which would advance the field in both of these directions.

First, the even denser instrumentation of DeepCore would allow the energy threshold for atmospheric neutrinos to be lowered to below 10 GeV, making the detector sensitive to the matter effects of neutrino oscillations inside the Earth and allowing the fundamental question of the neutrino mass ordering to be addressed. The Precision IceCube Next Generation Upgrade (PINGU) proposal would measure the neutrino mass hierarchy with a statistical significance of 3 σ after only about 3.5 years of data taking. The PINGU letter of intent [1] was distributed to the community in January 2014.

Figure 1

Multi-PMT optical module that could be used for PINGU and the High-Energy Array

The second extension under consideration, the High-Energy Array, calls for up to 120 additional strings with an increased horizontal spacing and an instrumented volume of the order of 10 km^3. It could lead to the discovery of the sources of astrophysical neutrinos. In December 2014, our vision for the High-Energy Array [2] was published, and the optimisation of the detector design is proceeding with high momentum.

Both PINGU and the High-Energy Array could be constructed with well-established techniques and therefore pose very little risk. More ambitious ideas are also being explored. For example, the optical modules with a single 10 inch photomultiplier tube (PMT) could be replaced by one of several devices now being developed that will have considerably larger photon collection area and/or lower noise. Figure 1 shows one such device: a multi-PMT optical module adapted by the Erlangen Centre for Astroparticle Physics (ECAP) from a model used by the KM3NeT experiment [3]. A second candidate is the wavelength-shifting optical module (WOM) that is being developed by a collaboration of DESY and the University of Mainz. A first prototype module is expected in summer 2015.

Present plans call for PINGU to be deployed first and to serve as a platform for testing these new types of optical module and studying their in-ice performance and, thereby, their usability for the High-Energy Array and other future projects in Antarctica.

Contact:
Timo Karg, timo.karg@desy.de

References:

[1] M.G. Aartsen et al., arXiv:1401.2046
[2] M.G. Aartsen et al., arXiv:1412.5106
[3] S. Adrián-Martinez et al., Eur. Phys. J. C 74 3056 (2014)

Getting ready for CTA.

Last steps towards the start of construction

The next-generation gamma-ray observatory, the Cherenkov Telescope Array (CTA), will be built by a global consortium. In 2016, it will likely enter the construction phase with major contributions from DESY. CTA will observe the highly active non-thermal universe at energies above 30 GeV with unprecedented clarity, with the aim of understanding, among others, the sources and acceleration mechanisms of cosmic particles and the nature of dark matter.

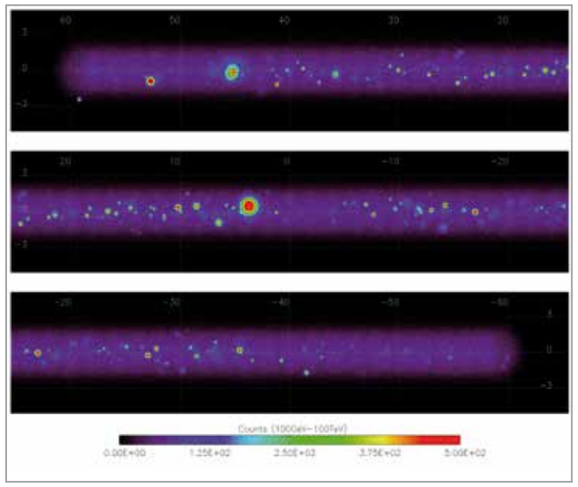

Figure 2

Simulated CTA survey image of the galactic plane for the inner region, $-60^0 < l < 60^0$, assuming a sensitivity of 2 mCrab and a population model considering only pulsar wind nebulae. CTA will discover about 1000 new gamma-ray sources.

Characteristics of CTA

CTA will consist of two observatories, sited in the northern and southern hemispheres. Each observatory will comprise an array of 20–100 imaging Cherenkov telescopes that measure the faint Cherenkov flashes emitted by air showers of secondary particles produced by gamma rays and charged particles in the atmosphere. Telescopes of three different sizes will operate in tandem to open up a sensitive energy range from 30 GeV to 300 TeV. The sensitivity of CTA will allow the detection of an unprecedented number of gamma-ray sources with exceptionally high spatial, spectral and temporal resolution. The sensitivity of CTA to steady sources will be a factor of 10 better than that of current instruments. The remarkable increase of the photon detection area will make CTA five orders of magnitude (!) more sensitive to hour-long gamma-ray flares at 30 GeV than NASA's Fermi Large Area Telescope (Fermi-LAT). The large field-of-view of the CTA telescopes will dramatically enhance its surveying and monitoring capabilities, allowing for the first time a deep, spatially well-resolved survey of both the whole galactic plane and a quarter of the extragalactic sky in very-high-energy gamma rays. DESY groups are developing new observing modes for surveys, which will use the large number of CTA telescopes and will further improve CTA's monitoring ability. CTA will be the first open, proposal-driven observatory in ground-based gamma-ray astronomy with data products, tools and user support for guest observers.

Figure 1

12 m diameter MST prototype in Berlin-Adlershof

Recent progress and schedule

CTA is the main project in gamma-ray astronomy at DESY. Group members hold various positions in the organisation of this international project and are responsible for the array control software and for the design and construction of the 12 m diameter mid-sized telescopes (MSTs). The technical design report (TDR) for the MSTs, which includes a work breakdown structure, production and assembly schedules and cost estimates, has been largely completed. 2014 saw many improvements of the design based on experience gained with a prototype telescope in Berlin-Adlershof (Fig. 1). The mechanical structure was stiffened, and tracking and pointing accuracy were greatly improved; a feedback system for reducing wind-induced oscillations was tested; an optimised camera support structure, produced in Brazil, was tested on the prototype telescope and, based on these extensive tests, redesigned mirrors are now being produced industrially in France, Italy and Poland. Before the design will be frozen later in 2015, a full-sized FlashCam will be mounted to test the interfaces and camera-mounting procedures, and an improved dish structure that could reduce costs, ease the assembly of dish and mirrors and improve accuracy will be tested.

In summer 2014, an interim legal entity, the CTAO GmbH, was established with DESY as one of its founding partners. Its tasks are the operation of the CTA Project Office through the pre-production and production phases, the preparation of the site decisions and the funding approval, and the management of the construction of the observatories.

In spring 2015, a critical design review will take place. It should certify that the CTA design has the technical maturity to go into construction. Site decisions are expected by the end of 2015, so that in early 2016, an international agreement on the start of funding could be reached and construction could begin. Early science runs with a partially completed array can be expected in 2017. Already then, CTA will be the world's most sensitive gamma-ray observatory. Completion of construction and full sensitivity are expected for 2020.

Main science drivers for CTA

The main science goals of CTA were formulated, with substantial contributions from the DESY CTA group, as part of the TDR. Research at CTA will cover three major themes: understanding the origin and role of relativistic cosmic particles; probing extreme environments, such as those around neutron stars and black holes; and exploring frontiers in physics, such as the nature of dark matter, quantum gravity effects and the search for axion-like particles.

Relativistic particles play a major role in a wide range of astrophysical systems, from supernova explosions to star-forming galaxies and active galactic nuclei. Cosmic rays are accelerated to energies of up to 10^{20} eV in unknown environments. In our own galaxy, the energy density of cosmic rays, gas pressure and magnetic fields is about the same, yet the connection between them, which is of great importance for the evolution of galaxies and galaxy clusters, is not well understood. CTA will address these issues by providing both a census of particle accelerators in the universe and high-precision measurements of bright, nearby sources such as young supernova remnants or the radio galaxy M87.

The unprecedented sensitivity of CTA will allow stringent tests of fundamental physics at high energies. For example, it will reach the sensitivity needed to observe the thermal-relic cross section for self-annihilating dark matter (DM) for a wide range of DM masses, including those inaccessible to the LHC at CERN. It will also be sensitive to the energy-dependent variations of the speed of light expected from quantum gravity theories. Axion-like particles, a subject in which DESY scientists are especially active, should make the universe more transparent to high-energy photons. The large number of extragalactic gamma-ray sources that will be seen by CTA should allow these predictions to be either verified or refuted with great precision.

Contact:
Gernot Maier, gernot.maier@desy.de
Stefan Schlenstedt, stefan.schlenstedt@desy.de

Theoretical physics.

One of DESY's assets is a rich theory portfolio that ranges from collider phenomenology through cosmology to lattice gauge theory and string theory. Theorists in these different fields are collaborating closely – frequently stimulating new ideas and methods – and they maintain strong ties to the experimental groups. This is particularly beneficial in these exciting times where new LHC results and cosmological observations may bring us closer to understanding key questions about matter and the universe.

DESY theorists provide guidance to the experimentalists at the LHC and elsewhere, leading e.g. the efforts to determine the properties of the Higgs boson ("Cornering the Higgs", p. 72). Similarly, astroparticle theorists work on integrating the multitude of cosmic-ray data into a consistent multimessenger picture of potential sources ("Where do the cosmic rays come from?", p. 68). In cosmology, the study of dark matter provides a strong link to collider physics ("Precision physics probes dark matter", p. 70).

The string theory and lattice gauge theory activities at DESY provide groundbreaking results. String theorists strive to get a handle on the low-energy behaviour of gauge theories, which cannot be tackled by the usual methods of expanding in a small coupling constant ("What happens at strong coupling?", p. 78), whereas lattice calculations have made progress in characterising an intriguing property of quantum chromodynamics ("Testing spontaneous symmetry breaking in QCD", p. 76). Both lines of research aim at a deeper understanding of gauge theories, which are the basic language for our present description of the microcosm.

Where do the cosmic rays come from?

Neutrinos test theories for the origin of the most energetic cosmic rays

The most energetic cosmic rays observed today are presumably of extragalactic origin because they cannot be trapped by the magnetic fields in the Milky Way. Prime candidates for their origin are gamma-ray bursts – violent explosive ejections of material from a central engine at ultrarelativistic speeds. Neutrino observations start to probe this hypothesis, and the theory of the sources is key to a self-consistent multimessenger picture of gamma rays, neutrinos and cosmic rays.

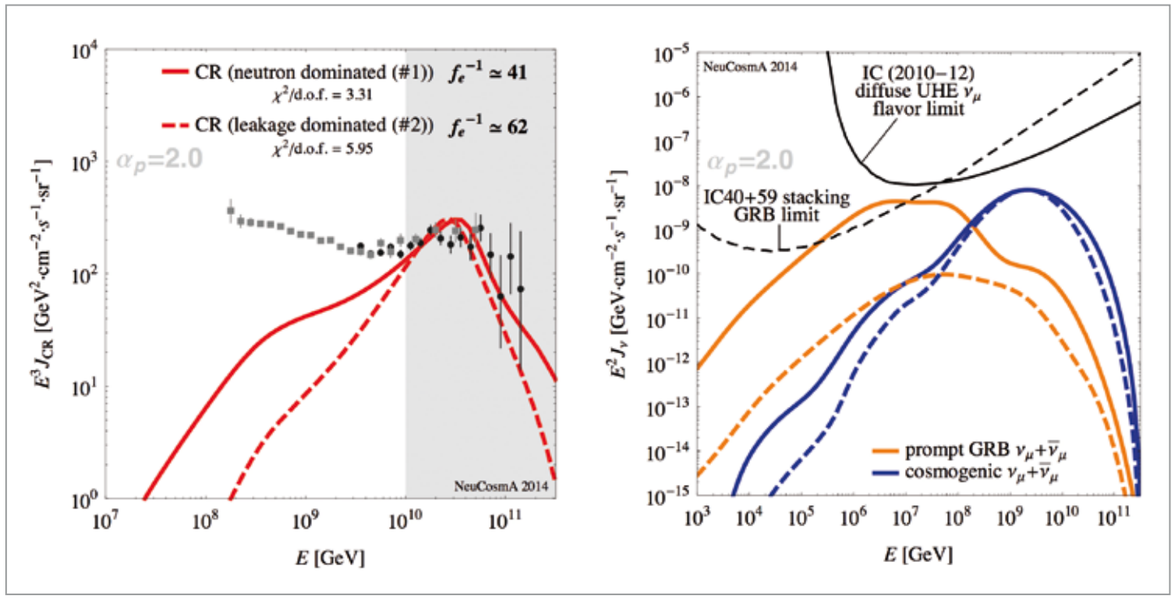

Figure 1

Cosmic-ray fluxes compared to HiRes data (left panel) and neutrino fluxes compared to IceCube data (right panel), described by two different parameter sets leading to different cosmic-ray escape mechanisms (solid and dashed curves). Both models describe the cosmic-ray data at the highest energies (left panel, grey-shaded region), whereas the prompt neutrino flux prediction is very different (right panel). Adapted from Ref. [2].

Neutrino astronomy has made groundbreaking advances in recent years, including the detection of a diffuse flux of highly energetic neutrinos of yet unknown origin by the IceCube experiment at the South Pole. The sensitivity to individual source classes depends on the efficiency with which the atmospheric muon and neutrino backgrounds can be rejected. A very successful strategy – so-called transients – can be used for astrophysical explosions: here, the timing information from gamma-ray satellite experiments, such as the Fermi Gamma-Ray Burst Monitor, can be used to reduce the search time window such that these backgrounds basically vanish. Therefore, the sensitivity to gamma-ray bursts is among the best of any individual object class detectable in a neutrino telescope. No neutrinos from gamma-ray bursts have been seen yet, and the current limit exceeds the observed flux by one order of magnitude, which challenges conventional production models for neutrinos in gamma-ray bursts [1].

If gamma-ray bursts are the sources of the highest-energy cosmic rays, the cosmic rays must interact with radiation in the sources, leading to secondary pions – and therefore neutrinos. There are several unknowns in this connection: for instance, the neutrino production efficiency depends on the radiation density in the source, which can be only crudely estimated from gamma-ray observations. In specific scenarios, however, the connection between neutrinos and cosmic rays is tight. Consider, for instance, the Δ resonance process:

$$p + \gamma \to \Delta^+ \to \begin{cases} n + \pi^+ & \frac{1}{3} \text{ of all cases} \\ p + \pi^0 & \frac{2}{3} \text{ of all cases} \end{cases}$$

Here, the neutrons and the charged pions, which will quickly decay into muons and neutrinos, are produced together by the same interaction. The neutrons may easily escape from the source because they are electrically neutral and cannot therefore be trapped by magnetic fields. Since they will decay into protons on the way to Earth, they could be a plausible candidate for the observable cosmic-ray protons. In this simple theory, the cosmic rays and neutrinos are intimately connected – no matter how often the process occurs in the source. Normalising the proton flux from all sources to the observed cosmic-ray spectrum at the highest energies, one can therefore predict the neutrino flux and compare it to observations. However, this scenario has been clearly excluded by recent neutrino data (see solid curves in Fig. 1).

This result imposes challenges on theory: Can the paradigm that gamma-ray bursts are the sources of the most energetic cosmic rays be ruled out? Or, perhaps, is this picture too simple? One of the keys to these questions is the cosmic-ray escape mechanism. If the primary protons in the process mentioned above can escape, the direct correlation with the neutrino production will be destroyed. We demonstrated that, even if the protons are trapped by magnetic fields, a fraction of them can leak out from the source. This leakage depends on the gamma-ray burst parameters and is the most conservative assumption one can make for direct proton escape. It may plausibly explain the non-observation of gamma-ray burst neutrinos even if these objects are the sources of the most energetic cosmic rays [2] (see dashed curves in Fig. 1).

In the standard theory of prompt gamma-ray burst emission, relativistic ejecta emitted from a central engine collide. In these collisions, shocks are formed and particles are accelerated. From this theory, it is expected that gamma-ray bursts are highly dynamical objects with emissions from different collision radii. Current results indicate that both neutron escape and direct leakage are competitive mechanisms present in most gamma-ray bursts – but at different radii [3]. Since data from the Pierre Auger Observatory in Argentina point towards a heavier composition of cosmic rays at the highest energies, future research will have to include the production and escape mechanisms of heavy nuclei. These processes will be investigated within a European Research Council (ERC) Consolidator Grant funded by the European Union with 1.75 million euro, named “Neutrinos and the origin of the cosmic rays“, which was awarded to DESY physicist Walter Winter.

Contact:
Walter Winter, walter.winter@desy.de

References:

[1] R. Abbasi et al. (IceCube Collaboration), Nature 484 351 (2012)
[2] P. Baerwald, M. Bustamante, W. Winter, Astropart. Phys. 62 66 (2015)
[3] M. Bustamante, P. Baerwald, K. Murase, W. Winter, Nature Comm. 6, 6783 (2015) [arXiv:1409.2874]

Precision physics probes dark matter.

What rare processes tell us about the dark world

While it is now firmly established that most of the matter in the universe is in the form of dark matter, the latter's nature remains a stubborn mystery. Current searches, however, might have seen the first glimpse of its particle physics identity.

There is overwhelming evidence for the existence of dark matter over a very large range of astrophysical scales, ranging from galactic to the largest observable scales in the universe. However, despite tremendous theoretical and experimental efforts over the past few decades, dark matter remains elusive, and its particle nature remains one of the great unknowns. Although the presence of dark matter has been inferred solely through gravitational interactions, it is very likely that dark-matter particles possess some non-gravitational (i.e. stronger) interactions, which would provide a production mechanism for them in the early universe. These additional interactions would imply that dark matter is detectable in several different ways: directly, through scattering off ordinary atoms in shielded underground detectors; indirectly, through observation of dark-matter annihilation products with satellites, balloons and ground-based telescopes; at accelerator experiments, finally, by attempting to produce it by colliding Standard Model particles at very high energies.

All these searches are currently being performed by a vast number of experiments. Neither direct-detection nor collider searches observe any signal, and they therefore provide strong bounds on the interactions of dark matter with Standard Model states. Indirect searches, on the other hand, suggest ongoing dark-matter annihilations in the galactic centre. More specifically, the Fermi-LAT instrument observes an excess of diffuse GeV energy gamma-ray emission from the galactic centre that could be explained by dark-matter annihilations. What is particularly intriguing about the dark matter explanation is that the required annihilation cross section is roughly what is needed to explain its relic abundance.

A natural question is therefore whether there are any viable particle physics models for dark matter that could explain the Fermi excess while being compatible with other searches. To put this question onto firm ground, one has to specify how the dark-matter particles actually interact with Standard Model particles. Amongst the many possibilities is a well-motivated assumption that the interactions are mediated by an additional new particle that couples very weakly to the visible sector (Fig. 1).

One possibility is that the new particle is a pseudoscalar (a particle that – unlike an ordinary scalar – looks different when viewed through a mirror), which is particularly interesting for several reasons. First, the recent discovery of the Higgs boson gives convincing evidence that fundamental scalars exist. Furthermore, many extensions of the Higgs sector naturally include additional pseudoscalar states. Pseudoscalar mediators are at the same time attractive from a purely phenomenological point of view, since they predict a very low event rate for direct-detection experiments. They thus satisfy most of the severe constraints on dark-matter interactions, but could also be responsible for the Fermi gamma-ray excess.

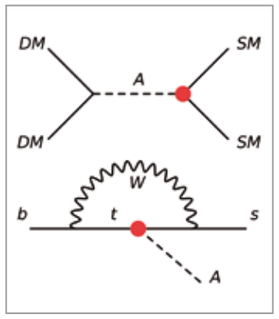

Figure 1
Feynman diagrams showing the annihilation of dark-matter particles into Standard Model states mediated by a pseudoscalar exchange particle (top). Because of loop diagrams, the coupling of the pseudoscalar also induces flavour-changing couplings, which can be constrained by rare meson decays (bottom).

There are stringent constraints, however, on new states coupling to Standard Model particles. For example, although not present at the classical level, quantum mechanical effects induce couplings of the pseudoscalar (denoted "A"), which would lead to so-called flavour violation, e.g. the transition from a bottom to a strange quark (see bottom of Fig. 1). At low energies, quarks are bound in hadrons; a bottom quark in a B meson and a strange quark in a kaon. Flavour-changing transitions such as $b \to s$ or $s \to d$ would therefore lead to rare meson decays, such as $B \to K, A$ or $K \to \pi, A$. The experimental observation that these decays are very rare, implies that the pseudoscalar couplings are very weak. Flavour observables therefore provide a unique opportunity to constrain the interactions of the dark sector with Standard Model particles via a light mediator. The resulting bounds on the coupling to Standard Model states as a function of the pseudoscalar mass are shown in Fig. 2.

The analysis shows that pseudoscalars with couplings large enough to explain the galactic centre excess have to be heavier than about 5 GeV in order not to be ruled out by rare decays, demonstrating that flavour physics is a valuable tool in the challenge to identify the properties of dark matter and its interaction with us.

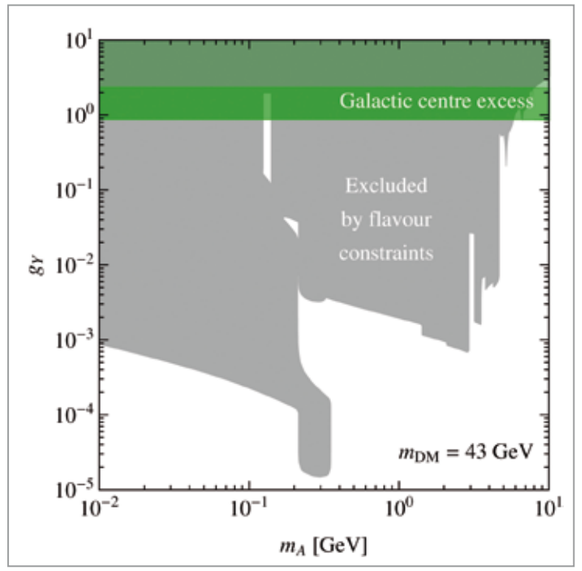

Figure 2
Bounds in the parameter plane spanned by the pseudoscalar mass and the coupling of the pseudoscalar to Standard Model states. The grey region is excluded by experimental bounds on rare meson decays. In the green region, the galactic centre excess can be explained with pseudoscalar mediators.

The overall realisation is that dark matter coupled to ordinary matter via pseudoscalar mediators with masses above that of B mesons is a natural explanation for the observed excess in gamma rays from the galactic centre. In order to confirm that this excess is really due to dark-matter annihilations, it should also be observed in other regions of the sky, with corresponding signals in e.g. dwarf spheroidal galaxies of the Milky Way – something that is on Fermi-LAT's agenda and should be clarified in the next couple of years.

To further pin down the particle nature of dark matter, however, laboratory searches are essential, with searches for flavour violation playing a major role. More specifically, if dark matter indeed couples via a pseudoscalar mediator, this might soon be inferred from an improved measurement of the rare decay $B_s \to \mu^+\mu^-$, demonstrating again the complementarity of particle physics and astrophysics that will be crucial to unravelling one of the greatest mysteries of all time – the nature the dark matter in our universe.

Contact:
Kai Schmidt-Hoberg, kai.schmidt.hoberg@desy.de

References:

Matthew J. Dolan, Christopher McCabe, Felix Kahlhoefer, Kai Schmidt-Hoberg, A taste of dark matter: Flavour constraints on pseudoscalar mediators, arXiv: 1412.5174

Cornering the Higgs.

The Higgs in every corner of phase space

After the discovery of a Higgs boson by the ATLAS and CMS experiments at the LHC at CERN in 2012, a major quest is to study the interactions of the new particle in detail. For this purpose, the production of Higgs particles is being measured in as many different decay channels and kinematic configurations as possible: the Higgs can be produced at rest, or with sizeable transverse momentum, with or without additional hadronic jets, together with *W* and *Z* bosons, or together with heavy quarks. Precise theory predictions for all measured kinematic regions are needed.

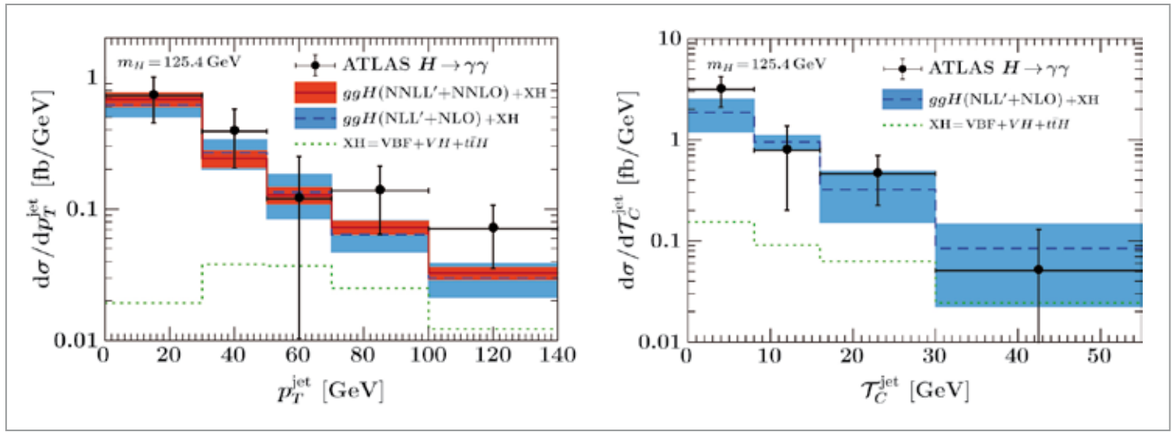

Figure 4

Measured Higgs cross section (data points) as a function of different kinematical quantities compared to theory predictions

In order to precisely test how the newly discovered Higgs boson interacts with all the other particles in the Standard Model – and if it possibly interacts with other, still unknown particles – we have to take a very detailed look at the Higgs events recorded by the ATLAS and CMS experiments. An important classification of these events is done using kinematic quantities, i.e. analysing whether the Higgs boson is produced almost at rest or with significant transverse momentum recoiling against a hadronic jet or a *W* or *Z* boson.

In events with no additional hard jets in the final state, momentum conservation forces the Higgs boson to have low transverse momentum. This is the case for the leading-order contribution to the cross section of the dominant $gg \to H$ production process (Fig. 1), and consequently this is what is observed in most of the events. Occasionally, however, in the process of producing a Higgs via gluon fusion, an energetic gluon is radiated, as shown in Fig. 2 (left). In this case, the Higgs boson has large transverse momentum, which balances against the transverse momentum of the gluon. The gluon itself will subsequently appear in the detector as a hadronic jet with large transverse momentum.

The Higgs can also be produced by coupling to *W* or *Z* bosons, as is also shown in Fig. 2 (centre and right). In these cases, the Higgs also tends to have large transverse momentum. Hence, to distinguish the different cases in Fig. 2, just measuring the transverse momentum of the Higgs itself is not enough. Instead, one needs to identify what kind of additional objects there are in the final state. That is, one needs to count the number of jets and of *W* or *Z* bosons. (Knowing the precise number of jets is also important for distinguishing Higgs events from background events, for example in the $H \to WW$ decay channel.)

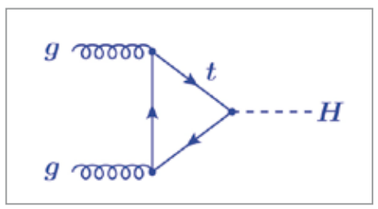

Figure 1

At lowest order, the Higgs is produced with no transverse momentum.

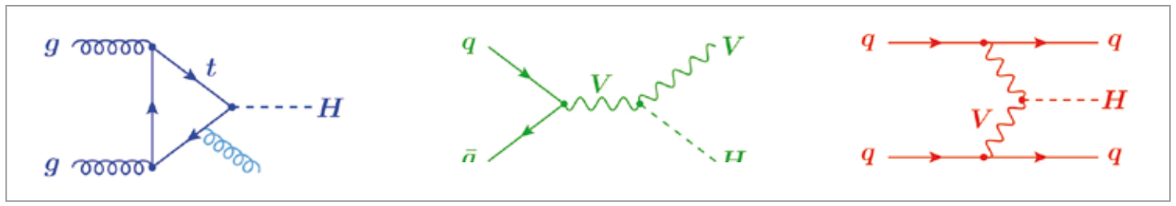

Figure 2

The Higgs can receive non-zero transverse momentum by recoiling against a gluon (left), a *W* or *Z* vector boson (middle), or quarks in vector boson fusion (right).

To count the number of jets in the final state, the jet phase space is divided according to the measured transverse momenta of the jets. This is illustrated in Fig. 3 for the case of 0 jets, 1 jet and 2 or more jets.

To make use of such detailed measurements, one also requires more detailed theory predictions for the cross section as a function of the Higgs boson transverse momentum or of the transverse momentum and number of jets. However, adding more details on top of the calculation of the total Higgs production cross section inevitably makes the predictions more involved. In particular, the jet momentum introduces sensitivity to a new energy scale, which induces large corrections at each order in the perturbative series. By employing an effective field theory description of jets and their interactions, we can break up the calculation into smaller and more manageable pieces, each describing the physics at a specific energy scale. Using renormalisation group evolution in the effective theory then allows us to sum up the dominant perturbative corrections to all orders in the strong coupling constant. In this way, accurate theory predictions can be obtained also for more differential cross sections that depend on additional momentum scales.

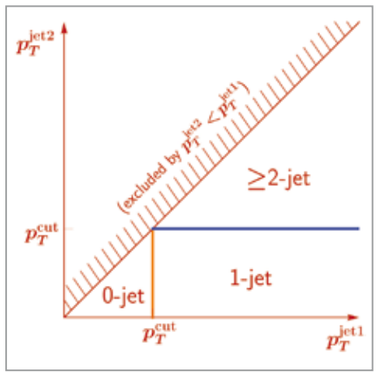

Figure 3

Counting jets by dividing up the jet phase space

The left plot in Fig. 4 shows the Higgs production cross section as a function of the transverse momentum of the hardest jet in the event. The right plot shows the cross section as a function of a novel jet variable that combines the jet's transverse momentum and rapidity, providing a different slicing of the allowed jet phase space. The data points show the measurements performed by the ATLAS experiment in the $H \to \gamma\gamma$ channel; the DESY ATLAS group was strongly involvement in this measurement (see p. 30). The blue and orange bands show our theory predictions [1, 2] at first and second order in resummed perturbation theory. For the jet transverse momentum on the left, these are the most precise theory predictions to date. The theory predictions on the right are the first for this observable. They are currently being extended to the second order and are expected to reach a similarly high precision.

With the new data from the upcoming LHC Run 2, we can expect a substantial decrease in the experimental uncertainties, thus allowing even more precise studies of differential Higgs cross sections.

Contact:
Frank Tackmann, frank.tackmann@desy.de

References:

[1] I. W. Stewart, F. J. Tackmann, J. R. Walsh, S. Zuberi, Phys. Rev. D 89 054001 (2014)
[2] S. Gangal, M. Stahlhofen, F. J. Tackmann, Phys. Rev. D91 054023 (2015)

Precision calculations for deep-inelastic production of heavy quarks.

Getting all the loops together

The present precision of the deep-inelastic world data requires QCD analyses and fits of the heavy quark masses m_c and m_b at 3-loop order [1]. While the massless corrections to this order are available, the heavy-flavour corrections are currently being computed. The results of these calculations will allow the precision data on QCD scaling violations taken at DESY's former HERA collider to be fully exploited at a theoretical accuracy that is better than the current experimental resolution.

The focus is on analytic calculations in the region $Q^2 >> m_Q^2$, which holds at the 1% level for the structure function $F_2(x, Q^2)$ if $Q^2/m^2 \geq 10$, and is a very good approximation for charm in HERA's kinematic regime. The 3-loop heavy-flavour corrections will allow the present theory errors on the parton distributions to be significantly reduced and thus provide refined input distributions for precision measurements at the LHC for various important observables studied there.

In 2009, a first milestone in the present research programme was accomplished – the calculation of a series of Mellin moments [2]. Later, we also studied a new class of 3-loop diagrams that contain both charm and bottom corrections, and computed their moments. Very recently, all logarithmic corrections were computed for the Wilson coefficients contributing to $F_2(x, Q^2)$ and for all transition matrix elements in the variable flavour number scheme (VFNS) to 3-loop order. Here, also the first two complete Wilson coefficients contributing at 3-loop order, $L_g^S(x, Q^2)$ and $L_q^{PS}(x, Q^2)$, were calculated. For the case of the longitudinal structure function $F_L(x, Q^2)$, the asymptotic 3-loop corrections are also known.

In the case of charged-current interactions, including single heavy-quark excitation, the 1-loop calculation had to be repeated because of conflicting results in the literature. At next-to-leading order (NLO), we corrected an earlier result by other authors.

We have by now also obtained complete results for a series of operator matrix elements (OMEs) and massive Wilson coefficients at 3-loop order, respectively, and the OMEs of complete contributions to individual colour factors. The contributions of $O(N_F\ T_F^2\ C_{F,A})$ to all OMEs were calculated, as were those of $O(T_F^2\ C_{F,A})$ to $A_{gg,Q}$. The solution of special higher topologies for ladder-, Benz- and V-graphs was worked out completely. So far, complete 3-loop results were obtained for the massive gluonic OME $A_{gg,Q}$ and in the non-singlet $A_{qq,Q}^{NS}$ and pure singlet A_{Qq}^{PS} cases [3,4]. In Fig. 1, we illustrate as one example the size of the 2- and 3-loop flavour pure singlet contributions, which are significant.

In the course of these calculations, various mathematical and computer-algebraic technologies had to be newly developed, up to new mathematical function spaces and analytic algebraic integration techniques. A recent review on these is given in Ref. [5]. These techniques are generally available for loop calculations in the case of other important high-energy processes with one and more mass scales. The analytic calculation of Feynman diagrams has thus a considerable impact on neighbouring disciplines like mathematics and computer algebra.

The present heavy-flavour corrections will help to improve our knowledge of fundamental parameters of the Standard Model and of the parton densities. In particular, high-luminosity measurements at proposed facilities such as the Electron–Ion Collider (EIC) or the Large Hadron Electron Collider (LHeC) [6] could test these corrections in further detail.

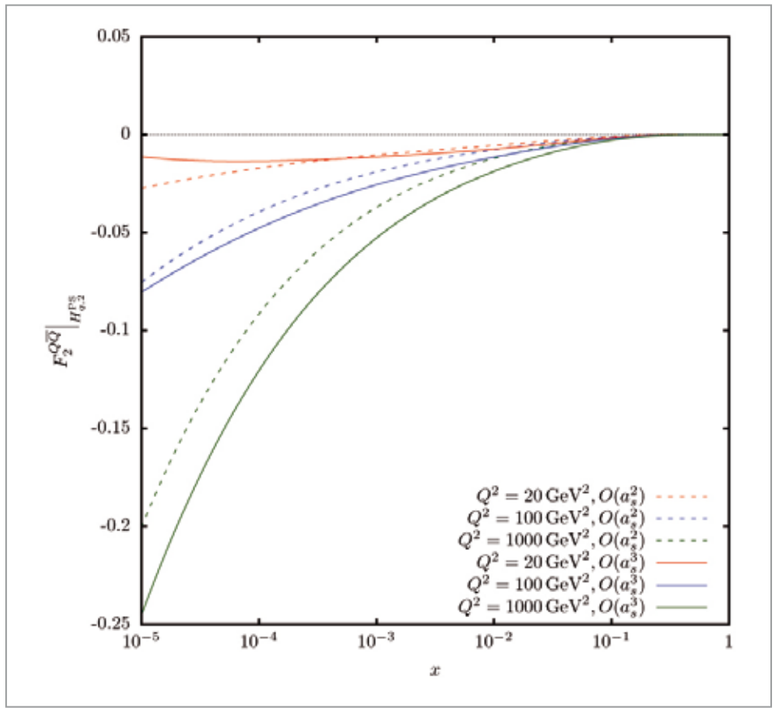

Figure 1

Charm contribution by the Wilson coefficient H_{Qq}^{PS} to the structure function $F_2(x, Q^2)$ as a function of x and Q^2, choosing $Q^2 = \mu^2$ and m_c = 1.59 GeV (on-shell scheme) using the parton distributions ABM12 [4]

Contact:

Johannes Blümlein, johannes.bluemlein@desy.de

References:

[1] S. Bethke et al., Proceedings of the 2011 Workshop on Precision Measurements of α_s, arXiv:1110.0016 [hep-ph];
S. Alekhin, J. Blümlein, K. Daum, K. Lipka and S. Moch, Precise charm-quark mass from deep-inelastic scattering, Phys. Lett. B 720 172 (2013) [arXiv:1212.2355 [hep-ph]]

[2] I. Bierenbaum, J. Blümlein and S. Klein, Mellin Moments of the $O(\alpha_s^3)$ Heavy Flavor Contributions to unpolarized Deep-Inelastic Scattering at $Q^2 >> m^2$ and Anomalous Dimensions, Nucl. Phys. B 820 417 (2009) [arXiv:0904.3563 [hep-ph]]

[3] J. Ablinger et al., The Transition Matrix Element $A_{gq}(N)$ of the Variable Flavor Number Scheme at $O(\alpha_s^3)$, Nucl. Phys. B 882 263 (2014) [arXiv:1402.0359 [hep-ph]];
J. Ablinger et al., The 3-Loop Non-Singlet Heavy Flavor Contributions and Anomalous Dimensions for the Structure Function $F_2(x,Q^2)$ and Transversity, Nucl. Phys. B 886 733 (2014) [arXiv:1406.4654 [hep-ph]];

[4] J. Ablinger et al., The 3-loop pure singlet heavy flavor contributions to the structure function $F_2(x,Q^2)$ and the anomalous dimension, Nucl. Phys. B 890 48 (2015) [arXiv:1409.1135 [hep-ph]]

[5] J. Ablinger and J. Blümlein, Harmonic Sums, Polylogarithms, Special Numbers, and their Generalizations, arXiv:1304.7071 [math-ph]

[6] D. Boer et al., Gluons and the quark sea at high energies: Distributions, polarization, tomography, arXiv:1108.1713 [nucl-th];
J. L. Abelleira Fernandez et al. [LHeC Study Group Collaboration], A Large Hadron Electron Collider at CERN: Report on the Physics and Design Concepts for Machine and Detector, J. Phys. G 39 075001 (2012) [arXiv:1206.2913 [physics.acc-ph]]

Testing spontaneous symmetry breaking in QCD.

Calculating the chiral condensate in lattice QCD

The research group "Particle Physics" at the John von Neumann Institute for Computing (NIC) at DESY is concerned with non-perturbative computations of quantum field theories. A particular emphasis is on quantum chromodynamics (QCD), the theory of the strong interactions between quarks and gluons (see p. 36). The NIC group recently achieved a quantitative determination of the chiral condensate as the order parameter of chiral symmetry breaking. The non-perturbative approach of lattice field theory was used to compute values of the chiral condensate. Employing two lattice discretisations, consistent results were found in the continuum limit, thus providing a most valuable crosscheck.

Figure 1
European sites coordinated by the NIC group. There are two Europe-wide collaborations, Coordinated Lattice Simulations (CLS) and the European Twisted Mass Collaboration (ETMC). The NIC group plays the leading role in driving the generation of the basic gluon field configurations on which physical observables are to be determined.

In the lattice QCD formulation, QCD is constructed on a discrete Euclidean lattice. Besides being a theoretically sound definition of QCD, lattice QCD also allows a numerical evaluation of the path integral that is taken to quantise the system to be performed.

The NIC group is leading and coordinating large collaborations of European institutes (Fig. 1) that perform large-scale computations in lattice QCD. The group is driving the effort to generate gluon field configurations, which are the basic data of lattice QCD, similar to single "events" at collider experiments. Physical observables are (sometimes complicated) functions of these field configurations, and the NIC group also engages in their design and evaluation. Other topics of the broad research programme are fundamental parameters of QCD, transition matrix elements and electroweak and flavour physics.

When QCD is considered for massless quarks, the Lagrangian of the theory is invariant under the exchange of left-handed and right-handed quarks – a phenomenon called chiral symmetry. By developing a chiral condensate, this symmetry can be spontaneously broken in the ground state. This mechanism leads to important consequences, the most notable one being that Goldstone modes are generated that manifest themselves as the pions. It explains why the pions as observed in nature are much lighter than other hadrons. The mechanism also removes the mass degeneracy of individual hadrons (e.g. the proton) with a partner of opposite parity, which would have to be there if chiral symmetry was not broken. The world would look very different without this symmetry breaking!

It is therefore of fundamental interest to test whether the phenomenon of spontaneous chiral symmetry breaking indeed emerges from QCD and to quantitatively determine the value of the order parameter, the chiral condensate.

For the evaluation of the chiral condensate – a main activity of the NIC group – two formulations of lattice QCD were employed. Their predictions differ at finite discretisation length of the theory. In the limit of zero discretisation length, i.e. the continuum limit, both results agree, which provides an excellent crosscheck.

The computations themselves were carried out using a method based on the Banks–Casher relation: the chiral condensate is given by the density of low-lying eigenvalues of the Dirac operator, which can be evaluated in a mathematically clean way by using so-called spectral projectors introduced by L. Giusti and M. Lüscher.

Based on gluon field configurations generated by both the CLS and the EMTC collaboration, the chiral condensate could be computed at various values of the lattice spacing, and for different physical volumes and a number of quark masses. This allowed the systematic errors of the calculations to be estimated on a quantitative level. In particular, it became possible to perform the limits to the continuum and also to zero quark mass. For the calculations, either only the first quark generation (up and down quarks) or the full first two quark generations (including the strange and the charm quark) were employed.

As a result, both collaborations found consistent values of the dimensionless quantity $r_0\Sigma^{1/3}$, where r_0 is a hadronic quantity related to the static potential between quarks ($r_0 \approx 0.5$ fm) and Σ denotes the chiral condensate. The obtained values are $r_0\Sigma^{1/3} = 689(33)$ (ETMC) and $r_0\Sigma^{1/3} = 665(22)$ (CLS) for the case of only the lightest quark family and $r_0\Sigma^{1/3} = 680(29)$ (ETMC) when the second family is also included.

The observed consistency of these values of $r_0\Sigma^{1/3}$ provides a most valuable crosscheck for these non-perturbative computations. Using the experimentally measured value of the kaon decay constant as input, the physical value of r_0 can be determined. The resulting value of the chiral condensate obtained by CLS is $[\Sigma^{MS}(2\ \text{GeV})]^{1/3} = 263(5)$ MeV. This result will influence the next review by the Flavour Lattice Averaging Group (FLAG) of low-energy properties of QCD computed using lattice QCD methods.

The Banks–Casher relation is not the only relation in which the chiral condensate enters, and in order to complete the picture, it is interesting to demonstrate that the numerical values obtained above are consistent with other expectations. In particular, the Gell-Mann–Oakes–Renner relation, i.e. the quark mass dependence of the pion masses, is an ideal tool due to the available high-accuracy results. The Banks-Casher relation was therefore studied by the CLS and ETMC collaborations. And indeed, the numerical value of the chiral condensate obtained from the Banks–Casher relation predicts the mass dependence seen in Fig. 2. This is a numerical proof that the picture of spontaneously broken chiral symmetry in QCD is indeed correct.

Most of the numerical calculations were performed at the Gauss Centre for Supercomputing (GCS), Germany's foremost supercomputing institution. Computing time was awarded to the NIC group through successful applications at the GCS itself or through the Partnership for Advanced Computing in Europe (PRACE).

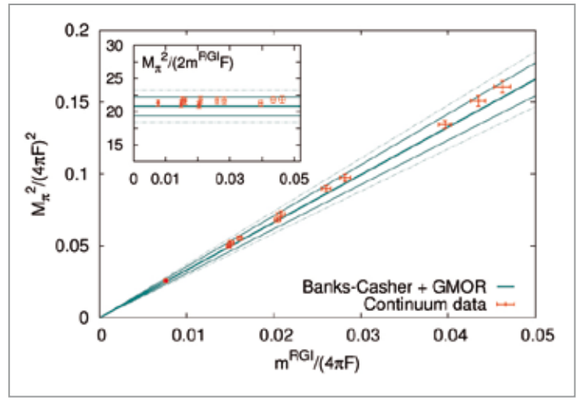

Figure 2
Square of the mass of the pion as a function of the quark mass (in the renormalisation-group-invariant convention), together with the prediction of the effective theory (line with error bands), given in terms of the chiral condensate

Contact:
NIC group:
Karl Jansen, karl.jansen@desy.de
Stefan Schaefer, stefan.schaefer@desy.de
Hubert Simma, hubert.simma@desy.de
Rainer Sommer, rainer.sommer@desy.de

References:

G.P. Engel, L. Giusti, S. Lottini and R. Sommer, Chiral symmetry breaking in QCD Lite, Phys. Rev. Lett. 114 (2015) 11, 112001 [arXiv:1406.4987 [hep-ph]]
K. Cichy, E. Garcia-Ramos and K. Jansen, Chiral condensate from the twisted mass Dirac operator spectrum, JHEP 1310 175 (2013) [arXiv:1303.1954 [hep-lat]]

What happens at strong coupling?

Non-perturbative physics of supersymmetric gauge theories

Gauge theories play a fundamental role in theoretical particle physics. They describe the interactions that bind the quarks into hadrons. It is well understood how these interactions behave at high energies: thanks to the phenomenon of "asymptotic freedom", the effective strength of the interactions depends on the energy scale and goes to zero for large energies. It is much less well understood how the interactions between quarks and gluons behave at low energies: the experimental evidence indicates that the interactions become strong enough to prevent complete separation of the quarks bound in a hadron ("confinement"). The theoretical understanding of this phenomenon has, however, remained elusive. Recently, the DESY theory group shed light on duality phenomena that could lead to an explanation of confinement.

When the interactions are weak, one may approximate the resulting effects reasonably well using perturbation theory. However, the calculation of higher-order effects in perturbation theory very quickly gets cumbersome. It is furthermore well known that additional effects exist that cannot be seen using perturbation theory. As an example, exponentially suppressed contributions to the effective interactions are caused by quantum-mechanical tunneling effects called instantons. From this point of view, the task of understanding the strong-coupling behaviour of gauge theories looks rather hopeless: it would require complete control over all perturbative and non-perturbative effects. In consequence, understanding the strong-coupling behaviour of gauge theories remains an important challenge for quantum field theory.

However, thanks to a phenomenon called duality, the situation has turned out to be better than one might thus have expected, at least in some gauge theories. Roughly speaking, duality means that there exist new field variables allowing us to construct a new perturbative expansion around a strong-coupling limit. The effectiveness of this perturbative expansion is controlled by a parameter that becomes small at strong coupling. In some examples, one may identify the expansion parameter with the inverse of the original coupling constant. The new field variables may be complicated functions of the old ones. Nevertheless, whenever the duality phenomenon is realised, it opens a window that gives a clear view on certain non-perturbative phenomena.

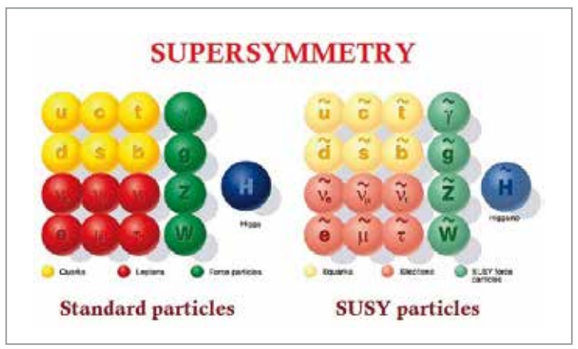

Figure 1

The particle spectrum of supersymmetry (Source: CERN)

Early proposals of G. 't Hooft for the explanation of confinement used a conjectured variant of the duality phenomenon called electric–magnetic duality. It was furthermore conjectured by A. Polyakov and others that instantons play a key role for the emergence of electric–magnetic dualities. Verifying such proposals seemed hopeless for quite some time. However, thanks to some recent spectacular developments in the investigation of supersymmetric versions of the gauge theories, there now exists a large class of example gauge theories where the duality conjectures have been confirmed with the help of some highly non-trivial calculations. Certain important physical quantities, such as expectation values of Wilson loops, have been calculated exactly in a series of works pioneered by V. Pestun. The existence of supersymmetry (SUSY) helps to study these examples. SUSY describes relations between bosons and fermions that may imply that most quantum corrections from bosonic degrees of freedom cancel against similar contributions coming from the fermions. Whatever remains may be exactly calculable.

It is clearly important to better understand how the duality phenomena come about. Recent work in the DESY theory group has shed some light on this question. It is often useful to regard space–time as the limit of a family of spaces of finite volume. The average values of all fields then represent particularly important observable quantities that have to be treated quantum-mechanically. Under certain conditions, one may argue that the dynamics of these average values dominates the physics at low energies. In supersymmetric field theories, for example, it is in many cases possible to demonstrate that the dynamics of the average values decouples from the fluctuations around the average values, as demonstrated in the work of V. Pestun and others. Understanding the dynamics of the average values is then sufficient for answering important physical questions about the low-energy dynamics.

Analysing the dynamics of the average values in finite-volume spaces may therefore help us to understand the origin of duality phenomena. If a duality occurs in a given gauge theory, it must be reflected in the low-energy physics. If the dynamics of the average values display a duality phenomenon, this strongly indicates that a similar phenomenon must be realised in the full theory: whatever the dynamics of the theory may be, it must be consistent with the dynamics of its average values.

The dynamics of the average values was recently determined exactly at DESY for an interesting family of supersymmetric gauge theories. It has an elegant description related to the mathematics of closed curves on two-dimensional surfaces. String theory offers a convenient framework guiding us to this prediction and to many possible generalisations. The gauge theories of interest are regarded as low-energy limits of string theories defined on higher-dimensional space–times with a compact part. The physics at low energies is effectively four-dimensional, but field content and dynamics are determined by the geometry of the compact part. If the compact part contains a two-dimensional surface, one gets a very direct link between closed curves on this surface and observable quantities in the corresponding four-dimensional gauge theory.

Direct physical arguments can then be used to demonstrate the validity of the predictions coming from string theory. We now have a precise abstract mathematical description of the quantum-mechanical system governing the dynamics of the average values. This may be used to derive highly non-trivial quantitative results on certain physical quantities, like Wilson loop expectation values in large families of supersymmetric gauge theories. With the help of these results, one may in particular analyse the origin of electric–magnetic dualities in great detail. As had been suspected for a long time, they are indeed the result of a resummation of instanton effects. This type of reasoning can furthermore be used to offer an explanation for the remarkable relations to two-dimensional conformal field theories recently discovered by L. Alday, D. Gaiotto and Y. Tachikawa, which have stimulated a huge amount of work in this field.

Even if supersymmetry has been crucial for getting exact results on gauge theories up to now, it seems likely that some of the lessons that can be learned by analysing supersymmetric field theories will hold in larger generality. As mentioned above, it had been conjectured for a long time that instantons play a key role for the behaviour of gauge theories at strong coupling. The exact results discussed above illustrate the importance of instanton effects beautifully. One may therefore hope that the study of supersymmetric field theories will allow us to further deepen our insights into non-perturbative phenomena in quantum field theories.

Contact:
Jörg Teschner, joerg.teschner@desy.de

References:

Jörg Teschner, Supersymmetric gauge theories, quantisation of moduli spaces of flat connections, and Liouville theory, arXiv:1412.7140 [hep-th]
Jörg Teschner, Exact results on N=2 supersymmetric gauge theories, arXiv:1412.7145 [hep-th]

Other experiments and experimental facilities.

DESY prides itself on its numerous smaller-scale experimental activities – its so-called “programme-independent research” and its state-of-the-art facilities that support research and R&D activities.

Currently, three small-scale experiments are being carried out at DESY: The OLYMPUS experiment (p. 82) aims at understanding discrepancies in different measurements of the proton’s electric-to-magnetic form factor ratio. The ALPS experiment (“Any Light Particle Search II”, p. 84) is a highly competitive light-shining-through-the-wall experiment that searches for hypothetical weakly interacting slim particles such as hidden photons or axion-like particles. Finally, the GRAVI experiment (p. 86) tests the law of gravitation at extremely small accelerations.

The test beam facility makes use of electron and positron beams delivered by the DESY II synchrotron. The facility is in high demand in many different communities and, in 2014, underwent major upgrade and refurbishment work (“All new in the test beam hall”, p. 88). The DESY Grid & Cloud Centre provides first-class computing resources to the German and international particle and astroparticle physics communities (“Grid and NAF at DESY”, p. 90). The electronics workshop expanded its expertise in bonding methods for detector components to be used in the LHC detector upgrades (“In-house bonding methods for 2D detectors”, p. 92). The library, finally, achieved major developments of the INSPIRE system and of the DESY publication database that already houses 14 300 publications in full text (“Inspire” and “DESY publication database”, pp. 94 and 95).

The OLYMPUS experiment.

Refining, improving and finalising the data analysis

Two-photon exchange is believed to be responsible for the large discrepancies observed between the measurements by several experimental groups of the electric-to-magnetic form factor ratio of the proton. The various analyses made different assumptions on the amount of two-photon exchange actually present; however, the magnitude of the two-photon exchange contribution has never been measured. The OLYMPUS experiment at DESY was designed to quantify the effect of two-photon exchange by measuring the ratio of the positron–proton elastic cross section to the electron–proton elastic scattering cross section over a wide kinematic range with high precision. The experiment used the intense beams of electrons and positrons stored in the DORIS ring at 2.0 GeV, which interacted with an internal windowless hydrogen gas target. The focus of the collaboration now lies on the analysis of the data and the derivation of final results.

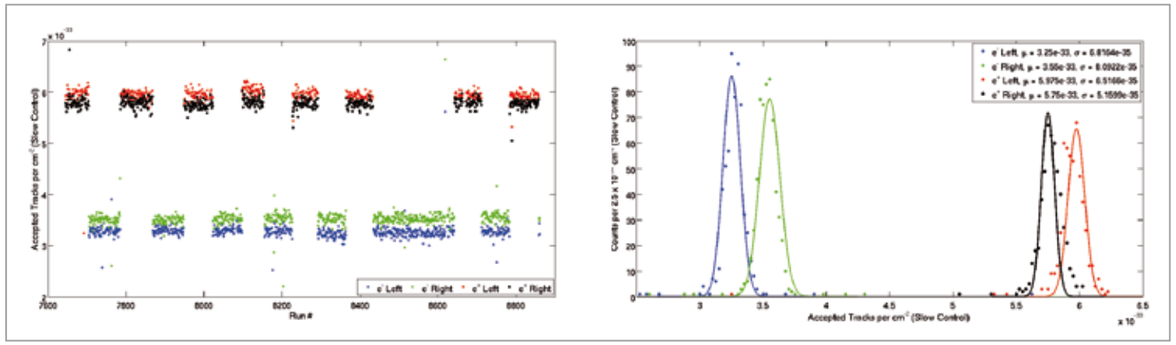

Figure 2

Left: Number of tracks normalised to luminosity in the left and right 12° luminosity detector telescopes for both electron and positron beams over a few weeks of running. Right: The distributions of numbers of tracks per unit luminosity for the data shown in the left plot. The width (sigma) of electron distributions is approximately 2% of the mean, while for positrons it is approximately 1% of the mean. The difference between electrons and positron and between left and right telescopes is due to geometry and acceptance. The uncertainty in the mean and hence integrated luminosity is of course much smaller.

The OLYMPUS experiment was designed to measure the contribution of two-photon exchange to lepton–proton scattering by counting the number of positron–proton elastic-scattering events observed when running with a positron beam and the number of electron–proton elastic-scattering events observed when running with an electron beam, as a function of the scattering angle. The ratio of the two numbers was then taken and corrected for various detector effects, radiative effects, background and luminosity differences between positron running and electron running periods. The needed data was collected at DORIS in 2012 and early 2013 with the former MIT BLAST detector, which had been transferred from MIT in the USA to DESY expressly for this purpose. As sketched in Fig. 1, the detector comprised a toroidal magnetic field with a left/right symmetric arrangement of tracking detectors, time-of-flight scintillation counters and luminosity monitors. The tracking detectors, which consisted of drift chambers, were used to measure the momenta, charges, scattering angles and vertices of out-going charged particles. The time-of-flight detector consisted of vertical scintillation bars in each sector. Their main purpose was to provide a trigger for event selection, but they are also being used for particle identification in the data analysis.

Three new detector systems were added to the original BLAST detector to provide independent and redundant measures of the luminosity. Two tracking telescopes, mounted at a scattering angle of 12°, where the contribution from two-photon exchange is expected to be negligible, were used to measure the rate of small-angle elastic scattering events. In addition, a completely independent system, consisting of symmetric Møller/Bhabha calorimeters, was positioned at 1.29°, very close to the beamline. (Møller/Bhabha scattering is precisely calculable, and a measurement of its rate can thus lead to a reliable luminosity estimate.)

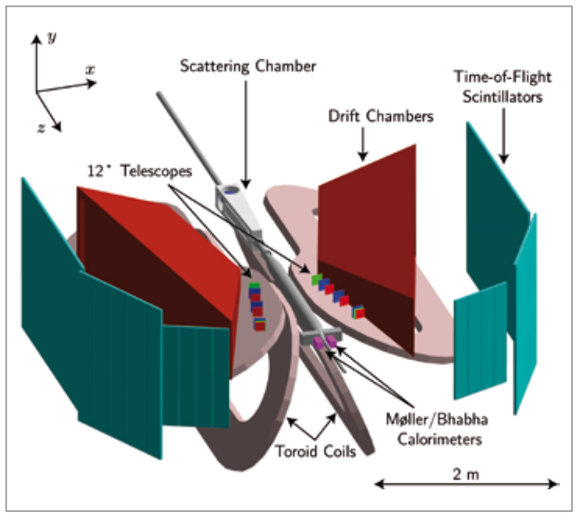

Figure 1

Schematic overview of the OLYMPUS detector

The OLYMPUS collaboration is now finalising its measurement of the cross section ratio, thereby determining the contribution of multiphoton exchange to lepton–proton scattering. The very demanding goal of achieving the needed measurement uncertainty of better than 1% requires a very detailed understanding of the detector performance, which is the present focus of the data analysis. A very large number of studies have been and are being made that are resulting in a much improved understanding of the detector and luminosity. Results include:

- Improvements in detector alignment due in part to a more complete inclusion of survey data into the alignment
- Better estimates of detection efficiency
- Improved Monte Carlo simulation
- Calibration of the beam position monitors in a dedicated test stand
- Improved description of the molecular gas flow of the target
- Better understanding of the non-linear effects in the readout system
- Better understanding of the energy loss in upstream collimators
- Better understanding of the sensitivity of the measurement to the beam positions and slopes
- Improved event model due to the introduction of an improved Møller/Bhabha event generator that includes radiative corrections into the simulation
- Better tracking efficiency and precision due to the introduction of an improved map of the complex toroidal field and to a refined method for extracting fine distance information from the drift chambers
- Better understanding of the Møller/Bhabha calorimeters due to the development of a method that uses the very-small-angle elastic electron–proton scattering observed in the Møller/Bhabha calorimeters to better understand the efficiency of the calorimeters (and also give a crosscheck on the luminosity)
- Better understanding of differences in detector behaviour when running with positron and electron beams

As an example of the improvements, the stability of the new luminosity measurement over the data-taking period is now approaching 1%, as illustrated in Fig. 2. The goal of achieving a ~1% uncertainty in the final result is in sight, and we are looking forward to finally analysing the data itself. The data is currently blinded in order to prevent the introduction of possible biases; it will only be let out of the box when all corrections are fully understood.

Contact:
Uwe Schneekloth, uwe.schneekloth@desy.de

References:

http://web.mit.edu/OLYMPUS/

Any Light Particle Search II.

Providing an intense photon source and evaluating site properties

In spite of the huge success of the Standard Model of particle physics, cosmological observations as well as theoretical considerations require its extension. The ALPS II experiment at DESY is searching for hypothetical "weakly interacting slim particles" (WISPs), focusing on hidden photons and axion-like particles. The hypothesis of the latter's existence receives additional support from different astrophysical observations.

ALPS II is a "light-shining-through-a-wall" (LSW) experiment that is striving for evidence of new particles beyond the known ingredients of the Standard Model. The principle of an LSW experiment is the following: Laser light is shone against an opaque barrier. If WISPs are produced (either by kinetic mixing with photons or by interactions of laser photons with a strong magnetic field), they could easily pass the light-tight barrier and may convert back to photons behind it, giving the impression of light shining through a wall. A clear observation of any light generated in a very well shielded environment could only be explained by such WISPs. Details of the planned ALPS II setup were given in *DESY Particle Physics 2012.*

In 2013, the ALPS II collaboration demonstrated the feasibility of the detector concept (ALPS II will use a superconducting transition edge sensor) and the possibility of straightening the HERA dipole magnets the experiment employs, which is required to provide a sufficient aperture for the light beams. In 2014, ALPS II has, among other achievements, reached important milestones concerning the optical system and evaluated the ambient seismic noise in the HERA tunnel where the final experiment will be located.

In order to further enhance the possibility of WISP production, the ALPS II experiment will generate a high photon flux in front of the wall. This is achieved with a combination of a 35 W continuous-wave laser and an optical resonator. The high performance of the laser in terms of frequency stability and spatial-mode profile allows most of its light to be coupled into the optical resonator, which stores the light for several microseconds and thus enhances the effective power of the light shining against the wall by a factor of 5000. For the current ALPS IIa experiment, located in the HERA west hall as a pathfinder for the final setup in the HERA tunnel, the optical resonator consists of two mirrors that are located on two optical tables 10 m apart from each other. A feedback control loop establishes the resonant condition for a long time and ensures robust operation.

A measure of the quality of the optical resonator is the internal light loss, which has to be extremely low to fulfil the demands of the ALPS II experiment. Losses originate from the surface quality of the two mirrors used to set up the optical resonator and from contaminations caused by dust particles. In order to avoid the latter, the experiment is set up in a cleanroom environment. The ALPS IIa resonator in front of the wall has now been operated for several months to study losses and ambient seismic noise in the lab. The optical resonator could be kept in the resonant condition continuously for more than one hour, showing very stable operation.

However, losses inside the optical resonator are currently higher than expected. An inspection of possible losses due to scattering on the mirror surfaces beyond specifications is currently under investigation (Fig. 1).

To investigate the suitability of the HERA tunnel to host the final ALPS II experiment, ambient-noise sources such as vibrational noise and acoustic noise have to be characterised in order to check if they can limit the performance of the optical resonator. Older data on the seismic motion of the tunnel and the HERA north hall were confirmed by new measurements from autumn 2014. With proper seismic isolation between the floor and the optical tables, the requirements for a stable operation of the optical cavities of ALPS II can be met. Data for slow motions (due to changes of the ground water level or changes of temperature) from water level systems in the tunnel sections and from an inclinometer in the hall of the GRAVI experiment show that the HERA infrastructure is well suited to host the ALPS II experiment.

In the context of ALPS II, a new small-scale activity on novel dark-matter searches has been started. Hidden photons, to which ALPS II will be sensitive already in its first experimental stage, belong to the theoretically well-motivated candidates for lightweight dark matter. A newly formed collaboration that also includes some ALPS members has thus begun to build a dedicated direct-detection setup, called FUNK (Finding U(1)'s of a Novel Kind), for such particles (Fig. 2).

Figure 1

Mirror of the high-power ALPS IIa resonator imaged with an infrared camera. The bright scatter points close to the mirror centre might hint at problems with the surface quality.

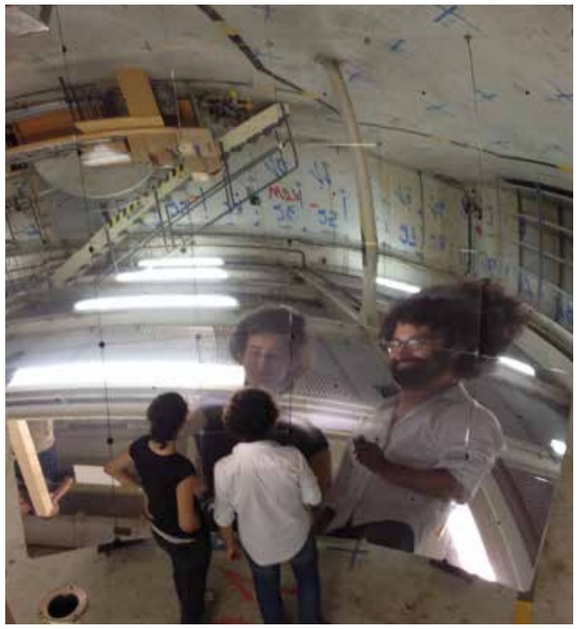

Figure 2

Dark matter composed of hidden photons can, due to the latter's electromagnetic coupling, excite electrons in conductors. The FUNK experiment in Karlsruhe, Germany, measures photonic signals in the centre of a large mirror as a hint to the existence of hidden-photon dark matter. The large mirror (roughly 13 m^2) was a prototype for a fluorescence detector of cosmic radiation and has now found novel and exciting discovery potential in FUNK.

Contact:

Axel Lindner, axel.lindner@desy.de
Andreas Ringwald, andreas.ringwald@desy.de

References:

A. Ringwald, Axions and Axion-Like Particles, arXiv:1407.0546 [hep-ph]
B. Döbrich et al., Hidden Photon Dark Matter Search with a Large Metallic Mirror, arXiv:1410.0200 [physics.ins-det]

The GRAVI experiment.

Testing the law of gravitation at very small accelerations

How does gravity work in a regime where its strength corresponds to only a millionth of a millionth of the gravitational acceleration we experience here on Earth? What might sound like a purely academic question is in fact linked to one of the biggest mysteries in physics today. When astronomers in the first half of the 20th century applied the law of gravitation to very distant astrophysical objects, they were faced with a severe problem. Galaxies toward the edge of galaxy clusters were moving far too fast – at least if their motions were to be explained by the gravitational influence of the other galaxies in the cluster. Astronomers took this as evidence that the cluster must contain a great deal of matter that we cannot see with our telescopes – the first evidence for dark matter. While the concept of dark matter has been adopted by the majority of astrophysicists and cosmologists, slight modification of Newton's law of gravity at very small accelerations below approximately 10^{-10} ms^{-2} cannot be excluded as the origin of the observed discrepancies. The GRAVI experiment at DESY is designed as a laboratory test of the law of gravitation at such small accelerations.

The nature of dark matter is one of the central puzzles in physics at present. Introduced also to explain the rotation velocities of stars in galaxies, dark matter has found a firm place in the Standard Cosmological Model. Still, many questions and difficulties remain (see e.g. [1]). None of the direct searches for dark matter at the LHC at CERN, at dedicated experiments operating in underground laboratories, or with X-ray telescopes have so far been able to produce conclusive evidence for the existence of this postulated elusive form of matter. In this context, the success of an alternative attempt to explain the phenomena attributed to dark matter – modified Newtonian dynamics or MOND – is remarkable [2]. MOND assumes that the gravitational law is slightly modified for small values of the acceleration on the order of $a_0 = 1.2 \cdot 10^{-10}$ m s^{-2}. As an alternative to a modification of Newton's law, MOND could also be interpreted as a violation of Newton's second axiom $F = m \cdot a$, irrespective of the nature of the force F. However, this latter aspect has been experimentally checked, using electromagnetic restoring forces, and Newton's axiom has been verified in several experiments down to accelerations of $5 \cdot 10^{-14}$ m s^{-2} [3]. Therefore, a possible modification according to MOND must rest with the gravitational force alone. The GRAVI experiment aims to test Newton's law using only gravitational forces at accelerations well below the characteristic scale a_0.
A schematic view of the experiment is shown in Fig. 1.

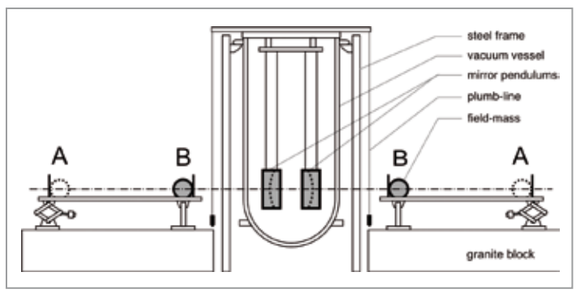

Figure 1
Schematic view of the GRAVI experiment

The apparatus had originally been built and operated at Wuppertal University for a precision measurement of the gravitational constant G [4]. It was later transferred to the former JADE hall at DESY's PETRA III storage ring, and a first measurement with accelerations down to approximately a_0 was carried out in the years 2009–2010.

The central part of the experiment is a microwave resonator, operated at a resonance frequency around 21 GHz. The resonator consists of two mirrors with spherical surfaces, separated by 0.24 m and suspended by thin wires of 2.67 m length, resulting in a pendulum period of 3.3 s. This part of the device is located in a cryostat evacuated to less than 10^{-4} mbar, thus reducing disturbances of the mirror positions from external sources. Two field masses are placed outside the vacuum vessel on either side of the resonator. Their positions alternate every 30 min between a far (A) and a near (B) position. The resulting change of their gravitational pull leads to a microscopic change of the average position of the two mirrors, causing a tiny change of the mean resonance frequency, which is measured twice per second in the experiment (Fig. 2). Averaging these frequency shifts over data-taking periods of several weeks yields a very sensitive measurement of the effect of the gravitational pull. Using the 2010 data, no significant deviations from Newton's law were observed [5].

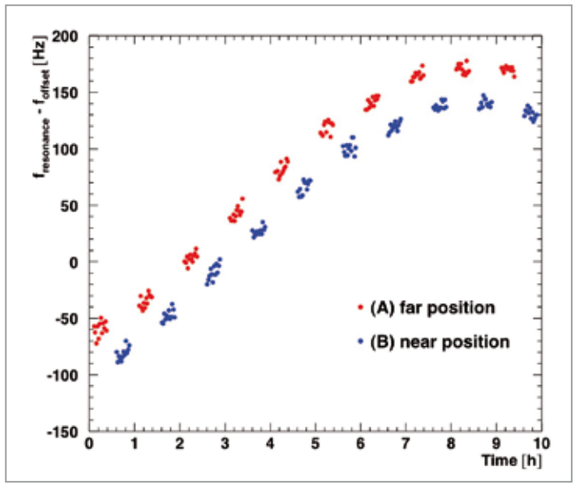

Figure 2
Resonance frequency versus time for a measurement with the 9 kg field masses. Each point corresponds to the average over 90 s. An offset of approximately 21 GHz has been subtracted. The slow drift of the measured frequency is caused by changes of external parameters like temperature and ambient pressure and is corrected for in the analysis.

The setup was subsequently moved to the former hall of the H1 experiment at HERA, which is located 25 m underground, and parts of the apparatus were rebuilt. Several important sources of mechanical noise and of electromagnetic disturbances from PETRA III could thus be eliminated, resulting in a significant improvement of the stability and accuracy of the measurements. As a further step towards avoiding systematic effects, the mechanism for periodically moving the field masses between the near and the far position has been significantly improved, and is still being optimised.

First preliminary measurements with the new setup have been carried out with five pairs of field masses, consisting of spheres of brass, granite, plastic and two hollow plastic spheres, with masses of 9.02 kg, 2.92 kg, 1.00 kg, 0.292 kg and 0.116 kg, respectively (Fig. 3).

The acceleration of a mirror caused by one of the 0.116 kg field masses in the near position is $2.4 \cdot 10^{-11}$ m s^{-2}, corresponding to 20% of a_0. This results in an expected change of the average distance between the two mirrors of about 0.006 nm, far less than an atomic radius. In order to measure changes of this order of magnitude, a change of the resonance frequency of 21 GHz must be measured to an accuracy of better than 0.2 Hz. First preliminary measurements with the 0.116 kg field masses indicate that this sensitivity can in principle be reached, but very subtle systematic effects that might affect the result still need to be thoroughly investigated.

After further improvements to the apparatus, a new accurate test of Newton's law at small accelerations will be performed. While any significant deviation from Newton's prediction would clearly have very far-reaching consequences, finding agreement with Newton would not necessarily invalidate alternative theories of gravitation, because there is no unambiguous way to calculate their predictions for the setup described here.

Figure 3
Field masses used in the experiment. All spheres have an outer diameter of 12.7 cm.

Contact:
Hinrich Meyer, hinrich.meyer@desy.de
Carsten Niebuhr, carsten.niebuhr@desy.de

References:

[1] P. Kroupa et al., arXiv:1006.1647v3; Astronomy and Astrophysics A32 523 (2010); P. Kroupa, arXiv:1406.4860v1
[2] M. Milgrom, Astrophys. J. 270 365 and 371 (1983)
[3] J.H. Gundlach et al., Phys. Rev. Lett. 98 150801 (2007)
[4] U. Kleinevoss et al., Meas. Sci. Technol. 10 439 (1999)
[5] H. Meyer et al., Gen. Rel. and Grav. 44 2537 (2012)

All new in the test beam hall.

Upgrading the pixel telescopes and the DESY II test beam facility

DESY operates the DESY II test beam facility for detector R&D projects from a wide range of communities. After the record year 2013 with far over 400 users, the test beam facility and the DESY II synchrotron itself were shut down for the largest part of 2014 – a great opportunity to upgrade the infrastructure of the facility and to continue to improve the pixel telescopes.

At its Hamburg site, DESY operates a test beam facility with three beamlines. The facility makes use of the electron and positron beams of 1–6 GeV delivered by the DESY II synchrotron via a secondary target. Each test beamline is fully controllable by the users in terms of beam energy and particle flux and provides extensive additional infrastructure. Its ease of use makes the DESY test beam a very popular facility for testing detector prototypes. To make effective use of the beam, however, the point of impact of beam particles with the device under test (DUT) must be measured with a precision that exceeds the expected resolution of the DUT. This is normally done with a so-called beam telescope. Traditionally, users would bring such telescopes with them along with the detector to be tested.

Figure 1
Laser alignment system (left) and beam monitor (right) mounted on the final collimator (yellow)

The DESY-led EUDET project has changed this approach by providing a precise, user-friendly and robust telescope that is sufficiently versatile to serve as a general-purpose, well-trusted device. The on-going high demand and a very active user community continue to strengthen the case for these instruments. An important factor for this continuous success is the strong support offered by DESY for both hardware and software.

Pixel telescope enhancements

2014 saw a lot of activity in the test beam area, particularly in the fields of data acquisition (DAQ) and reconstruction software for the pixel telescopes. These activities were driven by the goal to provide the users with an even more powerful infrastructure for their studies.

EUDAQ is the DAQ framework that has been successfully used since 2007. It allows the easy integration of the DUT and its DAQ with the pixel telescope DAQ. EUDAQ features a very modular design in which individual components communicate via TCP/IP and can run on different networked machines. EUDAQ 2.0 is the next-generation DAQ framework; its development has been driven by activities within the EU-funded AIDA project. It provides a new extended data format that allows storage of additional metadata, such as time stamps and multiple triggers per device readout. In order to be ready for increased trigger rates, EUDAQ 2.0 will be able to handle multiple data streams simultaneously. This makes the setup more flexible and allows bottlenecks to be avoided.

The additionally available metadata enable more thorough consistency checks. As all DUTs obtain their clock directly from the central DAQ, a loss of synchronisation and missed triggers can now be easily identified. Even with these fundamental changes with respect to EUDAQ, a lot of effort has been invested to make the modifications backward compatible in order to preserve existing solutions.

The EUTelescope reconstruction software suite, which encompasses tools for clustering, alignment, track reconstruction and data analysis, also generated a lot of activities. EUTelescope was originally developed for the EUDET pixel telescope, but has always been used in other setups. One key improvement implemented in 2014 is the improved handling of multiple-scattering effects in the track reconstruction. This is especially important for analysing data that were recorded at relatively low-energy beams, as provided for example by DESY II. Therefore, EUTelescope does now provide tracking based on the "general broken lines" (GBL) algorithm, which treats scattering in all present materials more accurately. GBL also offers alignment capabilities via a direct interface to Millepede-II. DESY contributes strongly to both the GBL and the Millepede-II package.

Furthermore, a new geometric clustering algorithm allowing generic pixel shapes and combinations has been developed together with a better detector geometry management system. These changes significantly simplify the analysis flow for the users, enabling an iterative alignment strategy, and improve the usability and run time speed. As a nice add-on, the new software suite can now run in a quasi-online mode, providing a very powerful online monitoring tool.

Improving the beam areas

The 2014 shutdown of DESY II was a great opportunity to further improve the test beam area at DESY. Besides a thorough cleanup, the focus was on the improvement of the safety and user-friendliness of the facility. The entire electrical safety system was overhauled, and flooring and wall paint were renewed. The DACHS access handling system was installed as a secure and standardised access system to the facility. Several enhancements were made both to the user areas and to the beamlines themselves in order to further increase the user-friendliness of the facility. To simplify the alignment of the detector setups with the beamlines, a laser alignment system was installed in all beam areas.

The primary beam targets inside DESY II were all replaced, after 25 years of service, by a new system that offers easier maintenance and control and that will take the test beam through the next 25 years of operations. In the same spirit, the magnet control system for the beamline magnets was replaced, with the new one being more user-friendly and easier to maintain.

A further important upgrade of the facility – among others – was the installation of additional beam monitoring, e.g. of a beam rate monitor right at the end of the beamline, which provides online measurements of the particle rates (Fig. 1). This information is also used to optimise the positions of the primary targets.

So, in eight months of shutdown in 2014, the DESY II test beam facility has seen numerous improvements and enhancements and is now ready for a successful run in 2015.

Simulating the beamlines

Another project during the 2014 shutdown was the implementation of the current beamline setup in a GEANT4-based simulation. The goal was to have a detailed model of the particle flux from the primary target in DESY II up to the entrance of the beam into the user area. One of the first results of this model was the redesign of the synchrotron light shielding with the aim of further reducing this background (Fig. 2).

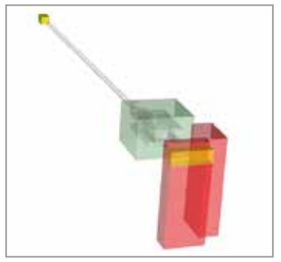

Figure 2
Simulation of the DESY II test beamline, showing the newly installed shielding (red) and the beamline magnet (green)

Outlook for 2015

The 2013 run was exceptionally successful, with over 400 users from all over the world. Out of these, 55% came to DESY for the first time. For the first half-year of 2015, the test beam is again in high demand. After a first call for proposals, 25 groups requested beam time. The LHC upgrade groups constitute the largest user group: 64% of the groups are connected to the LHC (Fig. 3). The pixel telescopes are again in high demand, with two-thirds of the groups requesting their usage. To meet this demand, a second pixel telescope will be permanently installed at DESY in 2015, making it the sixth out of a very successful series.

With the AIDA project ending in February 2015, it was very good news that the successor project – AIDA-2020 – has been approved and will provide travel support for researchers using the DESY II test beam facility for another four years.

The 2014 shutdown gave the DESY test beam and telescope teams the opportunity to implement many improvements to the existing facility. 2015 promises to be another successful year for the DESY II test beam facility, with lots of different user groups from all over the world. This success would not have been possible without the support from many individuals and groups from DESY-FH and DESY-M, and we would like to take this opportunity to thank everybody for their efforts.

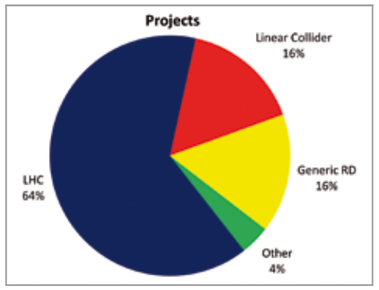

Figure 3
Test beam user groups from the 2015 request

Contact:
testbeam-coor@desy.de
Ralf Diener, ralf.diener@desy.de
Norbert Meyners, norbert.meyners@desy.de
Marcel Stanitzki, marcel.stanitzki@desy.de

References:
http://testbeam.desy.de

Grid and NAF at DESY.

Making use of federated resources

The DESY Grid sites in Hamburg (DESY-HH) and Zeuthen (DESY-ZN) federate computing resources, which allows free job slots to be provided to virtual organisations in an opportunistic usage model. A prominent example for this model are two Belle II Monte Carlo campaigns carried out in 2014 that benefited from reduced LHC computing activities. In consequence, DESY could provide more computing resources to Belle II than any other site worldwide. The National Analysis Facility (NAF) at DESY was redesigned (NAF 2.0) in order to adapt to changed community requirements. In the course of 2014, all users and resources were migrated to the rebuilt infrastructure.

Figure 1

DESY provides first-class computing and storage resources to many different communities through its Grid centres and the National Analysis Facility.

Overview

In the last ten years, the DESY Grid sites [1] have played major roles as members of the European Grid Infrastructure (EGI) [2] and as Tier-2 centres in the Worldwide LHC Computing Grid (WLCG) [3]. The facilities, complemented by the NAF [4], allowed physicists from ATLAS, CMS and LHCb as well as from the ILC community and Belle II to benefit from first-class computing and storage resources that have been reliably operated over the years.

Both DESY sites federate their computing resources and offer an opportunistic usage model to the approx. 20 supported virtual organisations (VOs), including non-LHC experiments and non-HEP groups. During the LHC shutdown in 2014 – a time with reduced computing needs from ATLAS, CMS and LHCb – this model allowed Belle II in particular to profit from the large surplus of computing resources at the DESY-HH site. In the two Monte Carlo campaigns of Belle II in spring and autumn 2014, DESY therefore became the world's biggest contributor to the Belle II computing, delivering roughly a third of the necessary resources. At the same time, DESY-ZN contributed to the astroparticle physics experiments CTA, IceCube and H.E.S.S.

The two DESY sites contribute more than a third to the available Grid computing, which is close to the contribution of the German Tier-1 centre at KIT in Karlsruhe and surpasses the sum of all university contributions.

The Grid

In 2014, numerous improvements and developments of the DESY Grid sites were carried out. All worker nodes were upgraded to deploy the network file system CVMFS natively rather than mounting a central NFS server. This meant a massive improvement of the performance and helps to avoid a single point of failure. In order to make use of recent developments in dCache, first tests of NFS4.1 mounts of the DESY storage space on the worker nodes were started. It is planned to finally deploy this data access strategy in 2015.

Some effort was spent to enable the efficient processing of jobs that request more than one CPU – so-called multicore jobs – on the Grid batch system. By further improving the scheduler developed in-house, which assigns queued jobs to the worker nodes, it is now possible to provide multicore job support to the VOs. Currently, the main customer is ATLAS.

Furthermore, in order to meet the LHC and Belle II 2015 pledges with up-to-date hardware, a significant part of the computing resources had to be renewed. By the end of 2014, the new resources were operated in addition to the old systems, which will be discharged in 2015. The recent values for computing and storage resources available at DESY are listed in Tab. 1. Figure 2 compares the delivered computing resources of all sites in Germany.

Table 1: Overview of the resources at the two DESY sites

Site	Job slots	kHS06	Disk space
DESY-HH	12 000	120	8.3 PB dCache (without HERA data)
DESY-ZN	1600	23	3.1 PB dCache
NAF	4500	55	800 TB Sonas

The NAF

The NAF has been in operation at DESY since 2007 and is well used, both by local groups and throughout Germany. In 2014, the initial design was adapted to meet new challenges and to respond to the evolving needs of the experiments. This involved e.g. providing more graphical tools and other software packages, including commercial products, and better remote access capabilities. Furthermore, new user communities, including the Belle II collaboration and the HERAFitter project, have joined, and legacy support for the HERA communities has started. In 2013, the NAF was redesigned and reimplemented, under the project name "NAF 2.0". During 2014, all resources were migrated from the old NAF to NAF 2.0, and the old NAF was finally decommissioned.

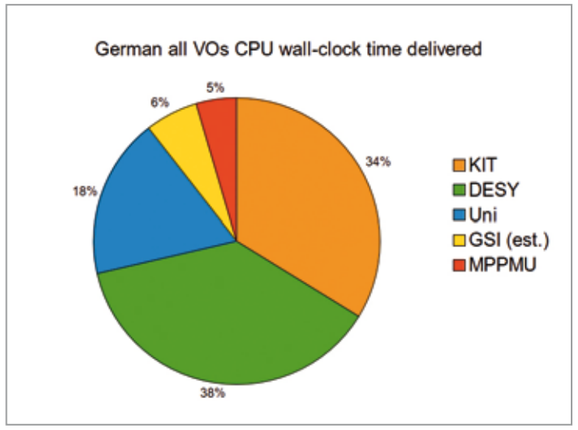

Figure 2

The Helmholtz centres DESY, GSI and KIT provide almost 80% of the delivered German Grid resources.

The NAF is now fully integrated in the existing DESY infrastructure:

- The DESY registry is used for account and access right management. The accounts are regular DESY accounts with username/password authentication.
- The workgroup server setup is similar to that of the standard DESY workgroup servers.
- The batch farm is integrated into the DESY BIRD facility, a general-purpose batch facility used by many DESY groups.
- The AFS cell used for home and group directories is the common desy.de cell.

In addition, to better address remote access needs, several NAF remote desktops were installed. These are server systems that run a desktop installation offering high-performance graphics access remotely. Finally, we denote that the mass storage system dCache, which is central to all HEP data analysis at DESY, is accessible by all computing resources, including NAF 2.0.

Contact:
Andreas Gellrich, andreas.gellrich@desy.de
Andreas Haupt, andreas.haupt@desy.de
Yves Kemp, yves.kemp@desy.de
Peter Wegner, peter.wegner@desy.de

References:

[1] http://grid.desy.de/
[2] http://egi.eu/
[3] http://wlcg.web.cern.ch/
[4] http://naf.desy.de/

In-house bonding methods for 2D detectors.

Flip-chip and wire bonding

Solid-state detectors are widely used in experiments at particle colliders and synchrotron facilities. Especially pixel detectors enjoy great popularity in these communities. These large-format sensors employ fine-pitch contact array patterns with several tens of thousands of electrical interconnections on one sensor chip. The signals are typically processed by CMOS circuits before being sent out to a data-collecting hybrid circuitry requiring several hundred interconnects. Automated high-density wire-bonding and flip-chip-bonding techniques are emerging as critical paths for a successful module assembly. DESY invested in corresponding equipment and applied the processes to the current barrel-pixel detector (BPIX) of the CMS experiment at CERN.

A photograph of the BPIX module is shown in Fig. 1. The hybrid setup consists of a bare silicon module mounted to a pair of Si_3N_4 base strips and a flexible high-density interconnection (HDI) circuit carrier in thin-film technology. The bare module contains a silicon sensor chip connected to 8-by-2 readout chips (ROCs) realised in 250 nm CMOS technology. The pixel contacts of the sensor are grouped in sixteen 80-by-52 pixel sections having two additional guard contacts each. Altogether, 66 592 solder connections exist between sensor and ROCs. Due to the larger ROC depth, a row of 35 wire bond pads per ROC sticks out laterally at the two long module edges (Fig. 5). In this way, 560 bond wires connect the ROC layer to the HDI carrier, which is glued to the sensor on the top (sensor rear side). The sensor is biased through a separate bond wire between the sensor rear side and the HDI carrier. This flexible carrier is assembled with a controller chip (TBM: token bit manager) and passive devices for decoupling and filtering. 78 bond wires connect the TBM chip. All supply voltages and signal channels are provided through a single connector.

DESY and Hamburg University will build a few hundred modules corresponding to about 20% of the new BPIX, where the present detector is planned to be replaced during the technical stop of the LHC in 2016/17. The bare modules will be produced and tested at the DESY FEC laboratory in close collaboration with the DESY CMS group. The attachments of the TBM chip to the HDI carrier, of the HDI carrier to the bare module, and of the bare module to the base strips are carried out at Hamburg University. The wire bonding of the TBM chip and of the bare module is done by the DESY ZE group. The equipment needed for the bare-module production was delivered in summer 2013, and tests were performed to find proper process parameters using ROC-sized bare modules. In 2014, the processes were applied to the large-format devices, and an optimisation of tooling and processes took place. At the same time, the subsequent processes of gluing and wire bonding were elaborated. The following sections describe the bonding methods and summarise first results of the BPIX demonstrator production.

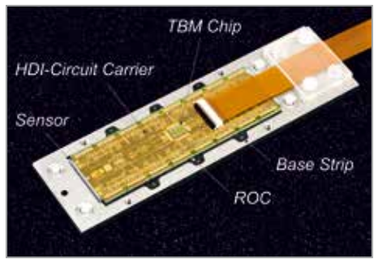

Figure 1
The BPIX module is a three-layer stack of 16 ROCs, a sensor and a HDI circuit carrier assembled with passive devices and a CMOS chip collecting the data of the ROCs.

Flip-chip bonding

After performing wafer-level tests of sensor and ROC wafers, the wafers are sent to an external service provider (PacTech GmbH) to process an under-bump metallisation (UBM) on all sensor and ROC contact pads through 30 µm and 15 µm wide passivation openings, respectively. A layer stack of 5 µm Ni, 200 nm Pd and 50 nm Au is chemically deposited (electroless plating). In this way, mushroom-like contacts (Fig. 2) are formed on the Al pads of the sensor and ROC before the bump metal is deposited. The ROC wafers are then thinned, and the wafers of both types diced and shipped to DESY.

DESY employs a ball-jetting method to deposit bumps on sensor pads without any solder flux or special tooling. Solder balls of 40 µm diameter are singulated from a reservoir and forced onto the pads through a capillary by a N_2 gas flow. A laser pulse melts the ball during its flight through the capillary. The molten ball solidifies again when hitting the cold UBM pad. The solder material is a lead-free Sn alloy with 3% Ag and 0.5% Cu (SAC305). The whole solder ball placement process is performed in an automatic production machine of the type SB²-Jet (PacTech GmbH) at a rate of about 6 h per sensor (~3 Hz jetting rate).

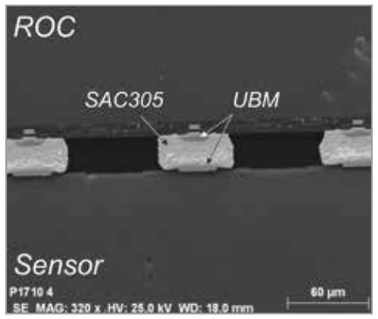

Figure 2
SEM micrograph showing solder bumps in a cross-sectional view after reflow. Each bump connects a UBM stack on the sensor pad to its counterpart on the ROC.

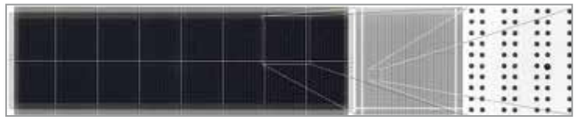

Figure 3
X-ray image of the bare module with sensor chip (right) and sixteen ROCs (left). Each black dot represents a single bump connecting the sensor pixel to the pixel electronics of the ROC.

For flip-chip mounting, DESY uses an automatic bonding machine of the type Fineplacer FEMTO (Finetech GmbH). The sensor is placed with its face up onto a base plate inside a chamber. First, a ball reflow process is performed under N_2 gas atmosphere enriched by formic acid. Then, the bond head picks up a ROC with its face down and places it accurately onto the sensor section at a certain force and temperature for a certain time (bonding). After bonding all 16 ROCs, an in-situ module solder reflow is performed inside the chamber. The complete bonding and reflow process for the module is carried out without any solder flux and takes about 100 min.

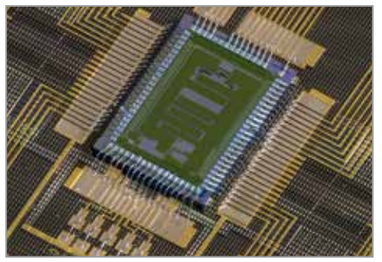

Figure 4
Picture of the bare module's TBM chip. 78 wires connect the TBM chip to the HDI carrier.

Figure 2 shows a cross section of a bare module inspected by means of a scanning electron microscope (SEM), demonstrating the achieved micrometre-level alignment accuracy and a void-free bonding and reflow process. The radiography of a bare module shown in Fig. 3 confirms the high homogeneity of both processes. The electrical interconnection yield exceeds 99.9%, indicating the high process stability.

Wire bonding

Ultrasonic (US) wire bonding takes place at two different stages of the production process. In a first step, 78 wire bonds were realised to connect the TBM chip to the flexible HDI carrier after chip attachment. Figure 4 shows a photograph of the TBM chip region. In a second wire-bonding process, the top layer (HDI carrier) is connected to the bottom layer (ROC) after gluing the HDI carrier to the bare module. Figure 5 displays a corner region with 35 wires per ROC. Both steps were carried out by using an automatic wire-bonding machine of the family G5, model 64000 (F&K Delvotec GmbH), with bond process control (BPC) using a 25 µm AlSi1 wire. The BPC monitors the whole process automatically and regulates the US power accordingly. The usage of a US frequency of 140 kHz with optimised process parameters has led to very stable bond connections without any anomalies. The first and second wire-bonding processes take about 90 and 150 min, respectively.

The on-site process capabilities of ball jetting, flip-chip bonding and wire bonding were successfully applied to build up first BPIX module demonstrators. As key technologies, they are also integral parts of the detector technology platform of the new “Matter and Technologies” programme of the Helmholtz Association.

Figure 5
Picture of the bare module's corner region illustrating details of the layer stack. 35 wires connect a single ROC to the HDI carrier.

Contact:
Karsten Hansen, karsten.hansen@desy.de
Otto-Christian Zeides, otto-christian.zeides@desy.de

INSPIRE.

A step into the future

In 2014, the DESY library and documentation group took first steps towards a fully integrated workflow for ingesting and curating records in the INSPIRE database. This new workflow is already used to process articles proposed by users. Intermittent procedures to process the bulk of the records coming from publishers and the arXiv preprint server were improved. The identification of authors does not rely on a semi-automatic algorithm (clustering) alone but is complemented by the use of ORCID identifiers.

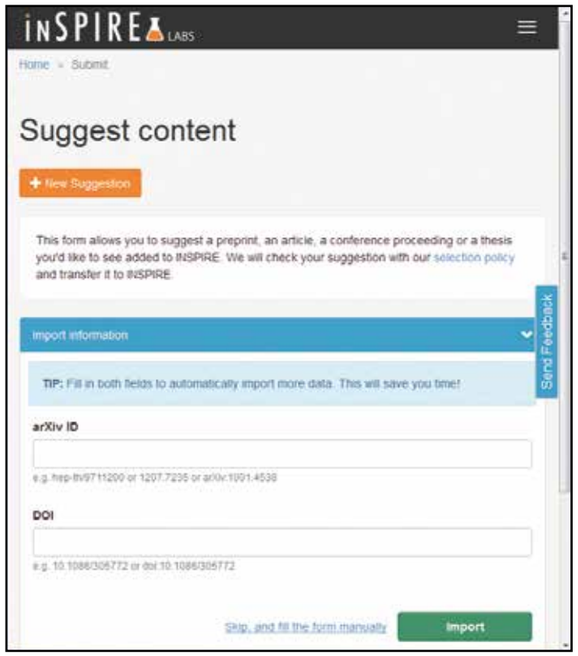

Figure 1

INSPIRE-HEP addition form

After the shutdown of the SPIRES database in February 2013, DESY set up and later further enhanced a temporary harvesting procedure for journal records. Matching of the journal record to the arXiv preprint was improved and now runs more reliably. Records are enriched in many ways to facilitate the manual selection of records based on their content: the enrichment not only determines keywords tagged as being relevant for HEP, it also checks the number of HEP publications by the authors and the corresponding HEP references. For some publishers, like APS, Elsevier and PoS, the conversion of the metadata is already done with the INSPIRE software. This will simplify the integration in the final workflow, where no locally installed procedures are used but everything is shared between the five laboratories running INSPIRE.

An agreement has been reached with the publisher of accelerator conferences JACoW to exchange metadata for the respective contributions. The format of the metadata has been defined, the conversion is set up by DESY, and from 2015 onwards, records will be included in INSPIRE shortly after publication. The JACoW author-ID is part of the metadata, which improves author identification and will help to import the metadata into the DESY publication database. The identifiers of the global Open Researcher Contributor Identification (ORCID) project will be heavily used by INSPIRE. Already now, publications that are not related to HEP, and hence not included in INSPIRE, are shown in the publication list of an author if his/her ORCID ID is known. While identifying authors by clustering works well for western authors, it fails for Asian names. Here, it is almost essential to have a global author identifier that is also used by publishers.

Another improvement that is directly visible for the user strongly optimises the processing by DESY staff: the old email-based form for suggesting new content for INSPIRE has been replaced by a new interactive form (Fig. 1). It can be pre-filled with content from arXiv or CrossRef. The user can add additional information like subject category or comments. Thanks to the login via ORCID, the identity of the submitter is known. Further processing of the record-to-be is done in an integrated workflow, which will finally be used for all sources of records. The form is implemented on the site https://labs.inspirehep.net/, which runs the latest version of INVENIO and is used for user testing of new features.

Contact:
Kirsten Sachs, kirsten.sachs@desy.de

DESY publication database.

Visible open access for science

Since 2006, the DESY publication database has been accounting for all publications resulting from research activities on the DESY campus. It stores bibliographic data as well as full texts for reference, access and long-term availability; and it is used to generate various publication lists on campus web pages, for the purpose of reporting for programme-oriented funding (POF) as well as for the annual report lists.

The DESY publication database is based on INVENIO, an open-source software also used by INSPIRE. Together with six other partners from the Helmholtz Association and RWTH Aachen, additional functionality was developed in the framework of the Just anOther INvenio INstance (JOIN²) project. In 2014, the system was upgraded to a new version of the underlying INVENIO software, which included various software enhancements for better end-user experience. To facilitate funding requirements and ease compliance for researchers with various funding rules, grant information was further enriched.

Over the entire year, the DESY library offered continuous practical training. Additionally, three specialised internal training courses were provided for the publication appointees.

To improve the visibility of DESY's achievements and to fulfill growing open-access requirements (e.g. EU Framework Programmes, the Helmholtz Initiative and Networking Fund, ongoing encouragement for open access by the German Research Foundation DFG, etc.), the DESY publication database follows the so-called “green way of open access” for the full texts. The DESY library implemented a workflow that will check and handle legal issues (e.g. embargoes and restrictions by copyright transfer) and make the full texts available online if possible.

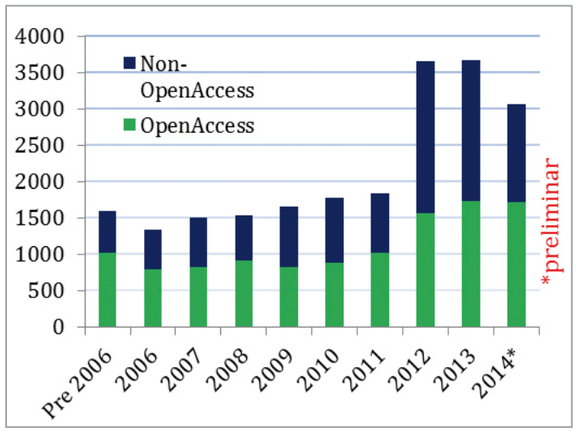

Figure 1

Open-access and non-open-access publication

Moreover, open access – the free and unrestricted online access to research publications – can give access to non-article results, like posters, slides, reports, preprints etc., that may raise the interest of fellow researchers.

Currently, the publication database gives access to about 14 300 publications in full text, which is about 50% of all entries. Additionally, we observe a marked increase in publication numbers since 2012. Also, DESY’s engagement in the Sponsoring Consortium for Open Access Publishing in Particle Physics (SCOAP³) allows for many publications of the DESY particle and astroparticle physics division to be included into open access, under the liberal CC-BY-4.0 license.

A growing number of DESY groups use automatic export functionalities built into the publication database to ease access and show their achievements online without additional work.

Contact:
Robert Thiele, robert.thiele@desy.de
Alexander Wagner, alexander.wagner@desy.de

References:

JOIN² project homepage: http://nbn-resolving.de/urn:nbn:de:0001-2015012904
Open access: http://openaccess.mpg.de/Berlin-Declaration

References.

Committees.

DESY Administrative Council

Representatives of the Federal Republic of Germany:

Gerda Winkler
(Federal Foreign Office)

MinR'in **O. Keppler**
(Federal Ministry of Education and Research)

Dr.-Ing. **B. Vierkorn-Rudolph** (Chair)
(Federal Ministry of Education and Research)

Representatives of the Free and Hanseatic City of Hamburg:

LRD Dr. **R. Greve**
(Ministry of Education and Research)

Christian Zierau
(Ministry of Education and Research)

Representatives of the Federal State of Brandenburg

Dr. **C. Menzel**
(Ministry of Finance)

Carsten Feller
(Ministry of Science, Research and Culture)

Representatives from science and industry

Prof. Dr. **U. Beisiegel**
(President, Georg-August-Universität Göttingen)

Dr. **M. Kraas**
(Olympus Surgical Technologies)

Dr. **G. Mecke**
(AIRBUS)

Dr. **C. Quitmann**
(Lund University)

DESY Board of Directors

Dr. **R. Brinkmann**
(Accelerator Division)

Prof. Dr. **H. Dosch**
(Chairman of the DESY Board of Directors)

Prof. Dr. **J. Mnich**
(Particle Physics and Astroparticle Physics Division)

C. Scherf
(Administrative Division)

Prof. Dr. **E. Weckert**
(Photon Science Division)

Prof. Dr. **C. Stegmann**
(Representative of the Directorate in Zeuthen)

DESY Scientific Council

Prof. Dr. **J. Daillant**
Soleil Synchrotron (FR)

Prof. Dr. **M. Danilov**
ITEP, Moscow (RU)

Prof. Dr. **P. Drell** (Chair)
SLAC National Accelerator Laboratory (USA)

Dr. **F. Gianotti**
CERN, Geneva (CH)

Prof. Dr. **K. Hämäläinen**
University of Helsinki (FIN)

Prof. Dr. **J. Hastings**
SLAC National Accelerator Laboratory (USA)

Dr. **N. Holtkamp**
SLAC National Accelerator Laboratory (USA)

Prof. Dr. **S. Larsen**
MAX IV Laboratory (SE)

Dr. **L. Merminga**
TRIUMF (CA)

Prof. Dr. **S. Ritz**
University of California (USA)

Dr. **E. Shaposhnikova**
CERN (CH)

Prof. Dr. **G. Wormser**
LAL, Orsay (FR)

Prof. Dr. **L. Young**
Argonne National Laboratory (USA)

and the chairs of

ECFA: Dr. **M. Krammer**
Institut für Hochenergiephysik, Wien (AU)

DESY MAC: Prof. Dr. **A. Jankowiak**
HZB

DESY PRC: Prof. Dr. **A. White**
U Texas (USA)

DESY PSC: Prof. Dr. **M. Drescher**
U Hamburg

DESY Scientific Board: Dr. **M. Kasemann**
DESY

European XFEL: Prof. Dr. **M. Altarelli**
European XFEL

DESY Scientific Board

M. Ackermann (DESY)
R. Balewski (DESY)
T. Behnke (DESY)
F. Beckmann (HZG)
M. Bieler (DESY)
K. Borras (DESY)
F. Brinker (DESY)
K. Büßer (DESY)
W. Buchmüller (DESY)
H. Chapman (DESY)
W. Drube (DESY)
G. Eckerlin (DESY)
H. J. Eckold (DESY)
E. Elsen (DESY)
K. Flöttmann (DESY)
B. Foster (DESY)
H. Franz (DESY)
H. Graafsma (DESY)
G. Grübel (DESY)
V. Gülzow (DESY)
T. Finnern (DESY)
I.-M. Gregor (DESY)
J. Haller (U Hamburg)
A. Kappes (DESY)
M. Kasemann (DESY, Chair)
F. Kärtner (DESY)
O. Kind (HU Berlin)
A. Meyer (DESY)
V. Miltchev (U Hamburg)
K. Mönig (DESY)
T. Naumann (DESY)
C. Niebuhr (DESY)
D. Nölle (DESY)
E. Plönjes-Palm (DESY)
M. Pohl (DESY)
B. Racky (DESY)
K. Rehlich (DESY)
A. Ringwald (DESY)
R. Röhlsberger (DESY)
R. Santra (DESY)
O. Seeck (DESY)
S. Schlenstedt (DESY)
J. Schmid (EMBL)
M. Schmitz (DESY)
T. Schörner-Sadenius (DESY)
V. Schomerus (DESY)
S. Schreiber (DESY)
C. Schrör (TU Dresden)
H. Schulte-Schrepping (DESY)
H. C. Schulz-Coulon (U Heidelberg)
A. Schwarz (DESY)
G. Sigl (U Hamburg)
J. Spengler (DESY)
A. Stierle (DESY)
M. Tischer (DESY)
T. Tschentscher (XFEL)
J. Viefhaus (DESY)
M. Vogt (DESY)
P. Wegner (DESY)
G. Weiglein (DESY)
H. Weise (DESY)
M. Wieland (U Hamburg)

Machine Advisory Committee (MAC)

Dr. **M. Borland** (ANL, USA)
Dr. **H. Braun** (PSI, CH)
Dr. **Massimo Ferrario** (INFN, IT)
Dr. **Zhitong Huang** (SLAC, USA)
Prof. Dr. **A. Jankowiak** (HZB, DE, Chair)
Dr. **K. Oide** (KEK, JP)
Dr. **Pantaleo Raimondi** (ESRF, FR)
Dr. **R. Schmidt** (CERN, CH)

Physics Research Committee (PRC)

Dr. **E. Aschenauer** (BNL, USA)
Prof. Dr. **M. Beneke** (RWTH Aachen)
Dr. **M. Carena** (Fermilab, USA)
Dr. **J. Haba** (KEK, JP)
Prof. Dr. **M. Kobel** (TU Dresden)
Prof. Dr. **L. Köpke** (U Mainz)
Prof. Dr. **R. Ong** (UCLA, USA)
Prof. Dr. **L. Rosenberg** (U Washington, USA)
Prof. Dr. **R. Wallny** (ETH Zürich, CH)
Prof. Dr. **A. White** (U Texas, Chair)
Dr. **R. Yoshida** (ANL, USA)

Ex-officio members:
Prof. Dr. **H. Dosch** (DESY)
Prof. Dr. **J. Mnich** (DESY)
Prof. Dr. **E. Weckert** (DESY)
Dr. **R. Brinkmann** (DESY)
Prof. Dr. **C. Stegmann** (DESY)

Helmholtz Alliance International Advisory Board

Prof. Dr. **J. Brau** (U Oregon, USA)
Dr. **N. Geddes** (RAL, UK)
Dr. **P. Jenni** (CERN, CH)
Dr. **D. Schlatter** (CERN, CH)
Prof. Dr. **B. Spaan** (U Dortmund)
Prof. Dr. **T. Virdee** (Imperial College London, UK)
Prof. Dr. **S. Yamada** (U Tokyo, JP)

German Committee for Particle Physics (KET)

Prof. Dr. **S. Bethke** (MPP München)
Dr. **K. Borras** (DESY)
Prof. Dr. **I. Brock** (U Bonn)
Prof. Dr. **S. Dittmaier** (U Freiburg)
Prof. Dr. **T. Hebbeker** (RWTH Aachen)
Prof. Dr. **W. Hollik** (MPP München)
Dr. **H. Kroha** (MPP München)
Prof. Dr. **T. Mannel** (U Siegen)
Prof. Dr. **J. Mnich** (DESY)
Prof. Dr. **T. Müller** (KIT)
Prof. Dr. **G. Quast** (KIT)
Prof. Dr. **P. Schleper** (U Hamburg, Chair)
Dr. **C. Rembser** (CERN, CH)
Prof. Dr. **R. Rückl** (U Regensburg)
Prof. Dr. **C. Zeitnitz** (U Wuppertal)

German Committee for Astroparticle Physics (KAT)

Prof. Dr. **J. Bluemer** (KIT)
Prof. Dr. **K. Danzmann** (U Hannover)
Prof. Dr. **R. Diehl** (MPE Garching)
Prof. Dr. **D. Horns** (U Hamburg)
Prof. Dr. **J. Jochum** (U Tübingen)
Prof. Dr. **K. Kampert** (U Wuppertal)
Prof. Dr. **M. Lindner** (MPP München)
Prof. Dr. **L. Oberauer** (TU München)
Prof. Dr. **E. Resconi** (TU München)
Prof. Dr. **G. Sigl** (U Hamburg)
Prof. Dr. **C. Stegmann** (DESY)
Prof. Dr. **C. Weinheimer** (U Münster)

Memberships.

ACOT - Advisory Committee of Triumf (CA)
Kerstin Borras

AIDA Steering Committee
Ties Behnke, Frank Gaede, Ingrid-Maria Gregor

Akademie der Wissenschaften Hamburg
Wilfried Buchmüller

Astroparticle Physics European Coordination (ApPEC), PRC
Christian Spiering (Chair)

ATLAS-Canada Review Committee on NSERC (CA)
Eckhard Elsen

ATLAS Executive Board
Klaus Moenig

Belle II Scrutiny Group
Bernd Löhr (Chair)

BMBF, Gutachterauschuss Physik der kleinsten Teilchen
Eckhard Elsen, Joachim Mnich, Hans Weise

CALICE Steering Board
Felix Sefkow

CERN Machine Advisory Committee
Reinhard Brinkmann

CERN Science Policy Committee
Christian Spiering

Cluster of Excellence for Fundamental Physics, Munich: Science Advisory Committee
Wilfried Buchmüller (Chair)

CMS Collaboration Board, Executive Board and Management Board
Matthias Kasemann

CMS Collaboration Board, Conference Committee and Finance Board
Kerstin Borras

Computing Resource Review Board, CERN
Volker Gülzow

Data Preservation and Long Term Analysis in High Energy Physics (DPHEP) International Steering Committee
Zaven Akopov, Cristinel Diaconu, Achim Geiser, Volker Gülzow, David South

Deutsches Kommitee für Astroteilchenphysik (KAT)
Christian Stegmann

DFG Allianz "Digitale Information"
Martin Köhler

Deutsches Forschungsnetz DFN Verwaltungsrat / Betriebsausschuss
Joachim Mnich / Volker Gülzow

DKE Deutsche Kommission Elektrotechnik, Elektronik und Informationstechnik im DIN und VDE, Kommission K967
Peter Göttlicher

DPG Beirat für Wissenschaftskommunikation
Thomas Naumann

DPG Beirat Fachverband Teilchenphysik
Christian Spiering

DPG Wissenschaftlicher Beirat des Physikzentrums
Georg Weiglein

EMI Project Technical Board (PTB)
Patrick Fuhrmann

European Committee for Future Accelerators (ECFA)
Kerstin Borras, Joachim Mnich

European Particle Physics Communication Network (EPPCN)
Thomas Zoufal

European Strategy Group for Accelerator R&D (ESGARD)
Eckhard Elsen

FAIR Machine Advisory Committee
Kay Wittenburg

Finance and Investment Board and Governance Review Group, UK Institute of Physics
Brian Foster

Gauss-Allianz Mitgliederversammlung und Grid-Koordinationsausschuss
Volker Gülzow

German Executive LHC Outreach Group (GELOG)
Ulrike Behrens, Klaus Ehret, Gerrit Hörentrup, Matthias Kasemann, Christian Mrotzek, Thomas Naumann, Barbara Warmbein, Thomas Zoufal

GridKA, Technical Advisory Board
Martin Gasthuber, Birgit Lewendel

Helmholtz Alliance, Institute Assembly
Ingrid-Maria Gregor

Helmholtz Alliance, Management Board
Ties Behnke (Scientific Coordinator), Karsten Büßer, Eckhard Elsen, Matthias Kasemann, Joachim Mnich, Klaus Mönig, Thomas Schörner-Sadenius

Helmholtz Alliance, Project Boards
Doris Eckstein, Eckhard Elsen, Volker Gülzow, Matthias Kasemann, Katja Krüger, Klaus Mönig, Thomas Schörner-Sadenius, Felix Sefkow, Georg Weiglein

Helmholtz Arbeitskreis Bibliotheks- und Informationsmanagement
Martin Köhler

Helmholtz Lenkungsausschuss Struktur der Materie
Ties Behnke, Reinhard Brinkmann, Helmut Dosch, Volker Gülzow, Joachim Mnich, Edgar Weckert

Helmholtz Programmsprecher für Elementarteilchenphysik
Joachim Mnich

Helmholtz Versammlung der Wissenschaftlich-Technischen Räte
Matthias Kasemann

Helsinki Institute of Physics, Scientific Advisory Board (SAB)
Wilfried Buchmüller

IEEE Radiation Instrumentation Steering Committee
Ingrid-Maria Gregor

ILC CLIC Physics and Detector Working Group
Felix Sefkow

ILC MDI Common Task Group
Karsten Büßer (Chair)

ILC Physics and Experiment Board
Ties Behnke, Karsten Büßer

ILC Programme Advisory Committee
Hans Weise

ILC Top Level Change Control Evaluation Panel
Karsten Büßer

ILD Executive Board
Ties Behnke, Karsten Büßer, Wolfgang Lohmann, Felix Sefkow

ILD Steering Boards
Ties Behnke, Felix Sefkow

INSPIRE Steuerungsgremium
Jürgen Reuter, Kirsten Sachs

Institute Pluridisciplinaire Hubert Curien, Advisory Board
Joachim Mnich

InterActions collaboration board
Christian Mrotzek

International Committee for Future Accelerators (ICFA)
Joachim Mnich

International Committee for Future Accelerators (ICFA), Panel on Advanced and Novel Accelerators
Siegfried Schreiber, Rainer Wanzenberg

International Lattice Data Grid
Karl Jansen

International Particle Physics Outreach Group (IPPOG)
Thomas Naumann

John von Neumann Institute for Computing (NIC)
Joachim Mnich (Director)

John von Neumann Institute for Computing (NIC), Scientific Council
Hubert Simma

Joint Institute of Nuclear Research JINR, Scientific Council
Joachim Mnich

KIT Center for Elementary Particle and Astroparticle Physics (KCETA), Advisory Board
Joachim Mnich

Koordinierungsaussschuss Datenverarbeitung der Helmholtz-Gemeinschaft (KODA)
Volker Gülzow

Komitee für Beschleunigerphysik
Hans Weise

Komitee für Astroteilchenphysik (KAT)
Christian Spiering

Komitee für Elementarteilchenphysik (KET)
Kerstin Borras, Joachim Mnich

Laboratoire Souterraine Modane, Advisory Board
Christian Spiering

L'Agence d'Evaluation de la Recherche et de l'Enseignement Superieur (AERES)
Eckhard Elsen

LHCC Experiments Committee (LHCC)
Eckhard Elsen (Chair)

LHC Resources Review Board (LHC-RBB)
Manfred Fleischer

LHC-RBB, Computing Resource Scrutiny Board
Martin Gasthuber

LHC-RRB Scrutiny Group
Carsten Niebuhr

LHC US Accelerator Research Program Advisory Committee
Kay Wittenburg

Linear Collider Board (LCB)
Joachim Mnich

Linear Collider Collaboration, European Director
Brian Foster

LPNHE, Wissenschaftlicher Rat
Klaus Mönig

MPI Munich, Scientific Advisory Board
Joachim Mnich (Chair)

Particle Data Group
Klaus Mönig, Georg Weiglein

PETA QCD Scientific Advisory
Karl Jansen

Rat Deutscher Sternwarten
Martin Pohl

Romanian CERN Project Funding Program of the Romanian Ministry of Education and Resaerch, Scientific Advisory Board
Eckhard Elsen

SFB676, Vorstand
Jenny List, Andreas Ringwald

Sponsoring Consortium for Open Access Publishing in Particle Physics (SCOAP3)
Florian Schwennsen

STFC, Oversight Committee for ATLAS UK
Bernd Löhr, Marcel Stanitzki

TTC Technical Board
Wolf-Dietrich Möller, Detlef Reschke, Hans Weise (Chair)

Collaborations.

H1

I. Physikalisches Institut, RWTH Aachen

Universiteit Antwerpen (BE)

VINCA Institute of Nuclear Sciences, Belgrade (CS)

School of Physics and Space Research, University of Birmingham (GB)

Inter-University Institute for High Energies ULB-VUB, Brussels (BE)

National Institute for Physics and Nuclear Engineering, Bucharest (RO)

Rutherford Appleton Laboratory, Chilton, Didcot (GB)

Henryk Niewodnicza□ski Institute of Nuclear Physics, Cracow (PL)

Institut für Physik, Technische Universität Dortmund

Joint Institute for Nuclear Research (JINR), Dubna (RU)

CEA, DSM-DAPNIA, CE Saclay, Gif-sur-Yvette (FR)

Deutsches Elektronen-Synchrotron DESY

Institut für Experimentalphysik, Universität Hamburg

Max-Planck-Institut für Kernphysik, Heidelberg

Kirchhoff Institut für Physik, Universität Heidelberg

Physikalisches Institut, Universität Heidelberg

Institute of Experimental Physics, Slovak Academy of Sciences, Košice (SK)

School of Physics and Chemistry, University of Lancaster (GB)

Oliver Lodge Laboratory, University of Liverpool (GB)

Queen Mary and Westfield College, London (GB)

Physics Department, University of Lund (SE)

Physics Department, University of Manchester (GB)

CPPM, Université de la Méditerranée, IN2P3-CNRS, Marseille (FR)

Departamento de Fisica Aplicada, CINVESTAV, Mérida (MX)

Departamento de Fisica, CINVESTAV, México (MX)

Institute for Theoretical and Experimental Physics (ITEP), Moscow (RU)

Russian Academy of Sciences, Lebedev Physical Institute, Moscow (RU)

Max-Planck-Institut für Physik, Werner-Heisenberg-Institut, München

LAL, Université Paris-Sud, IN2P3-CNRS, Orsay (FR)

Laboratoire Louis Leprince Ringuet, LLR, IN2P3-CNRS, Palaiseau (FR)

LPNHE, Université Paris VI et VII, IN2P3-CNRS, Paris (FR)

Faculty of Natural Sciences and Mathematics, University of Montenegro, Podgorica (YU)

Institute of Physics, Academy of Sciences of the Czech Republic, Prague (CZ)

Institute of Particle and Nuclear Physics, Charles University, Prague (CZ)

Dipartimento di Fisica, Università Roma 3 and INFN Roma 3, Rome (IT)

Institute for Nuclear Research and Nuclear Energy, Sofia (BG)

Institute of Physics and Technology, Mongolian Academy of Sciences, Ulaanbaatar (MN)

Paul Scherrer Institut, Villigen (CH)

Fachbereich Physik, Bergische Universität-GH Wuppertal

Yerevan Physics Institute, Yerevan (AM)

Institut für Teilchenphysik, ETH Zürich (CH)

Physik Institut, Universität Zürich (CH)

ZEUS

Department of Engineering in Management and Finance, University of the Aegean (GR)

Institute of Physics and Technology, Ministry of Education and Science of Kazakhstan, Almaty (KZ)

National Institute for Nuclear and High Energy Physics (NIKHEF), Amsterdam (NL)

Argonne National Laboratory (ANL), Argonne IL (USA)

Andrews University, Berrien Springs MI (USA)

University and INFN, Bologna (IT)

Physikalisches Institut, Universität Bonn

H.H. Wills Physics Laboratory, University of Bristol (GB)

Panjab University, Chandigarh (IN)

Rutherford Appleton Laboratory, Chilton, Didcot (GB)

Physics Department, Ohio State University, Columbus OH (USA)

Physics Department, Calabria University and INFN, Cosenza (IT)

The Henryk Niewodniczaski Institute of Nuclear Physics, Cracow (PL)

Department of Physics, Jagellonian University, Cracow (PL)

Faculty of Physics and Nuclear Techniques, AGH-University of Science and Technology, Cracow (PL)

University and INFN, Florence (IT)

Fakultät für Physik, Universität Freiburg

Department of Physics and Astronomy, University of Glasgow (GB)

Deutsches Elektronen-Synchrotron DESY

Institut für Experimentalphysik, Universität Hamburg

Nevis Laboratories, Columbia University, Irvington on Hudson NY (USA)

Institute for Nuclear Research, National Academy of Science and Kiew National University, Kiew (UA)

Department of Physics, Malaya University, Kuala Lumpur (MY)

Department of Physics, Chonnam National University, Kwangju (KR)

High Energy Nuclear Physics Group, Imperial College London (GB)

Physics and Astronomy Department, University College, London (GB)

Institute de Physique Nucléaire, Université Catholique de Louvain, Louvain-la-Neuve (BE)

Department of Physics, University of Wisconsin, Madison WI (USA)

Departamento de Fisica Teórica, Universidad Autónoma Madrid (ES)

Department of Physics, McGill University, Montreal (CA)

Moscow Engineering und Physics Institute, Moscow (RU)

Institute of Nuclear Physics, Moscow State University, Moscow (RU)

Max-Planck-Institut für Physik, München

Department of Physics, York University, North York (CA)

Department of Physics, University of Oxford (GB)

Dipartimento di Fisica, University and INFN, Padova (IT)

Department of Particle Physics, Weizmann Institute, Rehovot (IL)

Dipartimento di Fisica, Università La Sapienza and INFN, Roma (IT)

Polytechnic University, Sagamihara (JP)

Kyungpook National University, Taegu (KR)

School of Physics, University of Tel Aviv (IL)

Department of Physics, Tokyo Institute of Technology, Tokyo (JP)

Department of Physics, Tokyo Metropolitan University, Tokyo (JP)

Department of Physics, University of Tokyo (JP)

Università degli Studi di Torino and INFN, Torino (IT)

Università del Piemonte Orientale, Novara and INFN, Torino (IT)

Department of Physics, University of Toronto (CA)

Institute for Particle and Nuclear Study, KEK, Tsukuba (JP)

Department of Physics, Pennsylvania State University, University Park PA (USA)

Institute for Nuclear Studies, Warsaw (PL)

Institut of Experimental Physics, University of Warsaw (PL)

Faculty of General Education, Meiji Gakuin University, Yokohama (JP)

HERMES

National Institute for Subatomic Physics (NIKHEF), Amsterdam (NL)
Department of Physics and Astronomy, Vrije Universiteit, Amsterdam (NL)
Randall Laboratory of Physics, University of Michigan, Ann Arbor MI (USA)
Physics Division, Argonne National Laboratory, Argonne IL (USA)
Dipartimento di Fisica dell'Università and INFN, Bari (IT)
School of Physics, Peking University, Beijing (CN)
Nuclear Physics Laboratory, University of Colorado, Boulder CO (USA)
Joint Institute for Nuclear Research (JINR), Dubna (RU)
Physikalisches Institut, Universität Erlangen-Nürnberg
Dipartimento di Fisica dell'Università and INFN, Ferrara (IT)
Laboratori Nazionali di Frascati, INFN, Frascati (IT)
Petersburg Nuclear Physics Institute (PNPI), Gatchina (RU)
Department of Subatomic and Radiation Physics, University of Gent (BE)
Physikalisches Institut, Universität Gießen
School of Physics and Astronomy (SUPA), University of Glasgow (GB)
Deutsches Elektronen-Synchrotron DESY
P. N. Lebedev Physical Institute, Moscow (RU)
Institute for High Energy Physics (IHEP), Protvino (RU)
Institut für Theoretische Physik, Universität Regensburg
Gruppo Sanità, INFN and Physics Laboratory,
Istituto Superiore di Sanità, Rome (IT)
Department of Physics, Tokyo Institute of Technology, Tokyo (JP)
Department of Physics, University of Illinois, Urbana IL (USA)
TRIUMF, Vancouver (CA)
Andrzeij Soltan Institute for Nuclear Studies, Warsaw (PL)
Yerevan Physics Institute, Yerevan (AM)

OLYMPUS

INFN, Bari (IT)
Universität Bonn
Massachusetts Institute of Technology, Cambridge (USA)
University of New Hampshire, Durham (USA)
INFN, Ferrara (IT)
Petersburg Nuclear Physics Institute, Gatchina (RU)
University of Glasgow (UK)
Deutsches Elektronen-Synchrotron DESY
Hampton University, Hampton (USA)
Universität Mainz
MIT-Bates Linear Accelerator Center, Middleton (USA)
INFN, Rome (IT)
Arizona State University, Tempe (USA)
Yerevan Physics Institute, Yerevan (AM)

TESLA Technology Collaboration

Argonne National Laboratory (ANL), Argonne IL (USA)
Fermi National Accelerator Laboratory (Fermilab), Batavia IL (USA)
Peking University, Beijing (CN)
Institute for High Energy Physics (IHEP), Academia Sinica, Beijing (CN)
Tsinghua University, Beijing (CN)
Lawrence Berkeley National Laboratory, Berkeley (USA)
Helmholtz-Zentrum Berlin für Materialien und Energie
AGH-University of Science and Technology, Cracow (PL)
Henryk Niewodniza□ski Institute of Nuclear Physics, Polish Academy of Science, Cracow (PL)
Technische Universität Darmstadt
CCLRC, Daresbury & Rutherford Appleton Laboratory, Chilton, Didcot (GB)
Forschungszentrum Rossendorf, Dresden
Joint Institute for Nuclear Research (JINR), Dubna (RU)
Universität Frankfurt/Main
Laboratori Nazionali di Frascati, INFN, Frascati (IT)
Helmholtz-Zentrum Geesthacht
CERN, Geneva (CH)
CEA/DSM DAPNIA, CE-Saclay, Gif-sur-Yvette (FR)
Deutsches Elektronen-Synchrotron DESY
Universität Hamburg
Raja Ramanna Centre of Advanced Technology (RRCAT), Indore (IN)
Cornell University, Ithaca NY (USA)
Variable Energy Cyclotron Centre VECC, Kolkata (IN)
Istituto Nazionale di Fisica Nucleare (INFN), Legnaro (IT)
Technical University of Lodz (PL)
Royal Holloway University of London (RHUL/JAI), London (GB)
University College London (UCL), London (GB)
SLAC National Accelerator Laboratory (SLAC), Menlo Park CA (USA)
Istituto Nazionale di Fisica Nucleare (INFN), Milan (IT)
Institute for Nuclear Research (INR), Moscow (RU)
Moscow Engineering and Physics Institute (MEPhI), Moscow (RU)
Bhabha Atomic Research Centre (BARC), Mumbai (IN)
Jefferson Lab, Newport News VA (USA)
Budker Institute for Nuclear Physics (BINP), Novosibirsk (RU)
LAL, Université Paris-Sud, IN2P3-CNRS, Orsay (FR)
Andrzej Soltan Institute for Nuclear Studies, Otwock-□wierk (PL)
University of Oxford (JAI), Oxford (GB)
Institute for High Energy Physics (IHEP), Protvino (RU)
Istituto Nazionale di Fisica Nucleare (INFN), Rome II (IT)
Universität Rostock
Sincrotrone Trieste (IT)
Institute for Particle and Nuclear Study, KEK, Tsukuba (JP)
Canada's National Laboratory for Particle and Nuclear Physics (TRIUMF), Vancouver (CA)
Institute of High Pressure Physics, Polish Academy of Sciences, Warsaw (PL)
Warsaw University of Technology (WUT), Warsaw (PL)
Warsaw University, Department of Physics, Warsaw (PL)
Bergische Universität-GH Wuppertal
CANDLE, Yerevan (AM)
Yerevan Physics Institute, Yerevan (AM)

Publications.

Physics at the Terascale, Helmholtz Alliance

Rheinisch-Westfälische Technische Hochschule Aachen
Humboldt-Universität zu Berlin
Rheinische Friedrich-Wilhelms-Universität Bonn
Deutsches Elektronen-Synchrotron DESY
Technische Universität Dortmund
Technische Universität Dresden
Albert-Ludwigs-Universität Freiburg
Justus-Liebig-Universität Gießen
Georg-August-Universität Göttingen
Universität Hamburg
Ruprecht-Karls-Universität Heidelberg
Karlsruher Institut für Technologie – Großforschungsbereich
Karlsruher Institut für Technologie – Universitätsbereich
Johannes Gutenberg-Universität Mainz
Ludwig-Maximilians-Universität München
Max-Planck-Institut für Physik München
Universität Rostock
Universität Siegen
Julius-Maximilians-Universität Würzburg
Bergische Universität Wupperta

Adjunct Partner
Universität Regensburg

ALPS

Deutsches Elektronen-Synchrotron DESY
Universität Hamburg
Albert-Einstein-Institut Hannover
Johannes Gutenberg-Universität Mainz

Collaborations with DESY Participation

ATLAS Collaboration
Belle/Belle II Collaboration
CMS Collaboration
CALICE Collaboration
LCTPC Collaboration
John von Neumann Institute for Computing (NIC)

Amanda/IceCube
CTA
H.E.S.S.
MAGIC

ALPS

Published

E. Armengaud et al.
Conceptual design of the International Axion Observatory (IAXO).
Journal of Instrumentation, 9(05):T05002, and DESY-2014-02782.
doi: 10.1088/1748-0221/9/05/T05002.

A. G. Dias et al.
The quest for an intermediate-scale accidental axion and further ALPs.
Journal of high energy physics, 2014(6):37, and DESY-2014-02855.
doi: 10.1007/JHEP06(2014)037.

Group, Particle Data.
Review of Particle Physics.
Chinese physics / C, 38(9):090001, and PUBDB-2014-03548.
doi: 10.1088/1674-1137/38/9/090001.

Ph.D. Thesis

J. Dreyling-Eschweiler.
A superconducting microcalorimeter for low-flux detection of near-infrared single photons.
University of Hamburg, Hamburg, 2014.

J. E. von Seggern.
Constraining Weakly Interacting Slim Particles with a Massive Star and in the Laboratory.
University of Hamburg, Hamburg, 2014.

ATLAS

Published

S. Alekhin et al.
Nucleon PDF separation with the collider and fixed-target data.
37th International Conference on High Energy Physics, Valencia (Spain), 07/02/2014 - 07/09/2014.
Elsevier, Amsterdam, July 2014.

A. Altheimer et al.
Boosted Objects and Jet Substructure at the LHC.
The European physical journal / C, 74(3):2792, and PUBDB-2015-01073, arXiv:1311.2708; FERMILAB-PUB-13-669.
doi: 10.1140/epjc/s10052-014-2792-8.

S. Argyropoulos and T. Sjöstrand.
Effects of color reconnection on $t\bar{t}$ final states at the LHC.
Journal of high energy physics, 1411(11):43, and PUBDB-2014-04436, LU-TP-14-23; DESY-14-134; MCNET-14-15; arXiv:1407.6653.
doi: 10.1007/JHEP11(2014)043.

ATLAS Collaboration.
A Measurement of the Ratio of the Production Cross Sections for W and Z Bosons in Association with Jets with the ATLAS Detector.
The European physical journal / C, 74(12):3168, and PUBDB-2015-01045, CERN-PH-EP-2014-200; arXiv:1408.6510.
doi: 10.1140/epjc/s10052-014-3168-9.

ATLAS Collaboration.
A neural network clustering algorithm for the ATLAS silicon pixel detector.
Journal of Instrumentation, 9(09):P09009, and PUBDB-2014-03623, CERN-PH-EP-2014-120; arXiv:1406.7690.
doi: 10.1088/1748-0221/9/09/P09009.

ATLAS Collaboration.
A study of heavy flavor quarks produced in association with top quark pairs at $\sqrt{s} = 7$ TeV using the ATLAS detector.
Physical review / D, 89:072012, and DESY-2014-02661, CERN-PH-EP-2013-030; arXiv:1304.6386.
doi: 10.1103/PhysRevD.89.072012.

ATLAS Collaboration.
Comprehensive measurements of t-channel single top-quark production cross sections at $\sqrt{s}$ = 7 TeV with the ATLAS detector.
Physical review / D, 90(11):112006, and PUBDB-2014-04561, CERN-PH-EP-2014-133; arXiv:1406.7844.
doi: 10.1103/PhysRevD.90.112006.

ATLAS Collaboration.
Electron and photon energy calibration with the ATLAS detector using LHC Run 1 data.
The European physical journal / C, 74(10):3071, and PUBDB-2014-03805, CERN-PH-EP-2014-153; arXiv:1407.5063.
doi: 10.1140/epjc/s10052-014-3071-4.

ATLAS Collaboration.
Electron reconstruction and identification efficiency measurements with the ATLAS detector using the 2011 LHC proton-proton collision data.
The European physical journal / C, 74(7):2941, and DESY-2014-03161, CERN-PH-EP-2014-040; arXiv:1404.2240.
doi: 10.1140/epjc/s10052-014-2941-0.

ATLAS Collaboration.
Erratum: Search for new Phenomena in Final States with large Jet Multiplicities and missing Transverse momentum at $\sqrt{s}$ = 8 TeV Proton-Proton Collisions using the ATLAS Experiment.
Journal of high energy physics, 2014(1):109, and PUBDB-2015-01106, arXiv:1308.1841.
doi: 10.1007/JHEP01(2014)109.

ATLAS Collaboration.
Evidence for Electroweak Production of $W^{\pm}W^{\pm}jj$ in pp Collisions at $\sqrt{s} = 8$ TeV with the ATLAS Detector.
Physical review letters, 113:141803, and PUBDB-2014-03724, CERN-PH-EP-2014-079; arXiv:1405.6241.
doi: 10.1103/PhysRevLett.113.141803.

ATLAS Collaboration.
Fiducial and differential cross sections of Higgs boson production measured in the four-lepton decay channel in pp collisions at $\sqrt{s}$=8 TeV with the ATLAS detector.
Physics letters / B, 738:234, and PUBDB-2014-03725, CERN-PH-EP-2014-186; arXiv:1408.3226.
doi: 10.1016/j.physletb.2014.09.054.

ATLAS Collaboration.
Flavour tagged time dependent angular analysis of the $B_s \to J/\psi\phi$ decay and extraction of $\Delta\Gamma_s$ and the weak phase ϕ_s in ATLAS.
Physical review / D, 90(5):052007, and PUBDB-2014-03707, CERN-PH-EP-2014-43; arXiv:1407.1796.
doi: 10.1103/PhysRevD.90.052007.

ATLAS Collaboration.
Jet Energy Measurement and its Systematic Uncertainty in Proton - Proton Collisions at $\sqrt{s} = 7$ TeV with the ATLAS Detector.
The European physical journal / C, 75(1):17, and PUBDB-2015-00862, CERN-PH-EP-2013-222; arXiv:1406.0076.
doi: 10.1140/epjc/s10052-014-3190-y.

ATLAS Collaboration.
Light-Quark and Gluon Jet Discrimination in pp Collisions at $\sqrt{s} = 7$ TeV with the ATLAS Detector.
The European physical journal / C, 74(8):3023, and PUBDB-2015-01058, CERN-PH-EP-2014-058; arXiv:1405.6583.
doi: 10.1140/epjc/s10052-014-3023-z.

ATLAS Collaboration.
Measurement of χ_{c1} and χ_{c2} production with $\sqrt{s}$ = 7 TeV pp collisions at ATLAS.
Journal of high energy physics, 2014(7):154, and DESY-2014-03160, CERN-PH-EP-2013-202; arXiv:1404.7035.
doi: 10.1007/JHEP07(2014)154.

ATLAS Collaboration.
Measurement of differential production cross-sections for a Z boson in association with b-jets in 7 TeV proton-proton collisions with the ATLAS detector.
Journal of high energy physics, 10:141, and PUBDB-2014-04114, CERN-PH-EP-2014-118; arXiv:1407.3643.
doi: 10.1007/JHEP10(2014)141.

ATLAS Collaboration.
Measurement of dijet cross sections in pp collisions at 7 TeV centre-of-mass energy using the ATLAS detector.
Journal of high energy physics, 2014(5):59, and DESY-2014-02927, CERN-PH-EP-2013-192; arXiv:1312.3524.
doi: 10.1007/JHEP05(2014)059.

ATLAS Collaboration.
Measurement of distributions sensitive to the underlying event in inclusive Z-boson production in pp collisions at $\sqrt{s} = 7$ TeV with the ATLAS detector.
The European physical journal / C, 74(12):3195, and PUBDB-2014-04584, CERN-PH-EP-2014-162; arXiv:1409.3433.
doi: 10.1140/epjc/s10052-014-3195-6.

ATLAS Collaboration.
Measurement of event-plane correlations in $\sqrt{s_{NN}}$=2.76 TeV lead-lead collisions with the ATLAS detector.
Physical review / C, 90:024905, and PUBDB-2014-03510, CERN-PH-EP-2014-021.
doi: 10.1103/PhysRevC.90.024905.

ATLAS Collaboration.
Measurement of Flow Harmonics with Multi-Particle Cumulants in Pb+Pb Collisions at $\sqrt{s_{\rm NN}} = 2.76$ TeV with the ATLAS Detector.
The European physical journal / C, 74(11):3157, and PUBDB-2015-01036, CERN-PH-EP-2014-171; arXiv:1408.4342.
doi: 10.1140/epjc/s10052-014-3157-z.

ATLAS Collaboration.
Measurement of Four-Lepton Production at the Z Resonance in pp Collisions at $\sqrt{s}$ = 7 and 8 TeV with ATLAS.
Physical review letters, 112(23):231806, and DESY-2014-02895, CERN-PH-EP-2014-047; arXiv:1403.5657.
doi: 10.1103/PhysRevLett.112.231806.

ATLAS Collaboration.
Measurement of Higgs boson production in the diphoton decay channel in pp collisions at center-of-mass energies of 7 and 8 TeV with the ATLAS detector.
Physical review / D, 90(11):112015, and PUBDB-2015-00219, CERN-PH-EP-2014-198; arXiv:1408.7084.
doi: 10.1103/PhysRevD.90.112015.

ATLAS Collaboration.
Measurement of inclusive jet charged-particle fragmentation functions in Pb+Pb collisions at $\sqrt{s_{NN}}$ = 2.76 TeV with the ATLAS detector.
Physics letters / B, B739:320, and PUBDB-2014-04093, CERN-PH-EP-2014-101; arXiv:1406.2979.
doi: 10.1016/j.physletb.2014.10.065.

ATLAS Collaboration.
Measurement of long-range pseudorapidity correlations and azimuthal harmonics in $\sqrt{s_{\rm NN}}$ = 5.02 TeV proton-lead collisions with the ATLAS detector.
Physical review / C, 90:044906, and DESY-2014-03770, CERN-PH-EP-2014-201; arXiv:1409.1792.
doi: 10.1103/PhysRevC.90.044906.

ATLAS Collaboration.
Measurement of the Centrality and Pseudorapidity Dependence of the Integrated Elliptic Flow in lead-lead Collisions at $\sqrt{s_{\rm NN}} = 2.76$ TeV with the ATLAS detector.
The European physical journal / C, 74(8):2982, and PUBDB-2015-01038, CERN-PH-EP-2014-065; arXiv:1405.3936.
doi: 10.1140/epjc/s10052-014-2982-4.

ATLAS Collaboration.
Measurement of the cross section of high transverse momentum $Z \to b\bar{b}$ production in proton–proton collisions at $\sqrt{s}$=8 TeV with the ATLAS Detector.
Physics letters / B, 738:25, and PUBDB-2014-03644, CERN-PH-EP-2014-064;arXiv:1404.7042.
doi: 10.1016/j.physletb.2014.09.020.

ATLAS Collaboration.
Measurement of the cross-section of high transverse momentum vector bosons reconstructed as single jets and studies of jet substructure in pp collisions at $\sqrt{s}$ = 7 TeV with the ATLAS detector.
New journal of physics, 16(11):113013, and PUBDB-2014-04122, CERN-PH-EP-2014-123; arXiv:1407.0800.
doi: 10.1088/1367-2630/16/11/113013.

ATLAS Collaboration.
Measurement of the electroweak production of dijets in association with a Z-boson and distributions sensitive to vector boson fusion in proton-proton collisions at $\sqrt{s}$ = 8 TeV using the ATLAS detector.
Journal of high energy physics, 04:42, and DESY-2014-02591, CERN-PH-EP-2013-227.
doi: 10.1007/JHEP04(2014)031.

ATLAS Collaboration.
Measurement of the Higgs boson mass from the $H \to \gamma\gamma$ and $H \to ZZ^* \to 4\ell$ channels with the ATLAS detector using 25 fb^{-1} of pp collision data.
Physical review / D, 90(5):052004, and PUBDB-2014-03509, CERN-PH-EP-2014-122.
doi: 10.1103/PhysRevD.90.052004.

ATLAS Collaboration.
Measurement of the inclusive isolated prompt photons cross section in pp collisions at $\sqrt{s}$=7 TeV with the ATLAS detector using 4.6fb-1.
Physical review / D, 89(5):052004, and PUBDB-2015-01212, arXiv:1311.1440; CERN-PH-EP-2013-164.
doi: 10.1103/PhysRevD.89.052004.

ATLAS Collaboration.
Measurement of the low-mass Drell-Yan differential cross section at $\sqrt{s}$ = 7 TeV using the ATLAS detector.
Journal of high energy physics, 2014(6):112, and DESY-2014-02928, CERN-PH-EP-2014-020; arXiv:1404.1212.
doi: 10.1007/JHEP06(2014)112.

ATLAS Collaboration.
Measurement of the mass difference between top and anti-top quarks in pp collisions at $\sqrt{s} = 7$ TeV using the ATLAS detector.
Physics letters / B, 728:363, and DESY-2014-00169, CERN-PH-EP-2013-171.
doi: 10.1016/j.physletb.2013.12.010.

ATLAS Collaboration.
Measurement of the muon reconstruction performance of the ATLAS detector using 2011 and 2012 LHC proton-proton collision data.
The European physical journal / C, 74(11):3130, and PUBDB-2014-04482, CERN-PH-EP-2014-151; arXiv:1407.3935.
doi: 10.1140/epjc/s10052-014-3130-x.

ATLAS Collaboration.
Measurement of the parity-violating asymmetry parameter α_b and the helicity amplitudes for the decay $\Lambda_b^0 \to J/\psi\Lambda^0$ with the ATLAS detector.
Physical review / D, 89:092009, and DESY-2014-02877, CERN-PH-EP-2014-034; arXiv:1404.1071.
doi: 10.1103/PhysRevD.89.092009.

ATLAS Collaboration.
Measurement of the Production and Lepton charge asymmetry of W Bosons in Pb+Pb Collisions at $\sqrt{s_{\rm NN}} = 2.76$ TeV with the ATLAS Detector.
The European physical journal / C, 75(1):23, and PUBDB-2015-01026, CERN-PH-EP-2014-156; arXiv:1408.4674.
doi: 10.1140/epjc/s10052-014-3231-6.

ATLAS Collaboration.
Measurement of the production cross section of prompt J/ψ mesons in association with a $W^{\pm}$ boson in pp collisions at $\sqrt{s} =$ 7 TeV with the ATLAS detector.
Journal of high energy physics, 2014(4):172, and DESY-2014-02675, CERN-PH-EP-2013-184; arXiv:1401.2831.
doi: 10.1007/JHEP04(2014)172.

ATLAS Collaboration.
Measurement of the production cross-section of $\psi(2S) \to J/\psi(\to \mu^+\mu^-)\pi^+\pi^-$ in pp collisions at $\sqrt{s} = 7$ TeV at ATLAS.
Journal of high energy physics, 2014(9):79, and PUBDB-2014-03645, CERN-PH-EP-2014-095; arXiv:1407.5532.
doi: 10.1007/JHEP09(2014)079.

ATLAS Collaboration.
Measurement of the production of a W boson in association with a charm quark in pp collisions at $\sqrt{s}$ = 7 TeV with the ATLAS detector.
Journal of high energy physics, 2014(5):68, and DESY-2014-02875, CERN-PH-EP-2014-007; arXiv:1402.6263.
doi: 10.1007/JHEP05(2014)068.

ATLAS Collaboration.
Measurement of the top quark pair production charge asymmetry in proton-proton collisions at $\sqrt{s}$ = 7 TeV using the ATLAS detector.
Journal of high energy physics, 1402(2):107, and DESY-2014-02308, arXiv:1311.6724.
doi: 10.1007/JHEP02(2014)107.

ATLAS Collaboration.
Measurement of the total cross section from elastic scattering in pp collisions at $\sqrt{s} = 7$ TeV with the ATLAS detector.
Nuclear physics / B, B889:486, and PUBDB-2014-04116, CERN-PH-EP-2014-177; arXiv:1408.5778.
doi: 10.1016/j.nuclphysb.2014.10.019.

ATLAS Collaboration.
Measurement of the $t\bar{t}$ production cross-section using $e\mu$ events with b -tagged jets in pp collisions at $\sqrt{s} = 7$ and 8 TeV with the ATLAS detector.
The European physical journal / C, 74(10):3109, and PUBDB-2015-01047, CERN-EP-2014-124; arXiv:1406.5375.
doi: 10.1140/epjc/s10052-014-3109-7.

ATLAS Collaboration.
Measurement of the Underlying Event in Jet Events from 7 TeV Proton-Proton Collisions with the ATLAS Detector.
The European physical journal / C, 74(8):2965, and PUBDB-2015-01057, CERN-PH-EP-2014-077; arXiv:1406.0392.
doi: 10.1140/epjc/s10052-014-2965-5.

ATLAS Collaboration.
Measurement of the WW+WZ cross section and limits on anomalous triple gauge couplings using final states with one lepton, missing transverse momentum, and two jets with the ATLAS detector at $\sqrt{s} = 7$ TeV.
Journal of high energy physics, 2015(1):49, and PUBDB-2015-01027, CERN-PH-EP-2014-244; arXiv:1410.7238.
doi: 10.1007/JHEP01(2015)049.

ATLAS Collaboration.
Measurement of the Z/γ^* boson transverse momentum distribution in pp collisions at $\sqrt{s}$ = 7 TeV with the ATLAS detector.
Journal of high energy physics, 2014(9):145, and PUBDB-2014-03723, CERN-PH-EP-2014-075; arXiv:1406.3660.
doi: 10.1007/JHEP09(2014)145.

ATLAS Collaboration.
Measurements of fiducial and differential cross sections for Higgs boson production in the diphoton decay channel at $\sqrt{s} = 8$ TeV with ATLAS.
Journal of high energy physics, 2014(9):112, and DESY-2014-03771, CERN-PH-EP-2014-148; arXiv:1407.4222.
doi: 10.1007/JHEP09(2014)112.

ATLAS Collaboration.
Measurements of Higgs Boson Production and Couplings in the Four-Lepton Channel in pp Collisions at Center-of-Mass Energies of 7 and 8 TeV with the ATLAS Detector.
Physical review / D, 91(1):012006, and PUBDB-2015-00863, CERN-PH-EP-2014-170; arXiv:1408.5191.
doi: 10.1103/PhysRevD.91.012006.

ATLAS Collaboration.
Measurements of jet vetoes and azimuthal decorrelations in dijet events produced in pp collisions at $\sqrt{s}$ = 7 TeV using the ATLAS detector.
The European physical journal / C, 74:3117, and PUBDB-2014-04117, CERN-PH-EP-2014-132; arXiv:1407.5756.
doi: DOI 10.1140/epjc/s10052-014-3117-7.

ATLAS Collaboration.
Measurements of normalized differential cross-sections for $t\bar{t}$ production in pp collisions at $\sqrt{s} = 7$ TeV using the ATLAS detector.
Physical review / D, 90(7):072004, and PUBDB-2014-03800, CERN-PH-EP-2014-099; arXiv:1407.0371.
doi: 10.1103/PhysRevD.90.072004.

ATLAS Collaboration.
Measurements of spin correlation in top-antitop quark events from proton-proton collisions at $\sqrt{s} = 7$ TeV using the ATLAS detector.
Physical review / D, 90(11):112016, and PUBDB-2015-00098, CERN-PH-EP-2014-116; arXiv:1407.4314.
doi: 10.1103/PhysRevD.90.112016.

ATLAS Collaboration.
Monitoring and data quality assessment of the ATLAS liquid argon calorimeter.
Journal of Instrumentation, 9:P07024, and DESY-2014-03155, CERN-PH-EP-2014-045; arXiv:1405.3768.
doi: 10.1088/1748-0221/9/07/P07024.

ATLAS Collaboration.
Muon reconstruction efficiency and momentum resolution of the ATLAS experiment in proton-proton collisions at $\sqrt{s}$ = 7 TeV in 2010.
The European physical journal / C, 74:3034, and PUBDB-2014-03757, CERN-PH-EP-2013-154; arXiv:1404.4562.
doi: 10.1140/epjc/s10052-014-3034-9.

ATLAS Collaboration.
Observation of an Excited $B_c^{\pm}$ Meson State with the ATLAS Detector.
Physical review letters, 113(21):212004, and PUBDB-2014-04438, CERN-PH-EP-2017; arXiv:1407.1032.
doi: 10.1103/PhysRevLett.113.212004.

ATLAS Collaboration.
Operation and performance of the ATLAS semiconductor tracker.
Journal of Instrumentation, 9(08):P08009, and DESY-2014-03258, arXiv: 1404.7473; CERN-PH-EP-2014-049.
doi: 10.1088/1748-0221/9/08/P08009.

ATLAS Collaboration.
Search for a Multi-Higgs Boson Cascade in $W^+W^-b\bar{b}$ events with the ATLAS detector in pp collisions at $\sqrt{s} = 8$ TeV.
Physical review / D, 89(3):032002, and DESY-2014-02280.
doi: 10.1103/PhysRevD.89.032002.

ATLAS Collaboration.
Search for contact interactions and large extra dimensions in the dilepton channel using proton-proton collisions at $\sqrt{s}$ = 8 TeV with the ATLAS detector.
The European physical journal / C, 74(12):3134, and PUBDB-2014-04585, CERN-PH-EP-2014-135; arXiv:1407.2410.
doi: 10.1140/epjc/s10052-014-3134-6.

ATLAS Collaboration.
Search for dark matter in events with a hadronically decaying W or Z boson and missing transverse momentum in pp collisions at $\sqrt{s}$=8 TeV with the ATLAS detector.
Physical review letters, 112(4):041802, and DESY-2014-01856.
doi: 10.1103/PhysRevLett.112.041802.

ATLAS Collaboration.
Search for dark matter in events with a Z boson and missing transverse momentum in pp collisions at $\sqrt{s}$ = 8 TeV with the ATLAS detector.
Physical review / D, 90(1):012004, and DESY-2014-03162, CERN-PH-EP-2013-231; arXiv:1404.0051.
doi: 10.1103/PhysRevD.90.012004.

ATLAS Collaboration.
Search for direct pair production of the top squark in all-hadronic final states in proton-proton collisions at $\sqrt{s} = 8$ TeV with the ATLAS detector.
Journal of high energy physics, 2014(9):15, and PUBDB-2014-03499, CERN-PH-EP-2014-112.
doi: 10.1007/JHEP09(2014)015.

ATLAS Collaboration.
Search for direct production of charginos and neutralinos in events with three leptons and missing transverse momentum in $\sqrt{s}$ = 8 TeV pp collisions with the ATLAS detector.
Journal of high energy physics, 2014(4):169, and DESY-2014-02679, CERN-PH-EP-2014-019; arXiv:1402.7029.
doi: 10.1007/JHEP04(2014)169.

ATLAS Collaboration.
Search for direct production of charginos, neutralinos and sleptons in final states with two leptons and missing transverse momentum in pp collisions at $\sqrt{s} = 8$ TeV with the ATLAS detector.
Journal of high energy physics, 2014:71, and DESY-2014-02897, CERN-PH-EP-2014-037;arXiv:1403.5294.
doi: 10.1007/JHEP05(2014)071.

ATLAS Collaboration.
Search for direct top squark pair production in events with a Z boson, b-jets and missing transverse momentum in $\sqrt{s}$ = 8 TeV pp collisions with the ATLAS detector.
The European physical journal / C, 74(6):2883, and DESY-2014-03156, CERN-PH-EP-2014-035; arXiv:1403.5222.
doi: 10.1140/epjc/s10052-014-2883-6.

ATLAS Collaboration.
Search for direct top-squark pair production in final states with two leptons in pp collisions at $\sqrt{s} = 8$ TeV with the ATLAS detector.
Journal of high energy physics, 2014(6):124, and DESY-2014-02926, CERN-PH-EP-2014-014;arXiv:1403.4853.
doi: 10.1007/JHEP06(2014)124.

ATLAS Collaboration.
Search for $H \to \gamma\gamma$ produced in association with top quarks and constraints on the Yukawa coupling between the top quark and the Higgs boson using data taken at 7 TeV and 8 TeV with the ATLAS detector.
Physics letters / B, 740:222, and PUBDB-2014-04507, CERN-PH-EP-2014-179; arXiv:1409.3122.
doi: 10.1016/j.physletb.2014.11.049.

ATLAS Collaboration.
Search for Higgs boson decays to a photon and a Z boson in pp collisions at $\sqrt{s}$=7 and 8 TeV with the ATLAS detector.
Physics letters / B, 732:8, and DESY-2014-02429, CERN-PH-EP-2014-006.
doi: 10.1016/j.physletb.2014.03.015.

ATLAS Collaboration.
Search for high-mass dilepton resonances in pp collisions at $\sqrt{s} = 8$ TeV with the ATLAS detector.
Physical review / D, 90:052005, and PUBDB-2014-03643, CERN-PH-EP-2014-053; arXiv:1405.4123.
doi: 10.1103/PhysRevD.90.052005.

ATLAS Collaboration.
Search for Invisible Decays of a Higgs Boson Produced in Association with a Z Boson in ATLAS.
Physical review letters, 112(20):201802, and DESY-2014-02876, CERN-PH-EP-2013-210; arXiv:1402.3244.
doi: 10.1103/PhysRevLett.112.201802.

ATLAS Collaboration.
Search for long-lived neutral particles decaying into lepton jets in proton-proton collisions at $\sqrt{s} = 8$ TeV with the ATLAS detector.
Journal of high energy physics, 1411(11):88, and PUBDB-2014-04432, CERN-PH-EP-2014-209; arXiv:1409.0746.
doi: 10.1007/JHEP11(2014)088.

ATLAS Collaboration.
Search for microscopic black holes and string balls in final states with leptons and jets with the ATLAS detector at $\sqrt{s} = 8$ TeV.
Journal of high energy physics, 2014(8):103, and DESY-2014-03247, CERN-PH-EP-2014-072; arXiv:1405.4254.
doi: 10.1007/JHEP08(2014)103.

ATLAS Collaboration.
Search for neutral Higgs bosons of the minimal supersymmetric standard model in pp collisions at $\sqrt{s}$ = 8 TeV with the ATLAS detector.
Journal of high energy physics, 2014(11):56, and PUBDB-2014-04098, CERN-PH-EP-2014-210; arXiv:1409.6064.
doi: 10.1007/JHEP11(2014)056.

ATLAS Collaboration.
Search for new particles in events with one lepton and missing transverse momentum in pp collisions at $\sqrt{s}$ = 8 TeV with the ATLAS detector.
Journal of high energy physics, 2014(9):37, and PUBDB-2014-03507, CERN-PH-EP-2014-093.
doi: 10.1007/JHEP09(2014)037.

ATLAS Collaboration.
Search for new phenomena in events with a photon and missing transverse momentum in pp collisions at $\sqrt{s} = 8$ TeV with the ATLAS detector.
Physical review / D, 91(1):012008, and PUBDB-2015-01054, CERN-PH-EP-2014-245; arXiv:1411.1559.
doi: 10.1103/PhysRevD.91.012008.

ATLAS Collaboration.
Search for new resonances in $W\gamma$ and $Z\gamma$ Final States in pp Collisions at $\sqrt{s} = 8$ TeV with the ATLAS Detector.
Physics letters / B, 738:428, and PUBDB-2014-03876, CERN-PH-EP-2014-159; arXiv:1407.8150.
doi: 10.1016/j.physletb.2014.10.002.

ATLAS Collaboration.
Search for nonpointing and delayed photons in the diphoton and missing transverse momentum final state in 8 TeV pp collisions at the LHC using the ATLAS detector.
Physical review / D, 90(11):112005, and PUBDB-2014-04509, CERN-PH-EP-2014-215; arXiv:1409.5542.
doi: 10.1103/PhysRevD.90.112005.

ATLAS Collaboration.
Search for pair and single production of new heavy quarks that decay to a Z boson and a third-generation quark in pp collisions at $\sqrt{s} = 8$ TeV with the ATLAS detector.
Journal of high energy physics, 2014(11):104, and PUBDB-2014-04488, CERN-PH-EP-2014-188; arXiv:1409.5500.
doi: 10.1007/JHEP11(2014)104.

ATLAS Collaboration.
Search for pair-produced third-generation squarks decaying via charm quarks or in compressed supersymmetric scenarios in pp collisions at $\sqrt{s} = 8$ TeV with the ATLAS detector.
Physical review / D, 90(5):052008, and PUBDB-2014-03665, CERN-PH-EP-2014-141; arXiv:1407.0608.
doi: 10.1103/PhysRevD.90.052008.

ATLAS Collaboration.
Search for Quantum Black-Hole Production in High-Invariant-Mass Lepton + Jet Final States Using pp Collisions at $\sqrt{s}$ = 8 TeV and the ATLAS Detector.
Physical review letters, 112:091804, and DESY-2014-02321, CERN-PH-EP-2013-193.
doi: 10.1103/PhysRevLett.112.091804.

ATLAS Collaboration.
Search for Scalar Diphoton Resonances in the Mass Range $65 - 600$ GeV with the ATLAS Detector in pp Collision Data at $\sqrt{s}$ = 8 TeV.
Physical review letters, 113:171801, and PUBDB-2014-03831, CERN-PH-EP-2014-142; arXiv:1407.6583.
doi: 10.1103/PhysRevLett.113.171801.

ATLAS Collaboration.
Search for squarks and gluinos with the ATLAS detector in final states with jets and missing transverse momentum using $\sqrt{s} = 8$ TeV proton–proton collision data.
Journal of high energy physics, 2014:176, and PUBDB-2014-03753, CERN-PH-EP-2014-093; arXiv:1405.7875.
doi: 10.1007/JHEP09(2014)176.

ATLAS Collaboration.
Search for strong production of supersymmetric particles in final states with missing transverse momentum and at least three b-jets at $\sqrt{s} = 8$ TeV proton-proton collisions with the ATLAS detector.
Journal of high energy physics, 2014(10):24, and PUBDB-2014-03764, CERN-PH-EP-2014-110; arXiv:1407.0600.
doi: 10.1007/JHEP10(2014)024.

ATLAS Collaboration.
Search for supersymmetry at $\sqrt{s}$=8 TeV in final states with jets and two same-sign leptons or three leptons with the ATLAS detector.
Journal of high energy physics, 2014(6):35, and DESY-2014-02894, CERN-PH-EP-2014-044; arXiv:1404.2500.
doi: 10.1007/JHEP06(2014)035.

ATLAS Collaboration.
Search for supersymmetry in events with four or more leptons in $\sqrt{s} = 8$ TeV pp collisions with the ATLAS detector.
Physical review / D, 90(5):052001, and DESY-2014-03331, CERN-PH-EP-2014-074;arXiv:1405.5086.
doi: 10.1103/PhysRevD.90.052001.

ATLAS Collaboration.
Search for supersymmetry in events with large missing transverse momentum, jets, and at least one tau lepton in 20 fb^{-1} of $\sqrt{s} = 8$ TeV proton-proton collision data with the ATLAS detector.
Journal of high energy physics, 2014(9):103, and PUBDB-2014-03763, CERN-PH-EP-2014-144; arXiv:1407.0603.
doi: 10.1007/JHEP09(2014)103.

ATLAS Collaboration.
Search for the $b\bar{b}$ Decay of the Standard Model Higgs Boson in Associated $(W/Z)H$ Production with the ATLAS Detector.
Journal of high energy physics, 01:069, and PUBDB-2015-00979, CERN-PH-EP-2014-214; arXiv:1409.6212.
doi: 10.1007/JHEP01(2015)069.

ATLAS Collaboration.
Search for the lepton flavor violating decay $Z \to e\mu$ in pp collisions at $\sqrt{s}$ = 8 TeV with the ATLAS detector.
Physical review / D, 90(7):072010, and PUBDB-2014-03875, CERN-PH-EP-2014-195; arXiv:1408.5774.
doi: 10.1103/PhysRevD.90.072010.

ATLAS Collaboration.
Search for the Standard Model Higgs boson decay to $\mu^+\mu^-$ with the ATLAS detector.
Physics letters / B, 738:68, and PUBDB-2014-03722, CERN-PH-EP-2014-131; arXiv:1406.7663.
doi: 10.1016/j.physletb.2014.09.008.

ATLAS Collaboration.
Search for the X_b and other hidden-beauty states in the $\pi^+\pi^-\Upsilon(1S)$ channel at ATLAS.
Physics letters / B, 740:199, and PUBDB-2014-04504, CERN-PH-EP-2014-230; arXiv:1410.4409.
doi: 10.1016/j.physletb.2014.11.055.

ATLAS Collaboration.
Search for top quark decays $t \to qH$ with $H \to \gamma\gamma$ using the ATLAS detector.
Journal of high energy physics, 2014(6):8, and DESY-2014-02896, CERN-PH-EP-2014-036; arXiv:1403.6293.
doi: 10.1007/JHEP06(2014)008.

ATLAS Collaboration.
Search for top squark pair production in final states with one isolated lepton, jets, and missing transverse momentum in $\sqrt{s}$ = 8 TeV pp collisions with the ATLAS detector.
Journal of high energy physics, 11(11):118, and PUBDB-2014-04492, CERN-PH-EP-2014-143; arXiv:1407.0583.
doi: 10.1007/JHEP11(2014)118.

ATLAS Collaboration.
Search for WZ resonances in the fully leptonic channel using pp collisions at $\sqrt{s} = 8$ TeV with the ATLAS detector.
Physics letters / B, 737:223, and DESY-2014-03294, CERN-PH-EP-2014-094; arXiv:1406.4456.
doi: 10.1016/j.physletb.2014.08.039.

ATLAS Collaboration.
Searches for Heavy Long-Lived Charged Particles with the ATLAS Detector in Proton-Proton Collisions at $\sqrt{s} = 8$ TeV.
Journal of high energy physics, 2015(1):68, and PUBDB-2015-00980, CERN-PH-EP-2014-252; arXiv:1411.6795.
doi: 10.1007/JHEP01(2015)068.

ATLAS Collaboration.
Standalone vertex finding in the ATLAS muon spectrometer.
Journal of Instrumentation, 9(02):P02001, and DESY-2014-01850.
doi: 10.1088/1748-0221/9/02/P02001.

ATLAS Collaboration.
The differential production cross section of the ϕ (1020) meson in $\sqrt{s} = 7$ TeV pp collisions measured with the ATLAS detector.
The European physical journal / C, 74(7):2895, and DESY-2014-03158, CERN-PH-EP-2012-269; arXiv:1402.6162.
doi: 10.1140/epjc/s10052-014-2895-2.

ATLAS collaboration.
Search for the direct production of charginos, neutralinos and staus in final states with at least two hadronically decaying taus and missing transverse momentum in pp collisions at $\sqrt{s}$ = 8 TeV with the ATLAS detector.
Journal of high energy physics, 10:096, and PUBDB-2014-03877, CERN-PH-EP-2014-121; arXiv:1407.0350.
doi: 10.1007/JHEP10(2014)096.

R. Bates et al.
A Custom Online Ultrasonic Gas Mixture Analyzer With Simultaneous Flowmetry, Developed for the Upgraded Evaporative Cooling System of the ATLAS Silicon Tracker.
IEEE transactions on nuclear science, 61(4):2059, and PUBDB-2015-01075.
doi: 10.1109/TNS.2014.2326961.

J. Abdallah and K. Moenig.
Measurement of the Electron Structure Function F_2^e at LEP Energies.
Physics letters / B, 737:39, and PUBDB-2015-01110.
doi: 10.1016/j.physletb.2014.08.012.

S. Díez et al.
A double-sided, shield-less stave prototype for the ATLAS Upgrade strip tracker for the High Luminosity LHC.
Journal of Instrumentation, 9(03):P03012, and DESY-2014-03033.
doi: 10.1088/1748-0221/9/03/P03012.

S. Gonzalez-Sevilla et al.
A Double-Sided Silicon Micro-Strip Super-Module for the ATLAS Inner Detector upgrade in the High-Luminosity LHC.
Journal of Instrumentation, 9(02):P02003, and PUBDB-2015-01074.
doi: 10.1088/1748-0221/9/02/P02003.

K. Mahboubi et al.
The Front-End Hybrid for the ATLAS HL-LHC Silicon Strip Tracker.
Journal of Instrumentation, 9(02):C02027, and PUBDB-2015-01077.
doi: 10.1088/1748-0221/9/02/C02027.

Y. Unno et al.
Development of n$^+$-in-p large-area silicon microstrip sensors for very high radiation environments – ATLAS12 design and initial results.
The 9th International "Hiroshima" Symposium on Development and Application of Semiconductor Tracking Detectors, Hiroshima (Japan), 09/02/2013 - 09/05/2013.
North-Holland Publ. Co., Amsterdam, Sept. 2014.
doi: 10.1016/j.nima.2014.06.086.

E. G. Villani et al.
High voltage multiplexing for the ATLAS Tracker Upgrade.
01. 13th Topical Seminar on Innovative Particle and Radiation Detectors, Sienna (Italy), 10/10/2013 - 10/10/2013.
Inst. of Physics, London, Oct. 2014.
doi: 10.1088/1748-0221/9/01/C01032.

Ph.D. Thesis

J. Dassoulas.
Measurement of Z Boson Production with the ATLAS Experiment at the LHC.
University of Hamburg, Hamburg, 2014.

Astroparticle physics

Published

M. G. Aartsen et al.
Energy Reconstruction Methods in the IceCube Neutrino Telescope.
Journal of Instrumentation, 9(03):P03009, and PUBDB-2015-00729, arXiv:1311.4767.
doi: 10.1088/1748-0221/9/03/P03009.

M. G. Aartsen et al.
Improvement in fast particle track reconstruction with robust statistics.
Nuclear instruments & methods in physics research / A, 736:143, and DESY-2014-01329.
doi: 10.1016/j.nima.2013.10.074.

V. A. Acciari et al.
Observation of Markarian 421 in TeV gamma rays over a 14-year time span.
Astroparticle physics, 54:1, and DESY-2014-03044, arXiv:1310.8150.
doi: 10.1016/j.astropartphys.2013.10.004.

M. Ackermann et al.
Fermi-LAT Observations of the Gamma-Ray Burst GRB 130427A.
Science, 343(6166):42, and PUBDB-2015-01214, arXiv:1311.5623.
doi: 10.1126/science.1242353.

M. Ackermann et al.
High-Energy Gamma-Ray Emission from Solar Flares: Summary of FERMI Large Area Telescope Detections and Analysis of Two M-Class Flares.
The astrophysical journal, 787(1):15, and PUBDB-2015-01200.
doi: 10.1088/0004-637X/787/1/15.

M. Ackermann et al.
THE SPECTRUM AND MORPHOLOGY OF THE FERMI BUBBLES.
The astrophysical journal, 793(1):64, and PUBDB-2014-03721, arXiv:1407.7905.
doi: 10.1088/0004-637X/793/1/64.

M. Ajello et al.
Impulsive and Long Duration High-Energy Gamma-ray Emission From the Very Bright 2012 March 7 Solar Flares.
The astrophysical journal, 789(1):20, and PUBDB-2015-01151, arXiv:1304.5559.
doi: 10.1088/0004-637X/789/1/20.

J. Aleksić et al.
Black Hole Lightning due to Particle Acceleration at Subhorizon Scales.
Science, 346(6213):1080, and PUBDB-2015-01107, arXiv:1412.4936.
doi: 10.1126/science.1256183.

J. Aleksić et al.
Contemporaneous Observations of the Radio Galaxy NGC 1275 from Radio to very High Energy γ-Rays.
Astronomy and astrophysics, 564:A5, and PUBDB-2015-01215, arXiv:1310.8500.
doi: 10.1051/0004-6361/201322951.

J. Aleksić et al.
Detection of Bridge Emission above 50 GeV from the Crab Pulsar with the MAGIC Telescopes.
Astronomy and astrophysics, 565:L12, and PUBDB-2015-01206, arXiv:1402.4219.
doi: 10.1051/0004-6361/201423664.

J. Aleksić et al.
Discovery of TeV Gamma-Ray Emission from the Pulsar Wind Nebula 3C 58 by MAGIC.
Astronomy and astrophysics, 567:L8, and PUBDB-2015-01133, arXiv:1405.6074.
doi: 10.1051/0004-6361/201424261.

J. Aleksić et al.
Discovery of very high energy gamma-ray emission from the blazar 1ES 1727+502 with the MAGIC Telescopes.
Astronomy and astrophysics, 563:A90, and DESY-2014-00625, arXiv:1302.6140.
doi: 10.1051/0004-6361/201321360.

J. Aleksić et al.
First Broadband Characterization and Redshift Determination of the VHE Blazar MAGIC J2001+439.
Astronomy and astrophysics, 572:A121, and PUBDB-2015-01103, arXiv:1409.3389.
doi: 10.1051/0004-6361/201424254.

J. Aleksić et al.
MAGIC Gamma-Ray and Multi-Frequency Observations of Flat Spectrum Radio Quasar PKS 1510-089 in Early 2012.
Astronomy and astrophysics, 569:A46, and PUBDB-2015-01112.
doi: 10.1051/0004-6361/201423484.

J. Aleksić et al.
MAGIC Long-Term Study of the Distant TeV Blazar PKS 1424+240 in a Multiwavelength Context.
Astronomy and astrophysics, 567:A135, and PUBDB-2015-01130, arXiv:1401.0464.
doi: 10.1051/0004-6361/201423364.

J. Aleksić et al.
MAGIC reveals a complex morphology within the unidentified gamma-ray source HESS J1857+026.
Astronomy and astrophysics, 571:1, and PUBDB-2014-04521, arXiv:1401.7154.
doi: 10.1051/0004-6361/201423517.

J. Aleksić et al.
MAGIC upper limits on the GRB 090102 afterglow.
Monthly notices of the Royal Astronomical Society, 437(4):3103, and DESY-2014-01207.
doi: 10.1093/mnras/stt2041.

J. Aleksić et al.
Search for very high energy gamma-rays from the z = 0.896 quasar 4C +55.17 with the MAGIC telescopes.
Monthly notices of the Royal Astronomical Society, 440(1):530, and PUBDB-2014-04520, arXiv:1402.0291.
doi: 10.1093/mnras/stu227.

E. Aliu et al.
A Search for Enhanced very high Energy Gamma-Ray Emission from the 2013 March Crab Nebula Flare.
The astrophysical journal / 2, 781(1):L11, and DESY-2014-03038, arXiv:1309.5949.
doi: 10.1088/2041-8205/781/1/L11.

E. Aliu et al.
A Three-Year Multi-Wavelength Study of the Very-High-Energy γ-Ray Blazar 1ES 0229+200.
The astrophysical journal, 782(1):13, and PUBDB-2015-00943, arXiv:1312.6592.
doi: 10.1088/0004-637X/782/1/13.

E. Aliu et al.
Constraints on very High Energy Emission from GRB 130427A.
The astrophysical journal / 2, 795(1):L3, and PUBDB-2014-03844, arXiv:1410.5367.
doi: 10.1088/2041-8205/795/1/L3.

E. Aliu et al.
Investigating the TeV Morphology of MGRO J1908+06 with VERITAS.
The astrophysical journal, 787(2):166, and DESY-2014-03041, arXiv:1404.7185.
doi: 10.1088/0004-637X/787/2/166.

E. Aliu et al.
Observations of the Unidentified Gamma-Ray Source TeV J2032+4130 by VERITAS.
The astrophysical journal, 783(1):16, and DESY-2014-03045, arXiv:1401.2828.
doi: 10.1088/0004-637X/783/1/16.

E. Aliu et al.
Spatially Resolving the very high Energy Emission from MGRO J2019+37 with VERITAS.
The astrophysical journal, 788(1):78, and DESY-2014-03043.
doi: 10.1088/0004-637X/788/1/78.

S. Archambault et al.
Test of Models of the Cosmic Infrared Background with Multiwavelength Observations of the Blazar 1ES 1218+30.4 in 2009.
The astrophysical journal, 788(2):158, and PUBDB-2015-00478.
doi: 10.1088/0004-637X/788/2/158.

A. Archer et al.
Very-High Energy Observations of the Galactic Center Region by VERITAS in 2010-2012.
The astrophysical journal, 790(2):149, and PUBDB-2014-03727, arXiv:1406.6383.
doi: 10.1088/0004-637X/790/2/149.

P. Baerwald, M. Bustamante Ramirez and W. Winter.
Are gamma-ray bursts the sources of ultra-high energy cosmic rays?
Astroparticle physics, 62:66, and PUBDB-2014-04039, DESY 14-135; arXiv:1401.1820.
doi: 10.1016/j.astropartphys.2014.07.007.

A. Balzer et al.
The H.E.S.S. central data acquisition system.
Astroparticle physics, 54:67, and DESY-2014-00881.
doi: 10.1016/j.astropartphys.2013.11.007.

A. Barnacka et al.
PKS 1510-089: a Rare Example of a Flat Spectrum Radio Quasar with a very High-Energy Emission.
Astronomy and astrophysics, 567:A113, and PUBDB-2015-01141, arXiv:1307.1779.
doi: 10.1051/0004-6361/201322205.

A. Baushev.
Galaxy Halo Formation in the Absence of Violent Relaxation and a Universal Density Profile of the Halo Center.
The astrophysical journal, 786(1):65, and PUBDB-2015-00387, arXiv:1205.4302.
doi: 10.1088/0004-637X/786/1/65.

A. Baushev.
Relaxation of dark matter halos: how to match observational data?
Astronomy and astrophysics, 569:A114, and PUBDB-2015-00408, arXiv:1309.5162.
doi: 10.1051/0004-6361/201322730.

P. Belov et al.
Parton Distribution Functions at LO, NLO and NNLO with Correlated Uncertainties between Orders.
The European physical journal / C, 74(10):3039, and PUBDB-2015-01221.
doi: 10.1140/epjc/s10052-014-3039-4.

E. Bernardini et al.
Neutrino Masses and Oscillations.
Advances in high energy physics, 2014:1, and PUBDB-2015-01162.
doi: 10.1155/2014/823127.

S. M. Boucenna, S. Morisi and J. W. F. Valle.
Radiative neutrino mass in 3-3-1 scheme.
Physical review / D, 90(1):013005, and PUBDB-2014-03726, arXiv:1405.2332.
doi: 10.1103/PhysRevD.90.013005.

S. M. Boucenna, S. Morisi and J. W. F. Valle.
The Low-Scale Approach to Neutrino Masses.
Advances in high energy physics, 2014:1, and PUBDB-2015-01205, arXiv:1404.3751.
doi: 10.1155/2014/831598.

S. M. Boucenna et al.
Inflation and majoron dark matter in the neutrino seesaw mechanism.
Physical review / D, 90(5):055023, and PUBDB-2014-03714, arXiv:1404.3198.
doi: 10.1103/PhysRevD.90.055023.

R. Bühler and R. Blandford.
The surprising Crab pulsar and its nebula: a review.
Reports on progress in physics, 77(6):066901, and PUBDB-2014-03720, arXiv:1309.7046.
doi: 10.1088/0034-4885/77/6/066901.

X. Chen et al.
Magnetic Field Amplification and Flat Spectrum Radio Quasars.
Monthly notices of the Royal Astronomical Society, 441:2188, and PUBDB-2015-01142, arXiv:1404.2193.

Fermi-LAT Collaboration.
Dark Matter Constraints from Observations of 25 Milky Way Satellite Galaxies with the Fermi Large Area Telescope.
Physical review / D, 89(4):042001, and PUBDB-2015-01217, arXiv:1310.0828.
doi: 10.1103/PhysRevD.89.042001.

Fermi-LAT Collaboration.
Fermi Establishes Classical Novae as a Distinct Class of Gamma-Ray Sources.
Science, 345(6196):554, and PUBDB-2015-01119, arXiv:1408.0735.
doi: 10.1126/science.1253947.

Fermi-LAT Collaboration.
Inferred Cosmic-Ray Spectrum from Fermi Large Area Telescope γ-Ray Observations of Earth's Limb.
Physical review letters, 112(15):151103, and PUBDB-2015-01211.
doi: 10.1103/PhysRevLett.112.151103.

Fermi-LAT Collaboration.
Search for Cosmic-Ray-Induced Gamma-Ray Emission in Galaxy Clusters.
The astrophysical journal, 787(1):18, and PUBDB-2015-01195.
doi: 10.1088/0004-637X/787/1/18.

Fermi-LAT Collaboration and MAGIC Collaboration.
Multifrequency studies of the peculiar quasar 4C +21.35 during the 2010 flaring activity.
The astrophysical journal, 786(2):157, and PUBDB-2014-04518, arXiv:1403.7534.
doi: 10.1088/0004-637X/786/2/157.

H. E. S. S. Collaboration.
Discovery of the hard spectrum VHE γ-ray source HESS J1641-463.
The astrophysical journal / 2, 794(1):1, and PUBDB-2014-04056, DESY-14-156; arXiv:1408.5280.
doi: 10.1088/2041-8205/794/1/L1.

H. E. S. S. Collaboration.
Erratum: HESS J1640-465 - an Exceptionally Luminous TeV γ -Ray Supernova Remnant.
Monthly notices of the Royal Astronomical Society, 441(4):3640, and PUBDB-2015-01124.
doi: 10.1093/mnras/stu826.

H. E. S. S. Collaboration.
Flux upper limits for 47 AGN observed with H.E.S.S. in 2004-2011.
Astronomy and astrophysics, 564:A9, and PUBDB-2014-04519, arXiv:1402.2332.
doi: 10.1051/0004-6361/201322897.

H. E. S. S. Collaboration.
HESS J1640-465 - an exceptionally luminous TeV γ-ray supernova remnant.
Monthly notices of the Royal Astronomical Society, 439(3):2828, and PUBDB-2014-04522, arXiv:1401.4388.
doi: 10.1093/mnras/stu139.

H. E. S. S. Collaboration.
HESS J1818-154, a new composite supernova remnant discovered in TeV gamma rays and X-rays.
Astronomy and astrophysics, 562(A40):10, and DESY-2014-00666.
doi: 10.1051/0004-6361/201322914.

H. E. S. S. Collaboration.
H.E.S.S. observations of the Crab during its March 2013 GeV γ-ray flare.
Astronomy and astrophysics, 562:1, and PUBDB-2014-04525, arXiv:1311.3187.
doi: 10.1051/0004-6361/201323013.

H. E. S. S. Collaboration.
Search for Dark Matter Annihilation Signatures in H.E.S.S. Observations of Dwarf Spheroidal Galaxies.
Physical review / D, 90(11):112012, and PUBDB-2015-01046, arXiv:1410.2589.
doi: 10.1103/PhysRevD.90.112012.

H. E. S. S. Collaboration.
Search for extended γ-ray emission around AGN with H.E.S.S. and Fermi -LAT.
Astronomy and astrophysics, 562:A145, and PUBDB-2014-04524, arXiv:1401.2915.
doi: 10.1051/0004-6361/201322510.

H. E. S. S. Collaboration.
Search for TeV Gamma-ray Emission from GRB 100621A, an extremely bright GRB in X-rays, with H.E.S.S.
Astronomy and astrophysics, 565:A16, and PUBDB-2014-04515, arXiv:1405.0488.
doi: 10.1051/0004-6361/201322984.

H. E. S. S. Collaboration.
TeV γ-ray observations of the young synchrotron-dominated SNRs G1.9+0.3 and G330.2+1.0 with H.E.S.S.
Monthly notices of the Royal Astronomical Society, 441(1):790, and PUBDB-2014-04517, arXiv:1404.1613.
doi: 10.1093/mnras/stu459.

IceCube Collaboration.
IceCube Sensitivity for Low-Energy Neutrinos from Nearby Supernovae (Corrigendum).
Astronomy and astrophysics, 563:C1, and PUBDB-2015-01222.
doi: 10.1051/0004-6361/201117810e.

IceCube Collaboration.
Observation of High-Energy Astrophysical Neutrinos in Three Years of IceCube Data.
Physical review letters, 113(10):101101, and PUBDB-2015-00720, arXiv:1405.5303.
doi: 10.1103/PhysRevLett.113.101101.

IceCube Collaboration.
Observation of the Cosmic-Ray Shadow of the Moon with IceCube.
Physical review / D, 89(10):102004, and PUBDB-2015-00731, arXiv:1305.6811.
doi: 10.1103/PhysRevD.89.102004.

IceCube Collaboration.
Search for a Diffuse Flux of Astrophysical Muon Neutrinos with the IceCube 59-string Configuration.
Physical review / D, 89(6):062007, and PUBDB-2015-00728, arXiv:1311.7048.
doi: 10.1103/PhysRevD.89.062007.

IceCube Collaboration.
Search for Neutrino-Induced Particle Showers with IceCube-40.
Physical review / D, 89(10):102001, and PUBDB-2015-00727, arXiv:1312.0104.
doi: 10.1103/PhysRevD.89.102001.

IceCube Collaboration.
Search for Non-Relativistic Magnetic Monopoles with IceCube.
The European physical journal / C, 74(7):2938, and PUBDB-2015-00724, arXiv:1402.3460.
doi: 10.1140/epjc/s10052-014-2938-8.

IceCube Collaboration.
Searches for Extended and Point-like Neutrino Sources with Four Years of IceCube Data.
The astrophysical journal, 796(2):109, and PUBDB-2015-01104, arXiv:1406.6757.
doi: 10.1088/0004-637X/796/2/109.

IceCube Collaboration and LIGO Scientific Collaboration and Virgo Collaboration.
Multimessenger Search for Sources of Gravitational Waves and High-Energy Neutrinos: Initial Results for LIGO-Virgo and IceCube.
Physical review / D, 90(10):102002, and PUBDB-2015-00717, arXiv:1407.1042.
doi: 10.1103/PhysRevD.90.102002.

D. Kostunin et al.
Tunka-Rex: Status and results of the first measurements.
Nuclear instruments & methods in physics research / A, 742:89, and DESY-2014-00906, arXiv:1310.8477.
doi: 10.1016/j.nima.2013.10.070.

M. Kubliha et al.
Local atomic structure and electrical properties of $Ge_{20}Se_{80-x}Te_x$ (x=0, 5, 10, and 15) glasses doped with Ho.
Journal of alloys and compounds, 586:308, and DESY-2014-03227.
doi: 10.1016/j.jallcom.2013.10.059.

MAGIC Collaboration.
MAGIC search for VHE γ-ray emission from AE Aquarii in a multiwavelength context.
Astronomy and astrophysics, 568:A109, and PUBDB-2015-01115, arXiv:1407.3707.
doi: 10.1051/0004-6361/201424072.

MAGIC Collaboration.
Optimized Dark Matter Searches in Deep Observations of Segue 1 with MAGIC.
Journal of cosmology and astroparticle physics, 2014(02):008, and PUBDB-2015-01216, arXiv:1312.1535.
doi: 10.1088/1475-7516/2014/02/008.

MAGIC Collaboration.
Rapid and Multiband Variability of the TeV Bright Active Nucleus of the Galaxy IC 310.
Astronomy and astrophysics, 563:A91, and PUBDB-2015-01207.
doi: 10.1051/0004-6361/201321938.

D. Tescaro.
The upgraded MAGIC Cherenkov Telescopes.
Nuclear instruments & methods in physics research / A, 766:65, and PUBDB-2015-01227.
doi: 10.1016/j.nima.2014.04.037.

MAGIC Collaboration and Fermi-LAT Collaboration.
MAGIC Observations and Multifrequency Properties of the Flat Spectrum Radio Quasar 3C 279 in 2011.
Astronomy and astrophysics, 567:A41, and PUBDB-2015-01128, arXiv:1311.2833.
doi: 10.1051/0004-6361/201323036.

A. Merle, S. Morisi and W. Winter.
Common origin of reactor and sterile neutrino mixing.
Journal of high energy physics, 2014(7):39, and PUBDB-2014-03736, arXiv:1402.6332.
doi: 10.1007/JHEP07(2014)039.

Y. Mizuno et al.
Magnetic Field Amplification and Saturation in Turbulence behind a Relativistic Shock.
Monthly notices of the Royal Astronomical Society, 439(4):3490, and PUBDB-2015-00401, arXiv:1401.7080.
doi: 10.1093/mnras/stu196.

K.-I. Nishikawa et al.
Magnetic Field Generation in Core-Sheath Jets via the Kinetic Kelvin-Helmholtz Instability.
The astrophysical journal, 793(1):60, and PUBDB-2015-00385, arXiv:1405.5247.
doi: 10.1088/0004-637X/793/1/60.

Pierre Auger Collaboration.
A Targeted Search for Point Sources of EeV Neutrons.
The astrophysical journal / 2, 789(2):L34, and PUBDB-2015-00563, FERMILAB-PUB-14-192-AD-AE-CD-TD; arXiv:1406.4038.
doi: 10.1088/2041-8205/789/2/L34.

A. Letessier-Selvon and J. Knapp.
Highlights from the Pierre Auger Observatory.
5. 33rd International Cosmic Ray Conference, Rio de Janeiro (Brazil), 07/02/2013 - 07/09/2013.
Springer New York, New York, NY, July 2014.
doi: 10.1007/s13538-014-0218-6.

Pierre Auger Collaboration.
Origin of Atmospheric Aerosols at the Pierre Auger Observatory Using Studies of Air Mass Trajectories in South America.
Atmospheric research, 149:120, and PUBDB-2015-00600, arXiv:1405.7551.
doi: 10.1016/j.atmosres.2014.05.021.

Pierre Auger Collaboration.
Probing the radio emission from air showers with polarization measurements.
Physical review / D, 89(5):052002, and PUBDB-2014-03730, arXiv:1402.3677.
doi: 10.1103/PhysRevD.89.052002.

S. Pita et al.
Spectroscopy of High-Energy BL Lacertae Objects with X-Shooter on the VLT.
Astronomy and astrophysics, 565:A12, and PUBDB-2015-01209, arXiv:1311.3809.
doi: 10.1051/0004-6361/201323071.

R. Preece et al.
The First Pulse of the Extremely Bright GRB 130427A: A Test Lab for Synchrotron Shocks.
Science, 343(6166):51, and DESY-2014-00780.
doi: 10.1126/science.1242302.

V. V. Prosin et al.
Tunka-133: Results of 3 Year Operation.
4th Roma International Conference on Astroparticle Physics, Roma (Italy), 05/22/2013 - 05/24/2013.
North-Holland Publ. Co., Amsterdam, May 2014.
doi: 0.1016/j.nima.2013.09.018.

V. V. Prosin et al.
Tunka-133: Results of 3 year operation.
Nuclear instruments & methods in physics research / A, 756:94, and DESY-2014-00904.
doi: 10.1016/j.nima.2013.09.018.

P. Schellart et al.
Polarized radio emission from extensive air showers measured with LOFAR.
Journal of cosmology and astroparticle physics, 2014(10):014, and PUBDB-2014-03840, arXiv:1406.1355.
doi: 10.1088/1475-7516/2014/10/014.

A. Schulz et al.
Systematic search for high-energy gamma-ray emission from bow shocks of runaway stars.
Astronomy and astrophysics, 565:A95, and PUBDB-2014-04514, arXiv:1404.4059.
doi: 10.1051/0004-6361/201423468.

C. Spiering.
High-Energy Neutrino Astronomy: a Glimpse of the Promised Land.
Uspechi fiziceskich nauk, 184(5):510, and PUBDB-2015-01196.
doi: 10.3367/UFNr.0184.201405e.0510.

TAIGA Collaboration.
TAIGA the Tunka Advanced Instrument for cosmic ray physics and Gamma Astronomy - present status and perspectives.
Journal of Instrumentation, 9(09):C09021, and PUBDB-2015-00579.
doi: 10.1088/1748-0221/9/09/C09021.

M. Tluczykont et al.
The HiSCORE concept for gamma-ray and cosmic-ray astrophysics beyond 10TeV.
Astroparticle physics, 56:42, and DESY-2014-03032, arXiv:1403.5688.
doi: 10.1016/j.astropartphys.2014.03.004.

VERITAS Collaboration.
Investigating Broadband Variability of the TeV Blazar 1ES 1959+650.
The astrophysical journal, 797(2):89, and PUBDB-2015-01101, arXiv:1412.1031.
doi: 10.1088/0004-637X/797/2/89.

VERITAS Collaboration and Fermi LAT Collaboration.
DEEP BROADBAND OBSERVATIONS OF THE DISTANT GAMMA-RAY BLAZAR PKS 1424+240.
The astrophysical journal / 2, 785(1):L16, and DESY-2014-03042, arXiv:1403.4308.
doi: 10.1088/2041-8205/785/1/L16.

VERITAS Collaboration and H. E. S. S. Collaboration.
Long-Term TeV and X-Ray Observations of the Gamma-Ray Binary HESS J0632+057.
The astrophysical journal, 780(168):1, and DESY-2014-00768.
doi: 10.1088/0004-637X/780/2/168.

M. Walter, C. Spiering and J. Knapp.
100 Years of Cosmic Rays: The Anniversary of their Discovery by V.F. Hess.
Astroparticle physics, 53:1, and PUBDB-2015-00601.
doi: 10.1016/j.astropartphys.2013.10.006.

W. Winter, J. Becker Tjus and S. R. Klein.
Impact of secondary acceleration on the neutrino spectra in gamma-ray bursts.
Astronomy and astrophysics, 569:A58, and PUBDB-2014-03719, arXiv:1403.0574.
doi: 10.1051/0004-6361/201423745.

J. P. Yáñez et al.
Assessment of the capacity credit of wind power in Mexico.
Renewable energy, 72:62, and PUBDB-2015-00733.
doi: 10.1016/j.renene.2014.06.038.

H. Zhang, X. Chen and M. Böttcher.
Synchrotron Polarization in Blazars.
The astrophysical journal, 789(1):66, and PUBDB-2015-01153, arXiv:1401.7138.
doi: 10.1088/0004-637X/789/1/66.

Ph.D. Thesis

G. De Caneva.
Studies of Active Galactic Nuclei with the MAGIC Telescopes.
Humboldt-Universität zu Berlin, Berlin, 2014.

S. Federici.
Gamma-Ray Studies of the Young Shell-Type SNR RX J1713.7-3946.
Universität Potsdam, Potsdam, 2014.

BELLE

Published

Belle Collaboration.
Evidence for semileptonic $B^- \to p\bar{p}l^-\bar{\nu}_l$ decays.
Physical review / D, 89(1):011101, and DESY-2014-01707, Belle preprint 2013-10.
doi: 10.1103/PhysRevD.89.011101.

Belle Collaboration.
Evidence of $\Upsilon(1S) \to J/\psi + \chi_{c1}$ and search for double-charmonium production in $\Upsilon(1S)$ and $\Upsilon(2S)$ decays.
Physical review / D, 90(11):112008, and PUBDB-2014-04711, Belle Preprint 2014-14; arXiv:1409.7644.
doi: 10.1103/PhysRevD.90.112008.

Belle Collaboration.
Measurement of Branching Fractions and CP Violation Parameters in $B \to wK$ Decays with First Evidence of CP Violation in $B^0 \to wK^0_S$.
Physical review / D, 90:012002, and DESY-2014-03098, Belle Preprint 2013-28; arXiv:1311.6666.
doi: 10.1103/PhysRevD.90.012002.

Belle Collaboration.
Measurement of D^0-$\overline{D}^0$ Mixing and Search for Indirect CP Violation Using $D^0 \to K^0_S\pi^+\pi^-$ Decays.
Physical review / D, 89:091103, and DESY-2014-02872, BELLE-PREPRINT-2014-6; arXiv:1404.2412.
doi: 10.1103/PhysRevD.89.091103.

Belle Collaboration.
Measurement of the Branching Fraction $B(\Lambda_c^+ - pK^-\pi^+)$.
Physical review letters, 113:042002, and DESY-2014-03097, Belle Preprint 2013-30; arXiv:1312.7826.
doi: 10.1103/PhysRevLett.113.042002.

Belle Collaboration.
Measurement of the τ-lepton lifetime at Belle.
Physical review letters, 112(3):031801, and PUBDB-2014-04578, Belle preprint 2013-26; arXiv:1310.8503.
doi: 10.1103/PhysRevLett.112.031801.

Belle Collaboration.
Measurement of Time-Dependent CP Violation in $B^0 \to \eta' K^0$ Decays.
Journal of high energy physics, 10:165, and PUBDB-2014-04067, BELLE-PREPRINT-2014-10; arXiv:1408.5991.
doi: 10.1007/JHEP10(2014)165.

Belle Collaboration.
Measurements of Branching Fractions of τ Lepton Decays with one or more K^0_S.
Physical review / D, 89:072009, and DESY-2014-02585, Belle preprint 2014-3.
doi: 10.1103/PhysRevD.89.072009.

Belle Collaboration.
Measurements of the masses and widths of the $\Sigma_c(2455)^{0/++}$ and $\Sigma_c(2520)^{0/++}$ baryons.
Physical review / D, 89:091102(R), and DESY-2014-02786, BELLE-PREPRINT-2014-6; arXiv:1404.5389.
doi: 10.1103/PhysRevD.89.091102.

Belle Collaboration.
Observation of a new charged charmoniumlike state in $\overline{B}^0 \to J/\psi K^-\pi^+$ decays.
Physical review / D, 90(11):112009, and PUBDB-2014-04701, BELLE-PREPRINT-2014-12; arXiv:1408.6457.
doi: 10.1103/PhysRevD.90.112009.

Belle Collaboration.
Observation of $D^0 - \bar{D}^0$ Mixing in e^+e^- Collisions.
Physical review letters, 112(11):111801, and DESY-2014-02655, Belle Preprint 2013-31;arXiv:1401.3402.
doi: 10.1103/PhysRevLett.112.111801.

Belle Collaboration.
Observation of $e^+e^- \to \pi^+\pi^-\pi^0\chi_{bJ}$ and search for $X_b \to \omega\Upsilon(1S)$ at $\sqrt{s} \sim 10.867$ GeV.
Physical review letters, 113(14):142001, and PUBDB-2014-03703, BELLE-PREPRINT-2014-11; arXiv:1408.0504.
doi: 10.1103/PhysRevLett.113.142001.

Belle Collaboration.
Observation of the decay $B^0 \to \eta' K^*(892)^0$.
Physical review / D, 90:072009, and PUBDB-2014-03850, BELLE-PREPRINT-2014-13; arXiv:1408.6343.
doi: 10.1103/PhysRevD.90.072009.

Belle Collaboration.
Search for $B^0 \to p\bar{\Lambda}\pi^-\gamma$ at Belle.
Physical review / D, 89:051103(R), and DESY-2014-02656, BELLE-PREPRINT-2013-22; arXiv:1312.4228.
doi: 10.1103/PhysRevD.89.051103.

Belle Collaboration.
Search for $B^0_s \to \gamma\gamma$ and a measurement of the branching fraction for $B^0_s \to \phi\gamma$.
Physical review / D, 91(1):011101, and PUBDB-2015-00857, BELLE-PREPRINT-2014-18; arXiv:1411.7771.
doi: 10.1103/PhysRevD.91.011101.

Belle Collaboration.
Search for CP violation in $D^0 \to \pi^0\pi^0$ Decays.
Physical review letters, 112:211601, and DESY-2014-02825, arXiv:1404.1266; BELLE-PREPRINT-2014-7.
doi: 10.1103/PhysRevLett.112.211601.

Belle Collaboration.
Search for doubly charmed baryons and study of charmed strange baryons at Belle.
Physical review / D, 89:052003, and DESY-2014-02957, Belle preprint 2013-29; arXiv:1312.1026.
doi: 10.1103/PhysRevD.89.052003.

Belle Collaboration.
Search for the process $e^+e^- \to J/\psi + X(1835)$ at $\sqrt{s} \approx 10.6$ GeV.
Physical review / D, 89(3):032003, and DESY-2014-02657, Belle Preprint 2013-27;arXiv:1311.6337.
doi: 10.1103/PhysRevD.89.032003.

Belle Collaboration.
Updated Cross Section Measurement of $e^+e^- \to K^+K^-J/\psi$ and $K^0_SK^0_SJ/\psi$ via Initial State Radiation at Belle.
Physical review / D, 89(7):072015, and DESY-2014-02654, BELLE-PREPRINT-2014-2;arXiv:1402.6578.
doi: 10.1103/PhysRevD.89.072015.

K. Motohashi et al.
Evaluation of KEK n-in-p Planar Pixel Sensor Structures for Very High Radiation Environments with Testbeam.
9th International "Hiroshima" Symposium on Development and Application of Semiconductor Tracking Detectors, Hiroshima (Japan), 09/02/2013 - 09/05/2013.
North-Holland Publ. Co., Amsterdam, Sept. 2014.
doi: 10.1016/j.nima.2014.05.092.

CMS

Published

S. Alekhin et al.
Nucleon PDF separation with the collider and fixed-target data.
37th International Conference on High Energy Physics, Valencia (Spain), 07/02/2014 - 07/09/2014.
Elsevier, Amsterdam, July 2014.

R. Mankel.
Higgs searches beyond the Standard Model.
International journal of modern physics / A, 29(24):1430057, and PUBDB-2014-03765.
doi: 10.1142/S0217751X14300579.

CMS Collaboration.
Alignment of the CMS tracker with LHC and cosmic ray data.
Journal of Instrumentation, 9:P06009, and PUBDB-2014-03506, arXiv:1403.2286; CMS-TRK-11-002; CERN-PH-EP-2014-028.
doi: 10.1088/1748-0221/9/06/P06009.

CMS Collaboration.
Constraints on the Higgs boson width from off-shell production and decay to Z-boson pairs.
Physics letters / B, 736:64, and DESY-2014-03311, arXiv:1405.3455; CMS-HIG-14-002; CERN-PH-EP-2014-078.
doi: 10.1016/j.physletb.2014.06.077.

CMS Collaboration.
Description and performance of track and primary-vertex reconstruction with the CMS tracker.
Journal of Instrumentation, 9(10):P10009, and PUBDB-2015-00122, CMS-TRK-11-001; CERN-PH-EP-2014-070; arXiv:1405.6569.
doi: 10.1088/1748-0221/9/10/P10009.

CMS Collaboration.
Event activity dependence of Υ(nS) production in $\sqrt{s_{NN}}$=5.02 TeV pPb and $\sqrt{s}$=2.76 TeV pp collisions.
Journal of high energy physics, 2014(4):103, and DESY-2014-02848, arXiv:1312.6300; CMS-HIN-13-003; CERN-PH-EP-2013-219.
doi: 10.1007/JHEP04(2014)103.

CMS Collaboration.
Evidence for the 125 GeV Higgs boson decaying to a pair of τ leptons.
Journal of high energy physics, 2014(5):104, and PUBDB-2014-03542, arXiv:1401.5041; CMS-HIG-13-004; CERN-PH-EP-2014-001.
doi: 10.1007/JHEP05(2014)104.

CMS Collaboration.
Evidence for the direct decay of the 125 GeV Higgs boson to fermions.
Nature physics, 10(8):557, and PUBDB-2014-03541, arXiv:1401.6527; CMS-HIG-13-033; CERN-PH-EP-2014-004.
doi: 10.1038/nphys3005.

CMS Collaboration.
Evidence of b-Jet Quenching in PbPb Collisions at $\sqrt{s_{NN}} = 2.76$ TeV.
Physical review letters, 113(13):132301, and PUBDB-2015-01198, CMS-HIN-12-003; CERN-PH-EP-2013-037; arXiv:1312.4198.
doi: 10.1103/PhysRevLett.113.132301.

CMS Collaboration.
Identification Techniques for Highly Boosted W Bosons that Decay Into Hadrons.
Journal of high energy physics, 2014(12):17, and PUBDB-2015-00698, CMS-JME-13-006; CERN-PH-EP-2014-241; arXiv:1410.4227.
doi: 10.1007/JHEP12(2014)017.

CMS Collaboration.
Inclusive search for a vector-like T quark with charge 2/3 in pp collisions at sqrt(s) = 8 TeV.
Physics letters / B, 729:149, and DESY-2014-01751, arXiv:1311.7667; CMS-B2G-12-015; CERN-PH-EP-2013-215.
doi: 10.1016/j.physletb.2014.01.006.

CMS Collaboration.
Measurement of associated W + charm production in pp collisions at $\sqrt{s}$ = 7 TeV.
Journal of high energy physics, 2014(2):13, and DESY-2014-02649, arXiv:1310.1138; CMS-SMP-12-002; CERN-PH-EP-2013-149.
doi: 10.1007/JHEP02(2014)013.

CMS Collaboration.
Measurement of differential cross sections for the production of a pair of isolated photons in pp collisions at $\sqrt{s} = 7$ TeV.
The European physical journal / C, 74(11):3129, and PUBDB-2015-00120, CMS-SMP-13-001; CERN-PH-EP-2014-067; arXiv:1405.7225.
doi: 10.1140/epjc/s10052-014-3129-3.

CMS Collaboration.
Measurement of four-jet production in proton-proton collisions at $\sqrt{s} = 7$ TeV.
Physical review / D, 89(9):092010, and PUBDB-2014-03546, arXiv:1312.6440; CERN-PH-EP-2013-229; CMS-FSQ-12-013.
doi: 10.1103/PhysRevD.89.092010.

CMS Collaboration.
Measurement of Higgs boson production and properties in the WW decay channel with leptonic final states.
Journal of high energy physics, 2014(1):96, and DESY-2014-01750, arXiv:1312.1129; CMS-HIG-13-023; CERN-PH-EP-2013-221.
doi: 10.1007/JHEP01(2014)096.

CMS Collaboration.
Measurement of Higher-Order Harmonic Azimuthal Anisotropy in PbPb Collisions at $\sqrt{s_{NN}}$ = 2.76 TeV.
Physical review / C, 89(4):044906, and PUBDB-2015-01203, CMS-HIN-11-005; CERN-PH-EP-2013-196.
doi: 10.1103/PhysRevC.89.044906.

CMS Collaboration.
Measurement of inclusive W and Z boson production cross sections in pp collisions at $\sqrt{s}$ = 8 TeV.
Physical review letters, 112(19):191802, and DESY-2014-02846, arXiv:1402.0923; CMS-SMP-12-011; CERN-PH-EP-2013-217.
doi: 10.1103/PhysRevLett.112.191802.

CMS Collaboration.
Measurement of jet fragmentation in PbPb and pp collisions at $\sqrt{s_{NN}}$ =2.76 TeV.
Physical review / C, 90(2):024908, and PUBDB-2015-00114, CMS-HIN-12-013; CERN-PH-EP-2014-100; arXiv:1406.0932.
doi: 10.1103/PhysRevC.90.024908.

CMS Collaboration.
Measurement of jet multiplicity distributions in $t\bar{t}$ production in pp collisions at $\sqrt{s} = 7$ TeV.
The European physical journal / C, 74(8):3014, and PUBDB-2015-00136, CMS-TOP-12-018; CERN-PH-EP-2014-048; arXiv:1404.3171.
doi: 10.1140/epjc/s10052-014-3014-0.

CMS Collaboration.
Measurement of prompt J/ψ pair production in pp collisions at $\sqrt{s}$ = 7 Tev.
Journal of high energy physics, 2014(9):94, and PUBDB-2015-00113, CMS-BPH-11-021; CERN-PH-EP-2014-111; arXiv:1406.0484.
doi: 10.1007/JHEP09(2014)094.

CMS Collaboration.
Measurement of Prompt psi(2S) to J/psi Yield Ratios in PbPb and pp Collisions at sqrt(s[NN]) = 2.76 TeV.
Physical review letters, 113(26):262301, and PUBDB-2015-00702, CMS-HIN-12-007; CERN-PH-EP-2014-240; arXiv:1410.1804.
doi: 10.1103/PhysRevLett.113.262301.

CMS Collaboration.
Measurement of the muon charge asymmetry in inclusive $pp \to W + X$ production at $\sqrt{s} = 7$ TeV and an improved determination of light parton distribution functions.
Physical review / D, 90(3):032004, and PUBDB-2015-00137, CMS-SMP-12-021; CERN-PH-EP-2013-232; arXiv:1312.6283.
doi: 10.1103/PhysRevD.90.032004.

CMS Collaboration.
Measurement of the production cross section for a W boson and two b jets in pp collisions at sqrt(s) = 7 TeV.
Physics letters / B, 735:204, and PUBDB-2014-03545, arXiv:1312.6608; CMS-SMP-12-026; CERN-PH-EP-2013-223.
doi: 10.1016/j.physletb.2014.06.041.

CMS Collaboration.
Measurement of the production cross sections for a Z boson and one or more b jets in pp collisions at $\sqrt{s}$ = 7 TeV.
Journal of high energy physics, 1406:120, and PUBDB-2014-03539, arXiv:1402.1521; CMS-SMP-13-004; CERN-PH-EP-2014-005.
doi: 10.1007/JHEP06(2014)120.

CMS Collaboration.
Measurement of the properties of a Higgs boson in the four-lepton final state.
Physical review / D, 89(9):092007, and DESY-2014-02849, arXiv:1312.5353; CMS-HIG-13-002; CERN-PH-EP-2013-220.
doi: 10.1103/PhysRevD.89.092007.

CMS Collaboration.
Measurement of the ratio $B(t \to Wb)/B(t \to Wq)$ in pp collisions at $\sqrt{s}$ = 8 TeV.
Physics letters / B, 736:33, and DESY-2014-03312, arXiv:1404.2292; CMS-TOP-12-035; CERN-PH-EP-2014-052.
doi: 10.1016/j.physletb.2014.06.076.

CMS Collaboration.
Measurement of the ratio of inclusive jet cross sections using the anti-k_T algorithm with radius parameters R=0.5 and 0.7 in pp collisions at $\sqrt{s} = 7$ TeV.
Physical review / D, 90(7):072006, and PUBDB-2015-00116, CMS-SMP-13-002; CERN-PH-EP-2014-068; arXiv:1406.0324.
doi: 10.1103/PhysRevD.90.072006.

CMS Collaboration.
Measurement of the $t\bar{t}$ production cross section in the dilepton channel in pp collisions at $\sqrt{s}$ = 8 TeV.
Journal of high energy physics, 1402(2):24, and DESY-2014-02287, arXiv:1312.7582; CMS-TOP-12-007; CERN-PH-EP-2013-234.
doi: 10.1007/JHEP02(2014)024.

CMS Collaboration.
Measurement of the t-channel single-top-quark production cross section and of the $|V_{tb}|$ CKM matrix element in pp collisions at $\sqrt{s}$= 8 TeV.
Journal of high energy physics, 2014:90, and PUBDB-2014-03504, Xiv:1403.7366; CMS-TOP-12-038; CERN-PH-EP-2014-032.
doi: 10.1007/JHEP06(2014)090.

CMS Collaboration.
Measurement of the triple-differential cross section for photon+jets production in proton-proton collisions at $\sqrt{s}$=7 TeV.
Journal of high energy physics, 2014:9, and PUBDB-2014-03637, arXiv:1311.6141; CMS-QCD-11-005-003; CERN-PH-EP-2013-194.
doi: 10.1007/JHEP06(2014)009.

CMS Collaboration.
Measurement of the $t\bar{t}$ Production Cross Section in pp Collisions at s√=8 TeV in Dilepton Final States Containing one τ Lepton.
Physics letters / B, 739:23, and PUBDB-2015-00708, CERN-PH-EP-2014-167; CMS-TOP-12-026; arXiv:1407.6643.
doi: 10.1016/j.physletb.2014.10.032.

CMS Collaboration.
Measurement of the W gamma and Z gamma inclusive cross sections in pp collisions at $\sqrt{s}$ = 7 TeV and limits on anomalous triple gauge boson couplings.
Physical review / D, 89(9):092005, and PUBDB-2014-03650, arXiv:1308.6832; CMS-EWK-11-009; CERN-PH-EP-2013-108.
doi: 10.1103/PhysRevD.89.092005.

CMS Collaboration.
Measurement of top quark-antiquark pair production in association with a W or Z boson in pp collisions at $\sqrt{s}$ = 8 TeV.
The European physical journal / C, 74(9):3060, and PUBDB-2015-00085, CMS-TOP-12-036; CERN-PH-EP-2014-136; arXiv:1406.7830.
doi: 10.1140/epjc/s10052-014-3060-7.

CMS Collaboration.
Measurement of WZ and ZZ production in pp collisions at $\sqrt{s}$ = 8 TeV in final states with b-tagged jets.
The European physical journal / C, 74(8):2973, and PUBDB-2014-03505, arXiv:1403.3047; CMS-SMP-13-011; CERN-PH-EP-2014-022.
doi: 10.1140/epjc/s10052-014-2973-5.

CMS Collaboration.
Measurements of the $t\bar{t}$ charge asymmetry using the dilepton decay channel in pp collisions at $\sqrt{s}$ = 7 TeV.
Journal of high energy physics, 2014(4):191, and DESY-2014-02845, arXiv:1402.3803; CMS-TOP-12-010; CERN-PH-EP-2014-010.
doi: 10.1007/JHEP04(2014)191.

CMS Collaboration.
Measurements of $t\bar{t}$ spin correlations and top-quark polarization using dilepton final states in pp collisions at $\sqrt{s}$ = 7 TeV.
Physical review letters, 112(18):182001, and DESY-2014-02854, arXiv:1311.3924; CMS-TOP-13-003; CERN-PH-EP-2013-211.
doi: 10.1103/PhysRevLett.112.182001.

CMS Collaboration.
Modification of Jet Shapes in PbPb Collisions at $\sqrt{s_{NN}} = 2.76$ TeV.
Physics letters / B, 730:243, and PUBDB-2015-01210, CERN-PH-EP-2013-189; CMS-HIN-12-002; arXiv:1310.0878.
doi: 10.1016/j.physletb.2014.01.042.

CMS Collaboration.
Observation of a peaking structure in the J/psi phi mass spectrum from B(+/-) to J/psi phi K(+/-) decays.
Physics letters / B, 734:261, and PUBDB-2014-03649, arXiv:1309.6920; CMS-BPH-11-026; CERN-PH-EP-2013-167.
doi: 10.1016/j.physletb.2014.05.055.

CMS Collaboration.
Observation of the associated production of a single top quark and a W boson in pp collisions at $\sqrt{s}$ = 8 TeV arXiv.
Physical review letters, 112(23):231802, and PUBDB-2014-03544, arXiv:1401.2942; CMS-TOP-12-040; CERN-PH-EP-2013-237.
doi: 10.1103/PhysRevLett.112.231802.

CMS Collaboration.
Observation of the diphoton decay of the Higgs boson and measurement of its properties.
The European physical journal / C, 74(10):3076, and PUBDB-2015-00084, CMS-HIG-13-001; CERN-PH-EP-2014-117; arXiv:1407.0558.
doi: 10.1140/epjc/s10052-014-3076-z.

CMS Collaboration.
Probing color coherence effects in pp collisions at $\sqrt{s} = 7$ TeV.
The European physical journal / C, 74(6):2901, and PUBDB-2014-03646, arXiv:1311.5815; CERN-PH-EP-2013-200; CMS-SMP-12-010.
doi: 10.1140/epjc/s10052-014-2901-8.

CMS Collaboration.
Search for anomalous production of events with three or more leptons in pp collisions at $\sqrt{s}$ = 8 TeV.
Physical review / D, 90(3):032006, and PUBDB-2015-00133, CMS-SUS-13-002; CERN-PH-EP-2014-039; arXiv:1404.5801.
doi: 10.1103/PhysRevD.90.032006.

CMS Collaboration.
Search for baryon number violation in top-quark decays.
Physics letters / B, 731:173, and DESY-2014-02648, arXiv:1310.1618; CMS-B2G-12-023; CERN-PH-EP-2013-179.
doi: 10.1016/j.physletb.2014.02.033.

CMS Collaboration.
Search for excited quarks in the γ + jet final state in proton-proton collisions at $\sqrt{s}$ = 8 TeV.
Physics letters / B, 738:274, and PUBDB-2015-00086, CMS-EXO-13-003; CERN-PH-EP-2014-129; arXiv:1406.5171.
doi: 10.1016/j.physletb.2014.09.048.

CMS Collaboration.
Search for flavor-changing neutral currents in top-quark decays t to Zq in pp collisions at sqrt(s) = 8 TeV.
Physical review letters, 112(17):171802, and DESY-2014-02850, arXiv:1312.4194; CMS-TOP-12-037; CERN-PH-EP-2013-208.
doi: 10.1103/PhysRevLett.112.171802.

CMS Collaboration.
Search for Heavy Neutrinos and W Bosons with Right-Handed Couplings in Proton-Proton Collisions at s√=8TeV.
The European physical journal / C, 74(11):3149, and PUBDB-2015-00712, CMS-EXO-13-008; CERN-PH-EP-2014-161; arXiv:1407.3683.
doi: 10.1140/epjc/s10052-014-3149-z.

CMS Collaboration.
Search for invisible decays of Higgs bosons in the vector boson fusion and associated ZH production modes.
The European physical journal / C, 74(8):2980, and PUBDB-2014-03503, arXiv:1404.1344; CMS-HIG-13-030; CERN-PH-EP-2014-051.
doi: 10.1140/epjc/s10052-014-2980-6.

CMS Collaboration.
Search for jet extinction in the inclusive jet-p_T spectrum from proton-proton collisions at $\sqrt{s} = 8$ TeV.
Physical review / D, 90(3):032005, and PUBDB-2015-00117, CMS-EXO-12-051; CERN-PH-EP-2014-108; arXiv:1405.7653.
doi: 10.1103/PhysRevD.90.032005.

CMS Collaboration.
Search for massive resonances decaying into pairs of boosted bosons in semi-leptonic final states at $\sqrt{s} = 8$ TeV.
Journal of high energy physics, 2014:174, and PUBDB-2014-03502, arXiv:1405.3447; CMS-EXO-13-009; CERN-PH-EP-2014-076.
doi: 10.1007/JHEP08(2014)174.

CMS Collaboration.
Search for massive resonances in dijet systems containing jets tagged as W or Z boson decays in pp collisions at $\sqrt{s}$ = 8 TeV.
Journal of high energy physics, 2014:173, and PUBDB-2014-03501, arXiv:1405.1994; CMS-EXO-12-024; CERN-PH-EP-2014-071.
doi: 10.1007/JHEP08(2014)173.

CMS Collaboration.
Search for neutral MSSM Higgs bosons decaying to a pair of tau leptons in pp collisions.
Journal of high energy physics, 10(10):160, and PUBDB-2015-00082, CMS-HIG-13-021; CERN-PH-EP-2014-192; arXiv:1408.3316.
doi: 10.1007/JHEP10(2014)160.

CMS Collaboration.
Search for new physics in events with same-sign dileptons and jets in pp collisions at $\sqrt{s}$=8 TeV.
Journal of high energy physics, 2014(1):163, and DESY-2014-01752, arXiv:1311.6736; CMS-SUS-13-013; CERN-PH-EP-2013-213.
doi: 10.1007/JHEP01(2014)163.

CMS Collaboration.
Search for new physics in the multijet and missing transverse momentum final state in proton-proton collisions at $\sqrt{s}$= 8 TeV.
Journal of high energy physics, 2014:55, and PUBDB-2014-03508, arXiv:1402.4770; CMS-SUS-13-012; CERN-PH-EP-2014-015.
doi: 10.1007/JHEP06(2014)055.

CMS Collaboration.
Search for new Resonances Decaying via WZ to Leptons in Proton-Proton Collisions at s√= 8 TeV.
Physics letters / B, 740:83, and PUBDB-2015-00715, CMS-EXO-12-025; CERN-PH-EP-2014-160; arXiv:1407.3476.
doi: 10.1016/j.physletb.2014.11.026.

CMS Collaboration.
Search for pair production of excited top quarks in the lepton + jets final state.
Journal of high energy physics, 2014:125, and PUBDB-2014-03647, arXiv:1311.5357; CMS-B2G-12-014; CERN-PH-EP-2013-206.
doi: 10.1007/JHEP06(2014)125.

CMS Collaboration.
Search for Pair Production of Third-Generation Scalar Leptoquarks and Top Squarks in Proton-Proton Collisions at $\sqrt{s} = 8$ TeV.
Physics letters / B, 739:229, and PUBDB-2015-00707, CMS-EXO-12-032; CERN-PH-EP-2014-190; arXiv:1408.0806.
doi: 10.1016/j.physletb.2014.10.063.

CMS Collaboration.
Search for supersymmetry in pp collisions at $\sqrt{s}$=8 TeV in events with a single lepton, large jet multiplicity, and multiple b jets.
Physics letters / B, 733:328, and PUBDB-2014-03648, arXiv:1311.4937; CMS-SUS-13-007; CERN-PH-EP-2013-209.
doi: 10.1016/j.physletb.2014.04.023.

CMS Collaboration.
Search for Supersymmetry with Razor Variables in pp Collisions at $\sqrt{s}$=7 TeV.
Physical review / D, 90(11):112001, and PUBDB-2015-00848, CMS-SUS-12-005; CERN-PH-EP-2014-057; arXiv:1405.3961.
doi: 10.1103/PhysRevD.90.112001.

CMS Collaboration.
Search for the Associated Production of the Higgs Boson with a Top-Quark Pair.
Journal of high energy physics, 1410:106, and PUBDB-2015-01105, CMS-HIG-13-029; CERN-PH-EP-2014-189; arXiv:1408.1682.
doi: 10.1007/JHEP10(2014)106.

CMS Collaboration.
Search for the associated production of the Higgs boson with a top-quark pair.
Journal of high energy physics, 2014(9):87, and PUBDB-2015-00131, CMS-HIG-13-029; CERN-PH-EP-2014-189; arXiv:1408.1682.
doi: 10.1007/JHEP09(2014)087.

CMS Collaboration.
Search for the standard model Higgs boson produced in association with a W or a Z boson and decaying to bottom quarks.
Physical review / D, 89(1):012003, and DESY-2014-01753, arXiv:1310.3687; CMS-HIG-13-012; CERN-PH-EP-2013-188.
doi: 10.1103/PhysRevD.89.012003.

CMS Collaboration.
Search for top squark and higgsino production using diphoton Higgs boson decays.
Physical review letters, 112(16):161802, and DESY-2014-02851, arXiv:1312.3310; CMS-SUS-13-014; CERN-PH-EP-2013-226.
doi: 10.1103/PhysRevLett.112.161802.

CMS Collaboration.
Search for Top-Quark Partners with Charge 5/3 in the Same-Sign Dilepton Final State.
Physical review letters, 112(17):171801, and DESY-2014-02852, arXiv:1312.2391; CMS-B2G-12-012; CERN-

PH-EP-2013-216.
doi: 10.1103/PhysRevLett.112.171801.

CMS Collaboration.
Search for top-squark pairs decaying into Higgs or Z bosons in pp collisions at $\sqrt{s}$=8 TeV.
Physics letters / B, 736:371, and PUBDB-2015-00128, CMS-SUS-13-024; CERN-PH-EP-2014-073; arXiv:1405.3886.
doi: 10.1016/j.physletb.2014.07.053.

CMS Collaboration.
Search for W' → tb decays in the lepton + jets final state in pp collisions at $\sqrt{s}$ = 8 TeV.
Journal of high energy physics, 2014:108, and PUBDB-2014-03525, arXiv:1402.2176; CMS-B2G-12-010; CERN-PH-EP-2014-011.
doi: 10.1007/JHEP05(2014)108.

CMS Collaboration.
Search for $WW\gamma$ and $WZ\gamma$ production and constraints on anomalous quartic gauge couplings in pp collisions at $\sqrt{s} = 8$ TeV.
Physical review / D, 90(3):032008, and PUBDB-2015-00135, CMS-SMP-13-009; CERN-PH-EP-2014-046; arXiv:1404.4619.
doi: 10.1103/PhysRevD.90.032008.

CMS Collaboration.
Searches for Electroweak Neutralino and Chargino Production in Channels with Higgs, Z, and W Bosons in pp Collisions at 8 TeV.
Physical review / D, 90(9):092007, and PUBDB-2015-00703, CMS-SUS-14-002; CERN-PH-EP-2014-216; arXiv:1409.3168.
doi: 10.1103/PhysRevD.90.092007.

CMS Collaboration.
Searches for electroweak production of charginos, neutralinos, and sleptons decaying to leptons and W, Z, and Higgs bosons in pp collisions at 8 TeV.
The European physical journal / C, 74(9):3036, and PUBDB-2015-00119, CMS-SUS-13-006; CERN-PH-EP-2014-098; arXiv:1405.7570.
doi: 10.1140/epjc/s10052-014-3036-7.

CMS Collaboration.
Searches for Heavy Higgs Bosons in Two-Higgs-Doublet Models and for t to ch Decay Using Multilepton and Diphoton Final States in pp Collisions at 8 TeV.
Physical review / D, 90(11):112013, and PUBDB-2015-00700, CMS-HIG-13-025; CERN-PH-EP-2014-239; arXiv:1410.2751.
doi: 10.1103/PhysRevD.90.112013.

CMS Collaboration.
Searches for light- and heavy-flavour three-jet resonances in pp collisions at $\sqrt{s} = 8$ TeV.
Physics letters / B, 730:193, and DESY-2014-02477, arXiv:1311.1799; CMS-EXO-12-049; CERN-PH-EP-2013-204.
doi: 10.1016/j.physletb.2014.01.049.

CMS Collaboration.
Studies of azimuthal dihadron correlations in ultra-central PbPb collisions at $\sqrt{s_{NN}} = 2.76$ TeV.
Journal of high energy physics, 1402(2):88, and DESY-2014-02476, arXiv:1312.1845; CERN-PH-EP-2013-214; CMS-HIN-12-011.
doi: 10.1007/JHEP02(2014)088.

CMS Collaboration.
Studies of dijet transverse momentum balance and pseudorapidity distributions in pPb collisions at $\sqrt{s_{\mathrm{NN}}} = 5.02$ TeV.
The European physical journal / C, 74(7):2951, and PUBDB-2014-03543, arXiv:1401.4433; CMS-HIN-13-001; CERN-PH-EP-2013-236.
doi: 10.1140/epjc/s10052-014-2951-y.

CMS Collaboration.
Study of double parton scattering using W + 2-jet events in proton-proton collisions at $\sqrt{s}$ = 7 TeV.
Journal of high energy physics, 1403(3):32, and DESY-2014-02475, arXiv:1312.5729; CMS-FSQ-12-028; CERN-PH-EP-2013-224.
doi: 10.1007/JHEP03(2014)032.

CMS Collaboration.
Study of hadronic event-shape variables in multijet final states in pp collisions at $\sqrt{s} = 7$ TeV.
Journal of high energy physics, 10:087, and PUBDB-2015-00083, CMS-SMP-12-022; CERN-PH-EP-2014-146; arXiv:1407.2856.
doi: 10.1007/JHEP10(2014)087.

CMS Collaboration.
Study of the production of charged pions, kaons, and protons in pPb collisions at $\sqrt{s_{NN}}$ =5.02 TeV.
The European physical journal / C, 74:2847, and PUBDB-2014-03651, arXiv:1307.3442; CMS-HIN-12-016; CERN-PH-EP-2013-096.
doi: 10.1140/epjc/210052-014-2847-x.

S. Spannagel.
Test Beam Campaigns for the CMS Phase I Upgrade Pixel Readout Chip.
Journal of Instrumentation, 9(12):C12001, and PUBDB-2015-01094, CMS-CR-2014-231; arXiv:1410.1399.
doi: 10.1088/1748-0221/9/12/C12001.

CMS Collaboration and TOTEM Collaboration.
Measurement of pseudorapidity distributions of charged particles in proton-proton collisions at $\sqrt{s}$ = 8 TeV by the CMS and TOTEM experiments.
The European physical journal / C, 74(10):3053, and PUBDB-2015-00132, CMS-FSQ-12-026; CERN-PH-EP-TOTEM-2014-002; CERN-PH-EP-2014-063; arXiv:1405.0722.
doi: 10.1140/epjc/s10052-014-3053-6.

J. Gao et al.
CT10 Next-to-Next-to-Leading Order Global Analysis of QCD.
Physical review / D, 89(3):033009, and PUBDB-2015-01102, SMU-HEP-12-23; arXiv:1302.6246.
doi: 10.1103/PhysRevD.89.033009.

M. Guzzi, P. M. Nadolsky and B. Wang.
Nonperturbative Contributions to a Resummed Leptonic Angular Distribution in Inclusive Neutral Vector Boson Production.
Physical review / D, 90(1):014030, and PUBDB-2015-01097, arXiv:1309.1393.
doi: 10.1103/PhysRevD.90.014030.

F. Hautmann and H. Jung.
Transverse Momentum Dependent Gluon Density from DIS Precision Data.
Nuclear physics / B, 883:1, and PUBDB-2015-01099, arXiv:1312.7875.
doi: 10.1016/j.nuclphysb.2014.03.014.

F. Hautmann, H. Jung and S. T. Monfared.
The CCFM uPDF evolution uPDFevolv Version 1.0.00.
The European physical journal / C, 74(10):3082, and PUBDB-2014-04557, DESY-14-060; RAL-arXiv:1407.5935; P-2014-010.
doi: 10.1140/epjc/s10052-014-3082-1.

F. Hautmann et al.
TMDlib and TMDplotter: library and plotting tools for transverse-momentum-dependent parton distributions.
The European physical journal / C, 74(12):3220, and PUBDB-2015-00311, DESY-14-059; NIKHEF-2014-024; YITP-SB-14-24; arXiv:1408.3015.
doi: 10.1140/epjc/s10052-014-3220-9.

J. L. Leonard et al.
Fast Beam Condition Monitor for CMS: performance and upgrade.
Nuclear instruments & methods in physics research / A, 765:235, and DESY-2014-03217, DESY 14-070.
doi: 10.1016/j.nima.2014.05.008.

A. V. Lipatov, M. A. Malyshev and N. Zotov.
Phenomenology of k_t-factorization for inclusive Higgs boson production at LHC.
Physics letters / B, 735:79, and DESY-2014-03182, DESY 14-062; arXiv:1402.6481.
doi: 10.1016/j.physletb.2014.06.014.

A. Lipatov and N. Zotov.
TMD parton densities in associated real and virtual photon and jet production at LHC.
Physical review / D, D90(9):094005, and PUBDB-2014-04204, DESY 14-197; arXiv:1409.0514.
doi: 10.1103/PhysRevD.90.094005.

I. Melzer-Pellmann and P. Pralavorio.
Lessons for SUSY from the LHC after the first Run.
The European physical journal / C, 74(5):2801, and PUBDB-2015-01100, arXiv:1404.7191.
doi: 10.1140/epjc/s10052-014-2801-y.

Z. Nagy and D. E. Soper.
A parton shower based on factorization of the quantum density matrix.
Journal of high energy physics, 2014(6):97, and DESY-2014-03297, DESY 13-241; arXiv:1401.6364.
doi: 10.1007/JHEP06(2014)097.

Z. Nagy and D. E. Soper.
Ordering variable for parton showers.
Journal of high energy physics, 2014(6):178, and DESY-2014-03280, DESY 13-242; arXiv:1401.6366.
doi: 10.1007/JHEP06(2014)178.

Z. Nagy and D. E. Soper.
Parton distribution functions in the context of parton showers.
Journal of high energy physics, 2014(6):179, and DESY-2014-03290, DESY 13-240; arXiv:1401.6368.
doi: 10.1007/JHEP06(2014)179.

Ph.D. Thesis

I. Asin Cruz.
Measurement of Top-Quark-Pair Differential Cross Sections in Proton-Proton Collisions at $\sqrt{s}$ = 8TeV with the CMS Experiment.
University of Hamburg, Hamburg, 2014.

P. Cipriano.
Forward-Central Jet Correlations in pp collisions at CMS.
University of Hamburg, Hamburg, 2014.

F. Costanza.
Search for Pair Production of Supersymmetric Top-Quark Partners in Events with a Single Lepton at CMS.
University of Hamburg, Hamburg, 2014.

J. Erfle.
Irradiation study of different silicon materials for the CMS tracker upgrade.
University of Hamburg, Hamburg, 2014.

M. Goerner.
Differential Cross Sections for Top-Quark-Pair Production in the e/μ+Jets Final State at $\sqrt{s} = 8$ TeV in CMS.
University of Hamburg, Hamburg, 2014.

N. Pietsch.
Search for Supersymmetry in Final States with a Single Lepton, B-Quark Jets, and Missing Transverse Energy at the CMS Experiment.
University of Hamburg, Hamburg, 2014.

J. Salfeld.
Search for the Higgs Boson Decaying into τ-Leptons in the Di-Electron Channel.
University of Hamburg, Hamburg, 2014.

Electronics Development

Published

D. Greiffenberg et al.
Towards AGIPD1.0: Optimization of the Dynamic Range and Investigation of a Pixel Input Protection.
Journal of Instrumentation, 9(06):P06001, and PUBDB-2015-01201.
doi: 10.1088/1748-0221/9/06/P06001.

D. Pennicard et al.
High-Speed Readout of High-Z Pixel Detectors with the LAMBDA Detector.
12. 10th International Conference on Position Sensitive Detectors, University of Surrey (UK), 09/07/2014 - 09/12/2014.
Inst. of Physics, London, Sept. 2014.
doi: 10.1088/1748-0221/9/12/C12014.

H1

Published

H1 Collaboration.
Measurement of Feynman-x spectra of photons and neutrons in the very forward direction in deep-inelastic scattering at HERA.
The European physical journal / C, 74:2915, and DESY-2014-03214, DESY-14-035; arXiv:1404.0201.
doi: 10.1140/epjc/s10052-014-2915-2.

H1 Collaboration.
Measurement of Inclusive ep Cross Sections at High Q^2 at $\sqrt{s}$ = 225 and 252 GeV and of the Longitudinal Proton Structure Function F_L at HERA.
The European physical journal / C, 74(4):2814, and PUBDB-2014-03638, DESY-13-211; arXiv:1312.4821.
doi: 10.1140/epjc/s10052-014-2814-6.

P. R. Newman and M. Wing.
The Hadronic Final State at HERA.
Reviews of modern physics, 86(3):1037, and PUBDB-2015-01144, arXiv:1308.3368.
doi: 10.1103/RevModPhys.86.1037.

Ph.D. Thesis

S. Bayesteh.
Transverse Electron Beam Diagnostic at REGAE.
University of Hamburg, Hamburg, 2014.

B. Pokorny.
Measurement of Diffractive Dijet Production in Deep Inelastic Scattering at HERA Collider.
Charles University, Prague, 2014.

HERMES

Published

S. Yashchenko.
An overview of recent DVCS results at HERMES.
1. The 20th International Symposium on Spin Physics, Dubna (Russian Federation), 09/17/2012 - 09/22/2012.
MAIK Nauka/Interperiodica, Moskva, Sept. 2014.
doi: 10.1134/S1063779614011127.

HERMES Collaboration.
Beam-helicity asymmetry in associated electroproduction of real photons ep→epγN in the Δ-resonance region.
Journal of high energy physics, 2014(1):77, and DESY-2014-01179, DESY 13-188; arXiv:1310.5081.
doi: 10.1007/JHEP01(2014)077.

M. Murray.
DVCS at HERMES.
1. The 20th International Symposium on Spin Physics, Dubna (Russian Federation), 09/17/2012 - 09/22/2012.
MAIK Nauka/Interperiodica, Moskva, Sept. 2014.
doi: 10.1134/S1063779614010675.

F. Giordano.
Flavor dependent azimuthal asymmetries in unpolarized semi-inclusive DIS at HERMES.
1. The 20th International Symposium on Spin Physics, Dubna (Russian Federation), 09/17/2012 - 09/22/2012.
MAIK Nauka/Interperiodica, Moskva, Sept. 2014.
doi: 10.1134/S1063779614010353.

V. A. Korotkov.
Measurement of the spin-structure function g_2 and the semi-inclusive double-spin asymmetries at HERMES.
1. The 20th International Symposium on Spin Physics, Dubna (Russian Federation), 09/17/2012 - 09/22/2012.
MAIK Nauka/Interperiodica, Moskva, Sept. 2014.
doi: 10.1134/S1063779614010511.

HERMES Collaboration.
Reevaluation of the parton distribution of strange quarks in the nucleon.
Physical review / D, 89(9):097101, and DESY-2014-03029, DESY 13-246; arXiv:1312.7028.
doi: 10.1103/PhysRevD.89.097101.

T.-A. Shibata.
Ring imaging Cherenkov counter of HERMES for pion, kaon, proton and anti-proton identification.
Eighth International Workshop on Ring Imaging Cherenkov Detectors, Shonan, Kanagawa (Japan), 12/02/2013 - 12/06/2013.
North-Holland Publ. Co., Amsterdam, Dec. 2014.
doi: 10.1016/j.nima.2014.04.070.

HERMES Collaboration.
Spin density matrix elements in exclusive ω electroproduction on ^{1}H and ^{2}H targets at 27.5 GeV beam energy.
The European physical journal / C, 74(11):3110, and PUBDB-2014-04143, DESY 14-116; arXiv:1407.2119.
doi: 10.1140/epjc/s10052-014-3110-1.

S. Belostotski.
Spin transfer to Λ and $\bar{\Lambda}$ hyperons in deep inelastic scattering at HERMES.
1. The 20th International Symposium on Spin Physics, Dubna (Russian Federation), 09/17/2012 - 09/22/2012.
MAIK Nauka/Interperiodica, Moskva, Sept. 2014.
doi: 10.1134/S1063779614010146.

L. L. Pappalardo.
Study of TMDs with polarized beam and/or targets.
1. The 20th International Symposium on Spin Physics, Dubna (Russian Federation), 09/17/2012 - 09/22/2012.
MAIK Nauka/Interperiodica, Moskva, Sept. 2014.
doi: 10.1134/S1063779614010766.

HERMES Collaboration.
Transverse polarization of Λ hyperons from quasireal photoproduction on nuclei.
Physical review / D, 90(7):072007, and PUBDB-2014-03849, arXiv:1406.3236; DESY 14-097.
doi: 10.1103/PhysRevD.90.072007.

HERMES Collaboration.
Transverse target single-spin asymmetry in inclusive electroproduction of charged pions and kaons.
Physics letters / B, 728:183, and DESY-2013-01334, arXiv:1310.5070; DESY 13-187.
doi: 10.1016/j.physletb.2013.11.021.

Ph.D. Thesis

I. Brodski.
Analysis of Hard Exclusive Scattering Processes of the HERMES Recoil Experiment.
Justus-Liebig-Universität Giessen, Giessen, 2014.

M. Golembiovskaya.
Exclusive phi meson production at HERMES.
University of Hamburg, Hamburg, 2014.

Linear Collider

Published

A. Cianchi and J. Osterhoff.
Summary of the Working Group 5: Plasma sources and instrumentation.
1st European Advanced Accelerator Concepts Workshop, La Biodola, Isola d'Elba (Italy), 06/02/2013 - 06/07/2013.
North-Holland Publ. Co., Amsterdam, June 2014.
doi: 10.1016/j.nima.2014.01.036.

M. Beckmann et al.
Spin Transport and Polarimetry in the Beam Delivery System of the International Linear Collider.
Journal of Instrumentation, 9(07):P07003, and DESY-2014-03218, DESY 14-071.
doi: 10.1088/1748-0221/9/07/P07003.

CALICE Collaboration.
Performance of the first prototype of the CALICE scintillator strip electromagnetic calorimeter.
Nuclear instruments & methods in physics research / A, 763:278, and PUBDB-2014-04795.
doi: 10.1016/j.nima.2014.06.039.

CALICE Collaboration.
Shower development of particles with momenta from 1 to 10 GeV in the CALICE Scintillator-Tungsten HCAL.
Journal of Instrumentation, 9(01):1, and DESY-2014-00776.
doi: 10.1088/1748-0221/9/01/P01004.

CALICE Collaboration.
The Time Structure of Hadronic Showers in Highly Granular Calorimeters with Tungsten and Steel Absorbers.
Journal of Instrumentation, 9(07):P07022, and PUBDB-2014-04796, arXiv:1404.6454; MPP-2014-147.
doi: 10.1088/1748-0221/9/07/P07022.

A. Fognini et al.
The role of space charge in spin-resolved photoemission experiments.
New journal of physics, 16(4):043031, and DESY-2014-02940.
doi: 10.1088/1367-2630/16/4/043031.

A. Fognini et al.
Ultrafast reduction of the total magnetization in iron.
Applied physics letters, 104(3):032402, and DESY-2014-02412.
doi: 10.1063/1.4862476.

J. Grebenyuk et al.
Beam-driven plasma-based acceleration of electrons with density down-ramp injection at FLASHForward.
First European Advanced Accelerator Concepts Workshop 2013- Proceedings , La Biodola, Isola d'Elba (Italy), 06/02/2013 - 06/07/2013.
North-Holland Publ. Co., Amsterdam, June 2014.
doi: 10.1016/j.nima.2013.10.054.

T. Mehrling et al.
HiPACE: a quasi-static particle-in-cell code.
8. Laser and Plasma Accelerator Workshop 2013, Goa (India), 09/01/2013 - 09/06/2013.
IOP Publ., Bristol, Sept. 2014.
doi: 10.1088/0741-3335/56/8/084012.

L. Schaper et al.
Longitudinal gas-density profilometry for plasma-wakefield acceleration targets.
1st European Advanced Accelerator Concepts Workshop, La Biodola, Isola d'Elba (Italy), 06/02/2013 - 06/07/2013.
North-Holland Publ. Co., Amsterdam, June 2014.
doi: 10.1016/j.nima.2013.10.052.

B. Schmidt and S. Wesch.
Echtzeitspektroskopie von Ferninfrarotstrahlung zur Strahldiagnose an Linearbeschleunigern - Real-time far-infrared spectroscopy as diagnostic tool for linear accelerators.
Technisches Messen, 81(3):137, and PUBDB-2014-04138.
doi: 10.1515/teme-2014-1023.

B. Vormwald.
Polarisation and beam energy measurement at a linear e + e collider.
Journal of Instrumentation, 9(08):C08012, and PUBDB-2015-01070.
doi: 10.1088/1748-0221/9/08/C08012.

B. Vormwald and J. List.
Bilinear R parity violation at the ILC: neutrino physics at colliders.
The European physical journal / C, 74(2):2720, and DESY-2014-01794.
doi: 10.1140/epjc/s10052-014-2720-y.

G. Xia et al.
Collider Design Issues based on Proton-Driven Plasma Wakefield Acceleration.
Nuclear instruments & methods in physics research / A, 740:173, and PUBDB-2015-01160, arXiv:1404.6107.
doi: 10.1016/j.nima.2013.11.006.

C. Xu et al.
Influence of X-ray irradiation on the properties of the Hamamatsu silicon photomultiplier S10362-11-050C.
Nuclear instruments & methods in physics research / A, 762:149, and PUBDB-2014-03702.
doi: 10.1016/j.nima.2014.05.112.

Master Thesis

C. Entrena.
Erzeugung und Transport von Doppelpaket-Elektronenstrahlen im FLASH Linearbeschleuniger(Generation and transport of double-bunch electron beams in the FLASH beamline).
University of Hamburg, Hamburg, 2014.

Ph.D. Thesis

T. Mehrling.
Theoretical and numerical studies on the transport of transverse beam quality in plasma-based accelerators.
University of Hamburg, Hamburg, 2014.

S. Schulz.
Implementation of the Laser-Based Femtosecond Precision Synchronization System at FLASH.
University of Hamburg, Hamburg, 2014.

A. Vauth.
A Quartz Cherenkov Detector for Polarimetry at the ILC.
University of Hamburg, Hamburg, 2014.

B. Vormwald.
From Neutrino Physics to Beam Polarisation - a High Precision Story at the ILC.
University of Hamburg, Hamburg, 2014.

C. Xu.
Study of the Silicon Photomultipliers and Their Applications in Positron Emission Tomography.
University of Hamburg, Hamburg, 2014.

OLYMPUS

Published

OLYMPUS Collaboration.
The OLYMPUS experiment.
Nuclear instruments & methods in physics research / A, 741:1, and DESY-2014-01887.
doi: 10.1016/j.nima.2013.12.035.

Ph.D. Thesis

O. Ates.
GEM Luminosity Monitors for the Olympus Experiment to determine the Effect of Two-Photon Exchange.
Hampton University, Hampton, 2014.

Theory

Published

A. Abdel-Rehim et al.
Disconnected quark loop contributions to nucleon observables in lattice QCD.
Physical review / D, 89(3):034501, and PUBDB-2014-03842, arXiv:1310.6339.
doi: 10.1103/PhysRevD.89.034501.

J. Ablinger et al.
Calculating massive 3-loop graphs for operator matrix elements by the method of hyperlogarithms.
Nuclear physics / B, 885:409, and PUBDB-2014-03832, DESY-13-063; DO-TH-14-02; SFB-CPP-14-12; LPN-14-046; HIGGSTOOLS –14-005; arXiv:1403.1137.
doi: 10.1016/j.nuclphysb.2014.04.007.

J. Ablinger et al.
Iterated Binomial Sums and their Associated Iterated Integrals.
Journal of mathematical physics, 55(11):112301, and PUBDB-2015-01108.
doi: 10.1063/1.4900836.

J. Ablinger et al.
The 3-loop non-singlet heavy flavor contributions and anomalous dimensions for the structure function $F_2(x,Q^2)$ and transversity.
Nuclear physics / B, 886:733, and PUBDB-2014-04119.
doi: 10.1016/j.nuclphysb.2014.07.010.

J. Ablinger et al.
The transition matrix element of the variable flavor number scheme at.
Nuclear physics / B, 882:263, and DESY-2014-02437.
doi: 10.1016/j.nuclphysb.2014.02.007.

A. Akhundov et al.
The ZFITTER project.
Physics of particles and nuclei, 45(3):529, and DESY-2014-03039, arXiv:1302.1395.
doi: 10.1134/S1063779614030022.

S. Alekhin, J. Blümlein and S. Moch.
The ABM parton distributions tuned to LHC data.
Physical review / D, 89(5):054028, and PUBDB-2014-04260, DESY-13-183; DO-TH-13-26; SFB-CPP-13-71; LPN-13-068; arXiv:1310.3059.
doi: 10.1103/PhysRevD.89.054028.

S. Alekhin, J. Blümlein and S.-O. Moch.
Statistical Issues in the Parton Distribution Analysis of the Tevatron Jet Data.
Journal of high energy physics, 2014(2):41, and DESY-2014-02387, DO-TH 12/34; LPN12-118; SFB/CPP-12-79.
doi: 10.1007/JHEP02(2014)041.

S. Alekhin et al.
Nucleon PDF separation with the collider and fixed-target data.
37th International Conference on High Energy Physics, Valencia (Spain), 07/02/2014 - 07/09/2014.
Elsevier, Amsterdam, July 2014.

C. Alexandrou et al.
A stochastic method for computing hadronic matrix elements.
The European physical journal / C, 74(1):2692, and DESY-2014-02959.
doi: 10.1140/epjc/s10052-013-2692-3.

C. Alexandrou et al.
Baryon spectrum with $N_f = 2+1+1$ twisted mass fermions.
Physical review / D, 90(7):074501, and PUBDB-2015-00870, DESY-14-096 , arXiv:1406.4310.
doi: 10.1103/PhysRevD.90.074501.

C. Alexandrou et al.
Evaluation of disconnected quark loops for hadron structure using GPUs.
Computer physics communications, 185(5):1370, and PUBDB-2014-03851, arXiv:1309.2256.
doi: 10.1016/j.cpc.2014.01.009.

A. Ali, A. Y. Parkhomenko and A. V. Rusov.
Precise calculation of the dilepton invariant-mass spectrum and the decay rate in $B^{\pm} \to \pi^{\pm}\mu^{+}\mu^{-}$ in the SM.
Physical review / D, 89(9):094021, and DESY-2014-02907, DESY-13-153.
doi: 10.1103/PhysRevD.89.094021.

S. Alioli et al.
Matching fully differential NNLO calculations and parton showers.
Journal of high energy physics, 2014(6):89, and DESY-2014-02910, DESY-13-194.
doi: 10.1007/JHEP06(2014)089.

S. Alioli et al.
Update of the Binoth Les Houches Accord for a standard interface between Monte Carlo tools and one-loop programs.
Computer physics communications, 185(2):560, and DESY-2014-00182.
doi: 10.1016/j.cpc.2013.10.020.

S. de Alwis et al.
Moduli spaces in AdS $_4$ supergravity.
Journal of high energy physics, 2014(5):102, and DESY-2014-02913, DESY-13-252.
doi: 10.1007/JHEP05(2014)102.

S. Aoki et al.
Review of lattice results concerning low-energy particle physics.
The European physical journal / C, 74(9):2890, and PUBDB-2014-04108, arXiv:1310.8555.
doi: 10.1140/epjc/s10052-014-2890-7.

C. Arina, V. Martín-Lozano and G. Nardini.
Dark matter versus h → γγ and h → γZ with supersymmetric triplets.
Journal of high energy physics, 2014(8):15, and PUBDB-2014-03891, DESY 14-039.
doi: 10.1007/JHEP08(2014)015.

E. Armengaud et al.
Conceptual design of the International Axion Observatory (IAXO).
Journal of Instrumentation, 9(05):T05002, and DESY-2014-02782.
doi: 10.1088/1748-0221/9/05/T05002.

H. M. Asatrian and C. Greub.
Next-to-leading logarithmic QCD contribution of the electromagnetic dipole operator to $\bar{B} \to X_s\gamma\gamma$ with a massive strange quark.
Physical review / D, 89(9):094028, and DESY-2014-03005, DESY-14-034.
doi: 10.1103/PhysRevD.89.094028.

I. Bah, M. Gabella and N. Halmagyi.
BPS M5-Branes as Defects for the 3d-3d Correspondence.
Journal of high energy physics, 2014(11):112, and PUBDB-2015-01082, arXiv:1407.0403.
doi: 10.1007/JHEP11(2014)112.

I. Bah, M. Gabella and N. Halmagyi.
Punctures from Probe M5-Branes and $\mathcal{N} = 1$ Superconformal Field Theories.
Journal of high energy physics, 2014(7):131, and PUBDB-2015-01084, arXiv:1312.6687.
doi: 10.1007/JHEP07(2014)131.

M. Baker et al.
Hyperfine splitting in positronium to $O(\alpha^7 m_e)$: one-photon annihilation contribution.
Physical review letters, 112(12):120407, and DESY-2014-03324, DESY 14-011; ALBERTA-THY-03-14; HIGGSTOOLS-14-04; LPN14-045; SFB-CPP-14-08; TTK-14-06; TTP14-005; TUM-HEP-930-14;arXiv:1402.0876.
doi: 10.1103/PhysRevLett.112.120407.

L. Bao et al.
Non-Lagrangian theories from brane junctions.
Journal of high energy physics, 2014(1):175, and DESY-2014-02298, DESY-13-176; HU-Mathematik-17-13; HU-EP-13/50; KIAS-P13058; RIKEN-MP-78; arXiv:1310.3841.
doi: 10.1007/JHEP01(2014)175.

T. Bargheer, J. A. Minahan and R. Pereira.
Computing three-point functions for short operators.
Journal of high energy physics, 2014(3):96, and DESY-2014-02619, DESY-13-201.
doi: 10.1007/JHEP03(2014)096.

J. Bartels, V. Schomerus and M. Sprenger.
Heptagon amplitude in the multi-Regge regime.
Journal of high energy physics, 2014(10):67, and PUBDB-2014-04099.
doi: 10.1007/JHEP10(2014)067.

P. Bechtle et al.
HiggsBounds-4: improved tests of extended Higgs sectors against exclusion bounds from LEP, the Tevatron and the LHC.
The European physical journal / C, 74(3):2693, and DESY-2014-02396, DESY-13-110.
doi: 10.1140/epjc/s10052-013-2693-2.

P. Bechtle et al.
HiggsSignals: Confronting arbitrary Higgs sectors with measurements at the Tevatron and the LHC.
The European physical journal / C, 74(2):2711, and DESY-2014-02292, DESY-13-078.
doi: 10.1140/epjc/s10052-013-2711-4.

P. Bechtle et al.
Probing the Standard Model with Higgs signal rates from the Tevatron, the LHC and a future ILC.
Journal of high energy physics, 2014(11):39, and PUBDB-2014-04086.
doi: 10.1007/JHEP11(2014)039.

A. Behring et al.
The logarithmic contributions to the $O(\alpha_s^3)$ asymptotic massive Wilson coefficients and operator matrix elements in deeply inelastic scattering.
The European physical journal / C, 74(9):3033, and PUBDB-2014-04121, arxiv:1403.6356.
doi: 10.1140/epjc/s10052-014-3033-x.

I. Ben-Dayan and T. Kalaydzhyan.
Constraining the Primordial Power Spectrum from SNIa Lensing Dispersion.
Physical review / D, 90(8):083509, and PUBDB-2015-01083, DESY-13-166; arXiv:1309.4771.
doi: 10.1103/PhysRevD.90.083509.

I. Ben-Dayan and T. Kalaydzhyan.
Constraining the primordial power spectrum from SNIa lensing dispersion.
Physical review / D, D90:83509, and PUBDB-2014-04081, DESY 13-166; arXiv:1309.4771.

I. Ben-Dayan, F. G. Pedro and A. Westphal.
Hierarchical Axion Inflation.
Physical review letters, 113(26):261301, and PUBDB-2015-00238, DESY-14-065; arXiv:1404.7773.
doi: 10.1103/PhysRevLett.113.261301.

I. Ben-Dayan et al.
Accidental inflation from Kähler uplifting.
Journal of cosmology and astroparticle physics, 2014(03):054, and DESY-2014-02615, DESY-13-155.
doi: 10.1088/1475-7516/2014/03/054.

I. Ben-Dayan et al.
R 2 log R quantum corrections and the inflationary observables.
Journal of cosmology and astroparticle physics, 2014(09):005, and PUBDB-2014-04091, DESY 14-064.
doi: 10.1088/1475-7516/2014/09/005.

I. Ben-Dayan et al.
Value of H_0 in the Inhomogeneous Universe.
Physical review letters, 112(22):221301, and PUBDB-2014-03762, DESY-13-091.
doi: 10.1103/PhysRevLett.112.221301.

M. Beneke et al.
Leptonic decay of the Upsilon(1S) meson at third order in QCD.
Physical review letters, 112(15):151801, and PUBDB-2014-04198, DESY 13-254; ALBERTA-THY-01-14; LPN14-004; SFB-CPP-14-04; SI-HEP-2014-02; TTK-14-02; TTP14-003; TUM-HEP-923-14; –SI-HEP-2014-02; arXiv:1401.3005.
doi: 10.1103/PhysRevLett.112.151801.

Z. Bern, A. De Freitas and L. Dixon.
Erratum: Two-loop helicity amplitudes for quark-gluon scattering in QCD and gluino-gluon scattering in supersymmetric Yang-Mills theory.
Journal of high energy physics, 2014(4):112, and PUBDB-2014-04272, arXiv:hep-ph/0304168.
doi: 10.1007/JHEP04(2014)112.

F. Bernardoni et al.
Decay Constants of B-Mesons from Non-Perturbative HQET with two Light Dynamical Quarks.
Physics letters / B, B735:349, and DESY-2014-03222, DESY 14-048; HU-EP-14-14; IFIC-14-24; CP3-ORIGINS-2014-011-DNRF90; DIAS-2014-11; LPT-ORSAY-14-19; MITP-14-026; MS-TP-14-18; SFB-CPP-14-20; TCD-14-03; arXiv:1404.3590.
doi: 10.1016/j.physletb.2014.06.051.

F. Bernardoni et al.
The b-quark mass from non-perturbative $N_f = 2$ Heavy Quark Effective Theory at $\mathrm{O}\left(1/m_h\right)$Bloss.
Physics letters / B, 730:171, and PUBDB-2014-04264.
doi: 10.1016/j.physletb.2014.01.046.

A. Bharucha, A. Goudelis and M. McGarrie.
En-gauging naturalness.
The European physical journal / C, 74(5):2858, and DESY-2014-02998, DESY-13-171.
doi: 10.1140/epjc/s10052-014-2858-7.

D. Blas, M. Garny and T. Konstandin.
Cosmological perturbation theory at three-loop order.
Journal of cosmology and astroparticle physics, 2014(01):010, and DESY-2014-02908, DESY-13-161.
doi: 10.1088/1475-7516/2014/01/010.

D. Blas et al.
Structure formation with massive neutrinos: going beyond linear theory.
Journal of cosmology and astroparticle physics, 2014(11):039, and PUBDB-2014-04632, DESY-14-143; arXiv:1408.2995.
doi: 10.1088/1475-7516/2014/11/039.

J. Blümlein, A. De Freitas and C. Schneider.
Higher Order Heavy Quark Corrections to Deep-Inelastic Scattering.
Nuclear physics / B / Proceedings supplements, 00:1, and PUBDB-2014-04270, DESY 14-159, DO–TH 14/22, SFB/CPP–14–73, LPN 14–113.

J. Blümlein and J. Brunner.
New exclusion limits on dark gauge forces from proton Bremsstrahlung in beam-dump data.
Physics letters / B, 731:320, and DESY-2014-02438.
doi: 10.1016/j.physletb.2014.02.029.

J. Blümlein, A. Hasselhuhn and T. Pfoh.
The $(0\frac{2}{s})$ heavy quark corrections to charged current deep-inelastic scattering at large virtualities.
Nuclear physics / B, 881:1, and DESY-2014-02282, DESY-13-247; DO-TH-13-34; SFB-CPP-14-005; LPN-14-006; Higgstools 14-2; TUM-HEP-921/13; arXiv:1401.4352.
doi: 10.1016/j.nuclphysb.2014.01.023.

G. Bohm and G. Zech.
Statistics of Weighted Poisson Events and its Applications.
Nuclear instruments & methods in physics research / A, 748:1, and PUBDB-2015-01191, arXiv:1309.1287.
doi: 10.1016/j.nima.2014.02.021.

M. Bonvini and S. Marzani.
Resummed Higgs cross section at $\mathrm{N^3LL}$.
Journal of high energy physics, 2014(9):7, and PUBDB-2014-04097, DESY 14-075.
doi: 10.1007/JHEP09(2014)007.

M. Bonvini et al.
Updated Higgs cross section at approximate $\mathrm{N^3LO}$.
Journal of physics / G, 41(9):095002, and DESY-2014-03154, DESY-14-052; IFUM-1026-FT; DCPT/14/62; IPPP/14/31.
doi: 10.1088/0954-3899/41/9/095002.

R. Boughezal et al.
Combining resummed Higgs predictions across jet bins.
Physical review / D, 89(7):074044, and DESY-2014-02765, DESY-13-244.
doi: 10.1103/PhysRevD.89.074044.

A. Broggio, A. S. Papanastasiou and A. Signer.
Renormalization-group improved fully differential cross sections for top pair production.
Journal of high energy physics, 2014(10):98, and PUBDB-2014-04244, DESY 14-104; PSI-PR-14-04; ZU-TH-21-14; arXiv:1407.2532.
doi: 10.1007/JHEP10(2014)098.

F. Brümmer and W. Buchmüller.
A low Fermi scale from a simple gaugino-scalar mass relation.
Journal of high energy physics, 2014(3):75, and DESY-2014-02617, DESY-13-174.
doi: 10.1007/JHEP03(2014)075.

F. Brümmer, M. McGarrie and A. Weiler.
Light third-generation squarks from flavour gauge messengers.
Journal of high energy physics, 2014(4):78, and DESY-2014-02758, DESY-13-152.
doi: 10.1007/JHEP04(2014)078.

M. Bruno et al.
Topological susceptibility and the sampling of field space in $N_f = 2$ lattice QCD simulations.
Journal of high energy physics, 2014(8):150, and PUBDB-2014-03536, DESY-14-101; SFB-CPP-14-29; arXiv:1406.5363.
doi: 10.1007/JHEP08(2014)150.

O. Buchmueller et al.
Implications of Improved Higgs Mass Calculations for Supersymmetric Models.
The European physical journal / C, 74(3):2809, and PUBDB-2015-01089, DESY-13-249; arXiv:1312.5233.
doi: 10.1140/epjc/s10052-014-2809-3.

O. Buchmueller et al.
The CMSSM and NUHM1 after LHC Run 1.
The European physical journal / C, 74(6):2922, and DESY-2014-03091, DESY-13-250.
doi: 10.1140/epjc/s10052-014-2922-3.

O. Buchmueller et al.
The NUHM2 after LHC Run 1.
The European physical journal / C, 74(12):3212, and PUBDB-2014-04633, DESY-14-144; arXiv:1408.4060.
doi: 10.1140/epjc/s10052-014-3212-9.

W. Buchmüller, V. Domcke and K. Schmitz.
The chaotic regime of D-term inflation.
Journal of cosmology and astroparticle physics, 2014(11):006, and PUBDB-2014-04243, DESY 14-099.
doi: 10.1088/1475-7516/2014/11/006.

W. Buchmuller, V. Domcke and C. Wieck.
No-scale D-term inflation with stabilized moduli.
Physics letters / B, 730:155, and DESY-2014-02297, DESY-13-157; arXiv:1309.3122.
doi: 10.1016/j.physletb.2014.01.040.

W. Buchmuller, C. Wieck and M. Winkler.
Supersymmetric moduli stabilization and high-scale inflation.
Physics letters / B, 736:237, and PUBDB-2014-04088, DESY 14-031.
doi: 10.1016/j.physletb.2014.07.024.

W. Buchmüller et al.
Large-field inflation and supersymmetry breaking.
Journal of high energy physics, 2014(9):53, and PUBDB-2014-03735.
doi: 10.1007/JHEP09(2014)053.

W. Buchmüller et al.
Hybrid inflation in the complex plane.
Journal of cosmology and astroparticle physics, 2014(07):054, and PUBDB-2014-04083, DESY 14-005.
doi: 10.1088/1475-7516/2014/07/054.

F. Burger et al.
Four-Flavour Leading-Order Hadronic Contribution to the Muon Anomalous Magnetic Moment.
Journal of high energy physics, 2014(2):99, and PUBDB-2015-01202, arXiv:1308.4327.
doi: 10.1007/JHEP02(2014)099.

V. V. Bytev, M. Kalmykov and S.-O. Moch.
HYPERDIRE: HYPERgeometric Functions DIfferential REduction: MATHEMATICA based Packages for Differential Reduction of Generalized Hypergeometric Functions: F_D and F_S Horn-type Hypergeometric functions of three variables.
Computer physics communications, 185(11):3041, and PUBDB-2015-01109, DESY-13-236; arXiv:1312.5777.
doi: 10.1016/j.cpc.2014.07.014.

F. Campanario et al.
Complete QED NLO Contributions to the Reaction $e^+e^- \to \mu^+\mu^-\gamma$ and their Implementation in the Event Generator PHOKHARA.
Journal of high energy physics, 2014(2):114, and PUBDB-2015-01035, DESY-13-263; arXiv:1312.3610.
doi: 10.1007/JHEP02(2014)114.

V. Cardoso and R. A. Porto.
Analytic Approximations, Perturbation Theory, Effective Field Theory Methods and their Applications.
General relativity and gravitation, 46(5):1682, and PUBDB-2015-01088.
doi: 10.1007/s10714-014-1682-6.

G. Chalons and F. Domingo.
Dimension-7 operators in the $b \to s$ transition.
Physical review / D, 89(3):034004, and DESY-2014-02291, DESY-13-056.
doi: 10.1103/PhysRevD.89.034004.

M. N. Chernodub et al.
On Chromoelectric (super)conductivity of the Yang–Mills Vacuum.
Physics letters / B, 730:63, and DESY-2014-01632, DESY 12-240; arXiv:1212.3168.
doi: 10.1016/j.physletb.2014.01.029.

K. Choi, K. Jeong and M.-S. Seo.
String theoretic QCD axions in the light of PLANCK and BICEP2.
Journal of high energy physics, 2014(7):92, and PUBDB-2014-04089.
doi: 10.1007/JHEP07(2014)092.

N. Christian et al.
Mesoscopic Behavior from Microscopic Markov Dynamics and its Application to Calcium Release Channels.
Journal of theoretical biology, 343:102, and PUBDB-2015-01218.
doi: 10.1016/j.jtbi.2013.11.010.

K. Cichy, E. Garcia-Ramos and K. Jansen.
Topological susceptibility from the twisted mass Dirac operator spectrum.
Journal of high energy physics, 2014(2):119, and PUBDB-2015-00884, DESY-13-208; HU-EP-13-64; SFB-CPP-13-114; arXiv:1312.5161.
doi: 10.1007/JHEP02(2014)119.

M. Cicoli et al.
Just enough inflation: power spectrum modifications at large scales.
Journal of cosmology and astroparticle physics, 2014(12):001, and PUBDB-2014-04630, DESY-14-117; arXiv:1407.1048.
doi: 10.1088/1475-7516/2014/12/030.

CSSM and QCDSF/UKQCD Collaborations.
Electric form factors of the octet baryons from lattice QCD and chiral extrapolation.
Physical review / D, 90(3):034502, and PUBDB-2014-04085, DESY 14-016.
doi: 10.1103/PhysRevD.90.034502.

CSSM and QCDSF/UKQCD Collaborations and CSSM Collaboration and QCDSF/UKQCD Collaboration.
Feynman-Hellmann approach to the spin structure of hadrons.
Physical review / D, 90(1):014510, and PUBDB-2014-04090, DESY 14-056.
doi: 10.1103/PhysRevD.90.014510.

CSSM Collaboration and QCDSF/UKQCD Collaboration.
Magnetic form factors of the octet baryons from lattice QCD and chiral extrapolation.
Physical review / D, 89(7):074511, and DESY-2014-02915, DESY-14-002.
doi: 10.1103/PhysRevD.89.074511.

G. Cullen et al.
GoSam-2.0: a tool for automated one-loop calculations within the Standard Model and beyond.
The European physical journal / C, 74(8):3001, and DESY-2014-03178, DESY 14-061; MPP-2014-145.
doi: 10.1140/epjc/s10052-014-3001-5.

M. Czakon et al.
Removing Gaps in the Exclusion of Top Squark Parameter Space.
Physical review letters, 113(20):201803, and PUBDB-2014-04245, DESY 14-107.
doi: 10.1103/PhysRevLett.113.201803.

A. G. Dias et al.
The quest for an intermediate-scale accidental axion and further ALPs.
Journal of high energy physics, 2014(6):37, and DESY-2014-02855.
doi: 10.1007/JHEP06(2014)037.

M. Diehl, T. Kasemets and S. Keane.
Correlations in double parton distributions: effects of evolution.
Journal of high energy physics, 2014(5):118, and DESY-2014-02912, DESY-13-243.
doi: 10.1007/JHEP05(2014)118.

E. Dudas.
Three-Form Multiplet and Inflation.
Journal of high energy physics, 2014(12):14, and PUBDB-2015-01081, DESY-14-132.
doi: 10.1007/JHEP12(2014)014.

J. Elias-Miró, J. R. Espinosa and T. Konstandin.
Taming infrared divergences in the effective potential.
Journal of high energy physics, 2014(8):34, and PUBDB-2014-04109.
doi: 10.1007/JHEP08(2014)034.

K. Enqvist, R. Lerner and T. Takahashi.
The minimal curvaton-higgs model.
Journal of cosmology and astroparticle physics, 2014(01):006, and DESY-2014-02759, DESY-13-180.
doi: 10.1088/1475-7516/2014/01/006.

L. Ferro et al.
Spectral Parameters for Scattering Amplitudes in $\mathcal{N}$ =4 Super Yang-Mills Theory.
Journal of high energy physics, 2014(1):94, and PUBDB-2015-01092, DESY-13-488; arXiv:1308.3494.
doi: 10.1007/JHEP01(2014)094.

N. Fischer et al.
Revisiting radiation patterns in e^+e^- e^+e^- collisions.
The European physical journal / C, 74(4):2831, and DESY-2014-02916, DESY-14-014.
doi: 10.1140/epjc/s10052-014-2831-5.

D. de Florian et al.
Approximate N^{3}LO Higgs-boson production cross section using physical-kernel constraints.
Journal of high energy physics, 1410(10):176, and PUBDB-2014-04047, DESY 14-123; LPN-14-088; LTH-1014; arXiv:1408.6277.
doi: 10.1007/JHEP10(2014)176.

M. Garny et al.
Majorana dark matter with a coloured mediator: collider vs direct and indirect searches.
Journal of high energy physics, 2014(6):169, and DESY-2014-03003, DESY-14-029; arXiv: 1403.4634.
doi: 10.1007/JHEP06(2014)169.

J. R. Gaunt.
Glauber gluons and multiple parton interactions.
Journal of high energy physics, 2014(7):110, and PUBDB-2014-04095, DESY 14-067.
doi: 10.1007/JHEP07(2014)110.

J. R. Gaunt, M. Stahlhofen and F. J. Tackmann.
The quark beam function at two loops.
Journal of high energy physics, 2014(4):113, and DESY-2014-02914, DESY-14-001.
doi: 10.1007/JHEP04(2014)113.

J. Gaunt, R. Maciula and A. Szczurek.
Conventional versus single-ladder-splitting contributions to double parton scattering production of two quarkonia, two Higgs bosons and $c\bar{c}c\bar{c}$.
Physical review / D, 90(5):054017, and PUBDB-2014-04046, DESY 14-120; arXiv:1407.5821.
doi: 10.1103/PhysRevD.90.054017.

J. Gaunt and M. Stahlhofen.
The fully-differential quark beam function at NNLO.
Journal of high energy physics, 12:146, and PUBDB-2015-00230, DESY-14-170; arXiv:1409.8281.
doi: 10.1007/JHEP12(2014)146.

N. Greiner.
GoSam 2.0: Automated one loop calculations within and beyond the Standard Model.
Nuclear physics / B / Proceedings supplements, PUBDB-2014-04036, DESY 14-183; arXiv:1410.3237.

C. Grojean et al.
Very boosted Higgs in gluon fusion.
Journal of high energy physics, 2014(5):22, and DESY-2014-02760, DESY-13-233.
doi: 10.1007/JHEP05(2014)022.

Group, Particle Data.
Review of Particle Physics.
Chinese physics / C, 38(9):090001, and PUBDB-2014-03548.
doi: 10.1088/1674-1137/38/9/090001.

L. Hadasz, M. Pawelkiewicz and V. Schomerus.
Self-dual continuous series of representations for $\mathcal{U}_q(sl(2))$ and $\mathcal{U}_q(osp(1|2))$.
Journal of high energy physics, 2014(10):91, and PUBDB-2014-03980, DESY 13-083.
doi: 10.1007/JHEP10(2014)091.

T. Hahn et al.
High-precision predictions for the light CP-even Higgs Boson Mass of the MSSM.
Physical review letters, 112(14):141801, and DESY-2014-02621, DESY-13-248.
doi: 10.1103/PhysRevLett.112.141801.

Y. Hamada et al.
More on cosmological constraints on spontaneous R-symmetry breaking models.
Journal of cosmology and astroparticle physics, 2014(01):024, and DESY-2014-01642, DESY 13-170.
doi: 10.1088/1475-7516/2014/01/024.

L. A. Harland-Lang et al.
Sharpening m T2 cusps: the mass determination of semi-invisibly decaying particles from a resonance.
Journal of high energy physics, 2014(6):175, and DESY-2014-03000, DESY-13-258; arXiv:1312.5720.
doi: 10.1007/JHEP06(2014)175.

Y. Hatsuda.
Wilson loop OPE, analytic continuation and multi-Regge limit.
Journal of high energy physics, 2014(10):38, and PUBDB-2015-01021, DESY-14-057; arXiv:1404.6506.
doi: 10.1007/JHEP10(2014)038.

Y. Hatsuda and K. Okuyama.
Probing non-perturbative effects in M-theory.
Journal of high energy physics, 1410(10):158, and PUBDB-2014-04045, DESY 14-126; arXiv:1407.3786.
doi: 10.1007/JHEP10(2014)158.

Y. Hatsuda et al.
Non-perturbative effects and the refined topological string.
Journal of high energy physics, 2014(9):168, and PUBDB-2014-03717.
doi: 10.1007/JHEP09(2014)168.

Y. Hatsuda et al.
Quantum Wronskian approach to six-point gluon scattering amplitudes at strong coupling.
Journal of high energy physics, 2014(8):162, and DESY-2014-03249, DESY 14-058.
doi: 10.1007/JHEP08(2014)162.

T. Higaki, K. Jeong and F. Takahashi.
Solving the tension between high-scale inflation and axion isocurvature perturbations.
Physics letters / B, 734:21, and DESY-2014-03004, DESY-14-033.
doi: 10.1016/j.physletb.2014.05.014.

T. Higaki, K. Jeong and F. Takahashi.
The 7 keV axion dark matter and the X-ray line signal.
Physics letters / B, 733:25, and DESY-2014-02918, DESY-14-022.
doi: 10.1016/j.physletb.2014.04.007.

T. Hiramatsu et al.
Instability of colliding metastable strings.
Journal of high energy physics, 2014(1):165, and DESY-2014-02290, DESY-13-039; arXiv:1304.0623.
doi: 10.1007/JHEP01(2014)165.

A. H. Hoang and M. Stahlhofen.
The top-antitop threshold at the ILC: NNLL QCD uncertainties.
Journal of high energy physics, 2014(5):121, and DESY-2014-02909, DESY-13-168.
doi: 10.1007/JHEP05(2014)121.

S. Höche, Y. Li and S. Prestel.
Higgs-boson production through gluon fusion at NNLO QCD with parton showers.
Physical review / D, 90(5):054011, and PUBDB-2014-04631, DESY-14-119; arXiv:1407.3773; SLAC-PUB 16011; MCNET 14-14.
doi: 10.1103/PhysRevD.90.054011.

M. Hoffmann et al.
Probing compositeness with Higgs Boson decays at the LHC.
The European physical journal / C, 74(11):3181, and PUBDB-2014-04425, DESY 14-094; arXiv:1407.8000.
doi: 10.1140/epjc/s10052-014-3181-z.

R. Horsley et al.
Nucleon axial charge and pion decay constant from two-flavor lattice QCD.
Physics letters / B, 732:41, and DESY-2014-02678, DESY-13-017.
doi: 10.1016/j.physletb.2014.03.002.

R. Horsley et al.
The SU(3) Beta Function from Numerical Stochastic Perturbation Theory.
Physics letters / B, 728:1, and PUBDB-2015-01091, DESY-13-127.
doi: 10.1016/j.physletb.2013.11.012.

M. Isachenkov, I. Kirsch and V. Schomerus.
Chiral primaries in strange metals.
Nuclear physics / B, 885:679, and PUBDB-2014-04087, DESY 14-028.
doi: 10.1016/j.nuclphysb.2014.06.004.

H. Ishida, K. Jeong and F. Takahashi.
7 keV sterile neutrino dark matter from split flavor mechanism.
Physics letters / B, 732:196, and DESY-2014-02917, DESY-14-017.
doi: 10.1016/j.physletb.2014.03.044.

K. Ishiwata.
Axino dark matter in moduli-induced baryogenesis.
Journal of high energy physics, 2014(9):122, and PUBDB-2014-04246, DESY 14-114.
doi: 10.1007/JHEP09(2014)122.

K. Ishiwata, K. Jeong and F. Takahashi.
Moduli-induced baryogenesis.
Journal of high energy physics, 2014(2):62, and DESY-2014-02289, DESY-13-235; arXiv:1312.0954.
doi: 10.1007/JHEP02(2014)062.

J. Jaeckel, J. Redondo and A. Ringwald.
3.55 keV hint for decaying axionlike particle dark matter.
Physical review / D, 89(10):103511, and DESY-2014-02781, DESY 14-023.
doi: 10.1103/PhysRevD.89.103511.

F. Jegerlehner.
About the Role of the Higgs Boson in the Evolution of the Early Universe.
7. 20th Cracow Epiphany Conference on the Physics at the LHC, Cracow (Poland), 06/08/2014 - 06/10/2014.
Inst. of Physics, Jagellonian Univ., Cracow, June 2014.
doi: 10.5506/APhysPolB.45.1393.

F. Jegerlehner.
The Standard Model as a Low-energy Effective Theory: What is Triggering the Higgs Mechanism?
Acta physica Polonica / B, 45(6):1167, and PUBDB-2015-01161, arXiv:1304.7813; DESY 13-074; HU-EP-13/23.
doi: 10.5506/APhysPolB.45.1167.

K. S. Jeong, M. Kawasaki and F. Takahashi.
Axions as hot and cold dark matter.
Journal of cosmology and astroparticle physics, 2014(02):046, and DESY-2014-02299, DESY-13-181; TU-948; ICRR-661-2013-10; IPMU13-0197; arXiv:1310.1774.
doi: 10.1088/1475-7516/2014/02/046.

K. S. Jeong, Y. Shoji and M. Yamaguchi.
Higgs mixing in the NMSSM and light Higgsinos.
Journal of high energy physics, 2014(11):148, and PUBDB-2014-04629, DESY-14-103; CTPU-14-10; TU-974; arXiv:1407.0955.
doi: 10.1007/JHEP11(2014)148.

A. Joseph.
Supersymmetric quiver gauge theories on the lattice.
Journal of high energy physics, 2014(1):93, and DESY-2014-02257, DESY-13-229.
doi: 10.1007/JHEP01(2014)093.

A. Joseph.
Two-dimensional $\mathcal{N}$ = (2, 2) lattice gauge theories with matter in higher representations.
Journal of high energy physics, 1407(7):67, and DESY-2014-03292, DESY14-030; arXiv:1403.4390.
doi: 10.1007/JHEP07(2014)067.

R. Kallosh, A. Linde and A. Westphal.
Chaotic inflation in supergravity after Planck and BICEP2.
Physical review / D, 90(2):023534, and PUBDB-2014-04092.
doi: 10.1103/PhysRevD.90.023534.

A. Kaminska et al.
A precision study of the fine tuning in the DiracNMSSM.
Journal of high energy physics, 2014(6):153, and DESY-2014-02999, DESY-13-256.
doi: 10.1007/JHEP06(2014)153.

R. Kappl and M. W. Winkler.
The cosmic ray antiproton background for AMS-02.
Journal of cosmology and astroparticle physics, 2014(09):051, and PUBDB-2014-03713.
doi: 10.1088/1475-7516/2014/09/051.

A. Karneyeu et al.
MCPLOTS: a Particle Physics Resource based on Volunteer Computing.
The European physical journal / C, 74(2):2714, and PUBDB-2015-01090, DESY-13-104;arXiv:1306.3436.
doi: 10.1140/epjc/s10052-014-2714-9.

T. Konstandin, G. Nardini and I. Rues.
From Boltzmann equations to steady wall velocities.
Journal of cosmology and astroparticle physics, 2014(09):028, and PUBDB-2014-04247, DESY 14-127.
doi: 10.1088/1475-7516/2014/09/028.

S. Krippendorf et al.
Rational F-theory GUTs without exotics.
Journal of high energy physics, 2014(7):13, and DESY-2014-03001, DESY-13-259; arXiv:1401.5084.
doi: 10.1007/JHEP07(2014)013.

M. C. Kumar and S.-O. Moch.
Phenomenology of Threshold Corrections for Inclusive Jet Production at Hadron Colliders.
Physics letters / B, 730:122, and PUBDB-2015-01219, arXiv:1309.5311; DESY 13-165; LPN 13-060.
doi: 10.1016/j.physletb.2014.01.034.

A. Kurz et al.
Anomalous magnetic moment with heavy virtual leptons.
Nuclear physics / B, 879:1, and DESY-2014-00188, SFB-CPP-13-81; TTP13-32; DESY-13-195; LPN13-084 ; arXiv:1311.2471.
doi: 10.1016/j.nuclphysb.2013.11.018.

Z. Ligeti and F. J. Tackmann.
Precise predictions for $B \to X_c \tau \nu$ decay distributions.
Physical review / D, 90(3):034021, and DESY-2014-03322, DESY 14-095.
doi: 10.1103/PhysRevD.90.034021.

N. A. Lo Presti, A. Almasy and A. Vogt.
Leading large-x logarithms of the quark-gluon contributions to inclusive Higgs-boson and lepton-pair production.
Physics letters / B, B737:120, and PUBDB-2014-04038, DESY 14-106; IPHT-T14-084; LTH-1013; LPN14-084; arXiv:1407.1553.
doi: 10.1016/j.physletb.2014.08.044.

P. Marquard and N. Zerf.
SLAM, a Mathematica interface for SUSY spectrum generators.
Computer physics communications, 185(3):1153, and PUBDB-2014-04297, Alberta Thy 5-13; DESY 13-156; LPN 13-059; TTP 13-024; arXiv:1309.1731.
doi: 10.1016/j.cpc.2013.12.005.

P. Marquard et al.
Three-loop matching of the vector current.
Physical review / D, 89(3):034027, and DESY-2014-02259, DESY-13-253; LPN14-003; SFB-CPP-14-03; SI-HEP-2014-01; TTP14-002; TTK-14-01; TUM-HEP-922-14.
doi: 10.1103/PhysRevD.89.034027.

L. McAllister et al.
The powers of monodromy.
Journal of high energy physics, 2014(9):123, and PUBDB-2014-03883.
doi: 10.1007/JHEP09(2014)123.

S. Melville and R. Lerner.
Quantifying the 'naturalness' of the curvaton model.
Journal of cosmology and astroparticle physics, 2014(07):026, and PUBDB-2014-04084, DESY 14-015.
doi: 10.1088/1475-7516/2014/07/026.

C. Meneghelli and G. Yang.
Mayer-Cluster Expansion of Instanton Partition Functions and Thermodynamic Bethe Ansatz.
Journal of high energy physics, 2014(5):112, and PUBDB-2015-01086, arXiv:1312.4537.
doi: 10.1007/JHEP05(2014)112.

M. D. Morte et al.
Matching of heavy-light flavour currents between HQET at order 1/m and QCD: I. Strategy and tree-level study.
Journal of high energy physics, 2014(5):60, and PUBDB-2015-00872, IFIC-13-69, DESY-13-231, MS-TP-13-33, arXiv:1312.1566.
doi: 10.1007/JHEP05(2014)060.

M. Papucci et al.
Fastlim: a fast LHC limit calculator.
The European physical journal / C, 74(11):3163, and PUBDB-2014-04628, DESY-14-010; arXiv:1402.0492; CERN-TH/2014-019; KCL-PH-TH/2014-04; MCTP-14-03.
doi: 10.1140/epjc/s10052-014-3163-1.

M. Pawelkiewicz, V. Schomerus and P. Suchanek.
The universal Racah-Wigner symbol for U q (osp(1|2)).
Journal of high energy physics, 2014(4):79, and DESY-2014-02614, DESY-13-129.
doi: 10.1007/JHEP04(2014)079.

F. G. Pedro and A. Westphal.
The scale of inflation in the landscape.
Physics letters / B, 739:439, and PUBDB-2014-04627, DESY-13-044.
doi: 10.1016/j.physletb.2014.10.022.

F. Pedro and A. Westphal.
Low-ℓ CMB power loss in string inflation.
Journal of high energy physics, 2014(4):34, and DESY-2014-02616, DESY-13-163.
doi: 10.1007/JHEP04(2014)034.

S. Plaetzer.
Summing large- N towers in colour flow evolution.
The European physical journal / C, 74(6):2907, and PUBDB-2014-03718.
doi: 10.1140/epjc/s10052-014-2907-2.

R. A. Porto, L. Senatore and M. Zaldarriaga.
The Lagrangian-Space Effective Field Theory of Large Scale Structures.
Journal of cosmology and astroparticle physics, 2014(05):022, and PUBDB-2015-01087, arXiv:1311.2168.
doi: 10.1088/1475-7516/2014/05/022.

A. Ramos.
The gradient flow running coupling with twisted boundary conditions.
Journal of high energy physics, 2014(11):101, and PUBDB-2015-00183, arXiv:1409.1445; DESY 13-151.
doi: 10.1007/JHEP11(2014)101.

J. Reuter, M. Tonini and M. Vries.
Littlest Higgs with T-parity: status and prospects.
Journal of high energy physics, 2014(2):53, and DESY-2014-02296, DESY-13-123; arXiv:1310.2918.
doi: 10.1007/JHEP02(2014)053.

M. Schlaffer et al.
Boosted Higgs shapes.
The European physical journal / C, 74(10):3120, and PUBDB-2014-04096, DESY 14-069.
doi: 10.1140/epjc/s10052-014-3120-z.

V. P. Spiridonov and G. S. Vartanov.
Vanishing Superconformal Indices and the Chiral Symmetry Breaking.
Journal of high energy physics, 2014(6):62, and PUBDB-2015-01085.
doi: 10.1007/JHEP06(2014)062.

M. Stahlhofen, F. J. Tackmann and J. Gaunt.
The gluon beam function at two loops.
Journal of high energy physics, 2014(8):20, and PUBDB-2014-04082, DESY 14-004.
doi: 10.1007/JHEP08(2014)020.

I. W. Stewart et al.
Jet p_T resummation in Higgs production at $NNLL' + NNLO$.
Physical review / D, 89(5):054001, and DESY-2014-02906, DESY-13-122.
doi: 10.1103/PhysRevD.89.054001.

J. Teschner and G. Vartanov.
6j Symbols for the Modular Double, Quantum Hyperbolic Geometry, and Supersymmetric Gauge Theories.
Letters in mathematical physics, 104(5):527, and DESY-2014-02955, DESY-12-035.
doi: 10.1007/s11005-014-0684-3.

C. Wieck and M. W. Winkler.
Inflation with Fayet-Iliopoulos terms.
Physical review / D, 90(10):103507, and PUBDB-2014-04248, DESY 14-139.
doi: 10.1103/PhysRevD.90.103507.

Master Thesis

D. Jung.
Visualizing Gravitational Lensing Phenomena in Real-time using GPU shaders in celestia.Sci.
International Space University (ISU), Strasbourg, 2014.

J. Kummer.
The Cosmological Constant in Theories with Finite Spacetime.
University of Hamburg, Hamburg, 2014.

Ph.D. Thesis

M. Sprenger.
High-Energy Scattering in strongly coupled $\mathcal{N} = 4$ super Yang-Mills Theory.
University of Hamburg, Hamburg, 2014.

M. Tonini.
Beyond the Standard Higgs at the LHC: present constraints on Little Higgs models and future prospects.
University of Hamburg, Hamburg, 2014.

M. de Vries.
Strongly Coupled Models at the LHC.
University of Hamburg, Hamburg, 2014.

L. K. Zeune.
Constraining supersymmetric models using Higgs physics, precision observables and direct searches.
University of Hamburg, Hamburg, 2014.

ZEUS

Published

L. L. Jenkovszky et al.
Low Missing Mass, Single- and Double Diffraction Dissociation at the LHC.
Physics of atomic nuclei, 77(12):1463, and PUBDB-2015-01143, arXiv:1211.5841.
doi: 10.1134/S1063778814120072.

H. Kowalski, L. Lipatov and D. Ross.
The Green Function for the BFKL Pomeron and the Transition to DGLAP Evolution.
The European physical journal / C, 74(6):2919, and PUBDB-2015-01145, arXiv:1401.6298.
doi: 10.1140/epjc/s10052-014-2919-y.

A. Luszczak and H. Kowalski.
Dipole Model Analysis of High Precision HERA Data.
Physical review / D, 89(7):074051, and PUBDB-2015-01146, arXiv:1312.4060.
doi: 10.1103/PhysRevD.89.074051.

P. R. Newman and M. Wing.
The Hadronic Final State at HERA.
Reviews of modern physics, 86(3):1037, and PUBDB-2015-01144, arXiv:1308.3368.
doi: 10.1103/RevModPhys.86.1037.

ZEUS Collaboration.
Deep inelastic cross-section measurements at large y with the ZEUS detector at HERA.
Physical review / D, 90(7):072002, and DESY-2014-03785, DESY-14-053; arXiv:1404.6376.
doi: 10.1103/PhysRevD.90.072002.

L. Stanco.
Elastic Z^0 production at HERA.
Nuclear physics / B / Proceedings supplements, 00:1, and PUBDB-2015-00134, arXiv:1410.3229.

ZEUS Collaboration.
Erratum: Measurement of $D^{*\pm}$ production in deep inelastic scattering at HERA.
Journal of high energy physics, 02:106, and DESY-2014-02399.
doi: 10.1007/JHEP02(2014)106.

ZEUS Collaboration.
Further studies of the photoproduction of isolated photons with a jet at HERA.
Journal of high energy physics, 2014(8):23, and DESY-2014-03355, DESY-14-086; arXiv:1405.7127.
doi: 10.1007/JHEP08(2014)023.

ZEUS Collaboration.
Measurement of beauty and charm production in deep inelastic scattering at HERA and measurement of the beauty-quark mass.
Journal of high energy physics, 2014(9):127, and PUBDB-2014-03752, DESY-14-083; arXiv:1405.6915.
doi: 10.1007/JHEP09(2014)127.

ZEUS Collaboration.
Measurement of D^* photoproduction at three different centre-of-mass energies at HERA.
Journal of high energy physics, 2014(10):3, and PUBDB-2014-03754, DESY-14-082; arXiv:1405.5068.
doi: 10.1007/JHEP10(2014)003.

ZEUS Collaboration.
Measurement of neutral current e+/-p cross sections at high Bjorken x with the ZEUS detector.
Physical review / D, D89(7):072007, and DESY-2014-02639, DESY-13-245.
doi: 10.1103/PhysRevD.89.072007.

ZEUS Collaboration.
Measurement of the Luminosity in the ZEUS Experiment at HERA II.
Nuclear instruments & methods in physics research / A, 744:80, and PUBDB-2015-01148, DESY-13-081; arXiv:1306.1391.
doi: 10.1016/j.nima.2014.01.053.

ZEUS Collaboration.
Photoproduction of isolated photons, inclusively and with a jet, at HERA.
Physics letters / B, 730:293, and DESY-2014-02047, DESY 13-234; arXiv:1312.1539.
doi: 10.1016/j.physletb.2014.01.062.

Photographs and graphics
Lars Berg / DESY
Heiner Müller-Elsner / DESY
DFZ Architekten / DESY
ATLAS experiment @ CERN 2013
Erik Butz
Hammeskrause Architekten
Humboldt Foundation / Albrecht G.W. Barthel
KEK
Christof Rieken
Semiconductor Laboratory Munich, MPG HLL
The figures were reproduced by permission of authors or journals.

Acknowledgement
We would like to thank all authors and everyone who helped in the creation of this annual report.

Imprint

Publishing and contact
Deutsches Elektronen-Synchrotron DESY
A Research Centre of the Helmholtz Association

Hamburg location:
Notkestr. 85, 22607 Hamburg, Germany
Tel.: +49 40 8998-0, Fax: +49 40 8998-3282
desyinfo@desy.de

Zeuthen location:
Platanenallee 6, 15738 Zeuthen, Germany
Tel.: +49 33762 7-70, Fax: +49 33762 7-7413
desyinfo.zeuthen@desy.de

www.desy.de
ISBN: 978-3-935702-97-3
doi: 10.3204/DESY_AR_ET2014

Editing
Ilka Flegel, Manfred Fleischer, Michael Medinnis, Thomas Schörner-Sadenius

Layout
Sabine Kuhls-Dawideit

Production
Britta Liebaug

Printing
ehs druck gmbh, Schenefeld

Editorial deadline
28 February 2015

Editorial note
The authors of the individual scientific contributions published in this report are fully responsible for the contents.

HELMHOLTZ
ASSOCIATION

Deutsches Elektronen-Synchrotron
A Research Centre of the Helmholtz Association

The Helmholtz Association is a community of 18 scientific-technical and biological-medical research centres. These centres have been commissioned with pursuing long-term research goals on behalf of the state and society. The Association strives to gain insights and knowledge so that it can help to preserve and improve the foundations of human life. It does this by identifying and working on the grand challenges faced by society, science and industry. Helmholtz Centres perform top-class research in strategic programmes in six core fields: Energy, Earth and Environment, Health, Key Technologies, Structure of Matter, Aeronautics, Space and Transport.

www.helmholtz.de